UNIVERSITY OF LIVERPOOL

Modulation of Neutrophil Migration by the Pneumococcal toxin, Pneumolysin

Thesis submitted in accordance with the requirements of the University of Liverpool for the degree of Doctor of Philosophy

Zuliza Mohamed
October, 2018

Authors Declaration

This thesis represents the unaided work of the author except where the help of other has been acknowledge

Zuliza Mohamed

October 2018

Abstract

Streptococcus pneumoniae is a common bacterial respiratory pathogen which often causes community-acquired pneumonia and is responsible for a huge burden of human disease and death. The initial innate immune response to promote clearance of this bacterium includes the heavy infiltration of neutrophils to the site of infection. However, excessive neutrophil recruitment, or uncontrolled neutrophil activity in response to the infection can result in massive damage to the host tissues.

Pneumolysin (PLY), is a membrane-damaging toxin synthesized by *S. pneumoniae*, which plays a multifunctional role as a pneumococcal virulence factor during infection. It has various biological activities, with distinct cytolytic and sub-lytic effects that interfere with cell function. It has been suggested this toxin can directly modulate neutrophil migration. However, the precise effects on neutrophil motility, and the molecular mechanism underpinning these changes, remain unknown. The effects of PLY on neutrophil migration form the basis of this PhD project, with the aim to understand the molecular mechanism used by PLY to alter neutrophil migration and function in *S. pneumoniae* infection.

We demonstrate that PLY inhibits murine neutrophil chemotaxis towards CXCL1/KC in 2- and 3-D, but does not competitively act as a chemoattractant for neutrophils. PdB, a toxoid derivative of PLY with greatly reduced haemolytic activity, did not inhibit neutrophil chemotaxis, suggesting full function of the toxin is required to inhibit chemotaxis. Consistent with this reduction in migration, we also show that PLY treated neutrophils have strong adhesion to tissue culture plastic, display enhanced actin polymerization, and express high levels of CD11b. Live bacteria were also able to inhibit neutrophil chemotaxis to varying degrees, but this did not strictly correlate with the haemolytic activity of the isolate.

Quantitative label-free proteomics of PLY-treated neutrophils revealed four proteins related to cell migration that significantly changed in abundance in PLY-treated neutrophils: Tyrosine-protein kinase Fes/Fps (FES), Grancalcin (GCA), Tyrosine-protein kinase CSK (CSK) and FYVE, RhoGEF and PH domain-containing protein 3

(FGD3). We also found a group of proteins changed in abundance in PLY-treated but not LPS treated neutrophils. These were enriched for cellular responses to calcium, and the presence of EF-hand domains, and were; Grancalcin (GCA), Peflin (PEF1) and Programmed cell death6 (PDCD6) Calpain (CAPN) and Sorcin(SRI) These proteins may offer potential clues to understanding the inhibitory effects of PLY on neutrophil chemotaxis. Preliminary experiments using HerbimysinA to inhibit Fes, revealed that chemotaxis of PLY-treated neutrophils towards KC could be partially restored.

The data presented here provide new insight into how PLY regulates neutrophil migration and function. In addition to advancing our understanding of the pathogenesis of *S. pneumoniae*, it is useful to understand how neutrophils migrate through inflamed tissues in order to develop therapies which can prevent neutrophil-mediated damage to host tissues in sterile injury.

Acknowledgements

First and foremost, I am grateful to God Almighty for giving me the opportunity to complete my PhD thesis. Without His numerous blessings, I can do nothing.

I owe a deep debt of gratitude to my sponsorships, the Ministry of Health Malaysia for the generous funding that allow me to embark on a PhD journey. I am also immensely grateful to both my supervisors for having accepted to be my advisors at the University of Liverpool.

I want to thank my primary supervisor Dr Janine Coombes for her patience, motivation and guidance, also for making me believe in my potential during the writing of this thesis. I sincerely appreciate her advice and instruction for me to be more focused whenever I was in confusion. I would also like to thank my secondary supervisor Prof Aras Kadioglu, for his suggestions and immense knowledge. I highly value to my both supervisor on their critical thinking that contributes to my experiments and analysis.

There are many members of the Coombes and Kadioglu group that I would like to thank who have directly helped me throughout this project, in particular Dr Laetitia Petit-Jentreau, Dr Laura Jacques, Heather Swift, Dr Lisa Luu, Emma Dearing, Dr Marie Yang and Dr Hesham Malak; their specific expertise allows my work be on track. For all other members in both groups, I feel so fortunate to have worked with diverse group of talented individuals. For all the help and advice that I have received in lab meetings, practice talks and whenever I had questions in the lab, thank you so much!

Also, I acknowledge the invaluable help that I have received from other groups; in particular Dr Stuart Armstrong in proteomic work and Ishtar for Western Blotting experiment. My gratitude also goes out to all technicians' team and individuals in IC2, RR and CCI Building who were always supportive with technical help and advice when needed.

A special word of thanks to all my friends (they know who they are) for their friendship and for the emotional support and enjoyable moment I experienced throughout my PhD.

Last but not least, the most profound appreciation goes to my mum and all my siblings to always believe in my ability. I do not think I would get this far without their continuous prayer and encouragement.

Table of Contents

List of Tables

List of Figures

Appendices

List of Abbreviations

2D	2-Dimensional
3D	3-Dimensional
AF647	Alexa Fluor 647
APC	Allophycocyanin
BSA	Bovine Serum Albumin
Calcein AM	Dye calcein acetoxymethyl ester
CBP	Choline-binding protein
CFSE	Carboxyfluorescein Succinimidyl Ester
DAPI	4′,6-diamidino-2-phenylindole
CPS	Capsular polysaccharide
FACS	Fluorescence Acitaved Cell Sorting
ECM	Extracellular Matrix
FMO	Fluorescence Minus One
EDTA	Ethylenediaminetetraacetic acid
Ca^{2+}	Calcium cation
F-actin	Filamentous Actin
FCS	Fetal Calf Serum
FMLP	N-formyl-Methionyl-Leucyl-Phenylalanine
FN	Fibronectin
FITC	Fluorescein isothiocyanat
HEPES	4-2-hydroxyethyl-1-piperazineethanesulfonic acid
JAM-A	Membrane-associated Adhesion Molecule
LPXTG	Sortase-Anchored Surface Protein
LPS	Lipopolysaccharide
LTB_4	Lipid leukotriene B_4
KC	Keratinocyte Chemoattractant
MAPK	Mitogen-Activated Protein Kinase;
MFI	Mean Fluorescence Intensity
Neu	Neutrophils
NET	Neutrophil Extracellular Trap
PBS	Phospahate Buffer Solution
PerCP	Peridinin Chlorophyll Protein Complex
PE	Phycoerythrin
PFA	Paraformaldehyde
PI3K	Phosphoinositide 3-kinase
PI3K γ	Phosphoinositide 3-kinase γ
PMN	Polymorhponuclear Neutrophils
PSGL	P-selectin Glycoprotein Ligand-1
PLA2	Phospholipase A2
PLY	Pneumolysin
PspA	Pneumococcal Surface Protein.
RPMI	Roswell Park Memorial Institute
ROS	Reactive oxygen
TNF	Tumor Necrosis Factor
SHG	Second-Harmonic Generation
SSL5	Superantigen-Like 5
TPEF	Two-photon excitation fluorescence)
WHO	Word Health Organisation

Chapter 1: Introduction

Neutrophils, together with other immune cell such as macrophages, dendritic cells (DC), mast cells and natural killer (NK) cells, are members of the innate immune system. Neutrophils are abundant in blood and are important first responders to sites of infection or inflammation, where they arrive rapidly in large numbers. Once there, they directly control infection three key processes: phagocytosis, degranulation and NETosis (release of neutrophil extracellular traps)(Kumar & Sharma 2010). Neutrophils can also modulate other aspects of the host innate and adaptive immune responses, for example (Amulic et al. 2012).

Neutrophils are distinguished by possession of a multi-lobed nucleus and neutrophilic granules, which form sequentially during maturation and contain substances with potent antimicrobial activity (Borregaard 2010). At the site of infection, these granules aid in the killing and digestion of microorganisms, but may also damage host tissues if released inappropriately (Borregaard et al. 2007; Perobelli et al. 2015).

The initial innate immune response to promote clearance of bacteria comprises a heavy infiltrate of neutrophils to the site of infection. However, excessive neutrophil recruitment, or uncontrolled neutrophil activity in response to the infection can result in massive damage to host tissues (Kolaczkowska & Kubes 2013; Craig et al. 2009). Better understanding of neutrophil migration and function is important both to optimising control of infection, and to protecting against host tissue damage (Kumar & Sharma 2010).

1.1 Neutrophil development

Neutrophils are the most abundant leukocytes in human peripheral blood, and are constantly generated in the bone marrow from myeloid precursors (Kolaczkowska & Kubes 2013). Neutrophil production is termed granulopoiesis, and occurs in haematopoietic cords in the venous sinuses of the bone marrow. In the bone marrow, the granulopoietic compartment can be divided into three broad categories: a haematopoietic stem cell pool, a mitotic pool (proliferating and differentiating granulocytic progenitor cells) and a post-mitotic pool (mature, fully differentiated neutrophils, ready to be released into the blood on demand) (Summers et al. 2010).

Before reaching maturation, neutrophils transition through the following developmental stages: haematopoietic stem cell, myeloblast, promyelocyte, myelocyte, metamyelocyte, band cell and PMN. This is accompanied by sequential development of granules, and segmentation of the nucleus, and occurs in response to a cocktail of growth factors and cytokines (Amulic et al. 2012). The basal rate of production of neutrophils in the bone marrow is about $5x10^{10}$–$20x10^{10}$ neutrophils/day in healthy human (Summers et al. 2010; Borregaard 2010; Rankin 2010).

Humans neutrophils make up 50-70% of the circulating white blood cells, and in mice, 10-25% (Doeing et al. 2003; Mestas & Hughes 2004). Neutrophils have a relatively short life-span, with an average circulatory lifespan of 5.4 days. Typically, the circulating half-life for mature neutrophils is about 8 hours in blood for humans, and 8-10 hours for mice (Galli et al. 2011; Pillay et al. 2010). They can spend approximately 2-3 days in the tissues. Their lives are mainly devoted to protecting

our body from infecting microorganisms, and after completing this function, the cells will die (Pillay et al. 2010).

1.1.1 Neutrophil release from bone marrow

Chemokines tightly control the release of bone marrow neutrophils into the blood stream in the healthy individual, and at the same time sustain a pool of cells in the bone marrow in case of infection (Amulic et al. 2012). In steady-state conditions, an equilibrium between signalling from the CXCR4 and CXCR2 chemokine receptors regulates the release of mature neutrophils from the bone marrow into the blood (Day & Link 2012). Bone marrow stromal cells produce the CXC chemokine, CXCL12 (stromal derived factor1/SDF-1α), which is a ligand for CXCR4 on neutrophils and promotes binding of (VLA)-4 on neutrophils to (VCAM)-1 on bone marrow endothelial and stromal cells to maintain them in the bone marrow, ready for immediate release (Borregaard 2010; Sadik et al. 2011).

Upon maturation of neutrophils CXCR4 will be down-regulated, and CXCR2 will be up-regulated. Bone marrow endothelial cells produce CXCL1 (KC) and CXCL2 (MIP-2), which bind CXCR2 on neutrophils, allowing effective mature neutrophil egress into the circulation (Summers et al. 2010; Sadik et al. 2011). During acute inflammation, neutrophils will be mobilized in greater numbers by a shifting balance between CXCL12 and CXCR2 ligands in the bone marrow, coordinated by G-CSF. G-CSF indirectly reduces production of CXCL12, at the same time increasing CXCL1 and CXCL2 production by bone marrow endothelial cells, promoting neutrophil egress (Summers et al. 2010; Sadik et al. 2011). During infection the lifespan of neutrophil will be prolonged, and together with increased granulopoiesis,

results in an increase in neutrophil numbers. This facilitates recruitment of large numbers of neutrophils to the site of infection (Quinn et al. 2014).

1.1.2 Neutrophil Homeostasis

Only around 1-2% of mature neutrophils circulate in blood, while the others are reserved in the bone marrow. Neutrophils adhere to blood vasculature, termed margination, to form intravascular pools in specific organs such as liver, spleen, bone marrow and lung. The size of the circulating neutrophil pool will be increased as the marginated pool of neutrophils decreases in these organs. During steady state, neutrophils will undergo apoptosis, which later promotes granulopoiesis through G-CSF production by macrophages. During inflammation, extravasated neutrophils will undergo apoptosis or necrosis and, also trigger the production of G-CSF. Thus, the rate of neutrophil development, release and death will determine the circulating number of neutrophils during infection and homeostatic conditions (Summers et al. 2010).

Neutrophils enter the site of infection, clear the pathogen and need to undergo apoptosis after that. However, if the dead cells are not cleared efficiently, they will cause inflammation and tissue damage by releasing cytotoxic proteins, such as MPO. At sites of inflammation, macrophages will clear apoptotic neutrophils (Summers et al. 2010). The uptake of apoptotic neutrophils by macrophages modulates macrophage inflammatory function. IL-23 production is suppressed, resulting in reduced IL-17 production by Th17 cells, ILCs, and others. As a result, G-CSF production is also reduced, decreasing granulopoiesis. This shifts the equilibrium between CXCR4-CXCR2 signalling towards CXCR4, retaining neutrophils in the

bone marrow, and attenuating the inflammatory response (Stark et al. 2005). Apoptotic neutrophil are not found in the circulation under non-inflammatory conditions. However, under homeostatic conditions, since neutrophils have a short half-life and are released in large numbers into the blood every day, they use a mechanism whereby the aging neutrophils will return to the bone marrow in response to the CXCR4/CXCL12 chemokine axis. In this process neutrophils are phagocytosed and thus, destroyed by resident macrophages, which in turn promotes the production of G-CSF, which further stimulates granulopoiesis (Rankin 2010).

1.2 Neutrophil recruitment to the site of infection and inflammation

Under steady state conditions neutrophils serve as security by patrolling in the blood vessels and looking for evidence of any initial inflammatory response without entering into the tissue. However, upon sensing inflammation or infection they will be primed and a recruitment cascade initiated, leading to migration from the blood into inflamed tissue, where they ingest and destroy invading microbes. Neutrophils are attracted to sites of infection after receiving chemoattractant signals which can be produced by resident macrophages, damaged cells, and bacteria. Neutrophil recruitment from blood to the site of infection involves a multistep process including extravasation from the vasculature, migration through the interstitial matrix, and at mucosal surfaces, transepithelial migration (Katanaev 2001; Bardoel et al. 2014).

1.2.1 Neutrophil Extravasation

Neutrophils have to move from the bloodstream to the site of infection in order to fight infection. In order to do this, endothelial cells must be activated to support

neutrophil attachment to the blood vessel endothelium. This multistep process involves slowing down of the neutrophil (tethering and rolling), firm adhesion of neutrophil (adhesion and crawling) and escape from blood vessel (transmigration). After crossing the endothelium and basement membrane, neutrophils enter the interstitial space and follow chemotactic cues towards the site of infection.

Extravasation from blood into the tissues, starts when, circulating neutrophils are slowed down near the infection site (Vestweber 2007). Sentinel cells resident in tissues, such as macrophages, DC and mast cells, produce pro-inflammatory mediators (IL-1β, TNF-a, chemokines) when they bind pathogen- and danger-associated molecular patterns (PAMPs and DAMPs) with their pattern recognition receptors (PRRs). The release of these pro-inflammatory mediators results in expression of P-selectin and E-selectin on endothelial cells. P-selectin glycoprotein ligand-1 (PSGL-1) recognises co-receptors on the inflamed endothelium. For example, interactions between P-selectin and PSGL-1 result in loosely adhesive contacts between neutrophils and endothelial cells, and together with the shearing force of the flow of the blood, cause the neutrophil to tether and roll along the vessel wall (Moore et al. 1995). The second step is firm adherence and full arrest of the neutrophil on the endothelial cell surface. This firm adhesion, will be influenced initially by the activation of a cascade of kinases following engagement of PSGL-1 and L-selectin on neutrophils (Amulic et al. 2012). At the same time, interactions between β2 (CD18) integrins, such as αLβ2 (LFA-1 or CD11a/CD18) and αMβ2 (MAC-1 or CD11b/CD18) on the surface of neutrophils, with intercellular adhesion molecule 1(ICAM-1) on endothelial cells occur (Diamond et al. 1990). Rolling neutrophils are exposed to chemoattractants, cytokines and bacterial products. Through a process of inside-out signalling, these drive the activation and clustering

of β2 integrins on the neutrophil surface, increase of affinity and avidity of the interaction with their ligands on endothelial cells. This results in firm adhesion and crawling of the neutrophil on the endothelial cells. Besides β2 integrins, neutrophils also use VLA-4 to interact with VCAM-1 during the rolling process (Ley et al. 2007). Subsequently, receptor-ligand interactions on both cells will result in transmigration to the interstitial space either through the endothelial junction (paracellular) or transcellularly through the endothelial cell (Phillipson et al. 2006; Spaan et al. 2013). It has been shown that neutrophils prefer paracellular migration. This is mediated by CD11b/CD18 and other adhesion molecules expressed in the endothelial junction, such as ICAM- 1 and 2, and PECAM-1 (Borregaard 2010). Subsequently, neutrophils cross the basement membrane and pericyte layers.

1.2.2 Interstitial neutrophil migration

Following extravasation, neutrophils will enter into the interstitial space where they encounter a large variety of chemotatic gradients. Studies have identified that there are significant differences in the adhesive, chemoattractant and signalling processes which regulate neutrophil migration in 2D- and 3D. *In vitro*, 2D migration is largely integrin-dependent, while 3D migration can be integrin-dependent or independent. Integrin-independent modes of migration are also dependent on actin polymerisation as it is the assembly and disassembly of the actin cytoskeleton that enables the cell to move toward cues such as chemoattractants.

In the interstitium, neutrophil chemotaxis to the site of infection is regulated by two types of chemoattractant gradient: "intermediary chemoattractants" found in the general area of infection and beginning at the endothelium (e.g. IL-8, LTB_4) and

"end-target chemoattractants" found at the infection site (e.g. complement, pathogen-derived chemoattractants). Neutrophils have to prioritize these gradients by following a hierarchy favouring end-target chemoattractants to reach the site of infection (Heit et al. 2002). The prioritization process uses two different signalling pathways: p38MAPK and CD11b/CD18 for end-target chemoattractants and PI3K and LFA-1 for intermediary chemoattractants (Heit 2005). This suggests that integrins play a role in neutrophil interstitial chemotaxis.

1.2.3 Neutrophil Activation

The interactions formed by neutrophils as they travel to sites of inflammation are accompanied by activation of complex signalling cascades that first prime neutrophils then result in their complete activation. At this point neutrophils elaborate killing functions such as phagocytosis, degranulation and NETosis. The activation of circulating neutrophils is crucial during inflammatory responses and involves a multistep process. Exposure of neutrophils to one stimulus (e.g. TNF α, IL-8, LTB4, microbial products, adhesion) leads to priming, and increases sensitivity to a second stimulus, which is necessary for full activation (Condliffe et al. 1998; Mayadas et al. 2014). Priming starts during the neutrophil recruitment cascade in blood vessels, through interaction with activated endothelial cells (Summers et al. 2010). Once neutrophils cross the endothelial barrier, the cells will become fully activated. These activated neutrophils, driven by chemoattractant cues, will release their antimicrobial contents at the site of infection. Activation also results in the release of cytokines by neutrophils, which recruit other immune cells (Amulic et al. 2012).

1.2.3.1 Pattern-recognition receptors (PRRs)

Neutrophils pattern recognition receptors (PRRs) recognise pathogen-associated molecular patterns (PAMPs) and danger-associated molecular patterns (DAMPs) (Mayadas et al. 2014).

PRR families include Toll-like receptors (TLRs), C-type lectin receptors (CLRs), Retinoic acid-inducible gene (RIG)-I-like receptors (RLRs) and NOD-like receptors (NLRs) (Takeuchi & Akira 2010). PRRs allow neutrophils to recognise a broad range of microbial features facilitating generation of the right response (Thomas & Schroder 2013). The primary endocytic PRRs of the neutrophil are the C-type lectin receptors of which Dectin-1 is the most important as it recognizes fungal β-glucan (Trinchieri & Sher 2007). Dectin-1 also induces the activation of CD11b/CD18 which is required for neutrophil cytotoxic responses (Chalovich & Eisenberg 2013). Meanwhile, the major type of non-phagocytic PRRs on neutrophils are the TLRs (Trinchieri & Sher 2007). Neutrophils have been shown to express TLR1, -2, -4, -5, -6, -8 and -10 (and, after GM-CSF treatment, TLR9) at the RNA level (Hayashi et al. 2003). It also been shown, neutrophils need to be 'primed' first before being fully activated. In the priming stage neutrophils can enhance their response to other stimuli by binding with TLR, which leads to increased cytokine release, and slows neutrophil apoptosis (Parker et al. 2005).

Peptidoglycan-related molecules of gram-negative bacteria are recognized by NOD1, and gram-positive bacteria by NOD2, which are cytosolic microbial sensors (Kanneganti et al. 2007). Recognition of PAMPs or DAMPS by NOD-like receptors results in nuclear translocation of NFkB, or activation of caspase 1 which cleaves pro-cytokines such as IL-1 and IL-18 to their active forms (Futosi et al. 2013).

NOD2 can also lead to IL-8 release after triggering by the appropriate proteoglycan (Ekman & Olaf 2009). RIG-like receptors are cytoplasmic receptors that mediate host defense against intracellular viruses (Futosi et al. 2013).

1.2.3.2 Opsonic receptors

Neutrophil-mediated uptake and degradation of opsonised pathogens occurs through Fcγ receptors or complement receptors (Mayadas et al. 2014).

1.2.3.3 G protein-coupled receptors

Neutrophils express a variety of G protein– coupled receptors (GPCRs) with roles in host defense. GPCRS are able to distinguish bacterial product (e.g. formyl peptides) and endogenous molecules such as leukotrienes and chemokines (Rabiet et al. 2007; Manuscript 2013; Ba et al. 2011). These GPCRs can strongly activate the chemotactic migration of neutrophils. Nevertheless, some GPCR ligands, and in particular formyl-peptides, lipid mediators and C5a, can activate other neutrophil responses such as ROS production and degranulation (Mayadas et al. 2014; Futosi et al. 2013).

1.2.4 Neutrophils and the elimination of pathogens

Once a neutrophil meets the invading microbe, it can react in a variety of different ways. The three major antimicrobial functions are phagocytosis, degranulation and the generation of neutrophil extracellular traps (NETs) (Amulic et al. 2012).

1.2.4.1 Phagocytosis

Neutrophils use phagocytosis as a major mechanism in removing pathogens and cell debris. Prior to phagocytosis, invading microbes are recognized by neutrophils, either directly (PRRs/PAMPs) or via recognition of an opsonin by opsonic receptors (e.g. Fcγ receptors or complement receptors). Following recognition, the neutrophil membrane engulfs the microbe into a vacuole called the phagosome. This process involves membrane lipids, intracellular signalling cascades and cytoskeletal rearrangements. The primary and secondary granule will release their antimicrobial contents after fusing with the phagosome to make a phagolysosome. The process is very rapid, particularly in the presence of opsonins, and can be enhanced by pre-activation of the neutrophil (Kruger et al. 2015; Bardoel et al. 2014).

During phagocytosis, the NADPH oxidase is formed (Kruger et al. 2015). This will convert oxygen into oxidizing molecules called reactive oxygen species (ROS) such as superoxide, hydrogen peroxide and halic acids. Together with antimicrobial contents and ROS this will lead to efficient killing of microbes (Bardoel et al. 2014)

1.2.4.2 Neutrophil Granules and Degranulation

Neutrophil granules contents have potent antimicrobial activity (Borregaard 2010). Neutrophil granules are classified into three different subsets based on their enzyme content and function. Primary (azurophilic) granules contain potent hydrolytic enzymes like myeloperoxidase (MPO), which is essential for the oxidative burst, various antimicrobial peptides such as defensins and lysozyme. Secondary (specific) granules contain lactoferrin which is important for stopping bacteria growing and assisting in cell wall breakdown. Tertiary (gelatinase) granules are rich in matrix

metalloproteinases (MMPs) (Borregaard 2010; Mayadas et al. 2014). In addition to this, secretory vesicles are classified as a granule subset. Secretory vesicles are highly mobilisable and serve as a reservoir for plasma membrane receptors, such as those involved in neutrophil adhesion and chemotaxis (Mayadas et al. 2014; Amulic et al. 2012).

Upon activation, granules are mobilized and fuse with the phagosome during pathogen uptake. This results in the release of stored proteinases and antimicrobial peptides into the phagosome. In addition, granule fusion with the plasma membrane can cause extracellular release of contents into the local tissue environment (Amulic et al. 2012; Mayadas et al. 2014). Extracellular release of granules risks damage to host tissues. Contents of secretory vesicles and tertiary vesicles can be released following modest activation, whereas release of secondary and primary granule contents most often occurs through unintentional leakage of the phagosome. In addition, during transmigration tertiary and secondary granules may mobilize to degrade the collagen in the basement membrane, assisting neutrophil exit into the tissue interstitium (Mayadas et al. 2014).

At the site of inflammation, neutrophil granules aid in tissue remodelling and the killing and digestion of microorganisms, but also possible damage to the host if released inappropriately (Borregaard et al. 2007; Perobelli et al. 2015).

1.2.4.3 Neutrophil Extracellular Traps (NETs)

Upon stimulation, neutrophils can release neutrophil extracellular traps (NETs) in form of cell death known as NETosis. During NETosis, chromatin is processed, scattered with antimicrobial enzymes such as neutrophil elastase and MPO, and

released into the extracellular space in the form of NETs (Amulic et al. 2012; Mayadas et al. 2014; Bardoel et al. 2014). NETs are involved in antimicrobial function by exposing pathogens to highly concentrated antimicrobial peptides and enzymes, and by physical trapping of microbes within the chromatin. They can also activate other immune cells.

1.2.5 Effect of neutrophil activation on host tissues

Neutrophil are considered to be the front line of defense against invading microorganisms, however the defensive mechanisms of neutrophils that aid in pathogen killing can also be harmful to host tissues. Inappropriate neutrophil activation is sometimes observed in sterile injury such as autoimmune and other chronic inflammatory diseases (Figure 1) (Mayadas et al. 2014). However, targeting specific neutrophil functions remains therapeutically challenging (Mayadas et al. 2014).

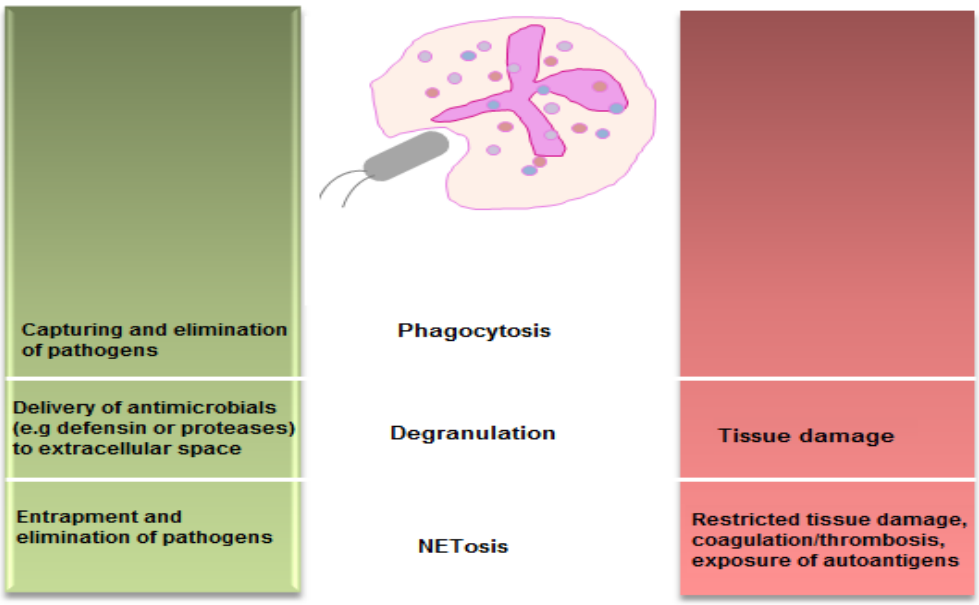

Figure 1: Neutrophil Activation: The Good and Bad Sides
(Green) indicate positive and (Red) indicate negative features related to neutrophils antimicrobial role which may affect the host. Picture adapted from (Bardoel et al. 2014)

1.3 Pathogen manipulation of neutrophil function

The primary role of neutrophils is host defense against pathogens, and they must be recruited in great numbers to the site of infection in order to provide the first line of defence to the host. Thus, the failure of neutrophils to infiltrate the site of infection, and deficiencies in activation, can lead to severe infections in the host. Here we provide one example of invading microorganism manipulation of neutrophils function;

A crucial defense system against *Staphylococcus aureus* is through neutrophil-mediated killing. However, this pathogen has developed many strategies to avoid killing at all levels including; i) extravasation ii) chemotaxis iii) priming and activation iv) opsonisation and phagocytosis, and v) NET Formation. The pathogen secretes a variety of molecules that resist neutrophil attack at the site of infection such as during extravasation neutrophil rolling on endothelial cells can be inhibited when staphylococcal superantigen-like 5 (SSL5) blocks PSGL-1 interaction with P-selectin and E-selectin on the neutrophil surface (Spaan et al. 2013). Another example, Liu *et al* have shown *Staphylococcus aureus*, produces a golden pigment (a virulence factor) with antioxidant properties and utilizes it to protect itself against ROS damage within the phagosome (Liu et al. 2005). In spite of the fact that *S. aureus* utilises multiple mechanisms to evade neutrophil responses, healthy people can still deal with this bacterium in an effective way.

1.4 Neutrophil Migration

To defend the host, neutrophils must migrate from the blood into the tissue through a multistep process, and then onwards through the tissue interstitium (Artemenko et al.

2011). During migration, the neutrophil activation state can be altered by extracellular signals which regulate the cytoskeleton, adhesiveness, shape and motility. These extracellular signals include; cytokines, chemokines, lipids, alarmins, formyl peptides, complement factors and adhesive ligands. From extracellular signal neutrophils will be able to translate the signals to intracellular signals that cause morphological changes and cell polarisation, resulting in migration (Lämmermann & Germain 2014).

1.4.1 Different types of migration

Environmental signals experienced by neutrophils are integrated and translated into a range of different morphological changes and migration modes. These include cytoskeletal activation, chemokinesis, chemotaxis, haptokinesis and haptotaxis (Figure 2).

Morphological shape changes without cell movement occur as a result of increased cytoskeletal activity in an homogeneous field of environmental signals. Chemotaxis and haptotaxis are directional, and occur along a soluble (chemotaxis) or substrate-bound (haptotaxis) gradients of chemoattractant. Different modes of haptotaxis exist, including migration on ECM-bound gradients, and on cell surface bound gradients. Meanwhile, chemokinesis and haptokinesis are non-directional. Chemokinesis (soluble), and haptokinesis (substrate-bound) occur in the presence of a uniformly applied stimulus (Tarabykina et al. 2000; Martin et al. 2015; Lyck & Enzmann 2015; Lämmermann & Germain 2014).

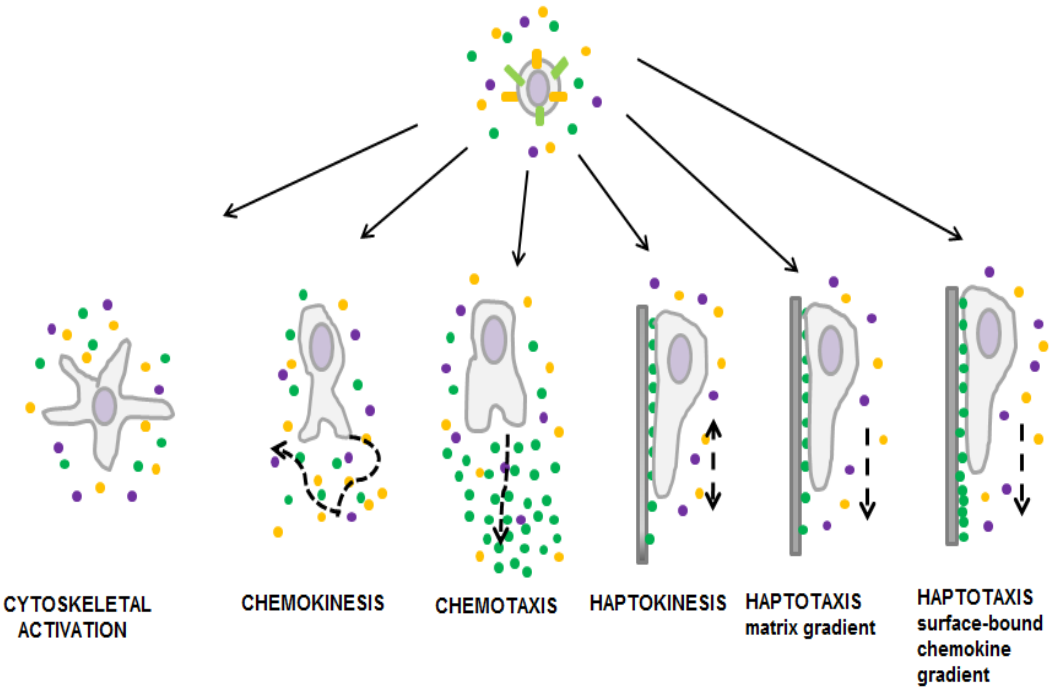

Figure 2: Changes in neutrophil shape, motility, and migration modes are induced by environmental signals
Neutrophils receive multiple signals from their surroundings, and then integrate them into intracellular signalling cascades to stimulate morphological changes and select different migration modes as above. Picture adapted from (Lämmermann & Germain 2014).

1.4.2 Methods for analysing neutrophil migration

A range of different migration assays have been developed and investigated by researchers over the years. They have been useful in unravelling the highly complex signalling pathways that contribute to different aspects of motility, such as two-dimensional (2D) and in three-dimensional (3D) migration. The combined effort of many researchers has led to improvements in *in vitro* models to produce more complex, physiologically relevant model environments for cells to migrate in (Artemenko et al. 2011). Elucidating the signalling pathways controlling neutrophil migration could lead to possible therapeutic approaches for treating conditions where neutrophils cause significant tissue damage and morbidity. There are many *in vitro*

2D and 3D models currently utilised to study cell migration, with those used in this thesis described below.

1.4.2.1 *In vitro* 2D models - Transwell Assay

Transwell assays are commonly used for analysing neutrophil chemotaxis. This assay is primarily used to study directed migration from the top compartment to the bottom compartment of a chamber, where a higher concentration of soluble chemoattractant has been applied to the bottom compartment (Nuzzi et al. 2007). The benefit of using this Transwell assay is the capability to perform multiple replicates, and to analyse the effect of various stimuli, inhibitors, or substrates on chemotaxis. However the results do not provide other evidence or details about the migration phenotype (Nuzzi et al. 2007), which need to be further analysed by other methods.

A basic transwell assay comprises two chambers separated by a microporous membrane (Figure 3a). Cells are placed in the upper chamber (Figure 3b) and allowed to migrate toward chemoattractants placed in the bottom chamber (Figure 3c) (Artemenko et al. 2011). Quantification of cells passing through the membrane can be done using MACS Quant Analyser, trypan blue exclusion, and image captured by microscope. Cells fluorescence can also be read using a fluorescent plate reader (Justus et al. 2014).

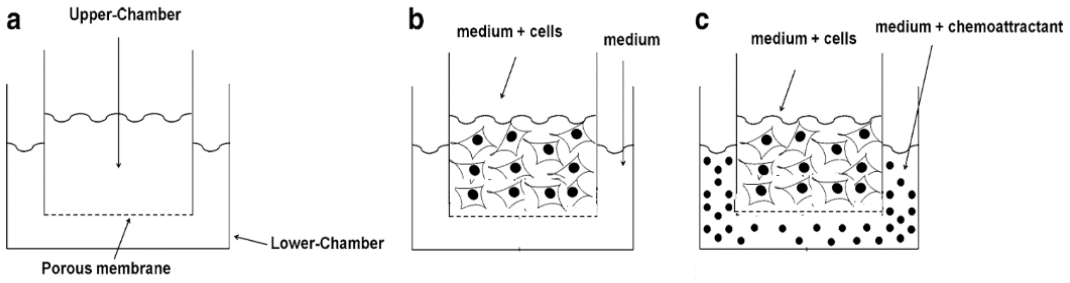

Figure 3: 2D Transwell® Assay
(a) Transwell® well have two different compartment; upper and lower which separated by a porous membrane (b) Cells are added onto upper compartment and lower compartment is filled with medium (with or without chemoattractant) (c) Cells are incubated for designated time to allow optimal migration. Once the incubation time for migration completed cells will collected and count (manually or using automation analyser such as MACS Quant Analyser)

1.4.2.2 *In vitro* 3D models

The majority of studies on neutrophil migration have used the 2D transwell assay described above, however one short coming of this 2D assay is that it does not closely relate to the reality of the environment encountered by neutrophils upon entering tissue. Better mimicking of the *in vivo* environment requires a 3D model where migrating cells can receive signals from the composition and structure of the tissue matrix. Furthermore in these models, migration in 2D has been identified as integrin dependent and migration 3D is integrin independent (Martin et al. 2015).

a) Transwell Invasion Assay

Transwell invasion assay can be modified to study cell migration in 3D environments. This can be done by overlaying a thin layer of specific extracellular matrix (ECM) components on the porous membrane before seeding the cells (Figure 4) (Artemenko et al. 2011; Justus et al. 2014). To move through a 3D matrix cells must modify their shape and interact with the ECM. In some cases, cells will squeeze through existing pores and channels in the matrix, while in other circumstances

active restructuring of the 3D environment by the migrating cell occurs. This is defined as invasion (Justus et al. 2014). Nowadays, commercially available inserts pre-coated with ECM are available. The assay is conducted as described in the previous section, but with longer timescales to allow the cells to traverse the 3D ECM. This assay has all the same advantages as the 2D assay, but is more representative of the *in vivo* environment.

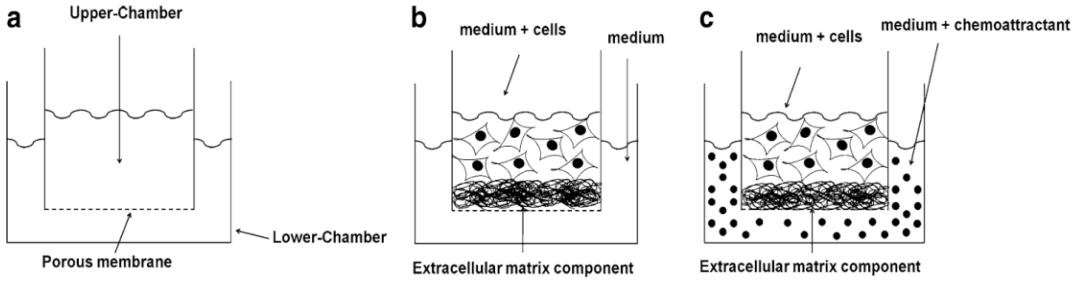

Figure 4: 3D Transwell® Assay
(a) Transwell® well have two different compartment; upper and lower which separated by membrane porous (b) Porous membrane is overlaid with collagen matrix and lower compartment filled with medium (with or without chemoattractant). Cells are added onto upper compartment and incubate for designated time to allow optimise migration. (c) After incubation the transmigrated cells have passed through the membrane. The upper chamber is removed. Migrated cells are visualised by microscopy and fixed and cell were counted using MACS Quant analyser.

b) 3D Chemotaxis using u-Slide Chemotaxis

The 3D transwell assay is a useful tool, but does not allow real-time visualisation of migrating cells, which may reveal important information about the mechanism of migration. A 3D migration assay developed by Ibidi addresses this shortfall. Neutrophils are embedded in a 3D collagen matrix in a central chamber, which is allowed to set before chemoattractant-free or chemoattractant containing medium is added to reservoirs on either side (Figure 5) (source https://ibidi.com/). The slides have cover glass bottoms, and three test samples can be observed concurrently in

each experiment. The slide chamber is sealed and placed onto a confocal microscope stage. Images are acquired every one minutes for several hours. The individual migration tracks of the cells can be analysed using software such as Fiji ImageJ manually or automatically. Using Chemotaxis Tool the information from the cell tracking for the parameter such as velocity, directionality, Euclidean distance and accumulated distance can be quantified statistically (Asano & Horn 2011). This assay allows heterogeneity in migration phenotypes to be more easily appreciated than in the transwell assay.

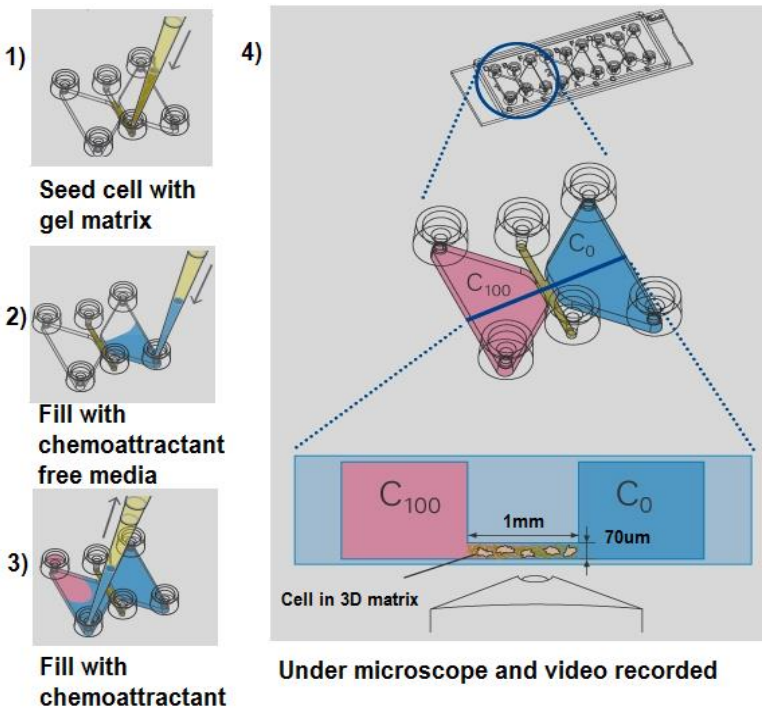

Figure 5: Schematic set up for 3D Chemotaxis using u-Slide Chemotaxis by ibidi®
The chamber was prepared as instructed in the manual from ibidi®. Three samples can be tested concurrently at one time. 1) Neutrophils were isolated and mixed with collagen. Samples were loaded into the chamber and allowed to solidify 2) Media without chemoattractant was added into the C_0 space and immediately before imagin, media with chemoattractant was added into C_{100} space. 4) Three positions of each sample were imaged. Cells were tracked using ImageJ-win64 from Fiji software. Image taken from https://ibidi.com/channel-slides/9--slide-chemotaxis-ibitreat.html.

1.4.3 Live cell imaging technique

While useful, extensive observations from 2D and 3D models still do not completely mimic the *in vivo* tissue environment, both structurally and in terms of the influence of interactions with other cell types. Thus to further improve our understanding of how cell migration is regulated in their native environment, live imaging technique in situ, such as by two photon laser scanning microscopy (TPLSM) is required (Dzhagalov et al. 2012). Commonly two techniques have been used to image cells *in situ,* which are post-mortem organ explant and intravital imaging in live anaesthetised mice. Two-photon imaging techniques using both methods have advantages and disadvantages (Sawtell 2015).

Tissue explant is performed by excision of the tissue of interest which is maintained in oxygen-perfused media during imaging. Tissues can be imaged whole (e.g. lymph nodes), or sliced with a vibratome to allow deeper imaging (e.g. thymus). The major advantage of this technique is that it allows imaging of tissue not easily accessible in a live animal, and avoids performing unnecessary procedures on living animals. However, using explant methods mean that blood and lymph circulation are interrupted which also may alter cell behaviour. Intravital imaging is superior in this regard, as tissues are imaged *in situ*, with intact blood and lymph perfusion, thus exact cell behaviour *in vivo* can be observed precisely. However, mice may experience surgical trauma and the use of anaesthetics during imaging may also interfere with imaging data. The data on motility of lymphocytes shows close agreement between the two methods (Dzhagalov et al. 2012).

The advantage of using TPLSM is that we are able to image deep into the tissue. Furthermore, this technique has the ability to visualize fibrillary collagen without

exogenous labelling, due to second harmonic generation (SHG). This offers extra visualisation of structural features of the tissue when investigating how cells move in 3D *in vivo*. The 4D images obtained by TPLSM can be analysed using software such as IMARIS for the quantification of migration parameters such as velocity and directionality (Sawtell 2015).

1.5 *Streptococcus pneumonaie*

1.5.1 Background

Streptococcus pneumoniae (commonly known as the pneumococcus) is a pathogenic extracellular, Gram-positive bacterium that colonises the mucosal surface of the human upper respiratory tract (Weiser et al. 2018). This microorganism lives in association with the human nasopharyngeal flora where it occurs asymptomatically as a commensal (Kadioglu et al. 2008). About 25% of the global population are estimated to be carriers (Paterson & Orihuela 2011). Under certain circumstances, the pneumococcus can spread into the lung, blood and brain and might lead to severe life-threatening disease such as pneumonia, sepsis and meningitis (Bogaert et al. 2004), particularly in situations when the host immune system is compromised (Kadioglu et al., 2008).

Encapsulated pneumococci are organised in pairs and can only be seen in a chain of varying lengths in blood cultures and liquid media (Alonso et al. 1995). Pneumococci are catalase-negative bacteria and facultative anaerobes, grouped as alpha-hemolytic due to the production of a green zone of hemolysis around colonies growing on blood agar plates (Obaro and Adegbola, 2002).

Pneumococci are a common cause of community-acquired pneumonia (CAP), which is accountable for a huge human disease and death toll in both economically developed and developing countries (Feldman & Anderson 2016). It is also the most common cause of hospitalisation and mortality in children in developing countries for pneumococcal septicemia (Kadioglu et al. 2008). While pneumococcal diseases may be tackled by the use of antibiotics, pneumococcal infections are associated with an unacceptably high rate of mortality and morbidity globally (Song et al. 2013) and may also lead to increasing risks of antibiotic resistance. In 2017, the pneumococcus was included by the WHO as one of the 12 priority pathogens causing continuous high burden disease and increasing rate of antibiotic resistance (Weiser et al. 2018).

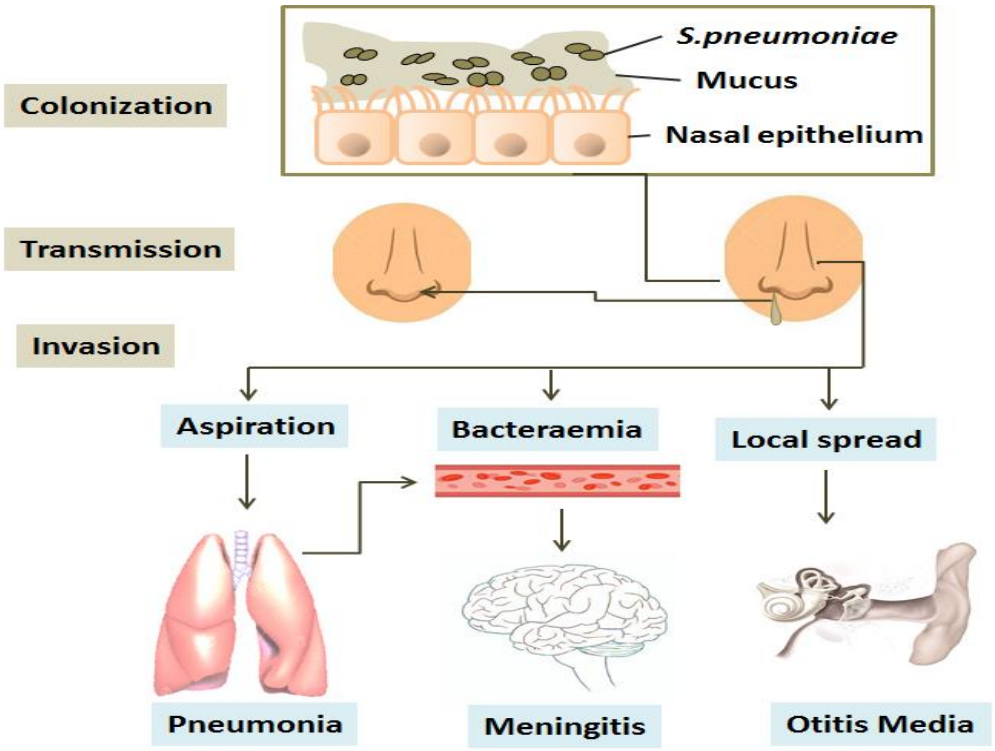

Figure 6: Life cycle of the pneumococcus and pathogenesis
Pneumococci colonise the mucosal surface of the upper respiratory tract (URT) and allows for the onset of disease and transmission from carriers to non-carriers. Carriers can shed pneumococci in their nasal discharge and allow transmission of the bacteria. The spreading can thru nasal epithelium, either by aspiration, bacteraemia or local spread, which further contribute to invasive diseases, such as pneumonia, meningitis and otitis media. Picture adapted from (Weiser et al. 2018)

1.5.2 Pneumococcal colonisation

Colonization of the nasopharynx is believed to be a prerequisite for the pneumococcus to develop into an infection. It lives in the upper respiratory track as a normal flora either entrapped in the nasal mucus, or attached to the surface of nasal epithelial cells. Pneumococcal transmission is believed to occur from one individual to another through droplets or aerosols. Invasion of the lower respiratory tract takes place when the pathogen gains entry into peripheral tissues either by local spread or aspiration, leading to mild diseases such as otitis media or life-threatening condition , such as bacteremia, pneumonia and meningitis (Figure 6) (Bogaert et al. 2004; Weiser et al. 2018).

Koppe *et al.* suggested that two overlapping scenarios needed to take place to result in invasive pneumococcal disease (IPD). Firstly, when the immunity of the host are not properly established this will likely favour colonisation by the bacteria (Koppe et al. 2012). Secondly, a breach needs to occur within the natural defense barriers or host immune balance present in the mucosal system (Koedel et al. 2002)

1.5.3 Pneumococcal disease

In 2000, the WHO reported that more than 800,000 deaths in children under 5 years of age and around 14.5 million cases were due to severe pneumococcal disease (Grant et al. 2003). Meanwhile, disease such as otitis media and sinusitis have also become prominent cases (Bogaert et al. 2004). Young children are the age group with the highest incidence rate of pneumococcal disease, however, the elderly and any other age group can also be affected (Obaro & Adegbola 2002).

Based on previous studies, the occurrence of IPD can be affected by a number of variables such as season, serotype, age, geographical location, and vaccination status of the population (Torres & Cilloniz 2014). Currently 98 serotypes have been described on the basis of their polysaccharide capsule (Weiser et al. 2018) and some of these serotypes are associated with colonisation in nasopharynx (Koppe et al. 2012).

A significant morbidity and mortality was reported in areas of Asia-Pacific where the highest incidence of pneumococcal diseases is found among young indigenous children with incidence rates ranging between 100-200 cases/100,000 children aged less than 2 years. Meanwhile, around 1500 cases/100,000 children aged <5 years were reported in India (Torres & Cilloniz 2014). Around 450 million people per year were affected by pneumococcal pneumonia (Rudan et al. 2008) associated with a high case fatality rate (15% of hospitalized patients) and a high incidence (Torres & Cilloniz 2014). In the UK, *S. pneumoniae* was reported to be amongst the most common cause of bacterial meningitis, after *Neisseria meningitidis,* in the very young children (Randle et al. 2011).

1.5.4 Pneumococcal virulence factors

The pneumococcus has a number of virulence factors which promote the success of colonisation and allow it to spread from the upper to the lower tract respiratory tract. It requires extensive and complex interactions between the pneumococcus and the nasopharyngeal microbiota (Weiser et al. 2018). The capsule is the major virulence factor, and contributes to resistance to phagocytosis, binding of immune complement (Weiser et al. 2018), and is important for the entrapment in neutrophil extracellular

traps (Koppe et al. 2012). The other major virulence factor is pneumolysin (PLY), which is a toxin capable of forming large pores into mammalian cell membranes and is essential to the mechanisms of pneumococcal infection (Koppe et al. 2012; Mitchell & Mitchell 2010). The pneumococcus has many virulence factors and the major ones are shown in Table 1 and on schematic diagram Figure 7.

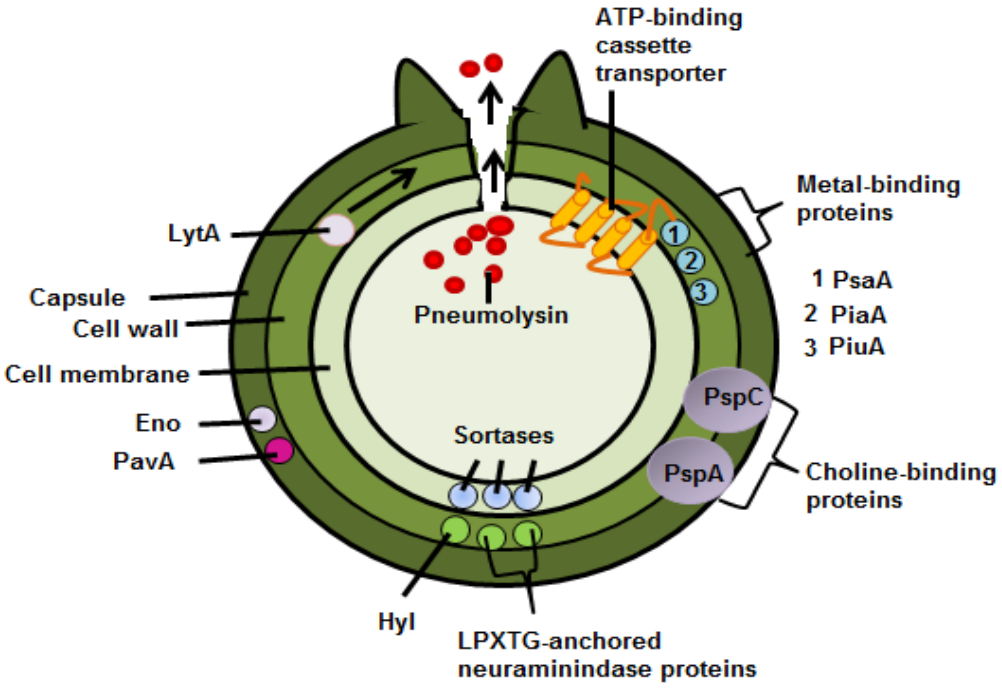

Figure 7: Schematic diagram of virulence factors of *S.pneumoniae*
Virulence factors on the pneumococcus compromise the capsule, cell wall, choline-binding pneumococcal surface proteins A and C, LPXTG-anchored neuraminidase, Hyl, Ply, Sortases, Eno, PavA and Lyt A. Picture adapted from (Kadioglu et al. 2008).

Table 1: Some of Penumococcal virulence factor and their functions

CBP, choline-binding protein; CPS, capsular polysaccharide; Fe, iron; iC3b, inactive C3b; LPXTG, sortase-anchored surface protein; MAPK, mitogen-activated protein kinase; Mn, Manganase; Ply, pneumolysin; PspA, pneumococcal surface protein. Part of the table taken from (Weiser et al. 2018).

Virulence Factor	Description	Function in pathogenesis
CPS	• Major surface antigen • 98 structurally distinct serotypes	• Prevent entrapment by mucus during colonization • Inhibits opsonophagocytosis by preventing the interaction of iC3b and the Fc fragment of IgG bound to deeper bacterial surface structures with receptors on phagocytic cells
Ply	• Pore-froming toxin • TLR4 ligand	• Cytotoxic and pro-apoptotic for a wide variety of host cells • Activates classical complement pathway and depletes serum opsonic activity • Highly pro-inflammatory at sub-lytic levels • Activates TLR4, NLRP3 inflammasome and p38-MAPK pathways
PspA	• CBP	• Limits C3 deposition on pneumococcal surface • Protects against bactericidal effects of free lactoferrin
CbpA (or PspC)	• CBP	• Binds C3 and factor H and limits C3b deposition on pneumococcal surface • Binds PIGR and laminin receptors through separate domains • Facilitates adherence and invasion respiratory epithelium and blood-brain barrier
LytA	• CBO • Autolysin	• Digest cell wall • Releases Ply and pro-inflammatory cell wall fragments • Mediates capsule shedding during cellular invasion
NanA	• Neuraminidase A • LPXTG	• Cleaves terminal sialic acid from host mucin and cell surface glycoconjugates • Unmasks receptors for adhesins • Important role in otitis media • Triggers TCF-B signalling to facilitate endothelial invasion
Hyl	• Hyaluronate lyase • LPXTG	• Degrades extracellular matrix • Facilitates tissue penetration
PsaA	• Lipoprotein • Solute-binding components of a single Mn-specific • ABC transporter	• Mn uptake in host environment • Essential for pneumococcal resistance to oxidative stress in vivo
PiuA, PiA and PitA	• Lipoprotein • Solute-binding components of iron-specific ABC transporter	• Fe acquisition in vivo
PavA and PavB	• Fibronection-binding protein • NCSP	• Adhere to host surface • Important during sepsis and meningitis
Eno	• Enolase • NCSP	• Binds and activates plasminogen • Facilitates tissue invasion

1.5.5 Pneumolysin

More than 100 years have passed from the first report that pneumococci make a hemolysin (Libman 1905). Pneumolysin (PLY) is a thiol-activated cytolysin and membrane-damaging toxin synthesized by *S.pneumoniae*. It plays a multifunctional role as a pneumococcal virulence factor during infection by using pore forming activity and complement activation. It consists of a single 53-kDa protein, comprised of 471 amino acid and is produced by all clinical isolates of the pathogen (Paton et al. 1993).

1.5.5.1 PLY structure and pore forming activity

The molecular model of PLY is long and rod-shaped with overall dimensions of 11nm x 35nm x 33nm and is composed of four domains (Figure 8) (Rossjohn et al. 1998). The N-terminal part of this molecule forms the domains 1-3, while the C-terminal end forms domain 4 (residue 360-469). Domain-4 was identified to be critical in the membrane-binding and pore formation ability of PLY (Tilley et al. 2005) and contains the undecapeptide sequence largely conserved in cholesterol dependent cytolysin (CDC) family (Anderluh & Gilbert 2014).

Upon activation, the lytic pore formation is formed when PLY monomers assemble into a circle after undergoing conformational changes, and then oligomerizes into a pore to penetrate the membrane of the cells (Tilley et al. 2005; Förtsch 2012). This formation of lytic action enable it to lyse membranes containing cholesterol that present in all eukaryotic cells (Cockeran, Anderson, et al. 2002). The diameter of the pore is 260 Å and is comprised of about 40 monomer subunits (Kadioglu et al. 2008).

PLY is known to have various biological activities, with distinct cytolytic and complement-activating activities effects that interfere with the cell function (Rijneveld et al. 2002). For example, studies by Jounblat *et al.* have shown that PLY's cytolytic and complement activities are involved in the inflammation and cellular influx in pneumonia, in the accumulation of T cells by complement-activating activity, and in the neutrophil recruitment into the lung tissue (Jounblat et al. 2003).

At relatively higher concentrations, PLY will cause widespread direct cellular and tissue damage as a result of its membrane pore forming properties causing lysis of the cell (Neill et al. 2015; Kadioglu et al. 2008). Meanwhile, at sub-lytic concentrations, the toxin can have a noticeable range of effects such as pro-inflammatory activation of neutrophils and macrophages (Cockeran, Anderson, et al. 2002) and eukaryotic cell signalling (Neill et al. 2015).

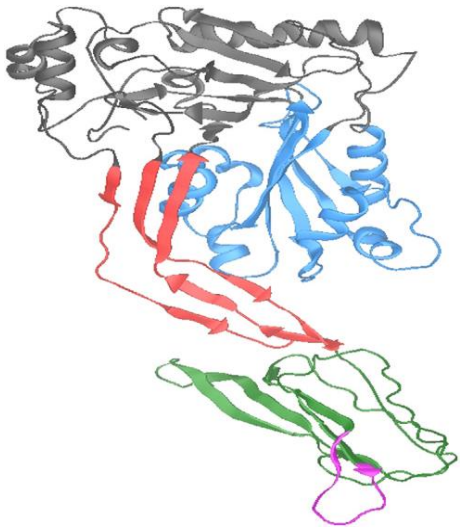

Figure 8: Structural Model of the Bacterial Toxin Pneumolysin
Pneumolysin (PLY) has four domains: domain 1 (in blue), domain 2 (in grey), domain 3 (in red), and domain 4 (in green). The N-terminal part of this molecule form domains 1-3 and the C-terminal end forms domain 4(residue 360-469). In pink is highlighted the undecapeptide conserved sequence characteristic of the cholesterol dependent cytolysin (CDC) family (Neill et al. 2015).

1.5.5.2 Effect of PLY on neutrophil function

Several pieces of evidence showed that PLY is capable of a range of effects on neutrophil activities. At sub-lytic concentration, PLY was shown to inhibit chemotaxis and random migration of polymorphonuclear leukocytes (PMNL) and also blocks respiratory burst (Paton & Ferrante 1983). Earlier studies have shown that PLY can activate human serum in a dose-dependent manner, and this toxin can act as chemoattractant for neutrophils and they also showed that PLY enhances neutrophil chemotaxis and secretion of lysosomal enzyme (Johnson et al. 1981).

Studies by Cockeran *et al.* showed that PLY can potentiate neutrophils pro-inflammatory activities resulting in Ca^{2+} influx and altering membrane potential. Treatment of human neutrophils with PLY showed an increased production of superoxide, release of elastase, upregulation of CD11b/CD18 expression, and increased activity of phospholipase A_2 (PLA_2) after subsequent exposure to FMLP (Cockeran, Theron, et al. 2001). Subsequent studies by the same authors also showed PLY increased production of prostaglandin E_2 and leukotriene B_4 by human neutrophils (Cockeran, Steel, et al. 2001), activates the synthesis and release of interleukin-8 (Cockeran, Durandt, et al. 2002) and also induce release of matrix metalloproteinase-8 and 9 (Cockeran et al. 2009).

Neutrophil recruitment mediated by PLY has been shown to involve MIP-2 and IL-6 (Rijneveld et al. 2002). Similarly, other studies showed PLY-induced neutrophil chemotaxis required a complex interaction between the pathogen and the host (Moreland & Bailey 2006). The release of sub-lytic concentrations of PLY by autolyzed pneumococci induces the activation of NADPH oxidase, and generation of reactive oxygen species (ROS). However, ROS is released into vesicular

compartments that lack microbes, which likely result in the deterioration and death of neutrophils and assist pneumococci to avoid phagocytic defence (Martner et al. 2008).

PLY can also induce K^+ efflux which mediates NLRP3/ASC inflammasome and caspase-1 activation for the secretion of IL-1β by neutrophils. This study has shown IL-1β is essential in bacterial clearance (Karmakar et al. 2015). Currently studies showed that PLY stimulates vital NETosis in human neutrophils, where this toxin was found to activate NET formation *in vitro*. Studies have shown that PLY has potential to induce NETs which is good for the host defence but on the other side might also induce the severity of the disease by damaging host tissues (Nel et al. 2016).

1.5.5.3 Effect of PLY on cell types other than neutrophils

Beside neutrophils, previous studies have also analysed PLY interaction on other immune cells. PLY was found to lyse platelets and activate serum to act as a chemoattractant (Johnson et al. 1981). Highly purified pneumolysin (at a concentration of 10ug/ml) was found to activate human complement *in vitro* (Paton et al. 1984).

Earlier studies by Rubins *et al.* showed that during experimental pneumonia, PLY facilitates intra alveolar replication, penetration into the interstitium of the lung and dissemination of pneumococci into the blood stream (Rubins et al. 1995).

At sub-lytic concentrations, PLY was found to stimulate the production of pro-inflammatory cytokines such as interleuking-1β (IL-1β) and tumor necrosis factor-α (TNF-α) produced by human mononuclear phagocyte monocytes (Houldsworth et al.

1994). Meanwhile, at the same concentration calcium-dependent pores and osmotic stress was induced by PLY in epithelial cells by activation of p38 mitogen-activated protein kinase (MAPK) signalling (Ratner et al. 2006). Other studies using sub-lytic concentrations have shown that PLY leads to formation of micro-pores in the plasma membrane, activation of rac1 and rhoA GTPases, and the formation of actin stress fibres in neuroblastoma cells (Iliev et al. 2007), inducing cytoskeletal rearrangements within the target cell involved in migration (Marriott et al. 2008).

Maus *et al.* showed in their studies that, in response to PLY challenge, macrophages phosphoinositide 3-kinase (PI3K)-γ was activated and necessary for the recruitment of inflammatory macrophages to the site of infection (Maus et al. 2007). Studies on human pharyngeal and bronchial epithelial cells *in vitro* has shown pro-inflammatory cytokines such as interleukin-6 and -8 release occurred upon stimulation with PLY(Küng et al. 2014).

1.6 General aims of the thesis

My research project has three main aims. The first aim (Chapter 3) was to determine whether *Streptococcus pneumoniae* and its toxin, pneumolysin (PLY), can inhibit neutrophil chemotaxis using two- and three-dimensional assays. The second aim (Chapter 4) was to elucidate the molecular mechanism through which PLY alters neutrophil migration and function. Following on from the work described in Chapters 3 and 4, the third aim (Chapter 5) was targeted at the global proteomic analysis of PLY-stimulated neutrophils, with the expectation that novel information would be discovered on the protein networks involved in PLY and its effect on neutrophil chemotaxis.

Chapter 2: Material and Methods

2.1 Use of mice for tissue harvest and *S. pneumoniae* infection models

2.1.1 Mice

In this study, female C57BL/6J mice (for *in vitro* study), aged 7- 12 weeks and female CD1 (for *in vivo* study), aged 7- 10 weeks, were used in accordance with project licenses granted under the Animals (Scientific Procedures) Act 1986, and approved by the University of Liverpool Animal Ethics Committee. Mice were culled by increasing CO_2 followed by cervical dislocation. Tissues were harvested into ice cold media, as described in 2.2.

2.1.2 Intranasal infection with *S. pneumoniae*

Murine infection models were performed by Dr Laura Jacques from Aras Kadioglu's Group. Briefly, CD1 (Female) mice (7-10 weeks) were infected intranasally with 50µL of 10^6 CFU of D39 bacteria strain whilst anaesthetized with 2.5% v/v Isofluorane over oxygen (1.4-1.6 litres/min) to induce pneumococcal pneumonia. After 24 hours, tissues (blood, lung and lymph nodes) from pneumococcal-infected and PBS-infected control mice were collected. Experiments were repeated three times and all work was carried out in the Biomedical Services Unit, University of Liverpool. Collected organs (blood, lung and mediastinal lymph nodes) were kept in 3mL of sterile PBS and put on ice. Bloods were collected by cardiac puncture and placed in heparin (5µL heparin/1mL blood) tubes before transportation to CIMI Laboratory for further experiment. Tissues and blood were prepared before analyses

on flow cytometry and 20μL was taken from homogenised tissue and blood for bacterial load (CFU) using the Miles and Misra method in Section 2.4.7.

2.2 Processing of Mouse Tissues

2.2.1 Isolation of Neutrophils from Bone Marrow

Following Schedule 1 cull, femurs and tibias of C57BL/6J mice were removed, excess tissue trimmed, and stored in media (RPMI-1640, 25mM HEPES, 10%FCS) on ice until ready to use.

Bone surfaces were sterilised by serially passing through four 60mm dishes containing 70% EtOH, then three containing ice-cold sterile PBS. Bones were finally transferred to a dish containing media (RPMI-1640, 25mM HEPES, 10%FCS). The bone marrow was exposed by cutting off the ends of the bones, and flushed out using a 25G needle into a new dish.

The clumps of marrow were dispersed by carefully pipetting using a P1000 pipette. A 70μm cell strainer was used to filter the cell suspension before transfer into a 50mL conical tube. Media (RPMI-1640, 25mM HEPES, 10%FCS, 2mM EDTA) was added to the cell suspension, and centrifuged for 7 minutes at 1400rpm.

The supernatant was discarded, and the cell pellet resuspended in 5mL of filtered Red Blood Cell Lysis (1xRBC Lysis Buffer, Ebioscience) for 4-5 minutes. Media (RPMI-1640, 25mM HEPES, 2%FCS) was added into the sample tube after the incubation and centrifuged for 7 minutes at 1400 rpm. The bone marrow sample was washed twice more with media before the cells were ready for neutrophil isolation.

Some of the bone marrow cells were kept aside for comparison of neutrophil purity.

Three protocols were trialled or optimised in order to obtain neutrophils of consistently high purity:

2.2.1a Percoll Density Gradient

The bone marrow pellet was resuspended in 5mL media (RPMI-1640, 25mM HEPES, 2%FCS). Then, 5mL of 62.5% Percoll (GE Healthcare) was carefully layered underneath the cell suspension and centrifuged at 2300 rpm for 30 minutes at medium acceleration and brakes off.

After centrifuging the cloudy interface (containing immature cells and non-granulocytes) at the 5mL 62.5% Percoll level was removed, and the last 3mL of Percoll retained (containing a loose pellet of neutrophils).

The cells were transferred into a fresh 15mL tube and washed twice with media at 1500rpm for 5 minutes. Lastly, the pellet was re-suspended in 1mL media and quantified using trypan blue to determine yield and viability.

2.2.1b Histopaque Density Gradient

The bone marrow pellet was resuspended in 1mL media (RPMI-1640, 25mM HEPES, 2%FCS). 3mL of Histopaque 1119 (density, 1.119 g/mL, Sigma) was added into the 15mL conical tube. Next, 3mL of Histopaque 1077 (density, 1.077 g/mL, Sigma) was carefully overlayed on top of the Histopaque 1119. Later the bone marrow cell suspension was overlayed on top of Histopaque 1077. The cells were centrifuged at 2000 rpm for 30 minutes, 25°C, medium acceleration and brakes off. After centrifugation, the neutrophils at the interface of the Histopaque 1119 and Histopaque 1077 layers were collected.

The collected neutrophils were washed twice with media and centrifuged at 1400 rpm for 7 minutes at 4°C. Lastly, the pellet was re-suspended into 1mL media and quantified using trypan blue to determine yield and viability.

2.2.1c MACS Neutrophil Isolation Kit (Miltenyi Biotech)

The bone marrow pellet was resuspended in 200µL of media (RPMI-1640, 25mM HEPES, 2%FCS) per 5×10^7 total cells and 50µL of neutrophil negative selection biotinylated antibody cocktail (Miltenyi) was added. After incubating for 10 minutes at 2−8 °C, 5-10 mL of media per 5×10^7 cells was added for washing and centrifuged at 300×g for 10 minutes. The supernatant was completely aspirated.

The cell pellet were re-suspended in 400µL media and 100µL of anti-biotin MicroBeads per 5×10^7 total cells, and were mixed well before incubating for 15 minutes in the refrigerator (2−8°C). After incubation, 5-10 mL of media per 5×10^7 cells were added for washing and centrifuged at 300×g for 10 minutes. The supernatant was completely aspirated. The pellet was re-suspended in 500µL of media before magnetic separation using an LS Column.

Cell suspensions were applied to an LS Column and unlabelled (representing the enriched neutrophils) cells which passed through the column were collected. The column was washed three times with 3mL media to ensure unlabelled cells were flushed through. The entire unlabelled cell fraction was centrifuged at 1400 rpm for 7 minutes. Lastly, the pellet was re-suspended in 1mL media and quantified using trypan blue to determine yield and viability.

2.2.2 Preparation of mouse lung cells

Lung tissue was harvested, weighed, placed into a petri dish and then cut into smaller pieces using small scissors and placed into 2.5mL of media (RPMI-1640, 25mM HEPES, 2%FCS) containing 1mg/mL Collagenase D (to help release of immune cells through enzymatic digestion) and 200µg/mL of DNase I was added. Samples were incubated at 37°C for 30 minutes in the water bath. After incubation, the contents of each tube were filtered through 70µm cell strainer into a 50mL centrifuge tube.

The lung pieces were mashed using the plunger of a 3mL syringe and all remaining cells through the filter were rinsed using 5mL media. 200µL of each sample was taken for CFU count. Single cell suspensions were centrifuged at 1500 rpm for 5 minutes at room temperature. After centrifugation, supernatants were discarded and 2mL of Red cell lysis buffer was added to the pellet. Samples were mixed well and incubated for 2 minutes at room temperature. Immediately afterwards, 5mL of media was added into each tube to restore the osmotic balance for the cells. Samples were centrifuged at 1500rpm for 5 minutes at room temperature and supernatant removed before re-suspended in 1mL media and placing on ice before staining for flow cytometry.

2.2.3 Preparation of mouse blood

Blood was collected by cardiac puncture on mice under terminal anaesthesia into Eppendorf tube containing heparin (5µL heparin/1mL blood). 20µL of blood from each Eppendorf tube was taken for CFU count by Miles and Misra method. All remaining cells were transferred into 50mL tubes, and 5mL of media (RPMI-1640, 25mM HEPES, 2%FCS) added into each tube. Cell suspensions were centrifuged for

5 minutes, at 1500 rpm, at room temperature. Supernatants were discarded and 2mL of Red cell buffer lysis were added to lyse red blood cells. Samples were mixed well and incubated for 2 minutes at room temperature. Immediately afterwards, 5mL of media was added into each tube to restore the osmotic balance for the cells. Samples were centrifuged at 1500rpm for 5 minutes at room temperature and supernatant removed before re-suspended in 1mL media and placing on ice before staining for flow cytometry.

2.2.4 Preparation of mediastinal Lymph nodes (mLN)

Each of mLN tissue was filtered through 70μm cell strainer (to eliminate clumps and debris) into labelled 50mL centrifuge tube. The MLN pieces were mashed using the plunger of a 3mL syringe and all remaining cells through the filter were rinsed using 5mL media. Samples were centrifuged at 1500 rpm for 5 minutes at room temperature and supernatant removed before re-suspended in 1mL media and kept on ice before staining for flow cytometry.

2.2.5 Preparation of living inguinal lymph node (iLN) slices for *ex vivo* analysis of neutrophil migration

Inguinal lymph nodes (iLN) were harvested from C57Bl/6J mice and kept on ice cold PBS. iLNs were carefully dissected to remove all connective tissues/fat and briefly dried before embedding in low melting point agarose (4% in PBS, Thermo Fisher) in Peel-A-Way embedding molds (Sigma). The molds were then put on ice for 5-10 minutes to allow the agarose to solidify.

The solidified agarose blocks were trimmed to make 1.5cm^2 blocks before mounting on a Vibratome (Ci Campden Intrument Ltd). 400μm slices were cut at amplitude 1.5mm, frequency 90Hz, advance speed 0.11mm/s.

Neutrophils were isolated as described in Section 2.2.1c, and labelled with CFSE dye. Briefly, cells were re-suspended in 5mM CFSE (Thermo Fisher) in PBS and incubated at 37°C in the water bath for 7 minutes. At the end of the incubation, neutrophils were washed twice in PBS+2%FCS (5 minutes, 1500rpm). Neutrophils ($2.5x10^6$cells/25μL) were then applied to iLN slices cultured at the air-liquid interface on transwell supports, and incubated at 37°C in CO_2 incubator for at least 2 hours before imaging.

iLN slices were imaged using the Zeiss LSM 880MP in the Centre for Cell Imaging (CCI), University of Liverpool, with the assistance of Dr. Laetitia Petit-Jentreau.

Prior to imaging, iLN slices were washed to remove neutrophils remaining on the surface of the tissue (DME, 1000mg/L glucose, sodium bicarbonate, without L-glutamine and phenol red) before being glued to cover glass. The cover glass was then put in the imaging chamber securely by spreading vacuum grease on the bottom. The sample was continuously perfused with oxygenated media, with or without added PLY. 15 minutes movies were recorded using the z-stack and time series functions in Zen Black (Zeiss). 50μm stacks were acquired at 2μm intervals, every minute. A W Plan-Apochromat 40x/1.0DIC objective was used, with filters combination of bandpass filter (emission filters) at 525nm and dichroic filters at 490nm (excitation filters). Cells were tracked using IMARIS (Bitplane version 7.7.1) software using spot tracking tool. Set up experiment as Figure 9.

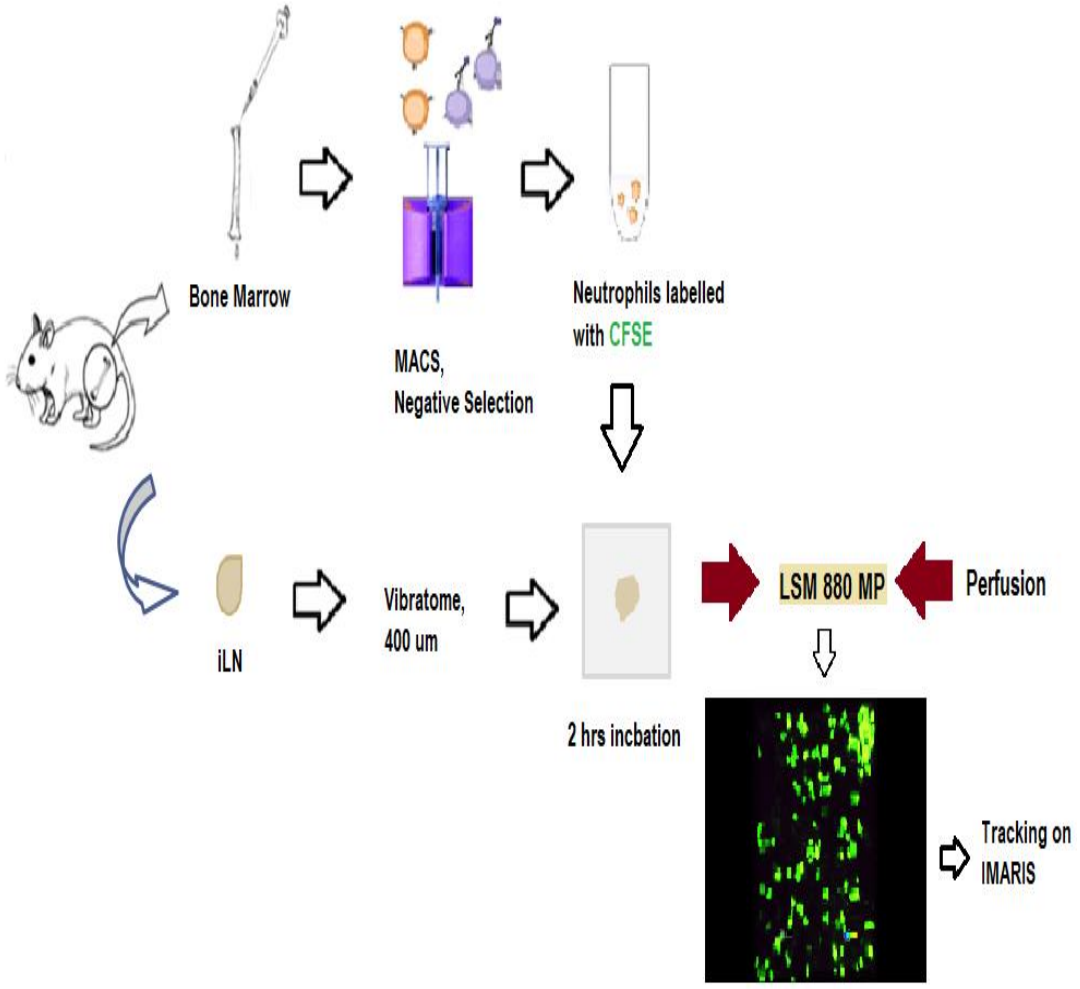

Figure 9: Schematic set up for *ex-vivo* experiment
Bone marrow and iLN were harvested. Neutrophils were isolated using MACS negative selection and labelled with CFSE dye. Vibratome-cut iLN slices were prepared and overlaid with labelled neutrophils. Sliced were incubated for 2 hours to allow neutrophils to migrate into the tissue. Live imaging was performed using Zeiss LSM 880MP microscope and cell migration analysed using IMARIS (Bitplane version 7.7.1).

2.3 Flow cytometry Analysis

Table 2: List of antibodies used for flow cytometric analysis

Marker	Label	Target	Isotypes	Dilution
	Fixable Viability dye (eFluor 450)	Live and Dead	-	1:1000
Anti-CD16/32, mouse /monoclonal		Fc Block		1:500
Anti Ly6G Clone :1A8	FITC	Neutrophils	Mouse IgG2aK FITC Clone :eBM2a	1:200
CD11b (αM) Clone:M1/70	APCeF780	Granulocytes, Monocytes, Neutrophils, NK, DCs, T cell, B cell, Macrophages	Rat IgG2b K APC-eFluor 780 Clone:eB149/10N 5	1:200
CD45 Clone:30-F11	eFluor 450	Pan-leukocyte	Rat/IgG2b, k Clone:eB149/10H 5	
CD45R(220) Clone:RA3-6B2	PeCy7	B cell	-	1:200
CD3e Clone:145-2C11	APC	T cell	-	1:200
CD18 (β2) Clone:M18/2	Biotin	Adhesion, Cell Signalling	IgG2a K Biotin Clone :eBR2a	1:200
	Streptavidin (PE)	Binding to biotin		1:400
CD18(β2)	PE (MACS)	Adhesion, Cell Signalling	Rat IgG2a K PE Clone:eBR2a	1:200
CD29(β1) Clone: eBioHMb1-1	PercP710	Cell Adhesion	Armenian Hamster/IgG PercP-eFluor 710	1:200
CD49b(α2) Clone :DX5	PE	Cell Adhesion / Collagen	Rat IgM PE	1:200
CD49b (α2) Clone:DX5	APC	Cell Adhesion/ Collagen	Rat IgM APC	1:200
CD49d(α4) Clone:R-2	PercP710	Cell Adhesion / Fibronectin	Rat IgG2b K Percp-eFluor710 Clone:RTK4530 Biolegend	1:200
CD49d(α4)	PE/Cy7	Cell Adhesion /Fibronectin	PE/Cy7 Rat IgG2b, k	1:200

2.3.1 Determination of Neutrophil Purity and Integrin Expression

Approximately $1x10^5$cells of whole marrow or isolated neutrophils were plated in a 96 well U-bottom plate for staining. The plate was centrifuged at 1500 rpm for 5 minutes and the supernatants were removed.

2.3.2 Live and dead staining

Live and dead stain (violet LIVE/DEAD dye, Ebioscience) was prepared by diluting 1μL dye in 1mL PBS (no protein). 100μL of LIVE/DEAD dye was used to re-suspend cell pellets, and incubated for 30 minutes at 4°C. After incubation, cells were washed twice in 100μL of media (RPMI-1640, 25mM HEPES, 2%FCS) for 5 minutes at 1500 rpm. Cells were re-suspended in 200μL PBS (with 2%FCS) for flow cytometry, or further stained with specific antibodies.

2.3.3 Fc-block and specific antibody staining

Cells were incubated with Fc Block (anti-CD16/32, mouse/monoclonal, Ebioscience) for 15 minutes at 4°C. After incubation, cocktails of specific antibodies (Table 2) were added, and the cells incubated for a further 30 minutes. 100μL of PBS (with 2%FCS) was topped up into each well after the incubation and plate was centrifuged for 5 minutes at 1500 rpm. Where biotinylated antibodies were used, further 30 minutes incubation with Streptavidin conjugates was performed. After washing in PBS (with 2%FCS) for 5 minutes at 1500rpm, cells were re-suspended with 200μL PBS (with 2%FCS), ready for flow cytometry.

2.3.4 Flow cytometry analysis

Flow cytometric analysis was performed using a MACS Quant analyser (Miltenyi®) version 2.11. Unstained and single stained samples were used to set voltages and perform compensation. Isotype and fluorescence minus one control (FMO) were used to determine gates.

2.4 Preparation of bacterial stocks

2.4.1 Growth Media

Standard growth media Blood agar base(BAB) and Brain heart infusion (BHI) were used during my PhD study as described in Tabel 3.

Table 3: Standard media used during PhD

Medium	Procedure
A. Blood agar base (BAB) (Sigma)	16g in 400mL dH2O
B. Brain heart infusion (BHI) (Sigma)	14.8g in 400mL dH2O

2.4.2 Blood agar base (BAB) culture plates

16 grams of (A) was added to 400mL of dH2O, then autoclaved for 30 minutes at 15psi (103kPA). Next, 20mL of sterile debrinated horse blood (Sigma) was added after the media has been cooled to approximately 56^{o}C before pouring into sterile petri dishes (90mm). Plates were left to dry and stored at 4^{o}C.

2.4.3 Blood agar base (BAB) culture plates with gentamicin (used in all murine *in vivo* experiments)

Preparation as above (2.4.2) but with addition of 2ug/mL of gentamicin (Sigma), which was added with 20mL of horse blood to 400mL of autoclaved BAB culture medium and gently mixed.

2.4.4 Brain heart infusion (BHI) broth

14.8 grams of (B) was added to 400mL of dH2O, then autoclaved for 30 minutes at 15psi (103kPA). Medium was stored at room temperature for up to 4 weeks.

2.4.5 BHI Serum broth

Preparation as above (2.4.4) with small alteration. To make up 80% v/v BHI broth and 20% v/v Foetal Bovine Serum (FBS), 20mL of FBS was added to 80mL of medium in (2.4.4). The BHI serum broth was prepared fresh for each use.

2.4.6 Preparing stocks of pneumococci

All bacterial stocks underwent a confirmation test to distinguish pneumococcus isolates from other bacteria species. These tests included: Gram stain, optochin (Ethylhydrocupreine hydrochloride) sensitivity, haemolytic test on blood agar plates and catalase tests. These were provided by a member of Aras's Kadioglu group.

To prepare pneumococcal stocks, laboratory bacterial bead collections of pneumococci were streaked onto blood agar base plates supplements with 5% v/v sterile defibrinated horse blood under sterile conditions and incubated invertedly at 37^{o}C 5% CO_2 overnight in a sealed jar. An optochin antibiotic disk (Oxiod) was also placed on the same plate to confirm pneumococci are present and no contamination has occurred.

After overnight growth on BAB plates, a sweep pneumococci was transferred from the plate and inoculated into 10mL sterile BHI broth. The inoculated broth was incubated overnight for 16-18 hours at 37^{o}C. The following day, cultured tubes were centrifuged at 3000 rpm for 15 minutes to pellet the bacteria so supernatants could be

discarded. Bacterial pellets were then resuspended in 1mL BHI serum borth (80% v/v BHI broth and 20% v/v Foetal Bovine Serum (FBS, Sigma). Into 10mL fresh BHI serum broth, 700µL of re-suspended bacterial pellet was added to make stock tubes. These stock tubes were incubated for between five and eight hours at 37^{o}C. When stock tubes reached an OD_{500} $\geq$1.2 value, they were divided into 500µL single use aliqouts in sterile cryotubes and stored at -80^{o}C.

The viability of the stocks was determined by a Miles and Misra count after 24 hours at -80^{o}C.

2.4.7 Viable counts of bacteria

The viable count of bacteria was determined using the Miles and Misra method, bacterial numbers are shown as colony forming units (CFU) in bacterial suspension or homogenate.

To examine the CFU of tissue homogenates, blood or in vitro culture supernatant:

20µL of the liquid culture (e.g. blood) was added to 180µL of sterile phosphate-buffered saline (PBS, Sigma) into sterile round-bottomed 96 well plates (Thermo Scientific) and serially diluted 10^{1}-10^{6}. The dilution contents were thoroughly mixed before changing to next dilution and the tip were discarded after each dilution. Next the blood agar plates were divided into six sections and 60µL (3x20µL) each dilution was spotted and plated on each corresponding sector. BAB culture plates were then incubated at 37^{o}C in a closed CO_2 jar, overnight.

Calculation of numbers of colony forming units: The grown pneumococcal colonies on BAB plates were counted on the dilution where between 30-100 colonies were

visible. The number of bacteria was determined as colony unit (CFUs) per mL, using the following equations:

CFU/mL = (Total number of colonies counted in sector) x dilution factor x (1000/60)

2.4.8 Preparation of D39 for neutrophil viability assay

The bacterial aliquot vial from -80^{o}C freezer was thawed and centrifuged at 13000 rpm for 2 minutes. Supernatant were removed and sample were re-suspended in media CFU/mL dilution at 1x10^{7}. Neutrophils were plated in a 24-well plate at 1x10^{6}/well. Bacteria were added at a range of MOI. Plates were incubated for 45 minutes at 37^{o}C. At the end of the incubation, neutrophil viability was assessed by flow cytometry as described in Section 2.3.2 and bacterial CFU was determined.

2.5 Purified pneumolysin (PLY)

Throughout my PhD study I also received purified PLY and PdB stocks which were prepared and tested for haemolytic activity by Emma Dearing and Hesham Malak from Aras Kadioglu's group.

PLY was produced *in vitro* by expressing the toxin on a pJW208 plasmid in MC1061 strain *Escherichia coli* (E.coli) as described by Mitchell *et al.* (Mitchell et al. 1989). The toxin was then purified from sonicated cell extract supernatant using the high performance Affinity chromatography system (GE healthare). The PLY concentration was determined by Nanodrop spectrometry at 280nm, and then purified toxin was passed through and EndoTrap endotoxin removal column (Profos AG, Germany) three times to remove LPS contamination. The batches received had an activity of 2.41 x 10^{4} Haemolytic Units (HU)/mg with a concentration of 352.5ug/mL. An endotoxin assay

also done to check Lipopolysaccharide (LPS) content of purified toxins using the Pierce® LAL Chromogenic Endotoxin Quantitation Kit with the detection limit of 0.1EU/mL (approximately 0.01ng endotoxin per mL). During this study, for *in vitro* experiments, the purified toxin had less than 0.4EU/µg of LPS. Previously published literature on PLY uses a concentration cut-off of <0.6 Endotoxin Units (EU)/µg protein).

2.5.1 Toxicity Assay

A series of PLY dilutions were prepared. Toxicity assays were performed at three different concentration ranges: (a) from 40.8 – 1305.6 HU PLY/mL, for 45 minutes (b) from 0.29-40.80 HU PLY/mL, for 45 minutes, and (c) from 1.2-2.5 HU PLY/mL, for 45 minutes, 2 hours and 4 hours.

Neutrophils were incubated with varying concentrations of PLY at $1x10^5$cells/well in a 96-well U-bottom plate. At the end of the incubation period, neutrophil viability was analysed by flow cytometry.

2.6 *In vitro* Migration Assays–using Transwell® 96 well plate

2.6.1 Preparation of Neutrophils

Neutrophils ($1\text{-}3x10^6$ cells/mL), PLY-treated neutrophils (final concentration 1.5HU PLY/mL), LPS-treated neutrophils (200ng/mL final concentration), and PdB-treated neutrophils (165ng/mL final concentration) were prepared and kept on ice during plating.

For assays using live bacteria, neutrophils were pre-mixed with bacterial isolates at an MOI of 10 (Table 4).

For analysis of the role of FES in neutrophil migration, neutrophils were treated with two different concentrations (1uM and 10uM) of a Fes inhibitor, Herbimysin A (sc-3518-Santa Cruz Biotechnology) or DMSO.

Table 4: List of bacterial stock strains and trigger molecules used

Strains /Triggers molecules	Concentration
D39 , serotype 2	$2x10^7$ CFU/mL
D39 Heat Killed, serotype 2	$2x10^7$ CFU/mL
PLN-A, serotype 2	$2x10^7$ CFU/mL
ST217, serotype 1	$2x10^7$ CFU/mL
ST306, serotype 1	$2x10^7$ CFU/mL
PLY	1.5 HU PLY/mL
PdB	165ng/mL
LPS	200ng/mL

2.6.2 Transwell® Migration/ Chemotaxis Assays

Transwell® 96 plates (HTS Transwell-96 Permeable Support with 5.0um Pore Polycarbonate Membrane, Corning) have an upper and lower compartment separated by a porous membrane (5.0um pore size) across which the cells migrate.

50µL ($1x10^5$) neutrophils, with or without chemoattractant (KC, 100ng/mL final concentration) were placed into the upper compartment (Figure 10). 50µL of media (RPMI-1640, 25mM HEPES, 2%FCS) with or without KC (100ng/mL final concentration) was placed in the lower compartment. Plates were incubated at 37^{o}C for 45 minutes and successful migration was confirmed by light microscopy. The number of neutrophils migrating (from upper to lower compartment) was determined

by counting neutrophils (count/mL) in the lower compartment using a MACS Quant analyser (Miltenyi®).

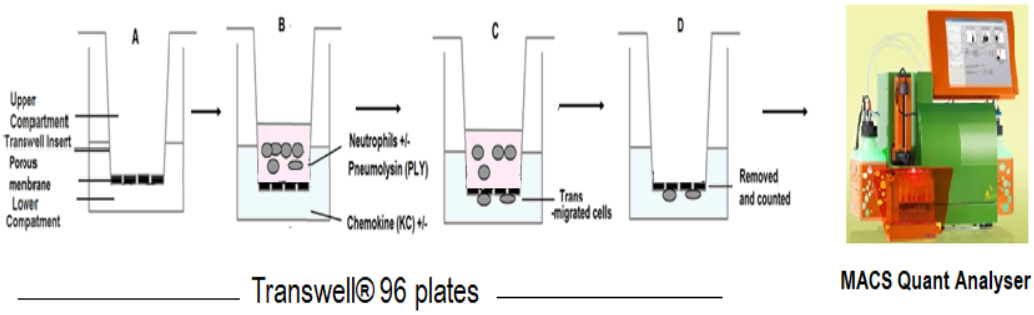

Figure 10: Schematic of basic set up for 2D Chemotaxis Assay using 96-well Transwell plates

(A) Prepare the plate (B) The neutrophils (+/- PLY) were placed into the upper compartment, and the chemoattractant (or media alone) placed in the lower compartment (C) The plate was incubated at 37^{o}C for 45 minutes and (D) confirmation of migration was checked using light microscopy. The absolute number of neutrophils migrating (from upper to lower compartment) was determined by counting neutrophils settling in the lower compartment using a MACS Quant flow cytometer (count/mL).

2.6.3 Transwell® Invasion Assays

Collagen gels (1.5mg/mL) were prepared in 1.5mL Eppendorf tubes according to Table 5, and kept on ice. Rat tail Collagen was kindly provided by Mark's Morgan Group (Nuffield Building, University of Liverpool).

Table 5: Preparation of 1.5mg/mL collagen gel for Invasion Assays

Component	Volume
10x DMEM Rat tail Collagen (7.1 mg/mL) H_2O	50µL 106µL 344µL
NaOH 1 M	As necessary to obtain neutral pH

15µL of collagen gel was added into each well to evenly cover the porous membrane. Care was taken not to create any bubbles. Gels were solidified in a 37^{o}C incubator for 30-45 minutes.

150µL of media with or without KC (100ng/mL final concentration) were added on the lower transwell compartment after the collagen gel had solidified. Plates were further incubated at 37^{o}C for 20 minutes to allow the chemoattractant to establish a gradient in the collagen gel. 50µL/1x10^{5} neutrophils treated as described in 2.6.1 were placed into the upper compartment. Plates were incubated at 37^{o}C for 2 hours.

20µL of 0.5M EDTA was added into each of the lower compartment to detach cells that had migrated across the membrane, but remained attached to the underside, incubated for 10 minutes on ice, and gently agitated.

The absolute number of neutrophils migrating (from upper to lower compartment) was determined by counting neutrophils (count/mL) in the lower compartment using the MACS Quant analyser (Miltenyi®).

2.7 *In vitro* Migration Assays - 3D Chemotaxis Assay using Ibidi u-Slide Chemotaxis Chambers

Ibidi u-slide chemotaxis contains two large-volume reservoirs separated by a smaller reservoir into which cells embedded in a 3D collagen gel are placed. When the reservoir on one side is filled with chemoattractant, this will form a concentration gradient inside the gel, stimulating chemotaxis.

Neutrophils prepared as above were embedded in rat tail collagen (1.5mg/mL) as described in Table 6.

Table 6: Preparation of 1.5mg/mL collagen gel for 3D Chemotaxis Assay using u-Slide Chemotaxis

Component	Volume
Rat tail collagen (stock 7.1mg/mL)	21.3µL
DMEM (10x)	10µL
NaOH (check pH)	as needed to adjust to neutral pH
Cell suspension (cell at $3x10^6$/mL)	67.2µL
Total	100µL

Media (RPMI-1640, 25mM HEPES, 2%FCS) with and without chemoattractant (KC, 100ng/mL final concentration) was prepared for the assay.

Collagen gels containing neutrophils were seeded into the central chamber of the u-Slide 3D Chemotaxis Chamber following the manufacturer's protocol in the Application Note 17 (ibdi GmbH 2016)**.** Reservoirs on either side of the gel were filled with media or media containing chemoattractant. Heather Swift provided assistance and guidance with the set-up and execution of this assay. The schematic set up for this experiment is shown in Figure 11.

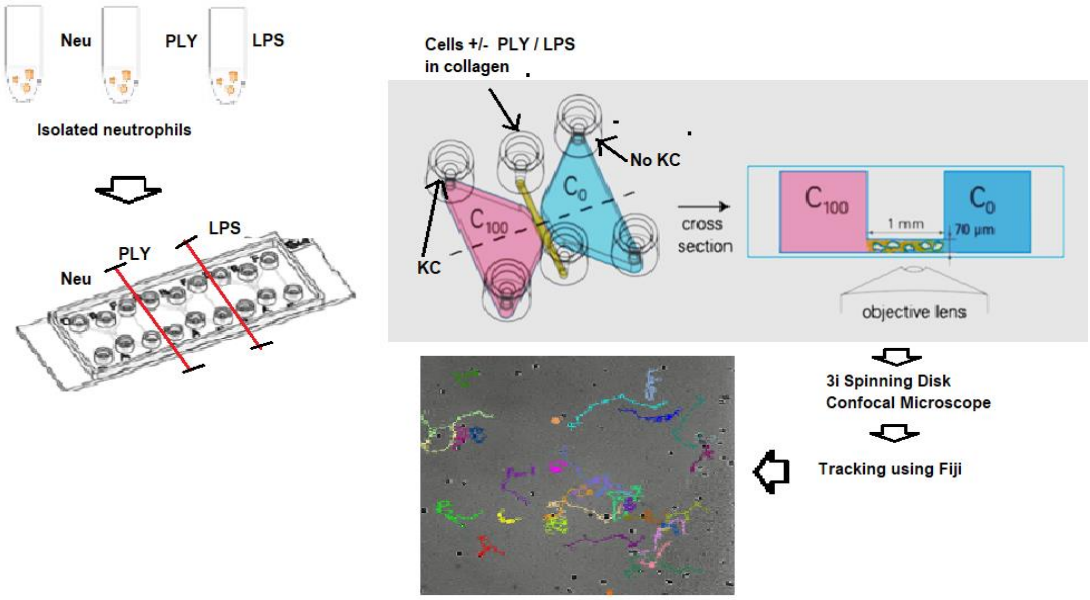

Figure 11: Schematic set up for 3D Chemotaxis using u-Slide Chemotaxis
Neutrophils were left untreated, or stimulated with PLY or LPS, and mixed into the collagen matrix. Collagen/neutrophil mixtures were loaded into the central chamber of u-slide chemotaxis, and allowed to solidify at 37°C. Media without KC was added into the C_0 space, and before the chamber put under the microscope, buffer with KC was added into the C_{100} space. Images were acquired at three stage positions per condition, at 1 minute intervals. Neutrophil migration in the resulting time-lapse movies was tracked using Fiji software. Figure adapted from (ibdi GmbH 2016)**.**

The u-slide chemotaxis chamber was placed in the incubation chamber of a Hamamatsu 3i spinning disk confocal microscope, and imaged using bright field and a 10x objective. The images were taken every 1minute for up to 8 hours.

Neutrophil migration was manually tracked for two hours, and the cells x and y positions at each time-point used to quantify; speed, directionality, Euclidean distance and accumulated distance using Fiji ImageJ-win64. The parameters feature can be seen in 2D trajectory plots in Figure 12. Data were also tracked by using auto-tracking in IMARIS x64 7.7.1 for speed.

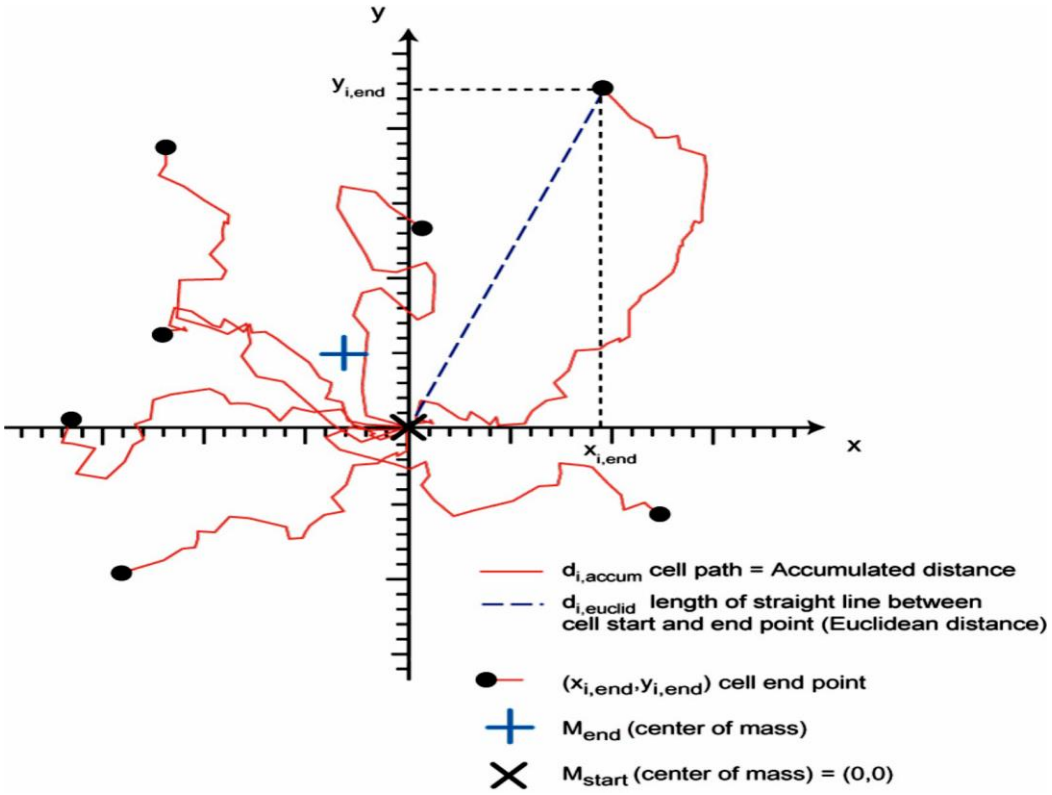

Figure 12: 2D trajectory plot

Plot shows the meaning of "i" is the index of different single cells.

Cells were manually tracked using MTrackJ in ImageJ-win64 and using the Migration and Chemotaxis Tool to quantify cell migration parameters. The cells x and y positions at each time-point were used to quantify; speed (um/min), euclidean distance (length of cell start and end point in straight line), accumulated distance (cell path taken for migration), and directionality/confinement index (Euclidean distance divided by Accumulated distance). Figure adapted from (Asano & Horn 2011).

2.8 Adhesion Assay

2.8.1 TC-treated plate (96 well flat bottom)

Neutrophils were re-suspended in RPMI at $5x10^6$/mL, and labelled with 5uM calcein AM (Vybrant™ Cell Adhesion Kit [V-131810]-Molecular Probes) for 30 minutes at 37°C before being washed twice with pre-warmed RPMI. Neutrophils were re-suspended at $5x10^6$/mL and left untreated or treated with 1.5HU PLY/mL, 200ng/mL LPS, or 165ng/mL PdB.

$5x10^5$ (100µL) neutrophils were then added to each well of a 96-well plate. Each condition was performed in triplicate. Plates were incubated at 37°C for 45 minutes, 2 hours or 4 hours. Non-adherent calcein-labelled cells were carefully removed by washing with pre-warmed RPMI. The washing steps were repeated four times and after the final wash, 200µL of PBS was added into each well. Sample fluorescence was measured using a Fluorescein filter set (494-517nm) on a Tecan Analyser.

2.8.2 Non-treated plated (96 well flat bottom)

96-well flat-bottom plates were pre-coated with 40µL bovine fibronectin (Thermo Scientific) at a concentration of 25ug/mL. Plated were incubated for 1 hour at 37°C or overnight at 4°C. Plates were washed three times with 200µL PBS. Plates were then blocked with blocking solution (PBS with 1% FCS) for 1 hour at room temperature and then washed three times with PBS. Adhesion assays were performed as described in 2.8.1.

2.9 Immunofluorescent Staining of F-actin and Grancalcin

Sterilised glass coverslips (round, 13mm, No1.5, VWR) were placed in 24-well flat bottom plates. Coverslips were submerged in 0.01% Poly-L-lysine (Sigma), and left overnight at 4^{o}C. Coated glass coverslips were washed twice with pre-warmed PBS$^{+Ca/Mg}$ without touching the glass. Neutrophils (1x10^{6} cells/mL), PLY-treated neutrophils (final concentration, 1.5HU PLY/mL), LPS-treated neutrophils (200ng/mL final concentration), and PdB-treated neutrophils (165ng/mL final concentration) were applied to the coated glass coverslips, and incubated for 45minutes at 37^{o}C. After incubation, media was gently aspirated and the glass coverslips washed gently with pre-warmed PBS$^{+Ca/Mg}$. Adhered cells on the coverslips were checked with the light microscope. The adhered cells were fixed by adding 4% paraformaldehyde/PFA (Pierce™16% Formaldehyde(w/v), Methanol-free, Thermo Fisher scientific) 400µL/well for 30 minutes at room temperature. After fixation, coverslips were washed twice with PBS, submerged in PBS, and left at 4^{o}C in the fridge overnight.

For F-actin staining, neutrophils were stained with Rhodamine-Phalloidin (1:250, Life Technologies) and DAPI (2 drops/mL, NucBlue@Fixed Cell Ready Probe-Thermofisher Scientific) in 1% Triton X-100 with 10% FCS. Samples were incubated for 1 hour at room temperature, before being washed gently three times for 5 minutes each with PBS. Glass coverslips were air-dried and mounted onto glass slides using Aquamount (VWR).

For Grancalcin staining, neutrophils were incubated in blocking solution (10% normal goat serum with 1% Triton x-100) for 1 hour on a rocker. Neutrophils were

then stained with anti-Grancalcin (1:200 in blocking solution) for 1 hour on a rocker. After 1 hour of incubation samples were carefully washed with PBS 3 times, with 3 minutes gap between each wash. Neutrophils were then incubated with goat anti-mouse-A647 (1:200), Rhodamine-phalloidin (1:250) and DAPI (2 drops per mL) in wash buffer (PBS, 1% FCS with 0.1% Triton x-100) for 1 hour. Neutrophils were carefully washed with PBS 3 times with a 3 minutes gap between each wash. Coverslips were air-dried and mounted onto glass slides using Aquamount (VWR).

Stained neutrophils were imaged on one of two confocal microscopes in the Centre for Cell Imaging:

1) Zeiss BioAFM880 using alpha Plan-Apochromat, 100x/1.46 oil DICM27 objective and 405nm (DAPI), 561nm (Rhodamine) laser lines.

2) Zeiss LSM780 using alpha Plan-Fluar, 100x/1.45oil objective and 405nm (DAPI), 561nm (Rhodamine) laser lines.

Images were further analysed using IMARIS (Bitplane version 7.7.1) software to obtain intensity mean of fluorescent actin, sphericity of neutrophils, and volume (um^3) of neutrophils using the surface area tool.

2.10 Label-free sample preparation of neutrophils for quantitative proteomics

2.10.1 Sample preparation

Bone marrow and neutrophil isolation steps were performed as described previously in Section 2.2.1c. Three independent experiments were performed, with bone marrow from four mice pooled for each experiment.

Neutrophils were plated alone, or with PLY or LPS and incubated at 37^{o}C for 4 hours in a 12 well flat bottom plate. After incubation, cells in suspension were harvested, and cells attached to the plastic wells were carefully scraped before being transferred into a 15mL conical tube. Small amounts of cell suspensions (100µL) were kept aside before and after incubation for FACS analyses of neutrophil purity and CD11b expression (Figure 13).

The remaining cell suspensions were centrifuged down at 1500 rpm for 5 minutes, and the supernatants were discarded. Pellets were then washed twice with PBS, and all the buffer were aspirated entirely from the sample. Sample pellets were immediately frozen on dry ice and stored at -20^{o}C for further proteomic analysis. Proteomic work and data analysis were performed by Dr. Stuart Armstrong, at the Infection Biology Department, University of Liverpool UK. Sample preparation for mass spectrometry and analysis was adapted from (Dong et al. 2017).

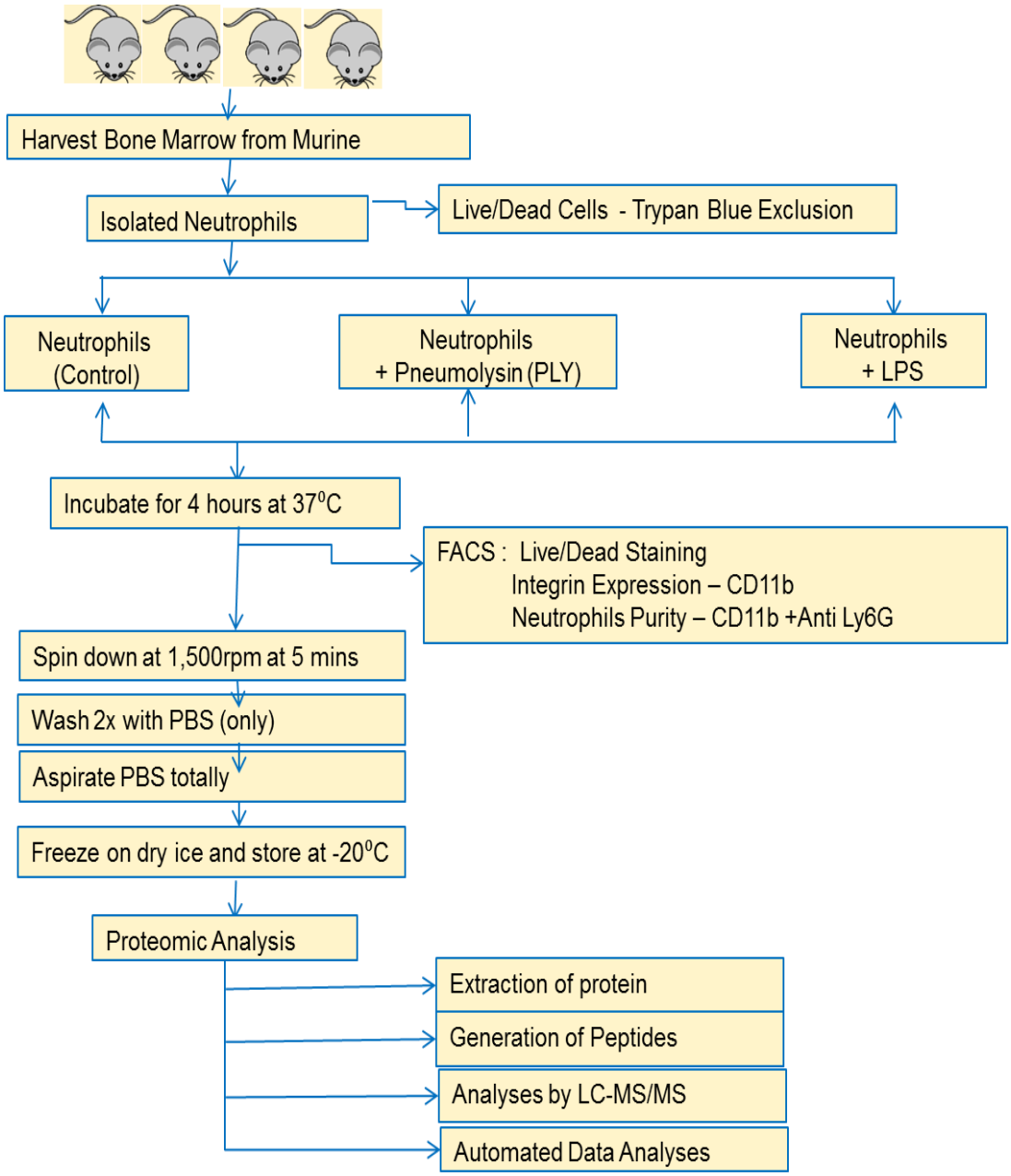

Figure 13: Schematic of Proteomic experimental

Bone marrow was harvested from four mice (expected neutrophil yield around 1.5 - 2 x 10^7 cells, sufficient for proteomic and FACS analysis). Cells underwent neutrophil isolation protocol as described Section 2.2.1c. Neutrophils were plated alone, or with PLY or LPS and incubated at 37°C for 4 hours. After incubation, cells were transferred into tubes, and aliquots withdrawn for FACS. Live/Dead Staining, CD11b expression and purity were assessed. Remaining cells were washed twice in PBS. All remaining serum was completely removed and samples immediately frozen. All subsequent proteomic analysis steps were performed by Dr Stuart Armstrong from Department of Infection Biology, IGH.

2.10.2 Homogenisation and protein digestion

Neutrophils, PLY-treated neutrophils, and LPS-treated neutrophils (in triplicate for each condition, n=9) each contained an average of 3.37 $x10^7$ neutrophils. Samples were lysed in 0.1% (w/v) RapiGest (Waters) in 50mM ammonium bicarbonate. Following that, 3 cycles of sonication on ice (Vibra-cell 130PB sonicator) at 20Hz using a microprobe with alternating 30 seconds incubation on ice and 10 seconds sonication was performed. Next, all samples were centrifuged at 13,000 x g for 10 minutes at 4°C and the supernatants were transferred to Eppendorf tube and stored at -80°C until use. Protein Assay Kit assay by Pierce Coomassie Plus (Bradford) (Thermo Scientific) was used to measure total protein concentration and protein content for each sample was normalised to 100ug.

Samples were heated at 80°C for 10 minutes and reduced with 10µl of 9.2mg/ml dithiothreitol (3mM final concentration (Sigma)) for 10 minutes at 60°C. Alkylation of the sample was performed by adding 10µl of 33mg/ml of iodoacetimde (9mM final concentration (Sigma)) and incubating at room temperature for 30 minutes in the dark. All these steps were performed with intermittent vortex-mixing. Proteomic-grade trypsin (Sigma) was added at 50:1 of protein:trypsin ratio and samples were incubated for overnight at 37°C. RapiGest was removed by adding Trifluoroacetic acid (TFA) to a final concentration of 0.5% (v/v) and the digest incubated for 45 minutes at 37°C. Finally, the peptide samples were centrifuged for 15 minutes at 13000 x g to remove precipitates. The supernatant were collected for subsequent mass spectrometric analysis (LC-MS/MS).

2.10.3 NanoLC MS ESI MS/MS analysis

In this experiment, we were using on-line nanoflow LC using the Ultimate 3000 nano system (Dionex/Thermo Fisher Scientific) for peptide analyses. 1µg of samples were loaded onto a trap column (Acclaim PepMap 100, 2cm × 75µm inner diameter, C18, 3µm, 100 Å) at 9µL/min with an aqueous solution containing 0.1% (v/v) TFA and 2% (v/v) acetonitrile. After 3 minutes, the trap column was set in-line with an analytical column (Easy-Spray PepMap® RSLC 50 cm × 75 µm inner diameter, C18, 2µm, 100 Å) fused to a silica nano-electrospray emitter (Dionex). The on-line nanoflow LC system was coupled to a Q-Exactive mass spectrometer (Thermo Fisher Scientific), and the trap column run at a constant temperature of 35°C. Chromatography was performed using a buffer system consisting of 0.1% formic acid (buffer A) and 80% acetonitrile in 0.1% formic acid (buffer B) and a linear gradient of 3.8 – 50% buffer B over 90 minutes at a flow rate of 300 nl/min was used to separate the peptides. The Q-Exactive mass spectrometer was run in data-dependent mode with survey scans acquired at a resolution of 70,000 at 200 m/z, with a scan range between 300 to 2000 m/z. Up to the 10 most abundant isotope patterns from the survey scan with charge states from +2 to +5 were picked with an isolation window of 2.0Thand fragmented by higher energy collisional dissociation with normalised collision energies of 30. The ion target value was set at 1E6 for survey scans and 1E4 for the MS/MS scans and maximum ion injection times were 250nm for the survey scan and 50ms for MS/MS scans. Acquisition was at a resolution of 17,500 for MS/MS events. The dynamic exclusion of the sequenced peptides for 20s was applied to minimize repetitive sequencing of peptides.

2.10.4 Protein Identification and Quantification

Thermo RAW files were imported into Progenesis LC–MS (version 4.1, Nonlinear Dynamics) for data analysis. Runs were aligned using default settings and the reference run automatically selected by the software. Only peaks with a charge state between +2 and +7 were chosen by the software using default settings. The reference run was used to normalise the peptide intensities and to highlight differences in protein expression between control and treated samples with supporting statistical analysis (ANOVA p-values). Spectral data were converted to .mgf files and exported to the Mascot (version 2.3.02, Matrix Science) search engine for peptide identification. Tandem MS data were searched against a database comprising; translated ORFs from the Mouse genome (Uniprot, Feb 2015), a background bovine genome (Uniprot, Feb 2015) and a contaminant database (cRAP, GPMDB, 2012) (combined 25513 sequences; 12610778 residues). The search parameters for this experiment were: 10 ppm for precursor mass tolerance, 0.01 Da for fragment mass tolerance, two missed tryptic cleavages and fixed modification for Carbamidomethylation (cysteine) and variable modification for oxidation (methionine). In addition to this, the machine learning algorithm Percolator embedded within Mascot was used to validate the search results. The false discovery rate was <1%, while individual percolator ion scores >13 indicated identity or extensive homology ($p < 0.05$) were utilised in the Mascot decoy database function before the results were imported into Progenesis LC–MS as .xml files.

2.10.5 Software used for data analysis

Analysis was performed using free online software with default settings during searches. The programmes used were:

STRING Database Version 10.5: This tool was used for assessing protein-protein interactions based on physical and functional interactions between the expressed proteins, which can give meaning biologically for their cellular function (Szklarczyk et al. 2017). In our sample we were using this tool to understand how proteins upregulated in PLY-treated neutrophils influenced neutrophil functions such as migration.

DAVID Bioinformatics Resources 6.8: This tool was using to understand biological meaning from large gene/protein where the information extracted systematically from set samples (Huang et al. 2009a; Huang et al. 2009b). Using this, we performed a functional annotation of proteins identified by pairwise analysis as being significantly changed in PLY-treated, but not LPS-treated, neutrophils.

Panther Classification System Version 13.1: Panther (Proteins Analysis Through Evolutionary Relationship) of gene families and annotated as; family and sub-family, protein class (biological process, molecular function and cellular component) and gene function (Mi et al. 2013; Thomas et al. 2003). We used this classification system to characterise the identified proteins according to biological process in our extracted neutrophils compared to mouse proteome.

Morpheus, https://software.broadinstitute.org/morpheus: This interactive tool the see the protein cluster display as a heat map base on intensity value in our dataset.

Venny 2.1.0 (Oliveros, J.C (2007 -2015) Venny, an interactive tool for comparing with Venn Diagram. http//bioinfogp.cnb.csic.es/tools/venny/index. html.): Using this tool we are able to visual the common share and unique protein identified across our samples in Venn diagrams.

2.11 Immunoblotting (Western Blotting (WB))

Neutrophil isolation steps were carried out as described earlier. Samples (neutrophil and neutrophil treated with 1.5HU/mL PLY) were prepared by incubating for 45 minutes at 37°C. Samples were centrifuged at 1500 rpm for 5 minutes and the supernatant removed. Each sample was mixed with lysis buffer (equivalent with pellet) and sonicated for 5 seconds and incubated for 10 minutes at 95°C to obtain neutrophil lysate. Samples were stored at -80°C until use.

10µL sample lysate and 8µL of Spectra^{TM} Multicolour Broad Range Protein Ladder(26634, Thermofisher) were loaded onto 12% SDS/acrylamide-separating gel (5mL of 1.5M Tris pH 8.8, 30% acrylamide (Acrylamide/Bis-acrylamide, 30% solution A3699-100mL, Sigma), dH_20, 20% SDS, 10%APS and N,N,N',N'-Tetramethylethylenediamine (TEMED, Sigma, T9281-25mL) and a 5% stacking (0.5M Tris pH6.8, 30% acrylamide, H_2O, 20% SDS, 10% APS and TEMED), and run in electrophoresis buffer at 60V, 200mA and 100W for 1:30 hour, the at 200V, 200mA for 1 hour till the end of running.

The protein was electrophoresed and blotted onto a nitrocellulose membrane (Immobilon-P Transfer Membrane, IVPH00010, Merck) in cold conditions and run at 200V, 350mA, and 100W for 1:15 hour in transfer buffer. Then, membranes were blocked in 5% skim milk/TBS-T (0.1% Tween 20, 5g NaCl, 20mL of Tris-HCL)

overnight with shaking at 4°C. The membranes were incubated with primary antibody (Table 7) for 2 hours on the shaking rotor at room temperature, after washing with TBS-T with shaking followed by incubation with conjugated secondary antibody (Table 8) for 1 hour.

The membrane was washed and processed for detection by chemiluminescence (ECL) reagents (Clarity™ Western ECL Substrate, 200mL #1705060, BioRad) and developed in ChemiDoc™ touch Imaging Systems (Bio-Rad,1708370).

Table 7: List of primary antibodies used in Western Blotting

Primary Antibodies / Supplier	**Source/Application**
Fes (E-1) : sc-166371 (Santa Cruz Biotechnology, Inc)	Mouse monoclonal of human origin. Detection - Fes of mouse , rat and human origin
Grancalcin (H-11) : sc-393681 (Santa Cruz Biotechnology, Inc)	Mouse monoclonal of mouse origin. Detection - Grancalcin on mouse.
Csk (B-7): sc-166513 (Santa Cruz Biotechnology, Inc)	Mouse monoclonal of human origin. Detection – Csk of mouse, rat and human origin
FGD3 (A-3) : sc-390256 (Santa Cruz Biotechnology, Inc)	Mouse monoclonal of mouse origin Detection – FGD3 of mouse, rat and human origin
GAPDH (GAIR)-MA5-15738/ Thermofisher	Loading Control Monoclonal antibody

Table 8: Secondary antibody used in Western Blotting

Control Antibodies / Supplier	**Application**
Goat anti-mouse IgG (A44d16/Sigma)	Secondary Antibody Control

2.12 Statistical Analyses

All statistical data were analysed using GraphPad Prism 7.0 unless stated. Results were analysed by one-way and two-way analysis of variance (ANOVA) followed by Tukey's multiple comparison tests to identify significant difference between individual groups. Probability (p) value <0.05 were considered statistically significant. Statistically significant differences in this work are indicated by *($p<0.05$), ** ($p<0.01$), *** ($p<0.001$), **** ($p<0.0001$).

Chapter 3: *Streptococcus pneumoniae* and its toxin, pneumolysin, inhibit neutrophil chemotaxis in two and three dimensional assays.

3.1 Brief Introduction

Neutrophils are the most abundant white blood cells in circulation, and play a crucial role in immune responses to pathogens during infection. To defend the host, they must migrate from the blood into the tissue through a multistep process, and then onwards through the tissue interstitium (Artemenko et al. 2011).

Neutrophil migration can occur in four main forms: random migration, chemokinesis, chemotaxis, and haptotaxis. Chemotaxis and haptotaxis are directional, and occur along a soluble (chemotaxis) or substrate-bound (haptotaxis) gradient of chemoattractant. Meanwhile, random migration and chemokinesis are non-directional. Chemokinesis occurs in the presence of a uniformly applied stimulus, and random migration occurs without stimuli (Martin et al. 2015).

Extravasation of neutrophils from blood capillaries is a multistep process which is initiated by tethering and rolling of the neutrophil, followed by slow rolling, activation of integrins, shear resistant arrest, crawling, diapedesis and, finally, migration across the epithelium and basement membrane (Lyck & Enzmann 2015). The neutrophil then migrates through the tissue interstitium to the site of infection, in response to chemoattractants. Extravasation is induced by chemokines and has been shown to be integrin dependent, however migration through the tissue is still poorly understood and may be either integrin dependent or independent. It is widely accepted that leukocyte migration on 2D surfaces requires adhesive forces (integrin-dependent), while migration in 3D environments largely depends on cytoskeletal

deformability rather than adhesion (integrin-independent). *In vivo* studies confirm the integrin-independence of leukocyte interstitial migration (Weninger et al. 2014; Lämmermann & Sixt 2009; Lämmermann et al. 2008). However, *in vitro* studies show that dendritic cells (DCs) can rapidly adjust their migration mechanisms by switching from adhesive (integrin-dependent) to non-adhesive (integrin-independent) modes, allowing maintenance of cell speed and amoeboid migration across different surfaces (Renkawitz et al. 2009). Similarly, in a model of sterile tissue damage, neutrophils switch from integrin-independent to integin-dependent migration at the boundary of the tissue interstitium and wound site (Lämmermann & Germain 2014). Furthermore, integrins and their regulatory proteins have been shown to play a role in facilitating chemotaxis of neutrophils in 3D environments. Efficient directed migration within 3D matrix has been shown needed both integrin regulatory protein talin-1 and RIAM for proper cell polarization toward chemoattractant gradient stimuli (Yamahashi et al. 2015). In lymph nodes, neutrophil migration mostly used a chemotactic mechanism involving phosphatidylinositde 3-kinase signalling and leukotriene B_4, but migration was not totally integrin independent. This indicated that neutrophil phenotype and behaviour is environment dependent, and indicate the complexity of neutrophils migration mechanisms (Sawtell 2015).

Pathogens such as *Streptococcus pneumoniae* or *Staphylococcus aureus* may manipulate neutrophil migration and function to avoid being killed by host cells. *S. pneumoniae* itself has many virulence factors such as its toxin pneumolysin (PLY) which has been shown in early studies to have the capability to inhibit neutrophil migration (Paton & Ferrante 1983). Likewise, *Staphylococcus aureus* has developed strategies to avoid neutrophil killing by secreting molecules that resist or fight back against neutrophil attack at the site of infection. For example, during extravasation

neutrophil rolling on endothelial cells can be inhibited when staphylococcal superantigen-like 5 (SSL5) blocks PSGL-1 interaction with P-selectin and E-selectin on the neutrophil surface (Spaan et al. 2013).

The interactions between neutrophils and PLY are complex (Johnson, Boese-Marrazzo, & Pierce, 1981). Neutrophils exposed to pneumolysin have enhanced production of superoxide and neutrophil elastase, increased expression of CD11b/CD18, and membrane depolarization (Cockeran, Theron, et al. 2001). Increased cell surface expression of CD18 on neutrophils leads to neutrophil adhesion to alveolar epithelial cells (Smith et al. 1998). Using human polymorphonuclear neutrophils (PMNs) from healthy volunteers, Johnson *et al* showed that pre-treatment with PLY at sub-lytic concentrations inhibited neutrophil chemotaxis and random migration. Similarly, Paton & Ferrante described significant inhibition of chemotaxis following treatment of human PMNs with PLY (Paton & Ferrante 1983). When PLY was used as a chemoattractant, PMN migration was initially enhanced, but then inhibited as the cells migrated up the gradient (Johnson et al. 1981). However, it is not clear if the chemoattractive effects of PLY compete with host chemokines, potentially explaining the impaired chemotaxis observed in neutrophils pre-treated with PLY.

Another *in vitro* study was done to examine the effects of serotype 2 (strain D39) *S. pneumoniae* and its pneumolysin-deficient mutant (PLN-A) on PMN migration across a monolayer of human pulmonary microvascular endothelial cells. They found that neutrophil migration was decreased in the presence of PLN-A, indicating that PLY promotes neutrophil endothethial transmigration (Moreland & Bailey 2006). Meanwhile, *in vivo* studies have found that treatment with PLY, but not its non- lytic

derivative, PdB, directly resulted in increased lung vascular permeability, which may lead to enhance neutrophil migration into the infected lung (Maus et al. 2004).

This chapter, aims to provide valuable insight into how pneumolysin (PLY) may affect neutrophil chemotaxis using purified murine bone marrow neutrophils. Both 2-D and 3-D *in vitro* chemotaxis assays were used to assess the effect of PLY on neutrophil migration. In addition these models were used to examine whether migration was an integrin dependent or independent process. Neutrophil migration within tissues and how the neutrophils and toxin interact in tissue microenvironments were determined using e*x vivo* experiments.

3.2 Results

3.2.1 Optimisation of Neutrophil Purification from Murine Bone Marrow

To study the effects of *S. pneumoniae* and PLY on neutrophil migration, a highly pure population of neutrophils was required. Three isolation methods were compared: Percoll density gradient centrifugation, Histopaque density gradient centrifucaton, and negative selection by magnetic-activated cell sorting (MACS). The detailed protocols are mentioned in Chapter 2. The purity of the isolated neutrophil fraction was assessed by flow cytometry, with cells double positive for both CD11b and Ly6G considered to be neutrophils. Viability of the cells was determined by trypan-blue exclusion.

Percoll Density Gradient Centrifugation was the first isolation method attempted. Briefly, bone marrow was resuspended in 5mL media. Next, 5mL of 62.5% Percoll was carefully layered underneath the cell suspension and centrifuged at 2300 rpm for 30 minutes. The cloudy interface (containing immature cells and non-granulocytes) was removed and the last 3mL of Percoll (containing a loose pellet of neutrophils) was retained. Using this method, $4.1x10^6 \pm 1.3x10^6$ cells /mouse were isolated, of which $66.7 \pm 3.4\%$ were $CD11b^+Ly6G^+$, and $94.1 \pm 2.8\%$ were viable (Figure 14), with n=7 independent experiments. Altering the media, FCS concentration, and centrifugation speed did not improve purity (data not shown).

The next isolation method attempted was Histopaque Density Gradient Separation (Histopaque 1119 and 1077). Briefly, bone marrow was resuspended in 1mL media. 3mL of Histopaque 1077 (density, 1.077 g/mL) was carefully overlayed on top of 3mL of Histopaque 1119 (density, 1.119 g/mL). The bone marrow cell suspension was then overlayed on top of the Histopaque 1077. The sample was centrifuged at

2000 rpm for 30 minutes, and the neutrophils at the interface of the Histopaque 1119 and Histopaque 1077 layers were collected. Using this method, $5.0x10^6 \pm 2.6x10^6$ cells/mouse were isolated, of which 46.7 $\pm$ 13.2% were $CD11b^+Ly6G^+$, and 93.5 $\pm$ 3.3% were viable (Figure 15), with n=12 independent experiments.

As neither protocol achieved sufficiently high purity, neutrophils were next isolated by negative selection using MACS. Briefly, bone marrow was labelled with a cocktail of antibodies to non-target (or unwanted) cells, which were removed from the mixture by retention in the MACS column. Meanwhile, the unlabelled neutrophils will run through the column and be collected. Using this method, $5.3x 10^6 \pm 1.7$ cells /mouse were isolated, of which 95.6 $\pm$ 2.7 % were $CD11b^+Ly6G^+$, and 96.8 $\pm$ 1.8% were viable (Figure 16), with n=12 independent experiments.

MACS isolation was superior to the Percoll Density Gradient Centrifugation and Histopaque Density Gradient. As this method consistently yielded high purity neutrophils, it was used for all future experiments.

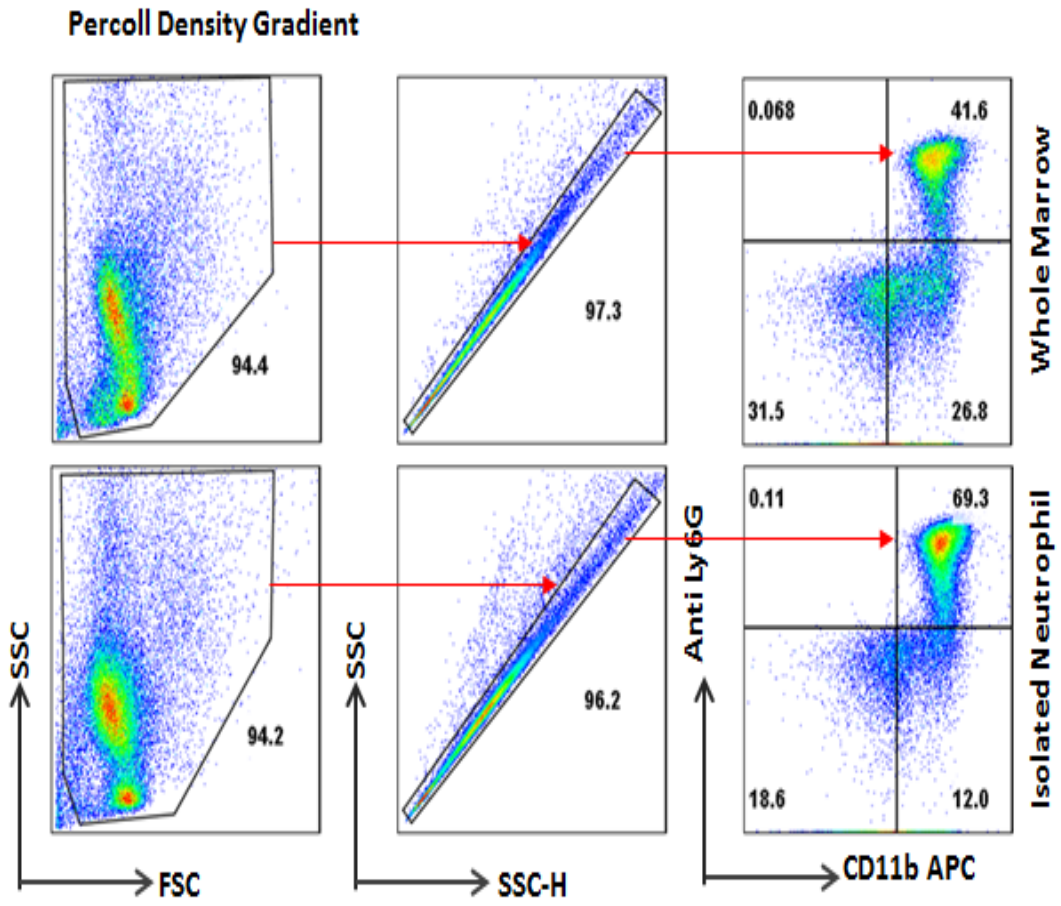

Figure 14: Optimisation of Neutrophil Purification from Murine Bone Marrow using Percoll Density Gradient

Flow cytometry analysis of whole marrow and purified neutrophils using Percoll Density Gradient The plots on the **left** show discrimination of live cells based on forward and side scatter, the **middle** plots show discrimination of single cells from doublets, and the **right** plots show percentage of cells stained with both CD11b and Ly6G in top right quadrant (neutrophils). Data are representative of 7 independent experiments.

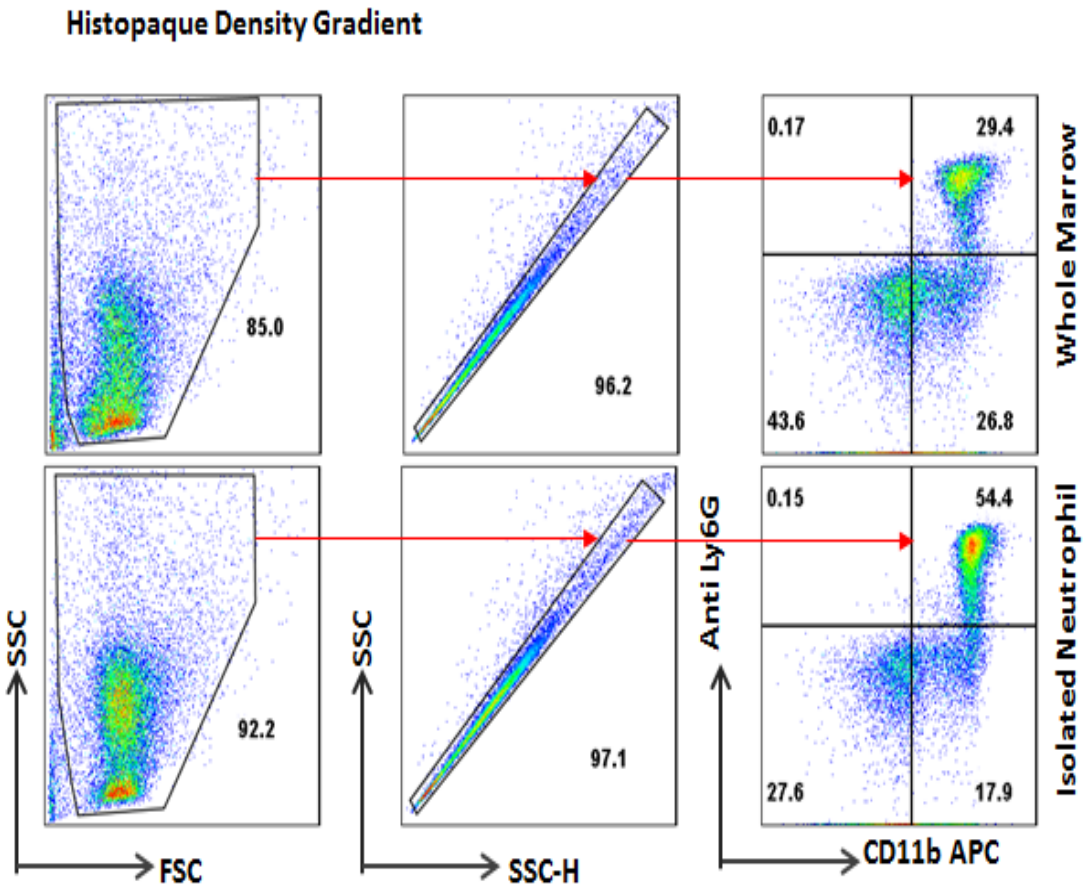

Figure 15: Optimisation of Neutrophil Purification from Murine Bone Marrow using Histopaque Density Gradient

Flow cytometry analysis of whole marrow and purified neutrophils using Histopaque Density Gradient. The plots on the **left** show discrimination of live cells based on forward and side scatter, the **middle** plots show discrimination of single cells from doublets, and the **right** plots show percentage of cells stained with both CD11b and Ly6G in top right quadrant (neutrophils). Data are representative of 12 independent experiments.

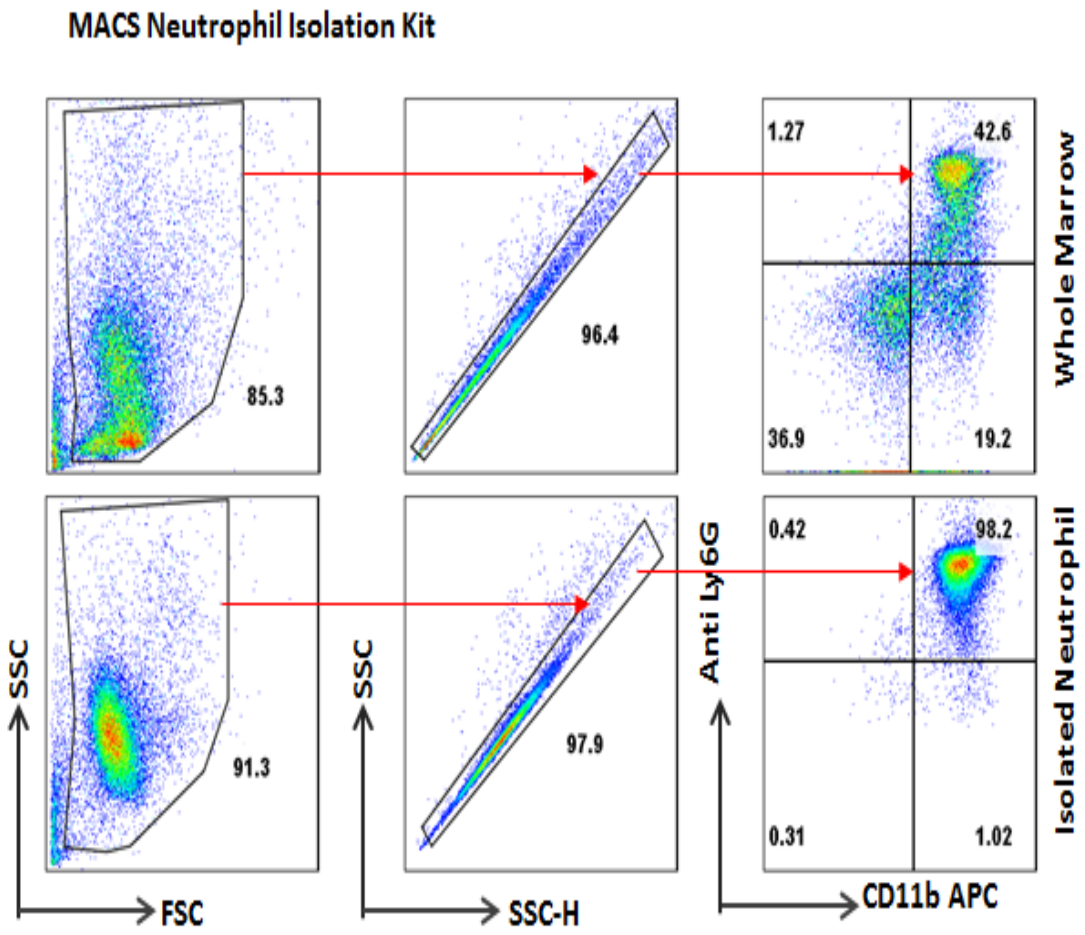

Figure 16: Optimisation of Neutrophil Purification from Murine Bone Marrow using MACS Neutrophil Isolation Kit

Flow cytometry analysis of whole marrow and purified neutrophils using MACS Neutrophil Isolation kit. The plots on the **left** show discrimination of live cells based on forward and side scatter, the **middle** plots show discrimination of single cells from doublets, and the **right** plots show percentage of cells stained with both CD11b and Ly6G in top right quadrant (neutrophils). Data are representative of 12 independent experiments.

3.2.2 Determination of a non-cytolytic, but biologically active, concentration of PLY

To assess the effect of PLY on neutrophil chemotaxis, we needed to determine the concentration of PLY that would produce a biological effect on neutrophils, but not cause significant cell death (sub-lytic). If cell death occurs, it will be impossible to determine if the toxin has a specific effect on neutrophil chemotaxis beyond general effects on cell viability. Throughout this thesis, purified PLY was provided by Aras Kadioglu's Group.

For each assay, freshly isolated neutrophils were treated with a range of concentrations of PLY, between 45 minutes and 4 hours. At the end of the incubation period, neutrophil viability was assessed by flow cytometry using a LIVE/DEAD fluorescent dye. We also assessed the ability of PLY to increase expression of CD11b (integrin αM) on neutrophils, to ensure that low, sub-lytic concentrations were still altering cell phenotype. Previous studies have shown that PLY increases expression of CD11b on neutrophils (Williams et al. 2003).

For the first experiment, a concentration range from 40.8 – 1305.6 haemolytic units (HU) PLY/mL was used (Figure 17A). At all concentrations, the toxin killed a high proportion of the neutrophils, as evidenced by uptake of the LIVE/DEAD dye (Figure 18). On the few remaining cells, the mean fluorescence intensity (MFI) of CD11b decreased dramatically relative to untreated cells. (Figure 17B) CD11b levels are expressed as a ratio of the MFI on PLY-treated neutrophils, relative to untreated controls.

For the next experiment, a concentration range between 0.29 – 40.80 HU PLY/mL was selected (Figure 17C and Figure 19). We observed good viability at PLY

concentrations of <3 HU/mL. However, neutrophil viability began to decrease at PLY concentrations of >5 HU/mL (Figure 17C). Surface expression of CD11b also increased at PLY concentrations of between 1.16 HU/mL and 5.73 HU/mL, but declined dramatically when cell viability was lost at higher concentrations (Figure 17 D).

From this experiment, it was determined that neutrophils stimulated for 45 minutes with PLY at a concentration range of 1.16 to 2.83 HU/mL were viable and showed increased surface expression of CD11b. To provide final confirmation that this concentration range was suitable for all of the assays performed in this chapter, neutrophil viability was next assessed for up to 4 hours following treatment with PLY.

This assay was performed at an optimal concentration range of 1.2 – 2.5 HU/mL (Figure 17E). More than 95% of neutrophils remained viable for the duration of the experiment (Figure 20) and the expression of CD11b (Figure 21) was also elevated at all time points.

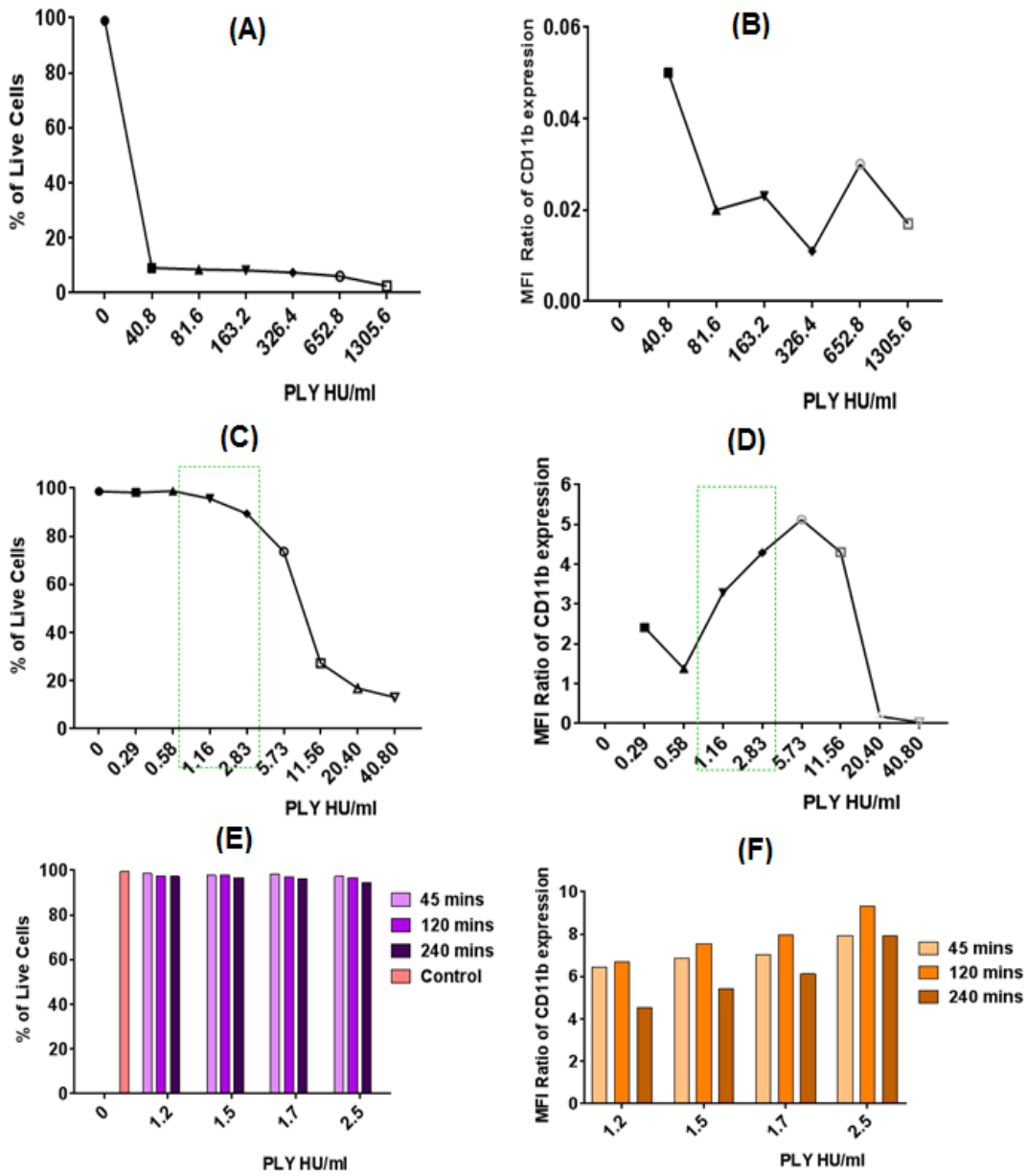

Figure 17: Determination of a non-cytolytic, but biologically active, concentration of PLY

Neutrophils were incubated with the indicated concentrations of PLY and stained with live/dead dye and antibody to CD11b before analysis by flow cytometry. The left column (A, C, E) Graphs depict flow cytometric analysis of neutrophil viability following stimulation with PLY. (B, D, F) Flow cytometric analysis of CD11b on PLY pre-treated neutrophils. CD11b levels are expressed as a ratio of the MFI on PLY-treated neutrophils, relative to untreated controls. Unless otherwise indicated, analysis was performed at 45 minutes post-stimulation.

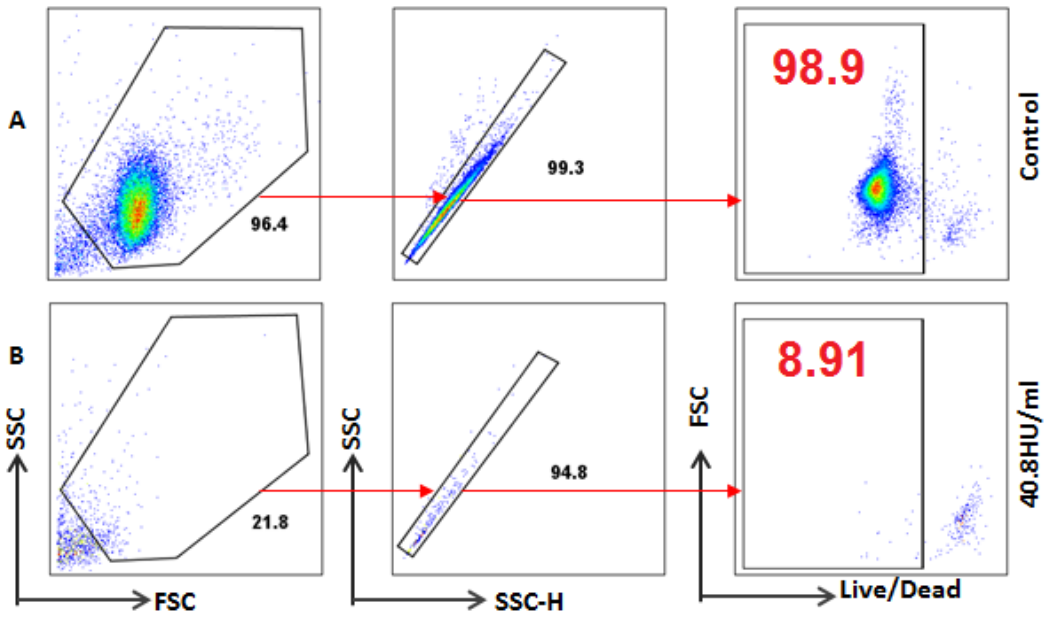

Figure 18: Representative flow cytometry plots for analysis of cell viability in Figure 17 (A)

Neutrophils were treated for 45 minutes with the indicated concentrations of PLY, followed by staining with a Live/dead dye (A) Flow cytometric analysis of untreated control neutrophils. (B) Flow cytometric analysis of neutrophils treated with 40.8 HU PLY/mL. Values in red are the percentage of live cells.

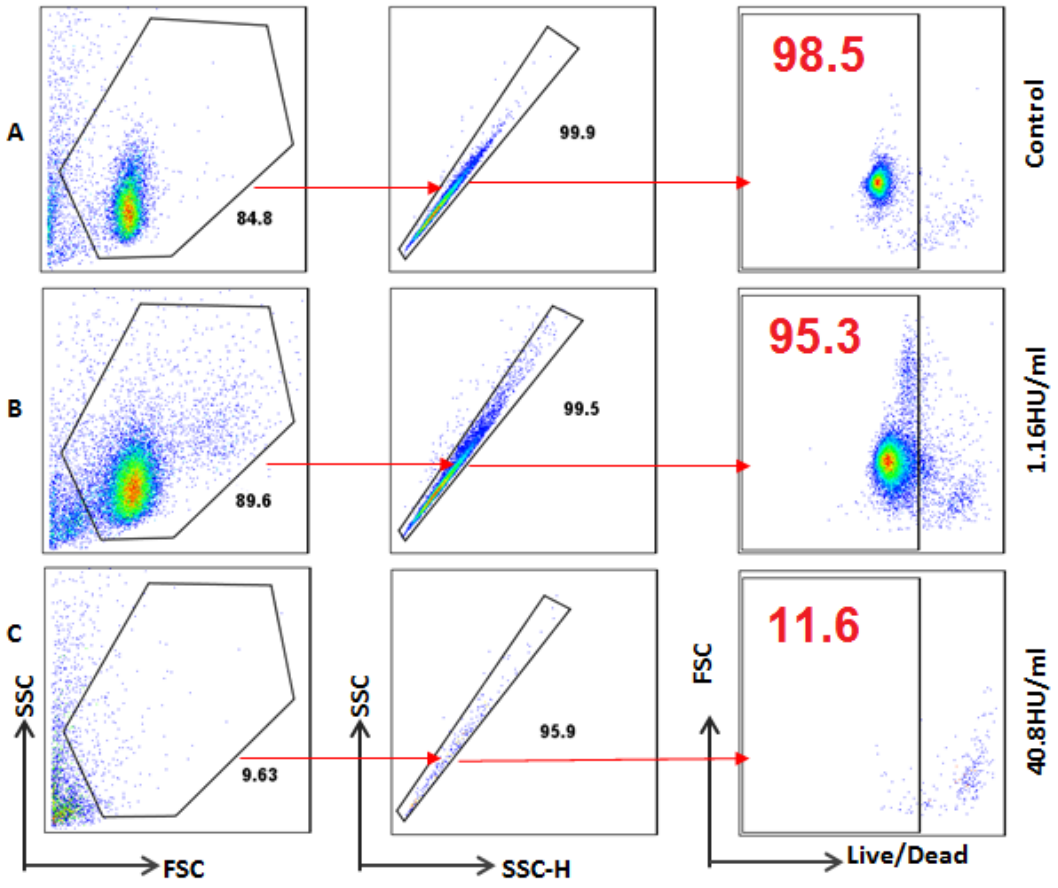

Figure 19: Representative flow cytometry plots for analysis of cell viability in Figure 17 (C)

Neutrophils were treated for 45 minutes with the indicated concentrations of PLY, followed by staining with a Live/dead dye (A) Flow cytometric analysis of untreated control neutrophils. (B) Flow cytometric analysis of neutrophils treated with 1.16 HU PLY/mL. (C) Flow cytometric analysis of neutrophils treated with 40.8 HU PLY/mL. Values in red are the percentage of live cells.

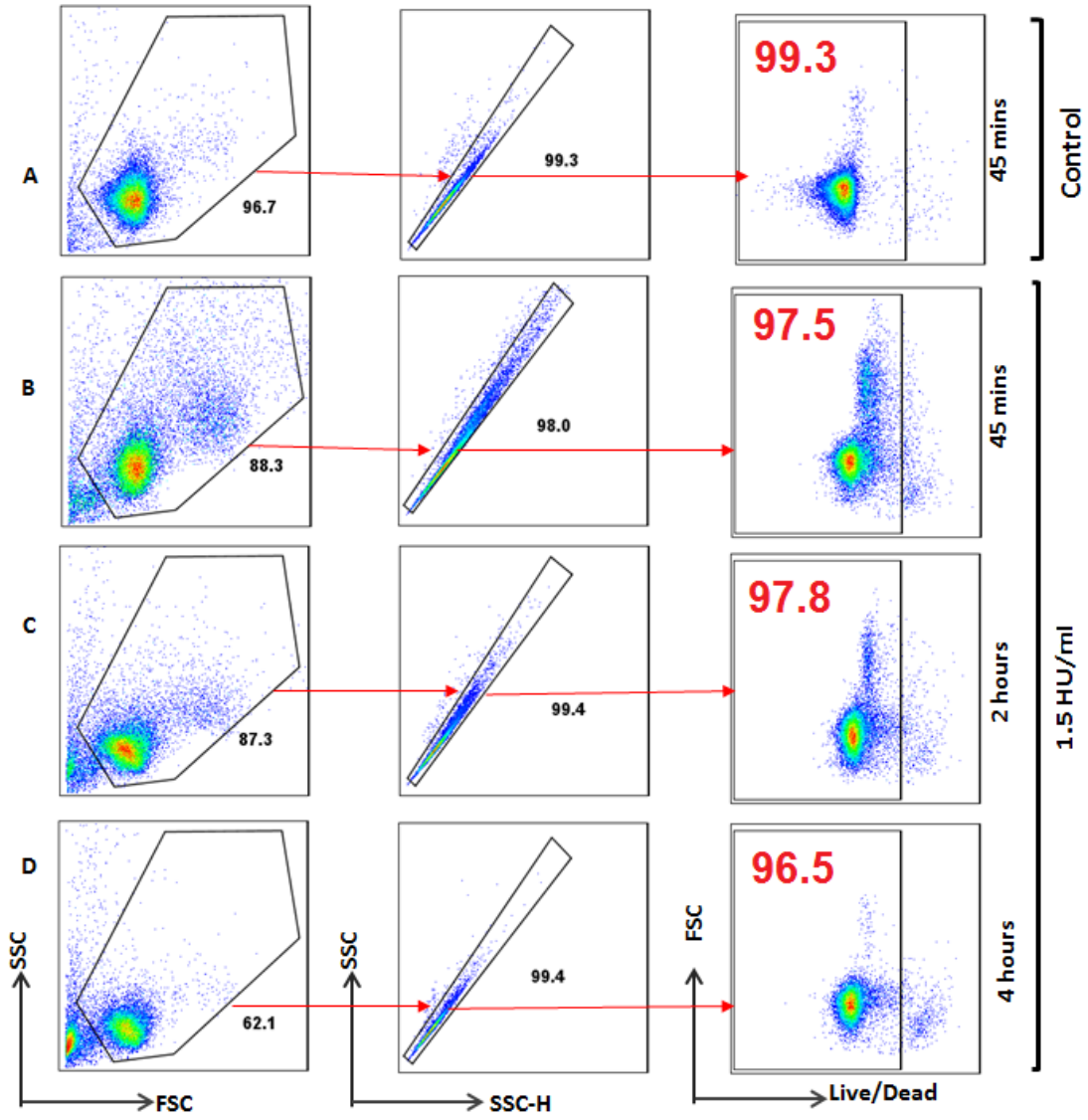

Figure 20: Representative flow cytometry plots for analysis of cell viability in 17(E) Neutrophils were treated for 45 minutes, 2 and 4 hours with 1.5 HU/mL PLY concentration of PLY, followed by staining with a fluorescent LIVE/DEAD dye (A) Flow cytometric analysis of untreated control neutrophils. (B-D) Flow cytometric analysis of neutrophils treated with 1.5HU PLY/mL on three different time points (45 minutes, 2 and 4 hours). Values in red are the percentage of live cells.

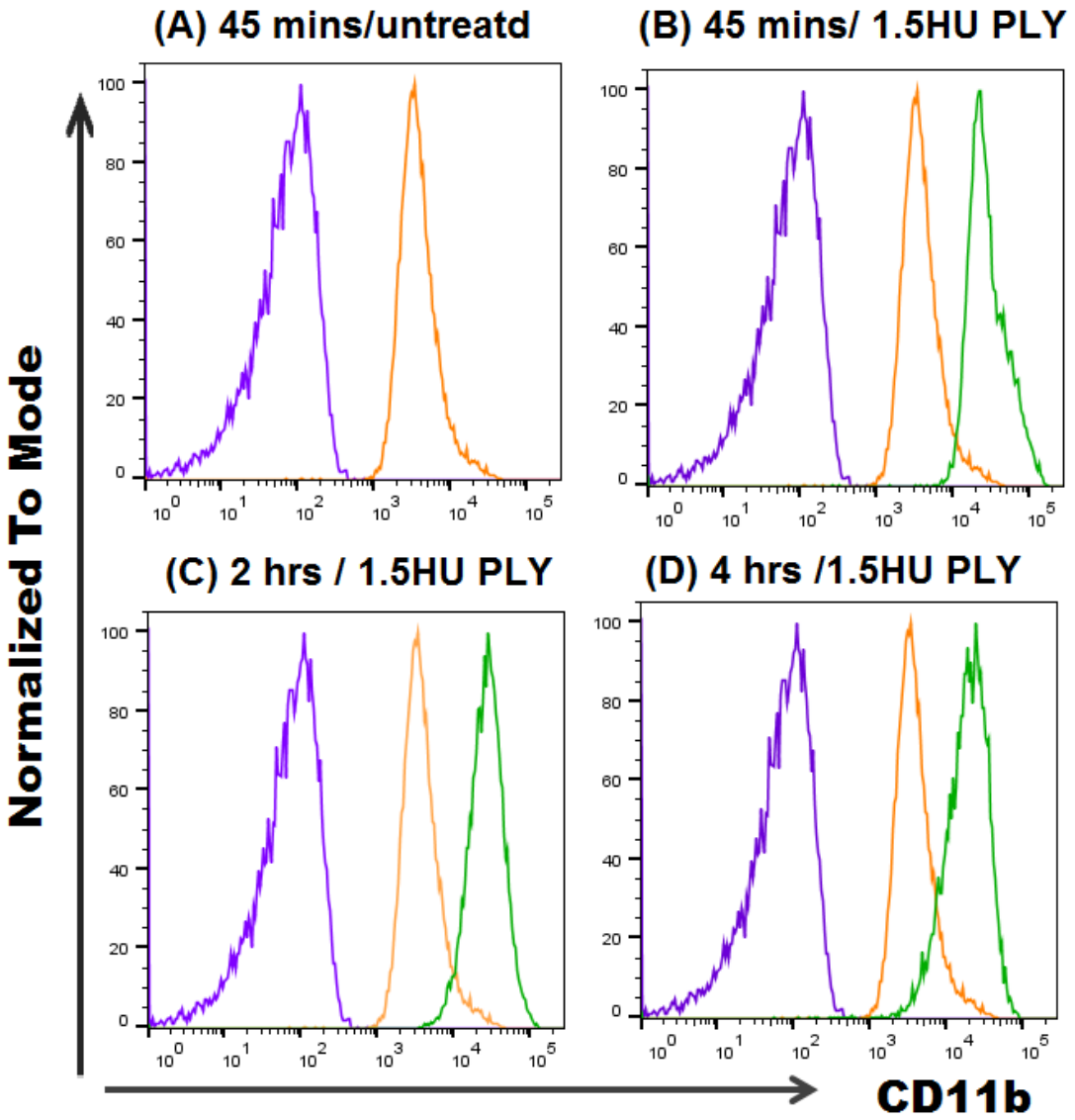

Figure 21: Representative flow cytometry histograms for analysis of CD11b expression on neutrophils treated with PLY in Figure 17(F)

Neutrophils were treated for 45 minutes, 2 and 4 hours with 1.5 HU/mL PLY, followed by staining with a Live/dead dye and an antibody to CD11b. The [purple] peak shows fluorescent intensity of unstained control cells. The [orange] peak shows CD11b staining on untreated neutrophils. The [green] peak shows CD11b staining on neutrophils treated with 1.5HU PLY/mL (A) Flow cytometric analysis of untreated control neutrophils. (B-D) Flow cytometric analysis of neutrophils treated with 1.5 HU PLY/mL for three different time points (45 minutes, 2 and 4 hours) respectively.

.

3.2.3 Neutrophils are more resistant to PLY-mediated cell death than whole bone marrow

Bone marrow derived cells and purified bone marrow neutrophils were treated with increasing concentrations of PLY (0.2 – 10 HU/mL), stained with a fluorescent live/dead dye, and analysed by flow cytometry. Interestingly, we found out that whole bone marrow was notably more susceptible to PLY-induced cell death than purified neutrophils (Figure 22). Flow cytometric analysis showed that the remaining cells were predominantly B cells ($CD45R^+$) and T cells ($CD3^+$), suggesting that lymphocytes are more sensitive to PLY than neutrophils (Figure 23).

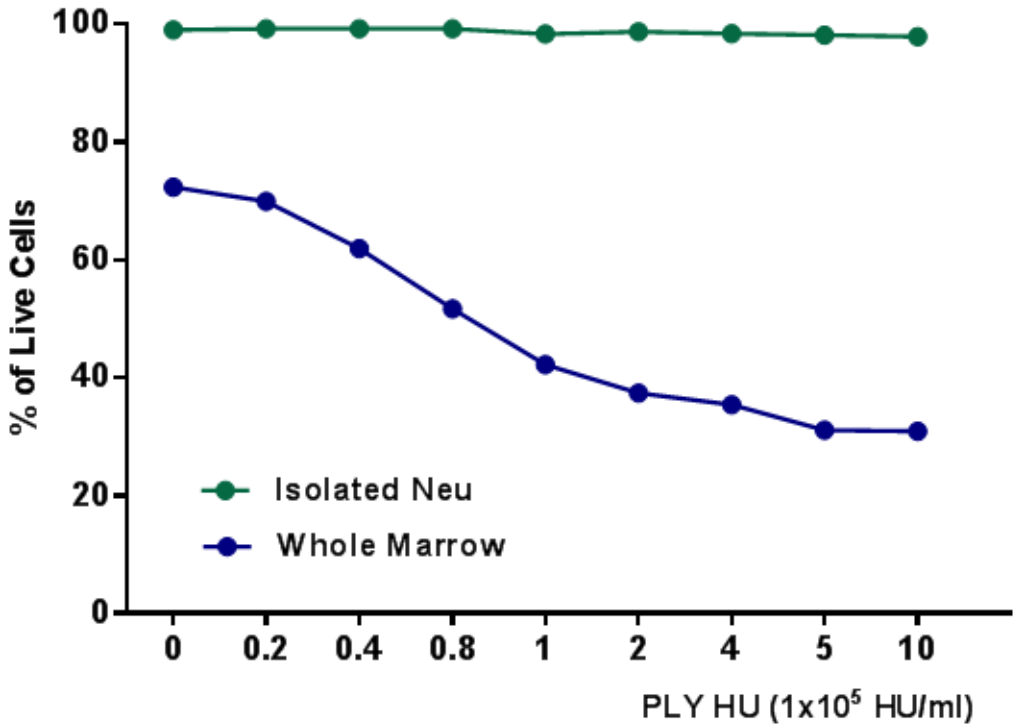

Figure 22: Neutrophils are more resistant to PLY-mediated cell death than whole bone marrow
Whole bone marrow and purified neutrophils were treated for 30 minutes with the indicated concentrations of PLY, before being stained with a fluorescent LIVE/DEAD dye and analysed by flow cytometry. Graph depicts the percentage of live cells.

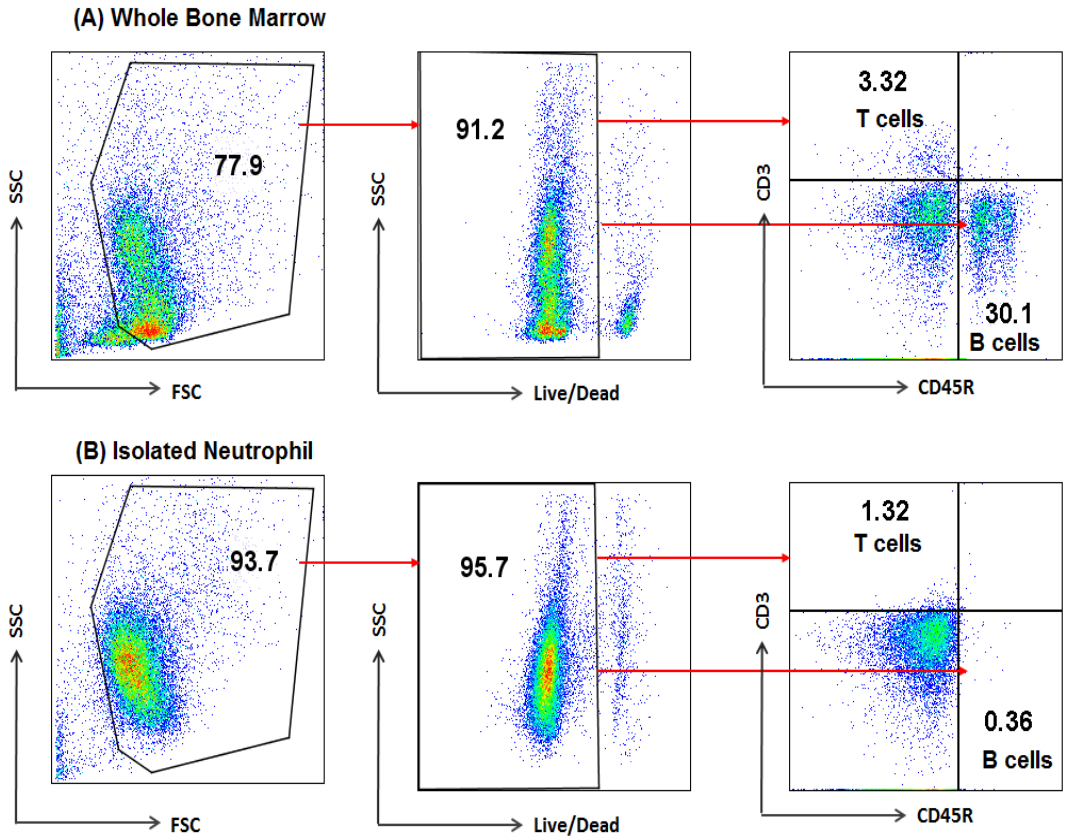

Figure 23: Representative flow cytometry plots for analysis of CD3 and CD45R expression on neutrophil and whole bone marrow treated PLY in Figure 22

Flow cytometry analysis of whole marrow and purified neutrophils using MACS Neutrophil Isolation kit. (A)Whole bone marrow and (B) Isolated neutrophils; From left to right, plots show discrimination of live cells based on forward and side scatter and next discrimination of live cells based on fluorescent LIVE/DEAD dye staining, percentage of cells stained with $CD45R^{+}$ (for B cells) and percentage of cells stained with $CD3^{+}$ (for T cells). Data are from a single preliminary experiment.

3.2.4 Optimisation of neutrophil transwell chemotaxis assay

The effect of PLY on neutrophil migration was first assessed using a basic transwell chemotaxis assay, which essentially models cell migration in 2D. Transwell® plates consist of a lower and an upper compartment separated by a porous membrane. Cells are plated in the upper compartment and the lower compartment is filled with media containing a neutrophil chemoattractant (KC). Next, cells are left to migrate for an appropriate time. The absolute number of cells migrating (from upper to lower compartment) through the Transwell® membrane is then determined by counting cells settling in the lower compartment.

To optimise this assay, we tested varying concentrations of the neutrophil chemoattractant, KC, and varying concentrations of FCS, in order to find a combination that produced high levels of neutrophil chemoattraction through the transwell, when compared to control wells lacking chemokine. $1x10^5$ cells neutrophils were added to the upper compartment, and 150μL of media (with or without KC) added to the lower compartment of a 96-well Transwell® plate. Migration was checked after 30 minutes using a light microscope, and the total number of neutrophils that had migrated to the lower compartment was counted using a MACS Quant Analyser. In the absence of FCS, cell migration toward 1μg/mL KC was twice that of the observed migration toward 100ng/mL KC. There was essentially no difference between the two chemokine concentrations on other conditions. In the presence of FCS, neutrophil chemotaxis increased above background levels but again there was no difference between the two chemokine concentrations (Figure 24). Therefore, 2% FCS, with 100ng/mL KC was used for all future experiments.

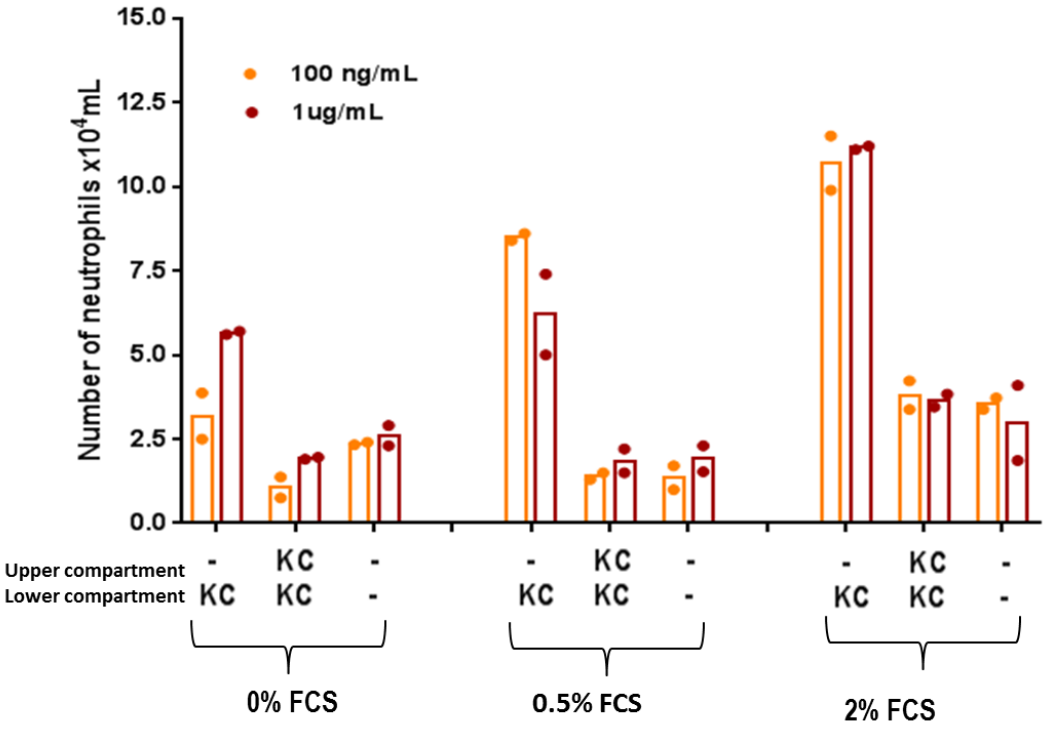

Figure 24: Optimisation of neutrophil Transwell chemotaxis assay
The neutrophils were placed into the upper compartment of 96-wells Transwell® plate. Chemoattractant (KC; 100ng/mL and 1µg/mL) was placed in the lower compartment to establish a gradient, or in both compartments to provide uniform stimulation of the cells. RPMI-1640 with three different percentages of FCS (0%, 0.5% and 2%) was utilised as indicated. The plate was incubated at 37°C for 30 minutes. The absolute number of neutrophils migrating (from upper to lower compartment) through Transwell® membrane was determined by counting neutrophils settling in the lower compartment using a MACS Quant Analyser. Graph depicts the total number of neutrophils migrating into the lower compartment for each condition. Data are from single experiment.

3.2.5 PLY inhibits neutrophil chemotaxis in a 2D Transwell Chemotaxis Assay

The optimised Transwell chemotaxis assay was used to assess the effect of PLY on neutrophil chemotaxis to KC. PLY significantly inhibited neutrophil chemotaxis towards KC, when compared to untreated control cells (Figure 25). PdB, a toxoid form of PLY mutant with dramatically reduced haemolytic activity, had no effect on neutrophil chemotaxis, suggesting that the pore forming function of the toxin is required for inhibition of neutrophil chemotaxis (Figure 25A). In some experiments, neutrophils were treated with LPS as an additional control. LPS also had no effect on neutrophil chemotaxis, indicating that any remaining LPS contamination in the PLY

samples was not responsible for the observed effects on neutrophil migration (Figure 25B).

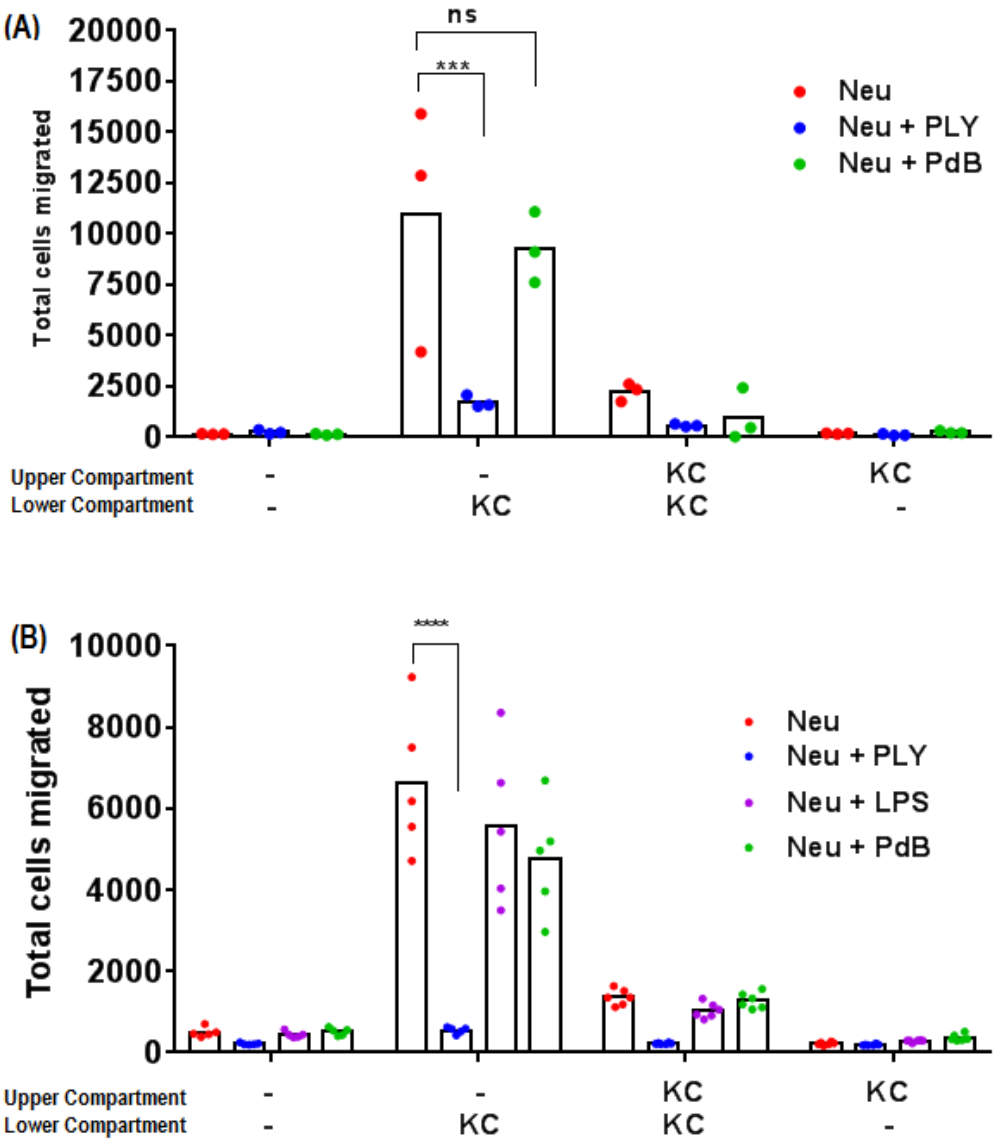

Figure 25: PLY inhibits neutrophil chemotaxis in a 2D Transwell Chemotaxis Assay
Neutrophils were treated with PLY, PdB or LPS and placed in the upper well of a 96-Transwell® plate. Chemotaxis towards KC placed in the lower compartment was assessed by counting the total number of migrated cells on a MACS Quant Analyser. (A-B) Graphs depict the total number of neutrophils migrating to the lower compartment under the indicated conditions. Untreated neutrophils are shown in red, PLY treated neutrophil in blue, LPS-treated neutrophils in purple, and PdB treated neutrophils in green. Each dot represents a single well of an assay performed in triplicate or greater. (A) Data are representative of 5 independent experiments with 3 - 4 replicate wells and (B) Data are representative of 2 independent experiments with 5 - 6 replicate wells. Statistical significance determined using two-way ANOVA with Tukey's multiple comparison ($p<0.05$) with *** ($p<0.001$),**** ($p<0.0001$) and ns denote not significant.

3.2.6 PLY-mediated inhibition of neutrophil chemotaxis cannot be solely explained by loss of cell viability.

Inhibition of neutrophil chemotaxis was not observed in the presence of PdB, a toxoid derivative of PLY with dramatically reduced haemolytic activity. To confirm that reduced migration was not driven solely by reduced viability of the neutrophils in the presence of PLY, flow cytometric analysis of cell viability was again performed. At conclusion of the experiment depicted in Figure 25A approximately 95% of cells were still viable, regardless of exposure to PLY (Figure 26C). For the experiment depicted in Figure 25B, a small reduction in cell viability was observed following PLY treatment. However this 23.0% reduction in viability cannot solely explain the more dramatic 91.7% reduction in cell migration.

We concluded from this experiment that treatment of neutrophils with PLY inhibits chemotaxis to KC, and that this effect cannot be explained solely by loss of cell viability.

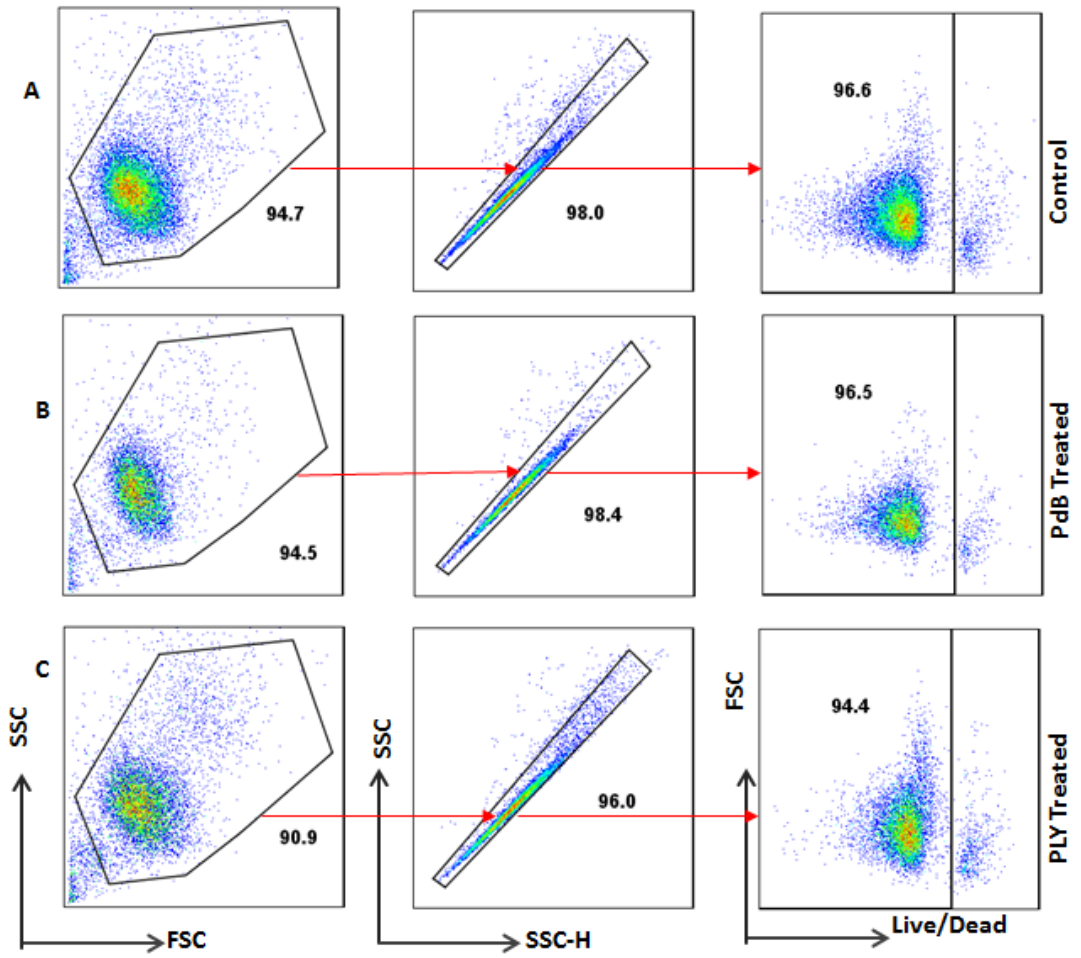

Figure 26 : Representative flow cytometry analysis of cell viability at conclusion of the chemotaxis assay in Figure 25(A)

Neutrophils were left untreated, or treated with PLY or PdB, then placed in the lower compartment of a transwell plate for the duration of the chemotaxis assay. At conclusion of the assay, neutrophils were stained with a fluorescent LIVE/DEAD dye and analysed by flow cytometry. (A) Untreated neutrophils (B) Neutrophils treated PdB (C) neutrophils treated with PLY. Plots are representative of two independent experiments.

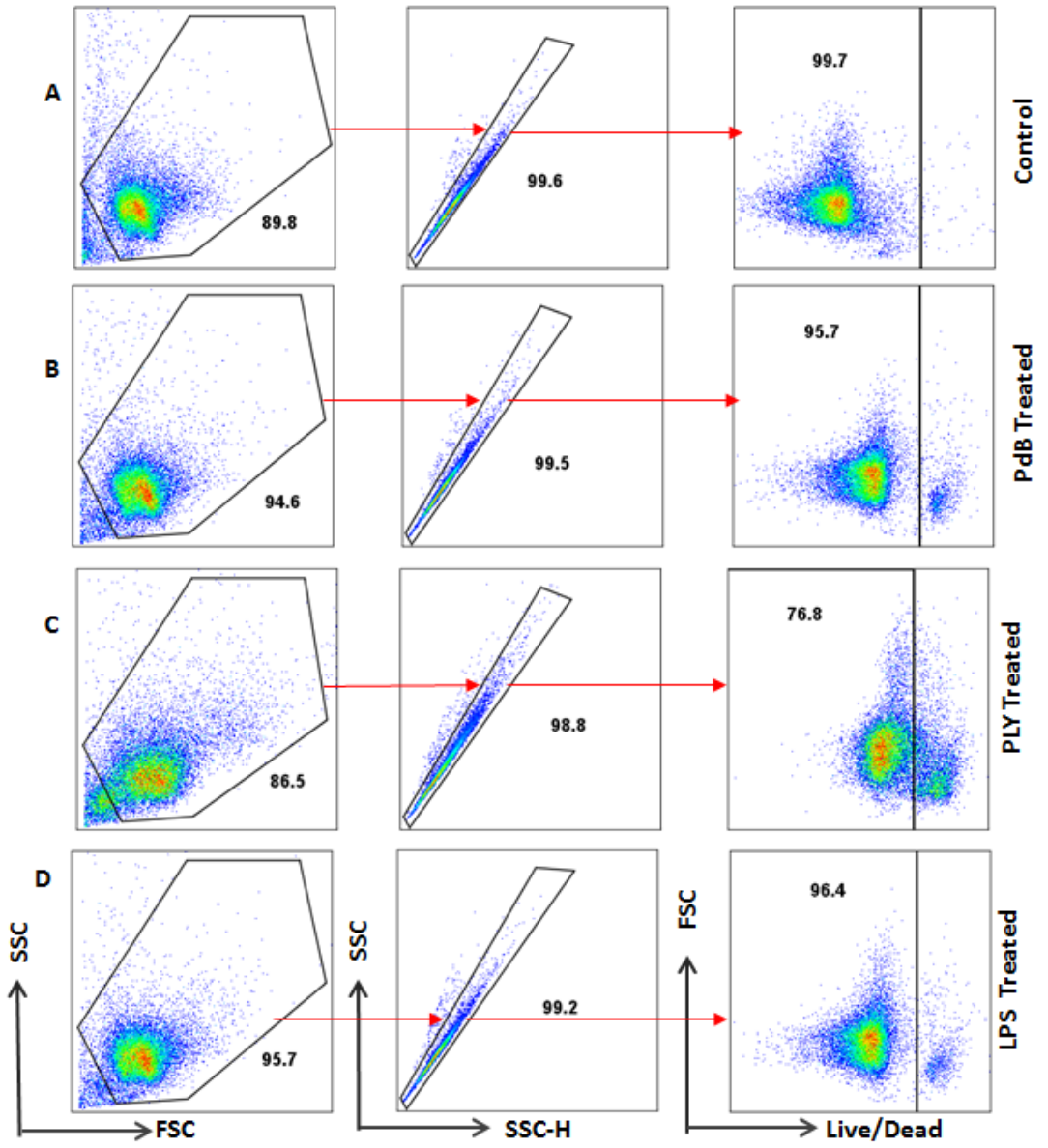

Figure 27: Representative flow cytometry analysis of cell viability at conclusion of the chemotaxis assay in Figure 25(B)

Neutrophils were left untreated, or treated with PLY or PdB, then placed in the lower compartment of a transwell plate for the duration of the chemotaxis assay. At conclusion of the assay, neutrophils were stained with a fluorescent LIVE/DEAD dye and analysed by flow cytometry. (A) Untreated neutrophils (B) Neutrophils treated PdB (C) Neutrophils treated with PLY (D) Neutrophils treated with LPS. Plots are representative of two independent experiments.

3.2.7 PLY does not act as a chemoattractant for neutrophils

The inhibitory effect of PLY on chemotaxis towards KC might be explained by PLY (added with neutrophils to the upper compartment) acting as a chemoattractant, and outcompeting KC (added to the lower compartment). Here, PLY was added to the bottom well of the transwell chemotaxis assay, and its ability to chemoattract neutrophils determined. We found that PLY does not act as chemoattractant for neutrophils in two independent experiments (Figure 28A and 28B). PdB and LPS also did not attract neutrophils. Unexpectedly, PdB had an inhibitory effect on neutrophil chemotaxis when placed in the lower compartment, in one of two experiments analysed. Since this effect was not seen in subsequent experiments, we cannot rule out that it was merely due to a technical issue with the transwell plate.

From these experiments, we concluded PLY does not act as chemoattractant for neutrophils. Therefore, PLY-mediated inhibition of neutrophil chemotaxis cannot be explained by PLY outcompeting KC as a chemoattractant.

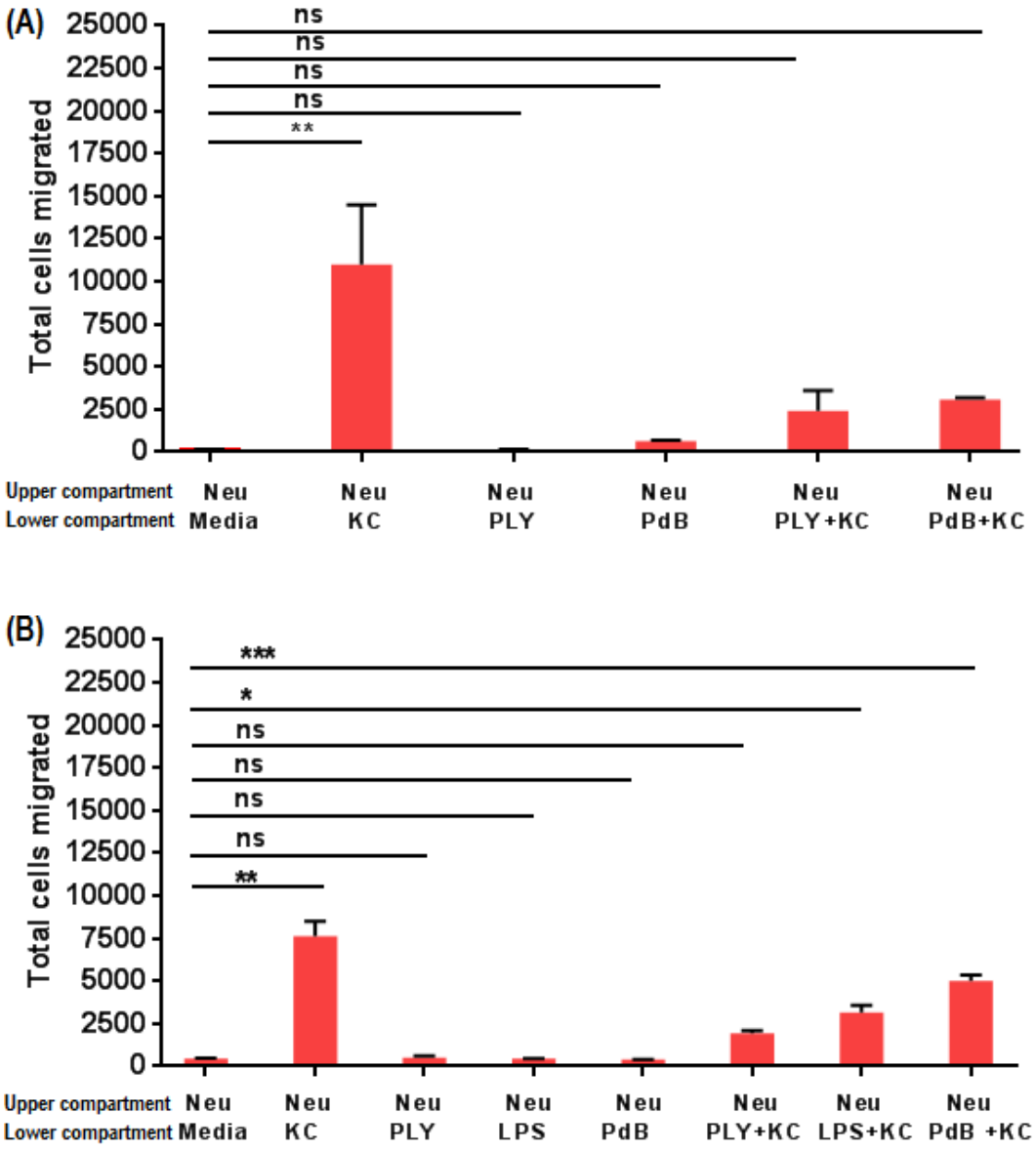

Figure 28: PLY does not act as a chemoattractant for neutrophils
Investigation of direct chemotactic effect of; (A) PLY, PdB and (B) PLY, PdB and LPS on neutrophils. Neutrophils were placed in the upper compartment of transwell, and PLY, PdB, LPS with or without KC placed in the lower compartment. Neutrophil chemotaxis towards PLY, PdB and LPS was assessed after 45 minutes migration. Mean $\pm$ SEM of triplicate wells. Data representative of 3 independent experiment for (A) and 2 independent experiment for (B). Statistical significance determined using one-way ANOVA with Tukey's multiple comparison with *($p<0.05$), **($p<0.01$),***($p<0.001$) and ns denote not significant.

3.2.8 Neutrophil chemotaxis is inhibited following incubation with live *S. pneumoniae*

We next assessed the effect of live bacteria on neutrophil chemotaxis. Pneumolysin (PLY) is expressed by virtually all clinical isolates of this pathogen (Rubins & Janoff 1998). To confirm the role of PLY in inhibiting neutrophil chemotaxis, I used different bacterial serotypes with varying levels of haemolytic activity in our *in vitro* chemotaxis assay. I used two serotype 1 clinical isolates: ST217, which is highly haemolytic, and ST306, which is non-haemolytic. I also included a serotype 2 (strain D39), and PLN-A, a PLY-deficient mutant of D39. Heat killed D39 was included as a control, in addition to PdB (non-lytic toxoid of PLY, with a Trp-433/Phe mutation)(Paton et al. 1991) and LPS (endotoxin of Gram negative bacteria). I then compared the ability of different strains of live bacteria to inhibit neutrophil chemotaxis with PLY.

3.2.8.1 Selection of an MOI that does not cause loss of neutrophil viability.

In order to study the effect of live bacteria on neutrophil chemotaxis, we needed to determine that co-incubation of neutrophils with bacteria would not adversely affect neutrophil viability. Since the purified PLY used at the beginning of the chapter came from the D39 strain background, D39 was used for the initial experiments.

Neutrophils were incubated with varying MOIs of D39, for 45 minutes, followed by staining with a fluorescent LIVE/DEAD dye and analysed by flow cytometry. Neutrophils were further stained with CD11b to check that sufficient bacteria were present to trigger a response in the neutrophils. We tested an MOI range of 0 – 50 (Table 9) in two separate experiments. Neutrophil viability remained high in the

presence of all concentrations of bacteria. CD11b expression was increased at MOI >10 (Figure 29). An MOI of 10 was therefore selected for chemotaxis experiments

Table 9: MOI Ratio of D39 strain bacteria infected on neutrophils
The highlighted box orange in color indicated the chosen MOI for the experiment

MOI	Live /Dead Staining	CD11b-MFI Ratio
50	**89.7 %**	**5.3**
25	**90.1%**	**4.2**
5	**95.6%**	**2.9**
0	**94.5%**	**-**
25	**97.2%**	**1.9**
10	**96.2%**	**1.8**
5	**99.2%**	**1.2**
2.5	**99.2%**	**1.0**
1	**99.2%**	**0.86**
0.5	**99.5%**	**0.66**
0	**97.6%**	**-**

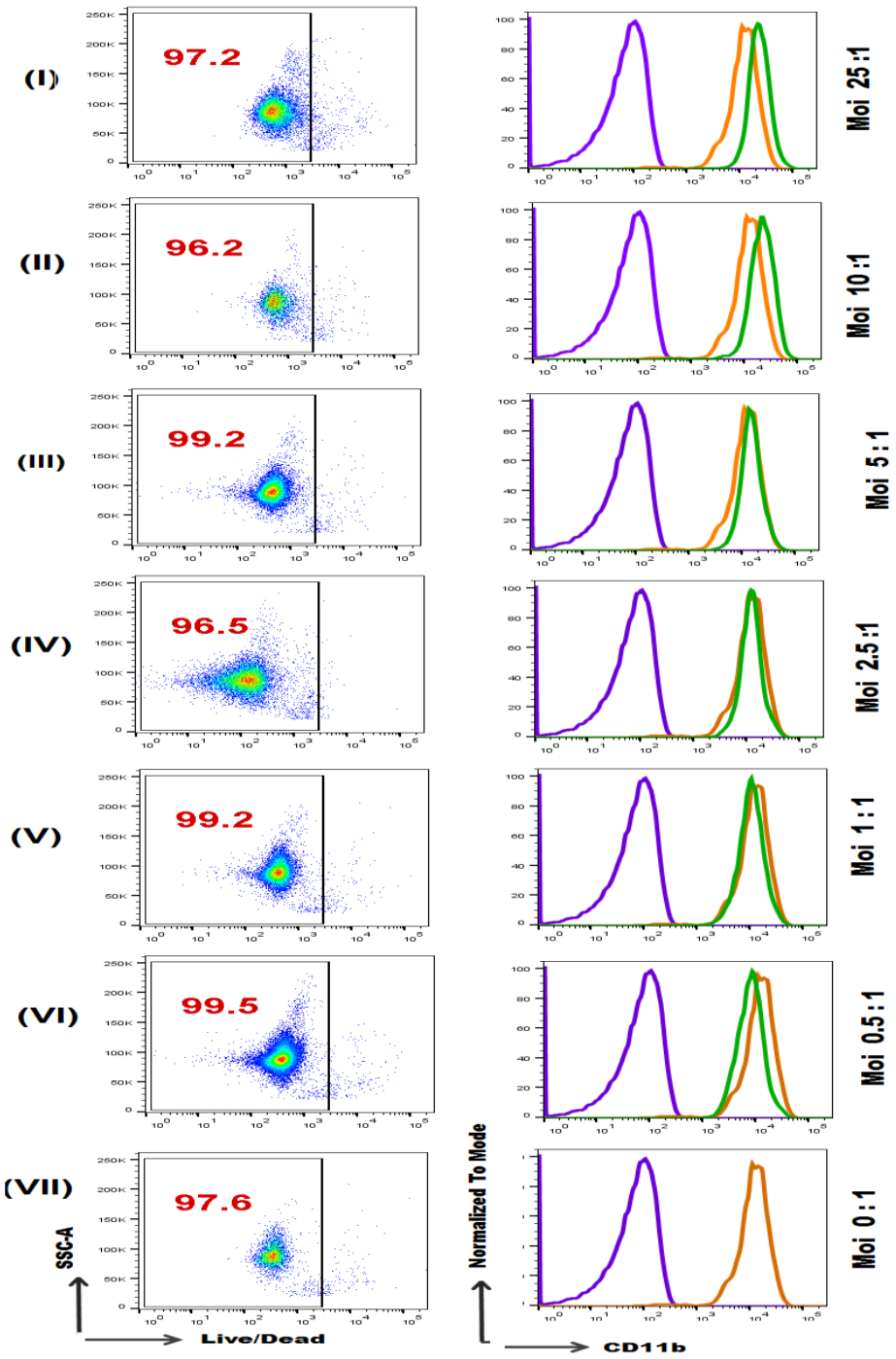

Figure 29: Cell viability and CD11b expression on neutrophils following incubation with varying MOI of D39

Neutrophils were incubated for 45 minutes with varying MOI of D39, serotype 2 bacteria, and stained with a fluorescent LIVE/DEAD dye and antibody to CD11b. (I-VII) Flow cytometry analysis of neutrophil viability (left column) and CD11b expression (right column) following incubation with the indicated MOI of D39, serotype 2 bacteria. The [purple] peak shows fluorescent intensity of unstained control cells. The [orange] peak shows CD11b staining on untreated neutrophils. The [green] peak shows CD11b staining on neutrophils treated with bacteria.

3.2.8.2 Effect of different *S. pneumoniae* isolates on neutrophil chemotaxis in 2D

Purified PLY inhibited neutrophil chemotaxis in the assays described in 3.2.5. To determine if live *S. pneumoniae* has a similar effect, and if it is dependent on PLY, we compared the ability of a panel of *S. pneumoniae* isolates with varying haemolytic activity to inhibit neutrophil chemotaxis in 2D. Neutrophils were mixed with PLY, PdB, LPS, or the panel of *S. pneumoniae* strains listed in Table 10, and placed in the upper compartment of a transwell plate. Migration towards KC, which was placed in the lower compartment, was assessed after 45 minutes.

Table 10: List of bacterial stock strains (highlighted in green) and trigger molecules

Strains/ trigger molecules	Description
D39	*S pneumoniae* serotype 2 (strain D39)
D39 HK	serotype 2, (strain D39) heat killed
Pln-A	pneumolysin deficient mutant of (strain D39)
ST217	clinical isolate of serotype 1, highly haemolytic
ST306	clinical isolate of serotype 1, non-haemolytic
PLY	Pneumolysin hemolytic
PdB	toxoid derivative of pneumolysin (mutation at Trp-433/Phe)(Paton et al. 1991)
LPS	lipopolysaccharide (endotoxin) of gram negative bacteria

Neutrophils were incubated with different *S.pneumoniae* isolates and placed in the upper compartments of transwell plate and incubated for 45 minutes then the total number of cells migrated to the lower compartment were counted. As expected, PLY inhibited neutrophil chemotaxis to KC, while PdB and LPS had minimal effects. Like PLY, D39 inhibited neutrophil chemotaxis to KC. As expected, heat killed D39, ST306 and PLN-A inhibited neutrophil chemotaxis to a lesser extent than PLY or D39 (Figure 30). However, the highly haemolytic isolate ST217 also inhibited

neutrophil chemotaxis but to a lesser extent compared to D39 or PLY (comparable to ST306). The inhibition of neutrophil chemotaxis by multiple strains of bacteria (and independently of PLY presence or haemolytic activity) may suggest the presence of other virulence factors besides the pore forming activities of PLY. In addition, I wanted to examine whether any of the bacterial strains had chemotactic effects on neutrophils. We showed that neutrophil migration across the transwell was enhanced when ST217, or ST306 were placed in the lower compartment, however D39, D39 HK, PLN-A PLY, PdB, and LPS showed no significant chemoattractive effect on neutrophils when compared to media alone (Figure 31).

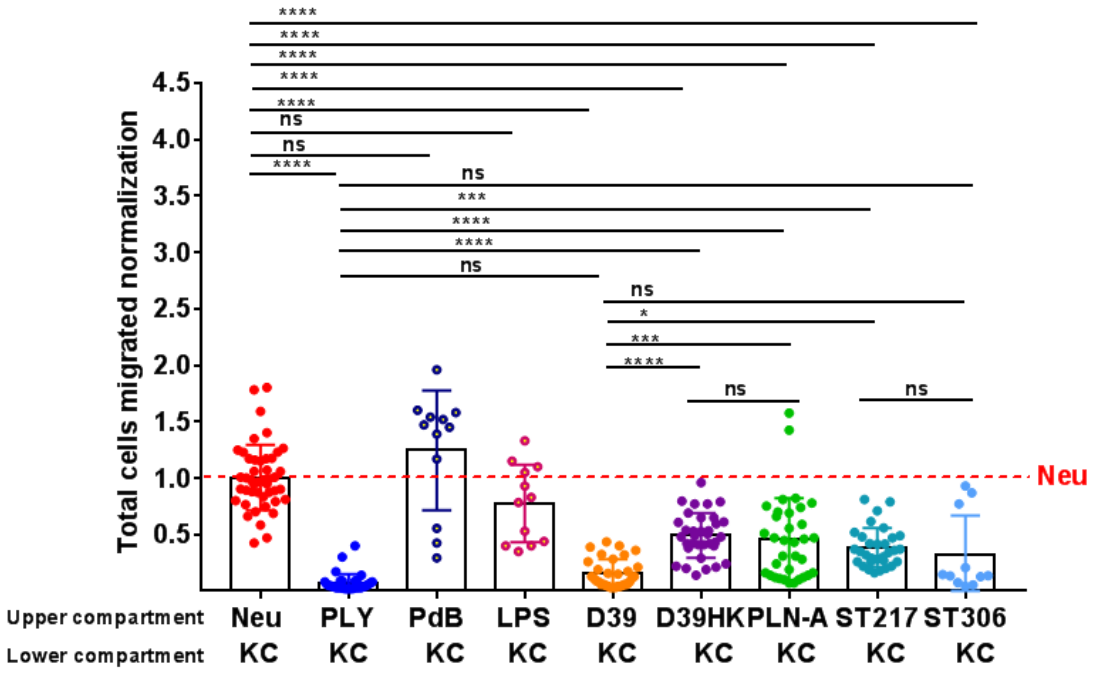

Figure 30: Effect of different *S. pneumoniae* isolates on neutrophil chemotaxis in 2D
Neutrophils were treated with the indicated stimuli and bacterial strains, and placed in the upper compartment of a transwell plate. After 45 minutes the total number of cells migrating towards KC in the lower compartment was assessed using a MACS Quant flow cytometer. Data are compiled from at least 3 independent experiments for each condition, and are normalised to the mean total number of neutrophils migrating towards KC in the absence of any bacterial stimulus, in each experiment. Each dot represents a single well from one of at least three independent experiments per condition. Statistical significance was determined using one-way ANOVA with Tukey's multiple comparisons test, with *($p<0.05$), ***($p<0.001$) and ****($p<0.0001$) and ns denote not significant.

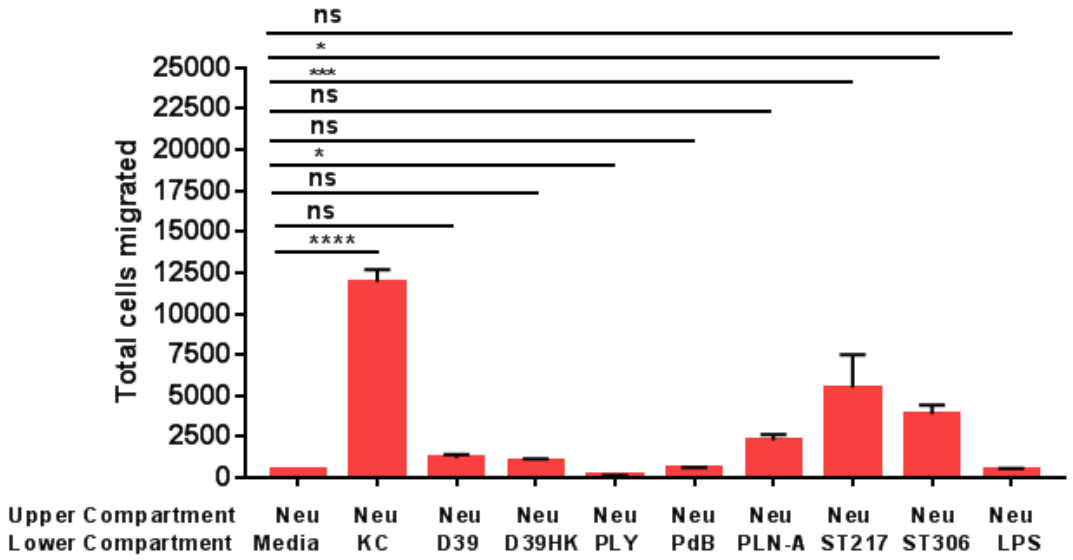

Figure 31: Effect of different stimuli on neutrophil migration
Investigation of the direct chemotactic effect of the indicated stimuli towards neutrophils. Here, neutrophils were placed in the upper compartment of the transwell, and all other stimuli in the lower compartment. Neutrophil chemotaxis from the upper compartment into the lower compartment was assessed by counting migrated cells on the MACS Quant. Graph depicts mean ± SEM for 4 replicate wells. Data are representative of two independent experiments. Statistical significance determined using one-way ANOVA with Bonferroni's multiple comparison, with *($p<0.05$), ***($p<0.001$), ****($p<0.0001$), and ns denote not significant.

3.2.8.3 Cell viability and CD11b expression on neutrophils following incubation with different *S. pneumoniae* isolates

To confirm that the observed reduction in neutrophil chemotaxis in the presence of live bacterial isolates was not due to cell death, we used a LIVE/DEAD dye to analyse neutrophil viability following 45 minutes incubation with different stimuli or *S. pneumoniae* isolates, in addition to CD11b expression on neutrophils. Both chemotaxis and FACS staining were performed concurrently. In Figure 32, we show that more than 90% of neutrophils were still viable at the end of the assay. Meanwhile CD11b expression was significantly increased in the presence of PLY, D39, ST217, but not PdB, D39HK, PLN-A, LPS and ST306 when compared to untreated neutrophils (Figure 33 and Figure 34).

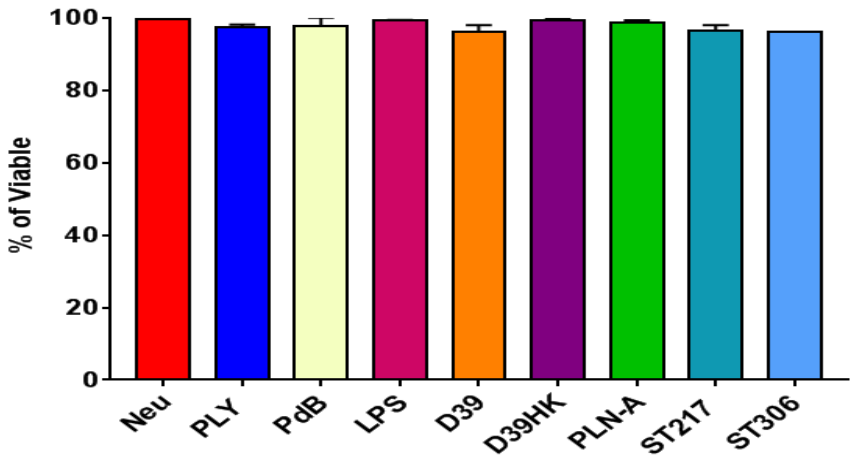

Figure 32: Neutrophil viablity following incubation with *S. pneumoniae* isolates
Neutrophils were treated with the indicated stimuli and after 45 minutes incubation, were stained with a fluorescent LIVE/DEAD dye and analysed on a MACS Quant Flow cytometer. Graph depicts the percentage of viable neutrophils following treatment with the indicated stimuli. Data are combination of 3 experiments except for ST306 from one experiment.

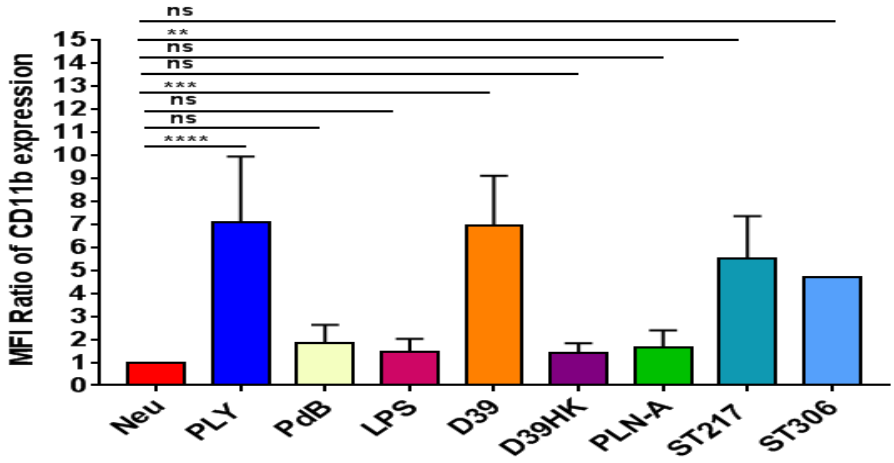

Figure 33: CD11b expression on neutrophils following incubation with *S. pneumoniae* isolates
Neutrophils were treated with the indicated stimuli and after 45 minutes incubation, were stained with a fluorescent LIVE/DEAD dye and an antibody to CD11b and analysed on a MACS Quant Flow cytometer. Graph depicts the fold-change in CD11b expression relative to unstimulated controls following treatment with the indicated stimuli. Data are combination of 3 experiments except for ST306 from one experiment. Statistical significance determined using one-way ANOVA with Tukey's multiple comparison, with **($p<0.01$), ***($p<0.001$), ****($p<0.0001$) and ns denote not significant.

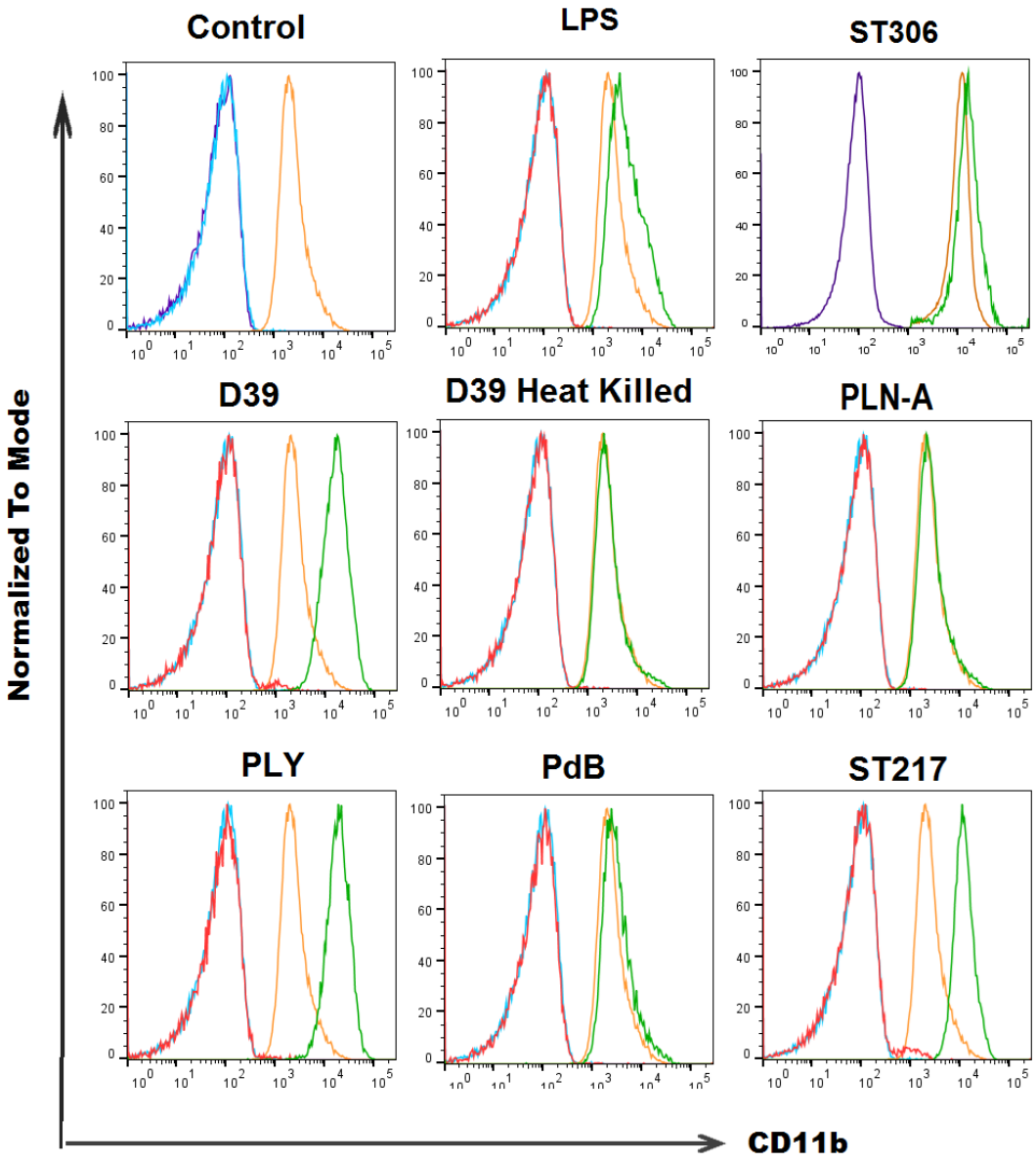

Figure 34: Representative histograms of CD11b expression on neutrophils treated with different stimuli in Figure 33

Neutrophils were treated with different stimuli and placed in the 96-U bottom well and stained with an antibody CD11b before analysis by flow cytometry. The [purple] peak shows fluorescence intensity of unstained control cells. The [blue] peak shows isotype control and [orange] CD11b staining for untreated neutrophils. The [red] peak shows isotype control for treated neutrophils and [green] peak for CD11b staining on treated neutrophils.

3.2.9 Effect of PLY on neutrophil chemotaxis in 3-D

Mechanisms of two-dimensional (2D) migration are different from three-dimensional (3D) migration, whereby cells use adhesion/integrin-independent modes of migration. Furthermore, using 3D migration assays are better representatives of the environment faced by neutrophils once they enter tissue. Therefore, the use of 3D *in vitro* models to mimic the *in vivo* tissue environment will increase the reliability of our understanding of the role of PLY in manipulating neutrophils migration. Here we have used collagen type I gels to represent interstitial migration. Two different 3D chemotaxis models were used, the first one was u-slide chemotaxis 3D chambers from Ibidi® where cells were embedded in a 3D collagen matrix and the migration of cells was recorded and tracked using specialist image analysis software (Fiji/IMARIS). The second model was a Transwell® Invasion Assay, where transwells were overlaid with a fibrous collagen gel, and neutrophils placed on top (details were described in Chapter 2). Neutrophils that migrated through the collagen to the bottom well were collected and counted using the flow cytometer.

3.2.9.1 PLY impairs the ability of neutrophils to chemotaxis in 3D environments.

Using u-slide chemotaxis 3D chambers from Ibidi®, neutrophils were embedded in a 3D collagen matrix and the reservoirs on either side of the matrix filled with either chemoattractant-free or chemoattractant-containing medium to establish a gradient. Collagen type I was chosen for these assays as it forms fibrillar gels that allow tissue interstitium to be modelled *in vitro*. Images were acquired every 60 seconds for a total of 8 hours using a 3i spinning disk confocal microscope. For the first 2 hours of the recorded migration, cells were manually tracked using MTrackJ from ImageJ-

win64 and cell velocity, directionality (confinement index), euclidean distance and accumulated distance were obtained using the Migration and Chemotaxis Tool from ImageJ-win64. Control, PLY, and LPS -treated neutrophils all migrated in the direction of the chemoattractant-containing well, as expected (Figure 35). However, PLY-treated neutrophil migration was more confined (Figure 36 I), and migration appeared to be slower compared to control and LPS treated neutrophils (Figure 36 II). Conversely, LPS treated neutrophils migrated faster, and were less confined in their migration that untreated neutrophils (Figure 35). Cell motility was not analysed after 2 hours, as neutrophils in all conditions showed loss of motility.

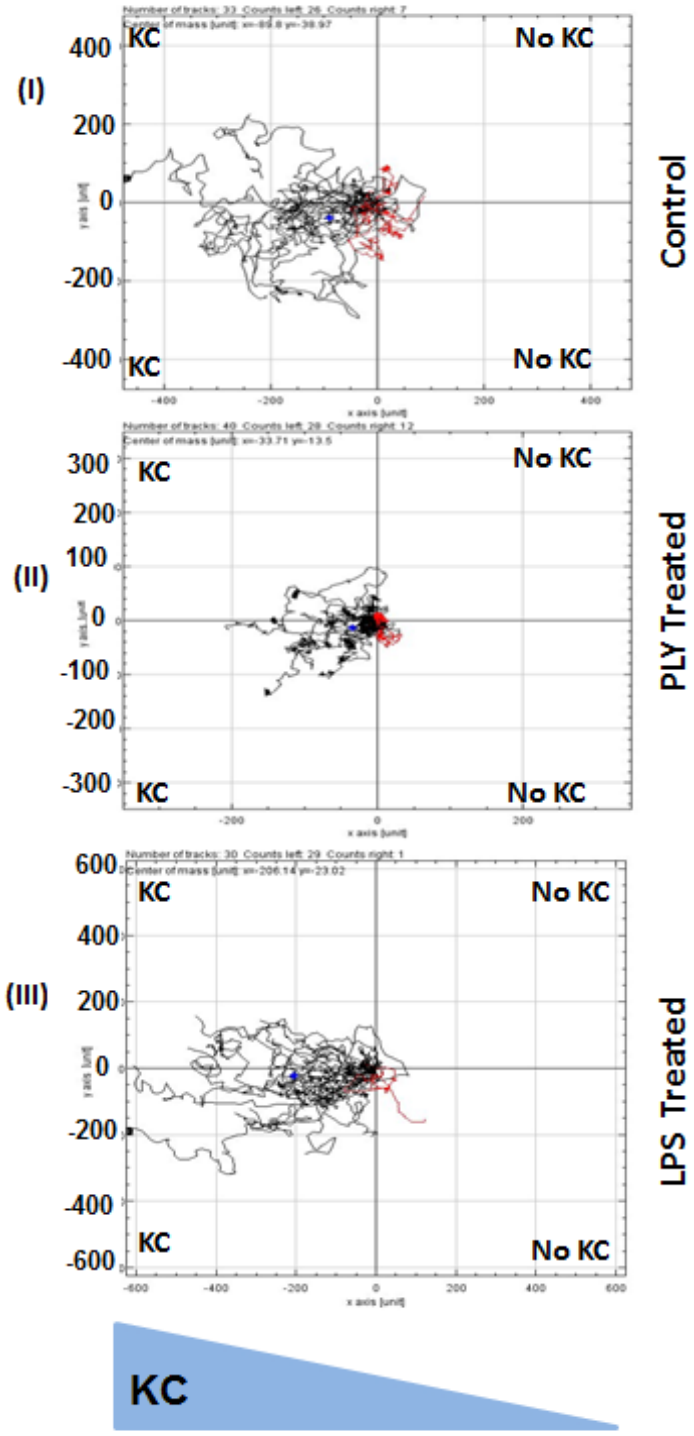

Figure 35: PLY impairs neutrophil ability to migrate toward KC in 3D collagen gels
Representative cell trajectory plots of neutrophil cells embedded in a 1.5mg/mL rat tail collagen type I gel in a u-slide 3D Ibidi® chamber (I) untreated neutrophils, (II) neutrophils treated with PLY and (III) neutrophils treated with LPS. Reservoirs were filled with either (left) chemoattractant-containing (KC) medium or (right) chemoattractant-free and the ability of the neutrophils to migrate towards KC was determined. Movies were recorded for 8 hours using the 3i spinning disk confocal microscope.

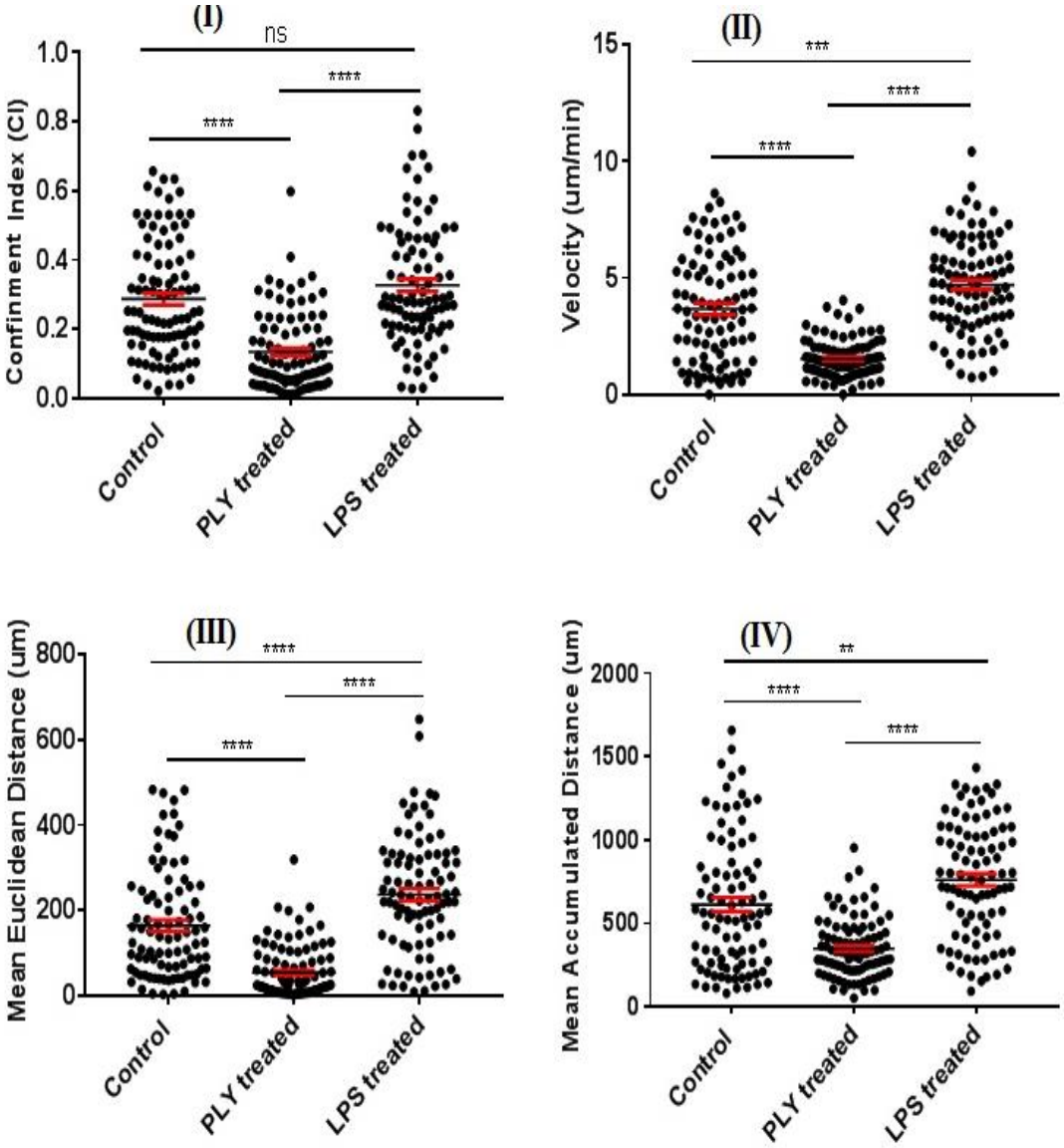

Figure 36: Summary of neutrophil migration characteristics represented in Figure 35
Cells were manually tracked for 2 hours at three different stage positions for each sample (control, PLY treated, LPS treated) (I) Confinement Index (CI), (II) Speed, (III) Mean Euclidean Distance and (IV) Mean Accumulated Distance were calculated. Analysis was done using ImageJ-win64 (Fiji Software) Data represent mean ± SEM. Each point represents an individual cell. Statistical significance was determined using one-way ANOVA with Tukey's multiple comparisons test, with ** ($p<0.01$), *** ($p<0.001$) and ****($p<0.0001$).

3.2.9.2 Pneumolysin (PLY) also inhibits neutrophil migration in a 3D transwell chemotaxis assay

As an alternative approach to assessing neutrophil migration in 3D, we also used Transwell® Invasion Assays where we coated the upper compartment of a transwell plate with a fibrillar type I collagen gel. Neutrophils were placed on the top of the gel and observed for migration to the lower compartment, using KC as a chemoattractant. Neutrophil migration through the collagen gel was found to be inhibited in the presence of PLY, whereas migration was enhanced in the presence of LPS and PdB (Figure 37A). We conclude from this experiment that treatment of neutrophils with PLY can also inhibit neutrophil migration in 3D.

.

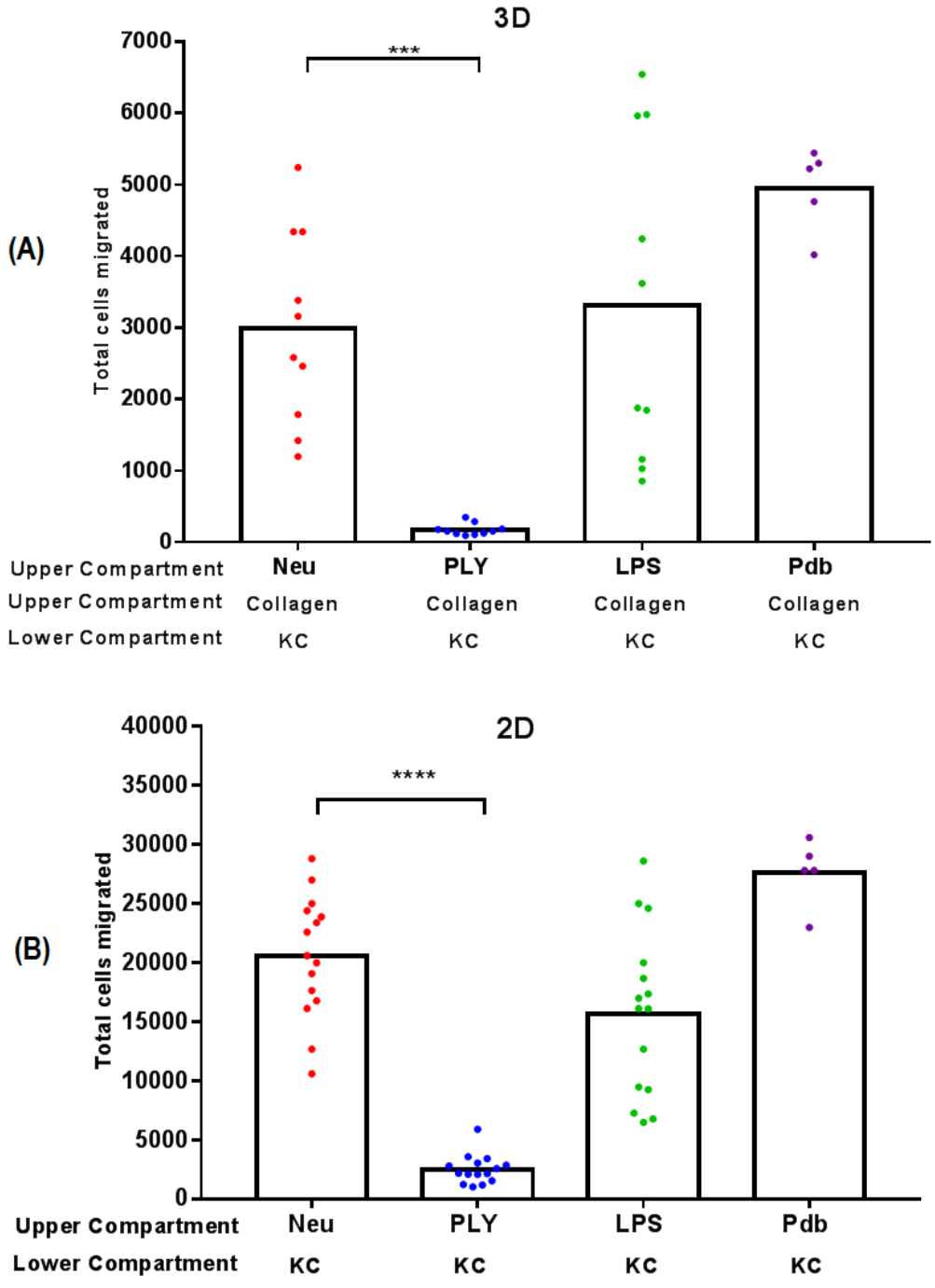

Figure 37: Pneumolysin (PLY) also inhibits neutrophil chemotaxis in 3D
Neutrophils were added to empty transwells (2D) or transwells containing collagen gels (3D). After 2 hours, migration of neutrophils towards KC in the lower compartment were assessed by counting migrated cells on the MACS Quant. (A) Effect of PLY, LPS and PdB on neutrophil 3D chemotaxis towards KC. (B) Effect of PLY, LPS and PdB on neutrophil 2D chemotaxis towards KC. Data are combined from three independent experiments. Statistical significance was determined using one-way ANOVA with Tukey's multiple comparisons test, with *** ($p<0.001$) and **** ($p<0.0001$).

3.2.10 *Ex vivo* experiment on neutrophil migration in lymphatic tissue

Despite the 3D collagen gel model being more representative of the tissue environment faced by neutrophils *in vivo*, key features such as presence of tissue resident cells and tissue-specific structures were missing (Condliffe et al. 2011; Martin et al. 2015; Perez-Castillejos 2010). We therefore wanted to investigate the effect of PLY on neutrophil migration in a living tissue environment. Explant imaging and intravital microscopy studies have been important in offering insight into immune cell migration *in vivo*. Neutrophils are recruited to lymph nodes (LN) following *S. pneumoniae* infection, where they appear to be highly dynamic and exhibit swarming behaviour (Sawtell 2015). We therefore decided to assess neutrophil migration in a lymph node slice model. To confirm that neutrophils are recruited into LN tissue, mice were infected intranasally with a high dose of D39 (10^6 CFU) for 24 hours to induce pneumonia (Kadioglu et al. 2000). Draining mediastinal LN (mLN) were analysed by flow cytometry at 24 hours post-infection. Following infection, neutrophils migrated to mLN, as can be seen in the increased percentage of neutrophils ($Ly6G^+CD11b^+$) in infected mice (Figure 38 and Figure 39).

3.2.10.1 Neutrophil migration in lymphatic tissue is enhanced by treatment with PLY

After confirming that neutrophils can migrate to lymph nodes, we next proceeded to image neutrophil migration in explanted and vibratome-sliced lymph node tissue. For *ex vivo* analysis of neutrophil migration, inguinal LN (iLN) were harvested and embedded in 4% agarose. 400µm slices were cut using a vibratome. Meanwhile, neutrophils were isolated from bone marrow by negative selection and labelled with

CFSE. Labelled cells were overlayed onto iLN slices and incubated for 2 hours to allow them to migrate into the tissue. Neutrophil migration was then assessed by two-photon microscopy. During imaging the sample was perfused with media alone, and later with media containing 1.5 HU PLY/mL.

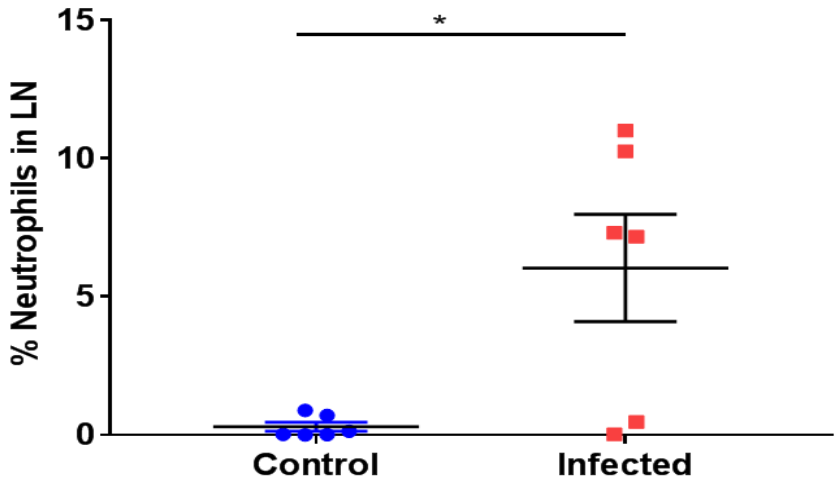

Figure 38: Neutrophils are recruited to mediastinal LN following infection with D39 strain bacteria

CD1 mice were infected intranasally with 10^6 CFU of D39 bacteria. Mice were culled at 24 hours post-infection and samples of mLN were collected from infected (n=6) and sham control (n=6) mice and processed for flow cytometry. Graphs depict proportion of neutrophils ($CD11b^+Ly6G^+$) after gating on $CD45^+$ cells. Mean $\pm$ SEM for 6 mice per condition is shown. Significance of $p<0.05$ was determined using an unpaired t-test (two-tailed) with *($p<0.05$).

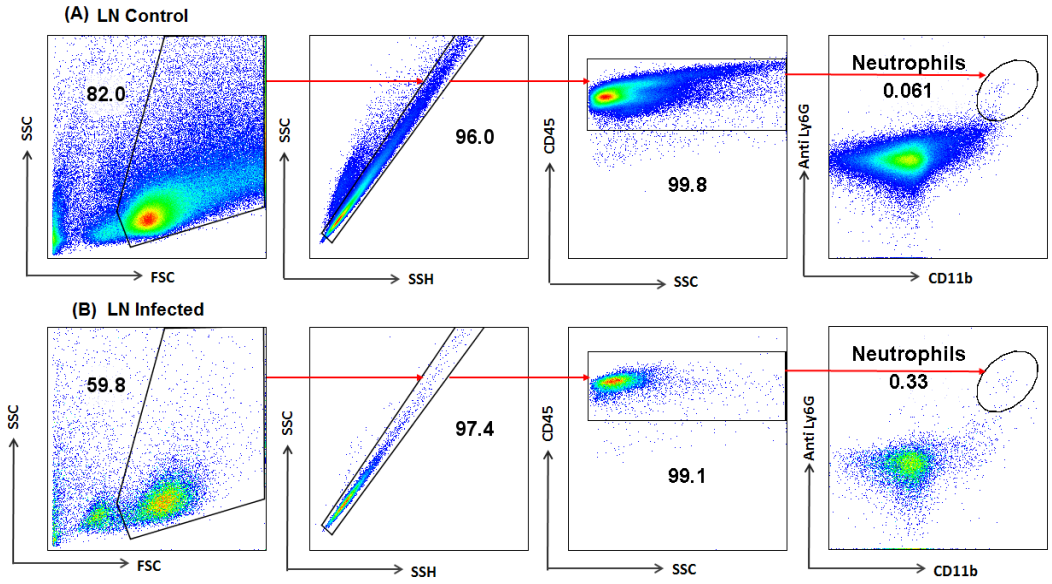

Figure 39: Neutrophils are recruited to mediastinal LN following intranasal infection with D39 strain bacteria

Mice were infected with D39 strain bacteria for 24 hours before mLN tissues were analysed for flow cytometry. First, SSC vs FSC for whole cell gate, next plot show discrimination of single cells from doublets (SSC-H vs SSC-A), and CD45 expression (for leukocyte). Last plot for neutrophils ($CD11b^{+}Ly6G^{+}$) cells were gated on.

Our analysis revealed that neutrophils migrated faster, had longer track lengths and were less confined, following perfusion with 1.5 HU/mL PLY (Figure 40, Figure 41and Figure 42). This result was unexpected, as our 3D chemotaxis assay using u-slide chambers (Figure 35 and Figure 36) showed that PLY inhibited neutrophil migration. However, another two-photon movie recording taken from separate experiment where we perfused lymph node tissues with 1.2 HU/mL PLY showed neutrophil migration did not increase following perfusion with PLY (Figure 43, Figure 44 and Figure 45).

It was therefore possible that PLY-treated neutrophils showed enhanced migration on live tissue dependent on the concentration of PLY. However, this experiment perfusing live tissue with 1.2 HU/mL PLY has only been performed once, and would need to be repeated multiple times to draw any conclusions.

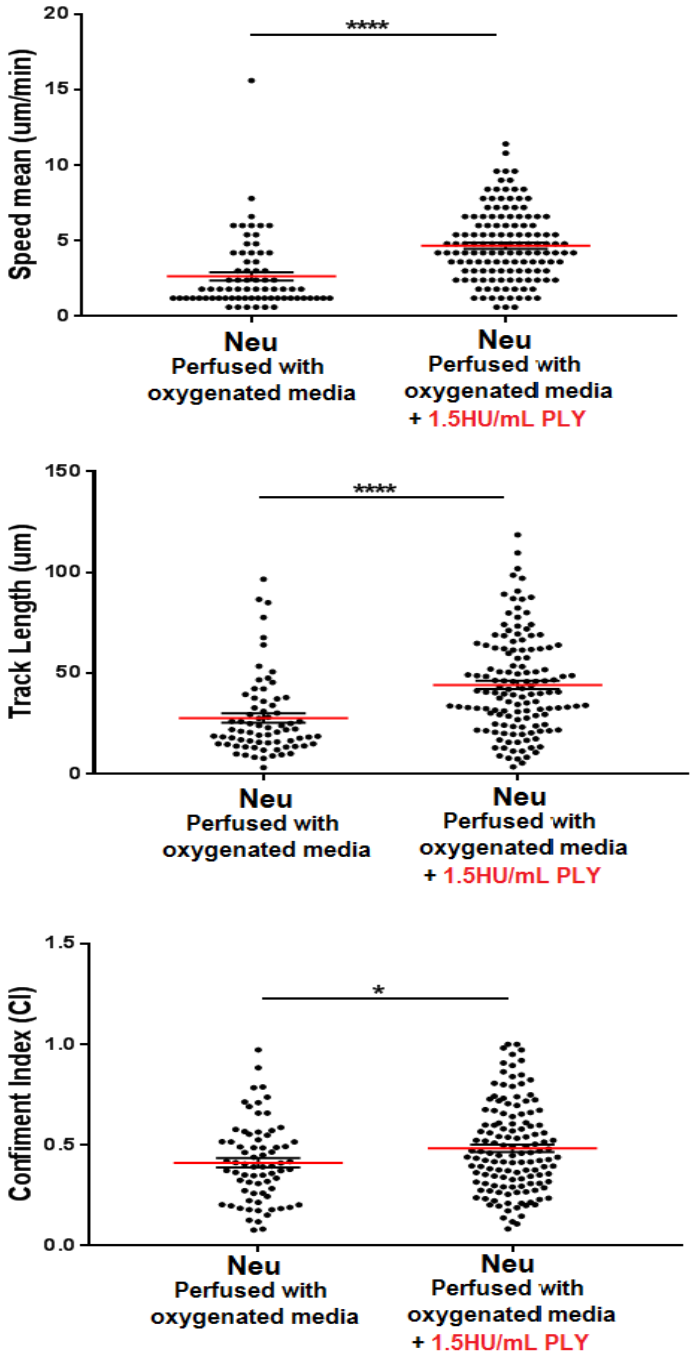

Figure 40: PLY enhanced neutrophil migration in lymphatic tissue
Neutrophils were tracked migrating in LN tissue slices before (left) and after (right) perfusion with 1.5 HU/mL PLY. Two movies per condition were recorded for 15 minutes each. Cell positions were tracked using IMARIS software, and cell speed (top), track length (middle) and confinement index (bottom) calculated. Graph shows mean $\pm$ SEM for 1 movie per condition (recorded at the same tissue position before and after PLY perfusion). Each point represents an individual cell. Statistical significance was determined using unpaired t-test (two-tailed) with *($p<0.05$) and ****($p<0.0001$).

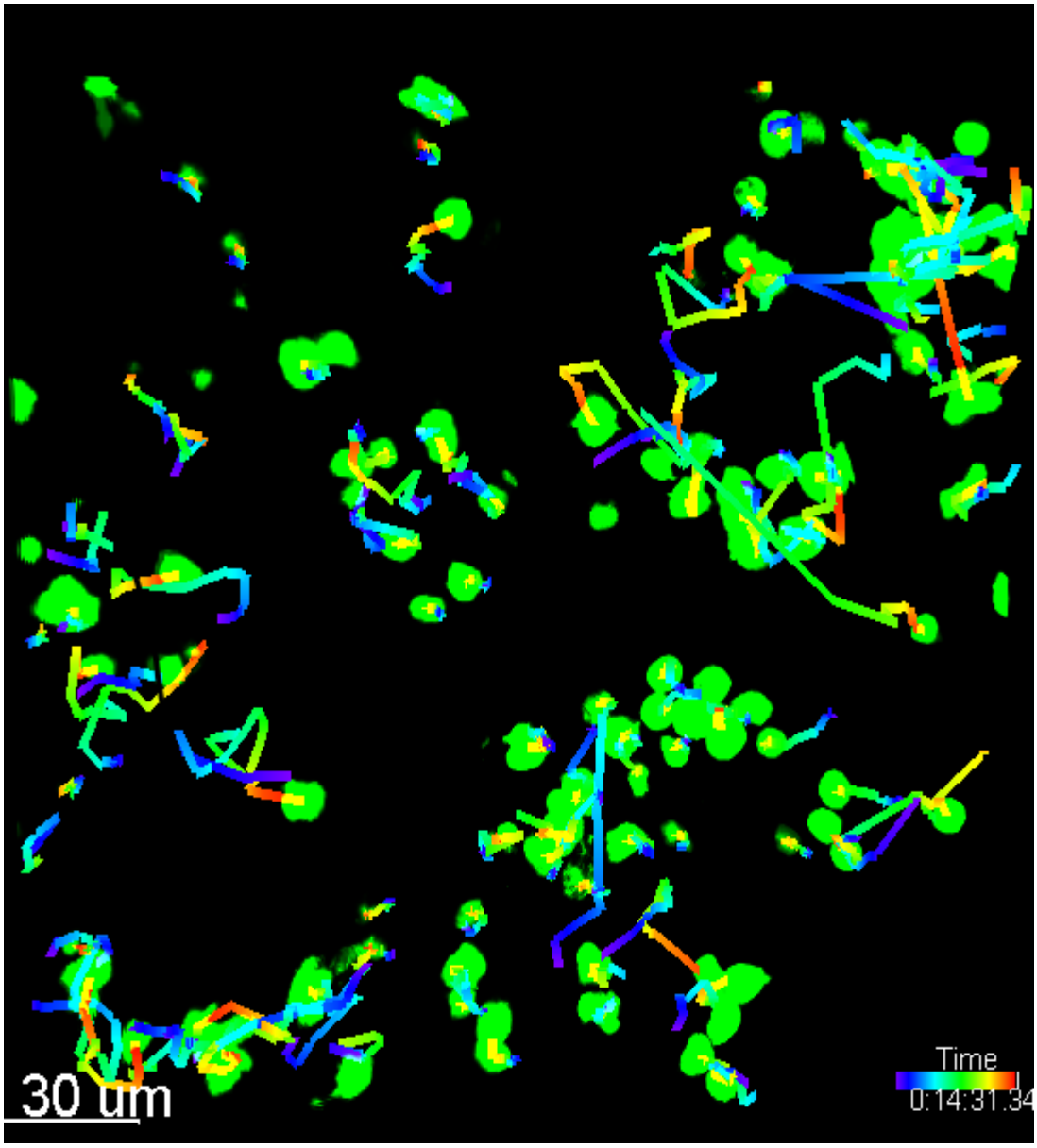

Figure 41: Neutrophils migration without PLY perfusion (Figure 40)
A single time point from a representative of two-photon movie of neutrophils labelled with CFSE (green) migrating in an inguinal LN slice. Neutrophil migration across the whole period of imaging is shown as time-coded tracks. Tissue was perfused with oxygenated media without PLY.

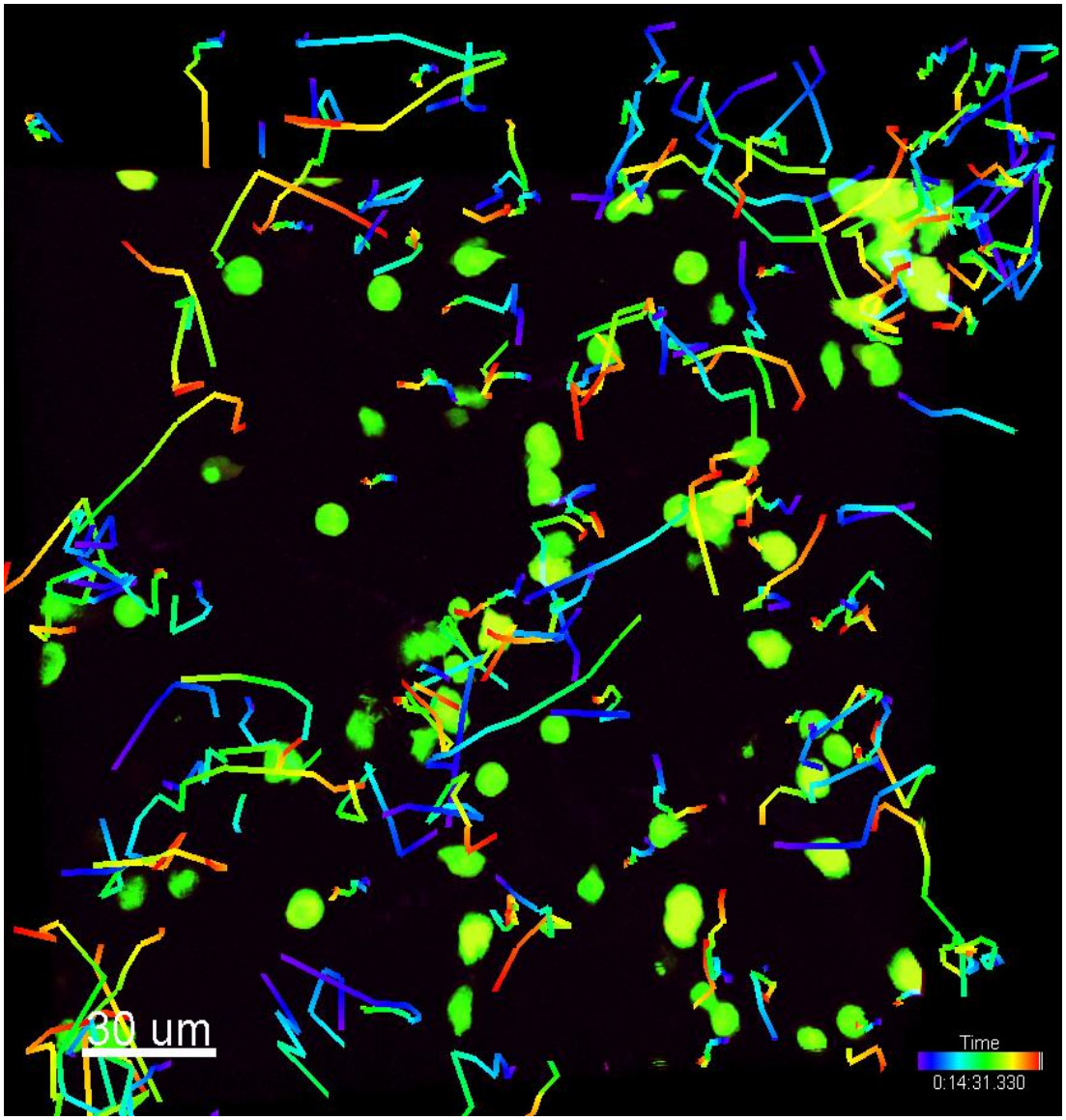

Figure 42: Neutrophil migration in lymph nodes was enhanced following perfusion with PLY at 1.5 HU/mL (Figure 40)
A single time point from a representative of two-photon movie of neutrophils labelled with CFSE (green) migrating in an inguinal LN slice. Neutrophil migration across the whole period of imaging is shown as time-coded tracks. Tissue was perfused with oxygenated media containing 1.5 HU/mL PLY.

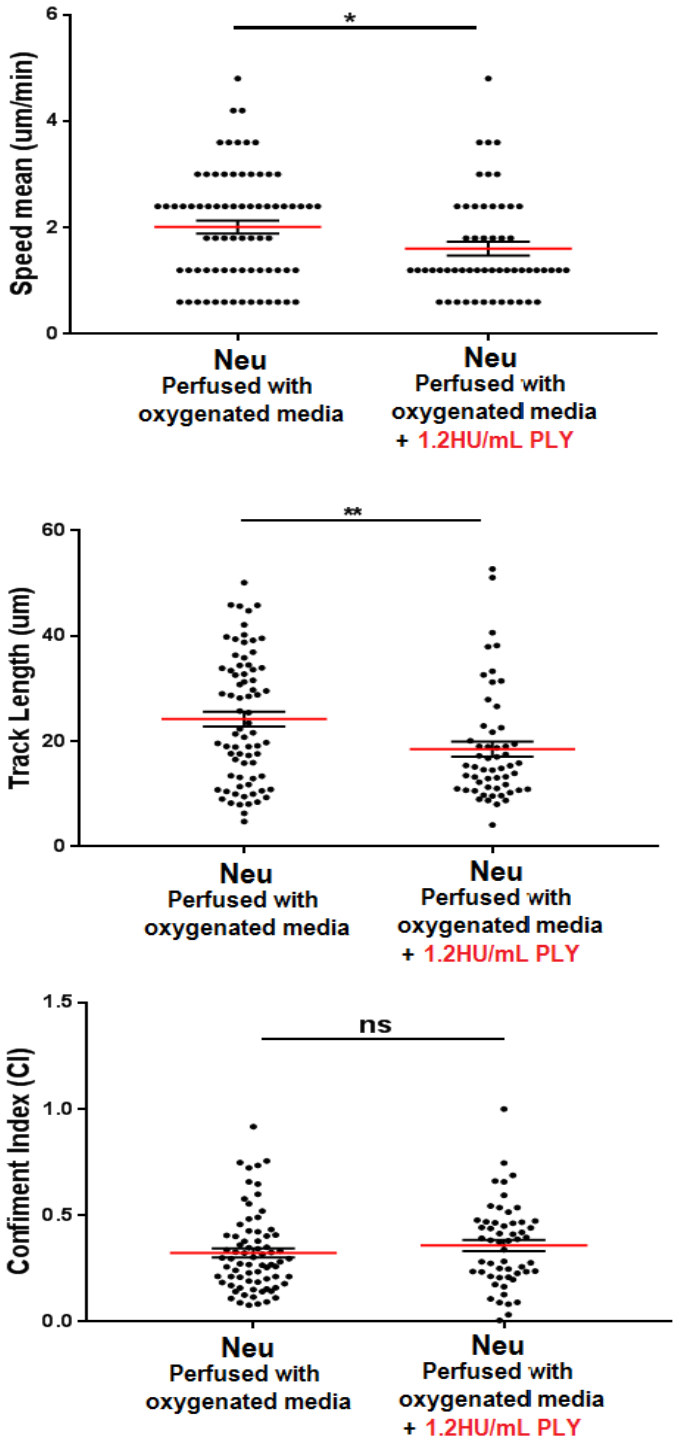

Figure 43: 1.2 HU/mL PLY did not enhance neutrophil migration in lymphatic tissue
Neutrophils were tracked migrating in LN tissue slices before (left) and after (right) perfusion with 1.2 HU/mL PLY. Two movies per condition were recorded for 15 minutes each. Cell positions were tracked using IMARIS software, and cell speed (top), track length (middle) and confinement index (bottom) calculated. Graph shows mean ± SEM for 1 movie per condition. Each point represents an individual cell. Statistical significance was determined using unpaired t-test (two-tailed) with * ($p<0.05$) and ** ($p<0.01$)

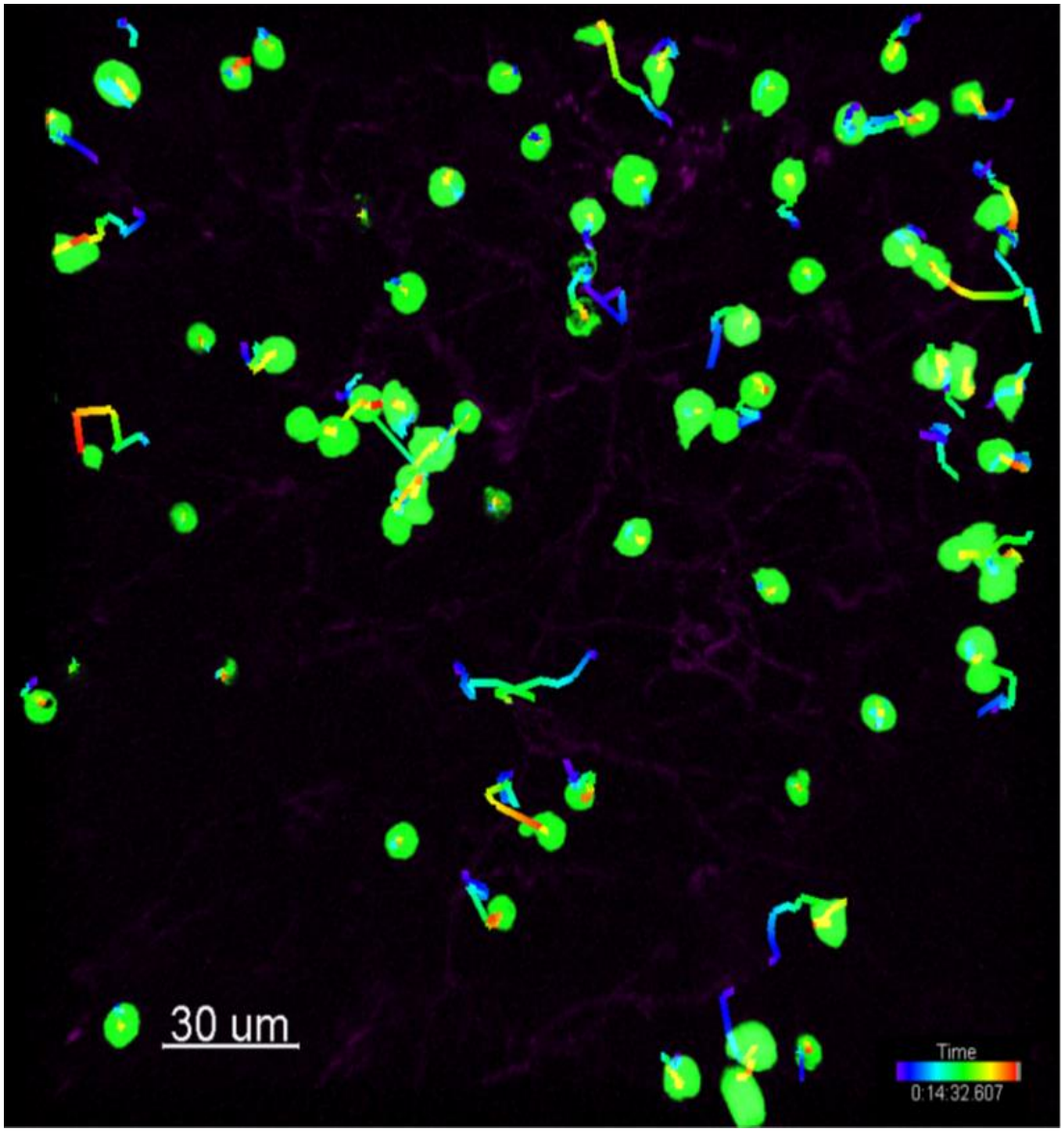

Figure 44: Neutrophils migration without PLY perfusion (1.2 HU/mL PLY) was enhanced on lymphatic tissue (Figure 43)
A single time point from a representative of two-photon movie of neutrophils labelled with CFSE (green) migrating in an inguinal LN slice. Neutrophil migration across the whole period of imaging is shown as time-coded tracks. Tissue was perfused with oxygenated media without PLY.

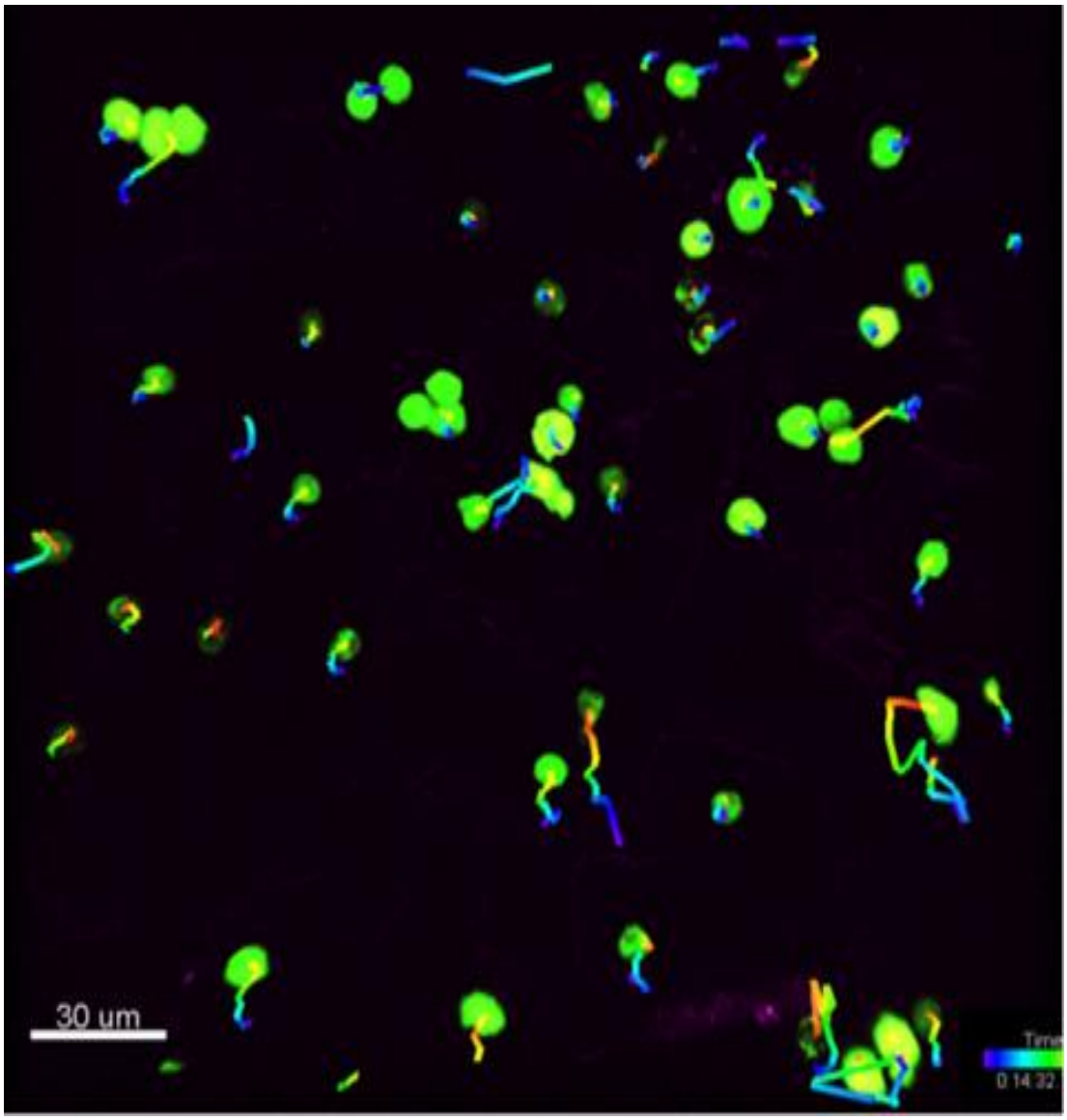

Figure 45: Neutrophils migration was not enhanced in lymph node slices following perfusion with PLY at 1.2 HU/mL (Figure 43)
A single time point from a representative of two-photon movie of neutrophils labelled with CFSE (green) migrating in an inguinal LN slice. Neutrophil migration across the whole period of imaging is shown as time-coded tracks. Tissue was perfused with oxygenated media with 1.2 HU/ml PLY.

3.3 Discussion

Previously published reports suggest that pneumolysin, a key virulence factor produced by *S. pneumoniae* can inhibit neutrophil migration (Paton & Ferrante 1983 ; Johnson et al. 1981 ;Paton et al. 1993). However, whether PLY targets particular modes of migration, or acts competitively, remains poorly understood. Here, we have shown that PLY can directly inhibit neutrophil migration in *in vitro* 2D assays, and in 3D assays, which are highly representative of the tissue interstitium. Live *S. pneumoniae* also inhibited neutrophil migration toward chemoattractant; however there did not seem to be a correlation between haemolytic activity of the different strains. These data contribute to our understanding of how neutrophil host defence may be impaired during a bacterial infection, specifically with *S. pneumoniae*

3.9.1 PLY inhibits neutrophil migration to KC, but not by acting competitively as a chemoattractant.

Previous studies using neutrophils isolated from the blood of healthy volunteers have shown that PLY inhibits chemotaxis (direct migration) and chemokinesis (random migration) (Paton & Ferrante 1983; Johnson et al. 1981; Paton et al. 1993). These are in agreement with our current data, whereby we demonstrate an inhibitory effect of PLY on chemotaxis of murine neutrophils in 2D and 3D environments. This could be the result of direct inhibition of neutrophil migration by the toxin, or by the toxin acting competitively as a chemoattractant. In support of the latter hypothesis, previous studies by Johnson *et al* suggested that PLY can chemoattract neutrophils at low concentrations *in vitro*, while instillation of PLY onto rabbit conjunctiva tissue led to neutrophil recruitment (Johnson et al. 1981). In contrast, in this study we found no chemoattractive effect on PLY on neutrophils. These differences may simply reflect

differences in experimental approaches. However, another possible explanation is that PLY acts on other cells resident in tissues and stimulates these cells to produce a neutrophil chemoattractant. Alternatively PLY activation of complement may contribute to neutrophil influx during infection (Rubins et al. 1995). Therefore PLY may indirectly enhance neutrophil influx into tissues, whilst also acting directly on neutrophils to constrain their migration upon arrival. Possible mechanisms for the direct inhibitory activity of PLY on neutrophil migration will be explored in subsequent chapters.

3.9.2 Inhibition of neutrophil chemotaxis by PLY depends on pore-forming activity, but is not accompanied by significant cell death.

PLY form pores has cell inhibition and activation properties (Kadioglu et al. 2008; McNeela et al. 2010). Both activities are required for *in vivo* virulence of the bacteria, but only the haemolytic activity regulates neutrophil recruitment (Jounblat et al. 2003). The pore-forming activity of PLY makes it toxic to a variety of cell types. When present in high concentration it can lyse any cell membrane that contains cholesterol. Meanwhile at sub-lytic concentrations, the functional effects of PLY on cells may also still be dependent on the formation of micropores (Martner et al. 2008) including inhibition of neutrophil chemotaxis, as we showed for the first time in this chapter. In our experiments, sub-lytic concentrations of PLY inhibited neutrophil chemotaxis without causing significant cell death. However, this effect was still be dependent on the pore forming activity of the toxin, since a toxoid derivate of PLY (PdB) did not alter neutrophil chemotaxis (Paton et al. 1991).

Similar to our data, a number of previous studies have demonstrated that the pore-forming activity of PLY is required to alter host cell behaviour at sub-lytic concentrations (i.e. independently of cell death). For example, nanomolar concentrations of PLY result in the formation of small numbers of sub-cytolytic pores in epithelial cell membranes. This leads to osmotic stress, activation of P38 mitogen-activated protein kinase, and innate responses, allowing them to act as an early warning system to the host immune response. This effect was dependent on pore formation, as it was lost in the presence of PdB (Ratner et al. 2006). In neuroblastoma cells, sub-lytic concentrations of PLY lead to formation of micro-pores in the plasma membrane, activation of rac1 and rhoA GTPases, and the formation of actin stress fibres (Iliev et al. 2007). This brought about cytoskeletal rearrangements within the target cells, and suggests a possible mechanism for the effects we observe on neutrophil migration (Marriott et al. 2008). Rac1 and RhoA are Rho GTPases which can produce morphological changes in the cell after responding to changes in the surrounding environment (Iliev et al. 2007). Both are involved in cell motility where rhoA facilitates actin-myosin contractility, and rac1 influences actin polymerization and the formation of lamellipodia (Wennerberg 2004). This suggests a possible mechanism for the effects we observe on neutrophil migration.

Sub-lytic concentrations of PLY also affect immune cell function, and again many of these effects are dependent on its pore-forming function. THP-1 monocytic cells exposed to PLY upregulate ICAM-1, but this effect is not seen in response to PdB (Thornton et al. 2005). In neutrophils, the release of sub-lytic concentrations of PLY by autolyzed pneumococci induces the activation of NADPH oxidase, and generation of reactive oxygen species (ROS) (Martner et al. 2008). However, contrary to our results, neutrophil recruitment into infected lung tissue was largely dependent on the

pore forming function of PLY (Jounblat et al. 2003). A possible explanation for this discrepancy is discussed below.

3.9.3 PLY can enhance neutrophil recruitment to the site of infection, but may subsequently inhibit interstitial migration

Our current study shows that PLY inhibits neutrophils chemotaxis *in vitro*. However, a number of murine infection studies have already demonstrated that PLY plays an important role in stimulating neutrophil recruitment to the site of infection. For example, a study by Kadioglu *et al*. has shown neutrophil recruitment to infected lungs is slower and less intense in the presence of PLY-mutant bacteria compared to WT controls (Kadioglu et al. 2000; Hirst et al. 2004). This function of PLY is dependent on its cytolytic, pore-forming activity (Jounblat et al. 2003). Furthermore, *in vitro* studies using Transwell system to study neutrophil migration across a pulmonary endothelial monolayer has demonstrated PLY to be necessary for pneumococcus-induced PMN recruitment (Moreland & Bailey 2006). As noted above, this discrepancy may be explained by PLY acting on endothelial or other stromal cells to indirectly enhance neutrophil recruitment, but then acting directly upon extravasated neutrophils to inhibit interstitial chemotaxis and function. We can't conclude here, are neutrophils stopping before reaching foci of live bacteria (bad) or are they receiving stop signal upon reaching foci of live bacteria (good, as that is where they need to be to perform function).

Despite the large influx of neutrophils in response to wild-type-pneumococci, susceptible hosts fail to eliminate bacteria from the lungs. This might be explained by neutrophil activity being significantly inhibited by PLY upon arrival in the lung, which is consistent with our results, and with earlier studies showing that pneumolysin-

treated mononuclear phagocytes showed significantly depressed ability to kill *S. pneumoniae in vitro* (Kadioglu et al. 2000; Mitchell et al. 1991; Nandoskar et al. 1986). Studies by Paton *et al*. have shown PLY to markedly depress the respiratory bust and bactericidal activity of PMNL cells (Paton & Ferrante 1983). In contrast, other studies have shown that PLY activates NADPH oxidase, and production of ROS. However, ROS produced in response to pneumolysin is formed mainly intracellularly, where it functions in cell signalling rather than bacterial killing. ROS is released into vesicular compartments lacking microbes, likely resulting in deterioration and death of the neutrophils and lessening pneumococci defence (Martner et al. 2008). Furthermore, PLY-induced damage to neutrophil membranes enhances release of lysozyme and possibly other hydrolytic enzyme from this cells, contributing to tissue damage (Johnson et al. 1981; Paton & Ferrante 1983).

Altogether, this work suggests that pneumolysin could function in pathogenesis by (1) stimulating a tissue inflammatory response that recruits large numbers of neutrophils (2) shifting the balance of neutrophil activity from bactericidal function to tissue damage, and (3) inhibiting neutrophil interstitial chemotaxis. Future studies should address the molecular details of how neutrophil behaviour is altered in lung tissue after PLY stimulation, or infection with *S. pneumoniae*.

3.9.4 Effect of live *S. pneumoniae* with varying haemolytic activity on neutrophil chemotaxis.

Our current results have shown that the haemolytic, pore-forming function of PLY is essential for inhibition of neutrophil chemotaxis. Thus, we hypothesised that the inhibitory effect of various bacterial strains on neutrophil migration would be dependent on their haemolytic activity, and might explain disease pathogenesis.

Reliant on the immunochemistry profile of their capsular polysaccharide, the pneumococci can be divided into 90 serotypes (Henrichsen 1995). However the serotypes that are found to cause the majority of disease account for less than 20% of all serotypes (Hausdorff et al. 2000). PLY is usually preserved in all serotypes of *S. pneumoniae,* and is needed for full invasive disease (Kirkham et al. 2006). ST217 and ST306 are serotype 1 pneumococci, which is known as one of the most common invasive serotypes (Kirkham et al. 2006). African ST217 is highly haemolytic while, European ST306 isolates have been shown to have mutations in their ply gene that have resulted in pneumolysin being unable to form functional pores in the host cell membrane, leaving no residual haemolytic activity (Marriott et al. 2008; Littmann et al. 2009). We therefore expected that ST217 would show greater inhibition of neutrophil chemotaxis in our assay than ST306. Surprisingly, however, both strains inhibited neutrophil migration to similar levels, albeit less than that of purified PLY or D39 serotype 2 pneumococci. Interestingly, ST306 does not require hemolytically active pneumolysin to cause invasive pneumococcal disease, nor to attract neutrophils to the site of infection. This suggests either the presence of other virulence factors, or alternative activities of PLY. Either could explain the reduction in neutrophil chemotaxis observed in our experiments. In support of the latter hypothesis, *S. pneumoniae* lacking the haemolytic activity of PLY was more virulent than *S. pneumoniae* in which the PLY gene was deleted (Alexander et al. 1998). However, we observed no inhibitory effect of PdB on neutrophil chemotaxis, suggesting other virulence factors are responsible for the observed effect.

3.4 Conclusion

We have shown that PLY is able to inhibit neutrophil migration in 2D and 3D chemotaxis assay. The 3D context is more representative of the tissue interstitium and helps us to understand further how neutrophils behaviour and interactions are modified by *S. pneumoniae* toxin, PLY. We hypothesise that *in vivo*, neutrophils are recruited from blood but are unable or delayed in their ability to reach foci of infection and use effective defence mechanisms to eradicate the pathogen. If we could understand the mechanism, we might be able to manipulate neutrophil migration in disease or inflammation to perform effective defensive action for killing the pathogen and minimise the risk of tissue damage to the host.

Chapter 4: Understanding the molecular mechanism through which PLY alters neutrophils migration and function

4.1 Brief Introduction

In chapter 3, we showed that *S.pneumoniae* and its toxin, PLY could inhibit neutrophil chemotaxis in 2D and 3D *in vitro* models. In this chapter, the molecular mechanism through which PLY alters neutrophil migration will be explored. Understanding how PLY inhibits neutrophil migration may reveal new ways to inhibit neutrophil migration in other disease settings, preventing them from damaging host tissues.

We have shown that neutrophil motility in 2D and 3D models is inhibited by PLY. Studies have identified that there are significant differences in the adhesive, chemoattractant and signalling processes which regulate neutrophil migration in 2D and 3D. *In vitro*, 2D migration is largely integrin-dependent, while 3D migration can be integrin-dependent or independent. *In vivo*, integrins play an important role in the recruitment of neutrophils from the blood stream into the site of *S. pneumoniae* infection by binding complementary receptors on endothelial cells, immobilising neutrophils (Hogg 1995). However, the role of integrins in subsequent chemotaxis of neutrophils through the tissue interstitium remains unclear.

One potential mode is using an adhesion-dependent pathway where neutrophils use extracellular matrix (ECM) as their platform of movement. In this pathway, integrins mediate interactions between neutrophils and extracellular matrix components (Weninger et al. 2014). Integrins are heterodimeric cell surface receptors which play

an important role in the transduction of cell-matrix adhesion signals (Wiesner et al. 2005). Integrins promote cell adhesion and migration, and connect the ECM with the actin cytoskeleton. They regulate actin based structures in the cell, which in turn regulate the stability of adhesions.

Integrins can play an important role in chemotaxis, even in 3D. This can be seen in studies done by Cera *et al*, where interstitial migration of neutrophils towards an inflammatory stimulus was impaired in the absence of JAM-A, which regulates integrin recycling (Cera et al. 2009). Studies by Heit *et al* have suggested that CD11b/CD18 (αMβ2, Mac1) is the dominant integrin involved in chemotaxis to fMLP, and CD11a/CD18 (αLβ2, LFA-1) is the dominant integrin involved in chemotaxis to IL-8, using a 3D agarose assay (Heit 2005).

In vivo studies by Werr *et al* demonstrated that neutrophil migration in extravascular tissues is crucially dependent on CD49b/CD29 (α2β1) function (Werr et al. 2000), and that CD29 is critically involved in the chemokinetic movement of neutrophils in rat extravascular tissue (Werr et al. 1998). Meanwhile another *in vivo* study has shown CD29 to be involved in the movement of neutrophils from the interstitium into alveoli using electron microscopy. It has also been suggested that CD49b and CD49d (α4) mediate CD18-independent neutrophil accumulation during pulmonary inflammation (Ridger et al. 2001).

Alternatively, other studies have shown neutrophil migration in 3D environments can be integrin-independent. Integrin-independent modes of migration are also dependent on actin polymerisation as it is the assembly and disassembly of the actin cytoskeleton that enables the cell to move toward cues such as chemoattractants.

Studies by Lammermann and colleagues, conducted both *in vivo* and in 3D *in vitro* assays, showed that murine leukocytes can migrate solely using the expansive force of the actin-network, that promotes protrusive flowing of the leading edge without integrin involvement (Lämmermann et al. 2008). Another study by Lammermann *et al* has shown that LTB_4 promotes rapid integrin-independent neutrophil recruitment through tissues, though integrins were required to maintain neutrophil swarms (Lämmermann et al. 2013). Other studies have shown, in the absence of integrins, alternative mechanisms of cell adhesion are utilised. Confinement of cells in a 3D matrix enables the cells to push against a substrate and use weaker affinity, integrin-independent, interactions. More transient interactions with matrix proteins allow for rapid motility required by leukocytes (Sahai & Pinner 2009).

We hypothesise that differences in integrin expression or function might explain the decrease in neutrophil motility in the presence of PLY. The assessment in this chapter will involve *in vitro* and *in vivo* experiments to determine the effect of *S. pneumonia*e or PLY on expression of selected integrins (CD11b, CD18, CD29, CD49b and CD49d) on neutrophils. The effect of PLY on actin polymerization and adhesion will also been assessed. The outcome of this study will be to better understand the molecular mechanism used by PLY to alter neutrophil migration.

4.2 Results

4.2.1 Effect of PLY on neutrophil adhesion

While working with PLY-treated neutrophils, we noticed that they were more difficult to dislodge from tissue culture plates than their untreated counterparts. We therefore assessed the effect of PLY treatment on neutrophil adhesion to TC-treated plastic, and to fibronectin-coated plates. Remodelling of the actin cytoskeleton is required for neutrophil chemotaxis. Our previous results in Chapter 3 have shown PLY inhibits neutrophil chemotaxis. Therefore we also investigated the effect of PLY-treatment on f-actin polymerisation, as measured by phalloidin staining.

4.2.1.1 Treatment with PLY increases neutrophil adherence to TC-treated plastic

To assess the effect of PLY on neutrophil adhesion, neutrophils were loaded with calcein-AM and treated with PLY, LPS or PdB before plating onto tissue culture treated plastic. Adhesion was quantified by measuring fluorescence of adhering cells at 45 minutes, 2 hours and 4 hours.

Neutrophils treated with PLY and LPS were more adhesive to tissue culture plastic than untreated controls (Figure 46 I–II). On the other hand, cells treated with PdB showed no difference in adhesiveness, compared to untreated controls (Figure 46 III). This finding is consistent with impaired chemotaxis seen in PLY- but not PdB- treated neutrophils.

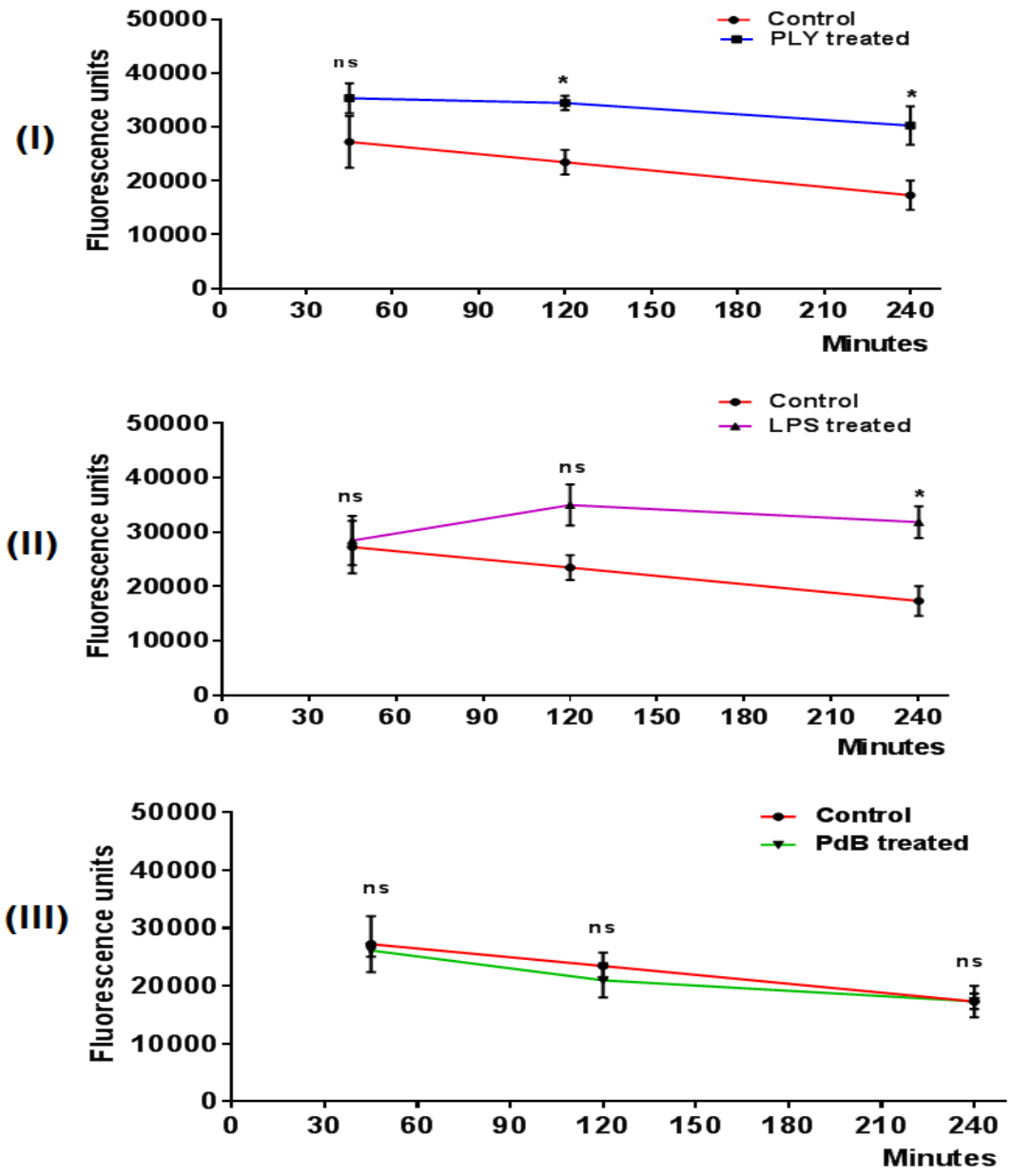

Figure 46 : PLY and LPS increase neutrophil adherence to TC treated plates
Neutrophils were stained with a fluorescent dye (Calcein AM) and incubated for 30 minutes at 37^{o}C before stimulation with PLY (I) or LPS (II) or PdB (III). Calcein-labelled neutrophils were allowed to adhere for three different time points (45 minutes, 2 hours and 4 hours). Thereafter non-adherent neutrophils were removed by washing, and the amount of neutrophils adhering to the plate was measured using a plate reader. Data are pooled from three independent experiments, each performed in triplicate. Graph show mean $\pm$ SEM. Statistical significance was determined using an unpaired t-test two-tailed analysis with *($p<0.05$).

4.2.1.2 PLY causes a transient increase in adhesion to fibronectin-coated plates

We next assessed adhesion of neutrophils to fibronectin (FN). Previous studies have shown CD11b/CD18-dependent neutrophil haptotaxis on FN (Henry et al. 2013). FN also has a role in inducing adherence of neutrophils on collagenous and non-collagenous substrates (Marino et al. 1985). FN is a ligand for CD49d/CD29 (α4β1) integrin (Plow et al. 2000), and CD49d/CD29 has been shown to be important for neutrophil recruitment during *S. pneumoniae* infection (Kadioglu et al. 2011).

Plates were pre-coated by adding 25µg/mL of fibronectin per well for 1 hour at 37^{o}C, or overnight at 4^{o}C. Neutrophils were loaded with calcein-AM and treated with PLY, LPS or PdB before plating onto fibronectin-coated plates. Adhesion was quantified by measuring fluorescence of adhering cells at 45 minutes and 3 hours.

After 45 minutes, we found that PLY- and LPS- treated neutrophils showed increased adhesion to fibronectin coated plates compared to control neutrophils. This effect was dependent on the pore-forming activity of the toxin, since neutrophils treated with PdB behaved similarly to untreated controls (Figure 47 I-II). However, after 3 hours, we observed that neutrophils treated with PLY no longer showed any increase in adherence compared to control neutrophils. In contrast, neutrophils treated with LPS showed a highly significant sustained increase in adhesion to fibronectin compared to untreated controls (Figure 47II). Untreated neutrophils showed no significant difference in adhesion to uncoated or fibronectin-coated wells, while PLY-, LPS- and PdB- treated neutrophils adhered significantly better to fibronectin-coated versus uncoated wells (Figure 47 I-II).

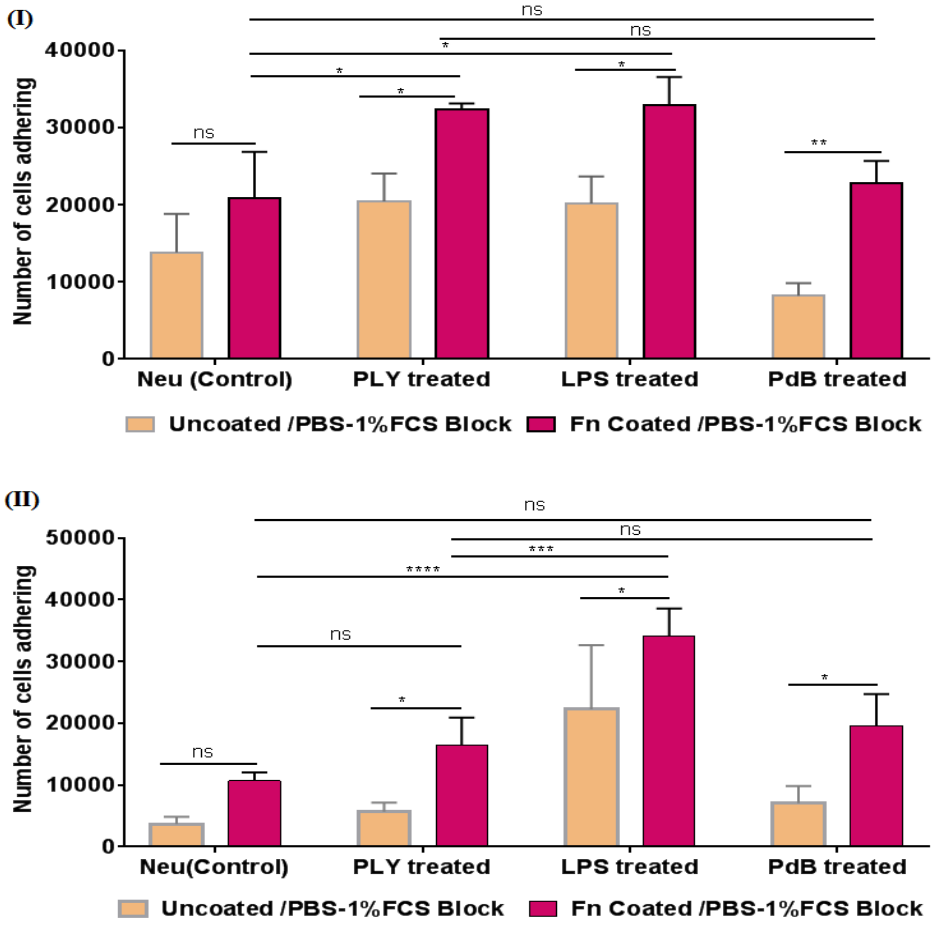

Figure 47: PLY causes a transient increase in adhesion to fibronectin-coated plates
Calcein-labelled neutrophils were allowed to adhere for 2 different time points 45 minutes (I) and 3 hours (II) at 37^{o}C. Non-TC treated plates were used and coated with 25µg/mL fibronectin. Thereafter, non-adherent neutrophil were removed by washing four times with PBS, and the fluorescence of adherent neutrophils to the plate was measured using a plate reader. Data represent mean ± SEM (n=3 wells per condition). Statistical significance was determined using two-way ANOVA with Tukey's multiple comparisons test, with *($p<0.05$), **($p<0.01$), ***($p<0.001$) and ****($p<0.0001$). Data is representative of 3 independent experiments.

4.2.1.3 Effect of PLY on neutrophil morphology and actin polymerization

LPS is known to increase neutrophil adhesion, and this is accompanied by actin filament re-arrangement (Watanabe et al. 2003). To assess if PLY induces changes in the actin cytoskeleton, we seeded neutrophils onto glass coverslips and treated with

PLY, LPS or PdB for 45 minutes. After fixing, neutrophil F-actin was labelled with Rhodamine-Phalloidin, before confocal imaging. Images were analysed using IMARIS software for the intensity mean of actin fluorescence and sphericity and volume of each neutrophil.

In an initial experiment, PLY treated neutrophils markedly increased their F-actin fluorescence intensity and volume but decreased in sphericity (Figure 48 and 49). However, when analysing collective data from a total of five experiments, there was some variation in the results for fluorescence intensity of F-actin staining and sphericity (Figure 50 I–II). Overall, no significant difference was observed between control and PLY treated neutrophils for either of these measures. An enhanced fluorescence intensity was observed in all experimental replicates, however was only statistically significant in three of five experiments (data not shown, $p<0.05$ using paired t-test). In contrast there was a statistically significant increase in volume in PLY treated neutrophils in the collective data (Figure 50 III, $p<0.05$). No significant difference was observed between PdB treated neutrophils and untreated neutrophils in all three measures (Figure 49). Meanwhile, LPS treated neutrophils showed a modest increased in their volume, and F-actin fluorescence intensity, but no changes in sphericity, when compared to untreated neutrophils (Figure 49). No collective data is presented for LPS and PdB as the experiment was performed for three times.

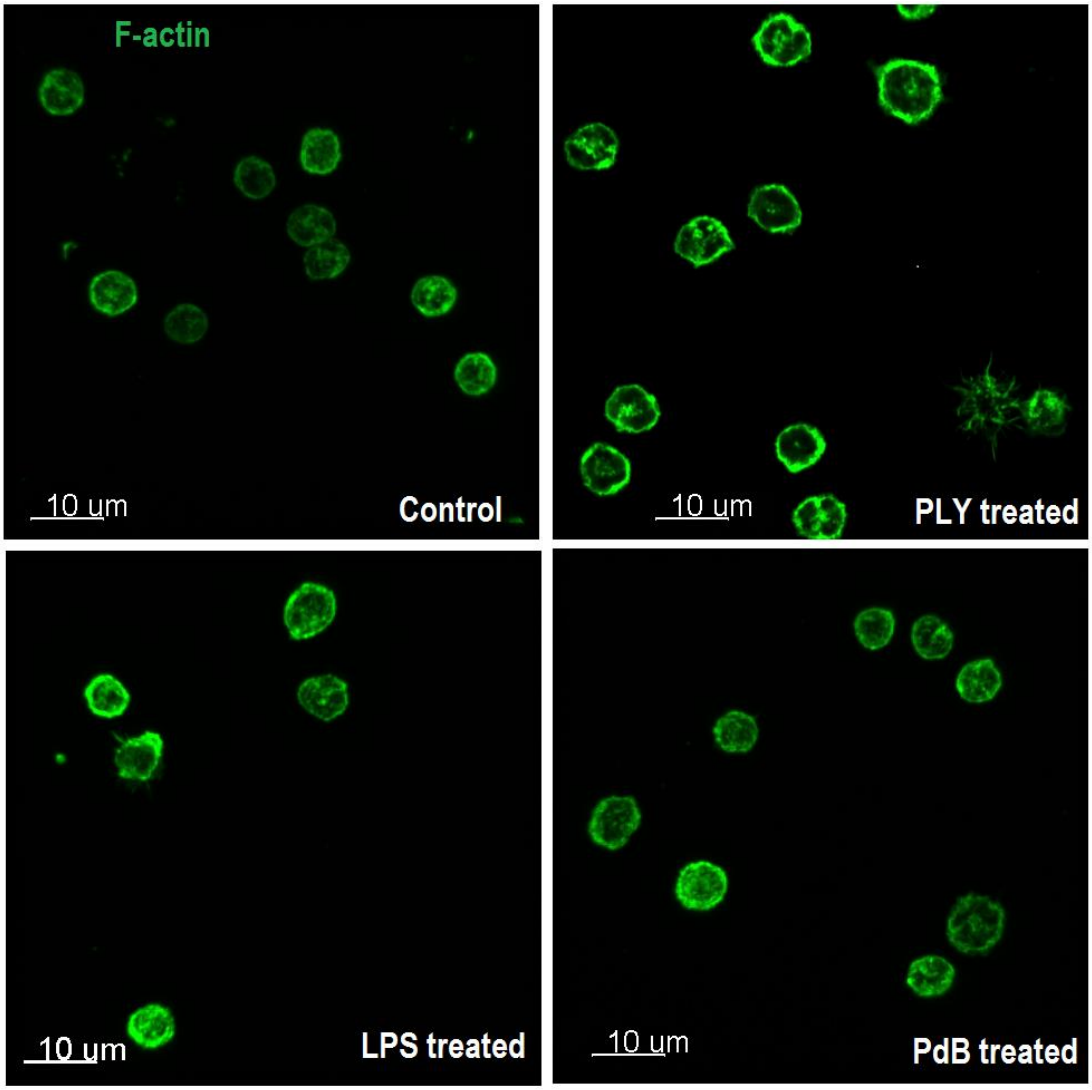

Figure 48: Neutrophils treated with PLY are larger and show increased F-actin polymerisation

Neutrophils were plated on glass coverslips and treated with PLY, LPS, or PdB for 45 minutes before fixation and staining with rhodamine-phalloidin (green) for F-actin. Neutrophils were observed using 100x objective mounted on the Zeiss BIOAFM 880 confocal microscope.

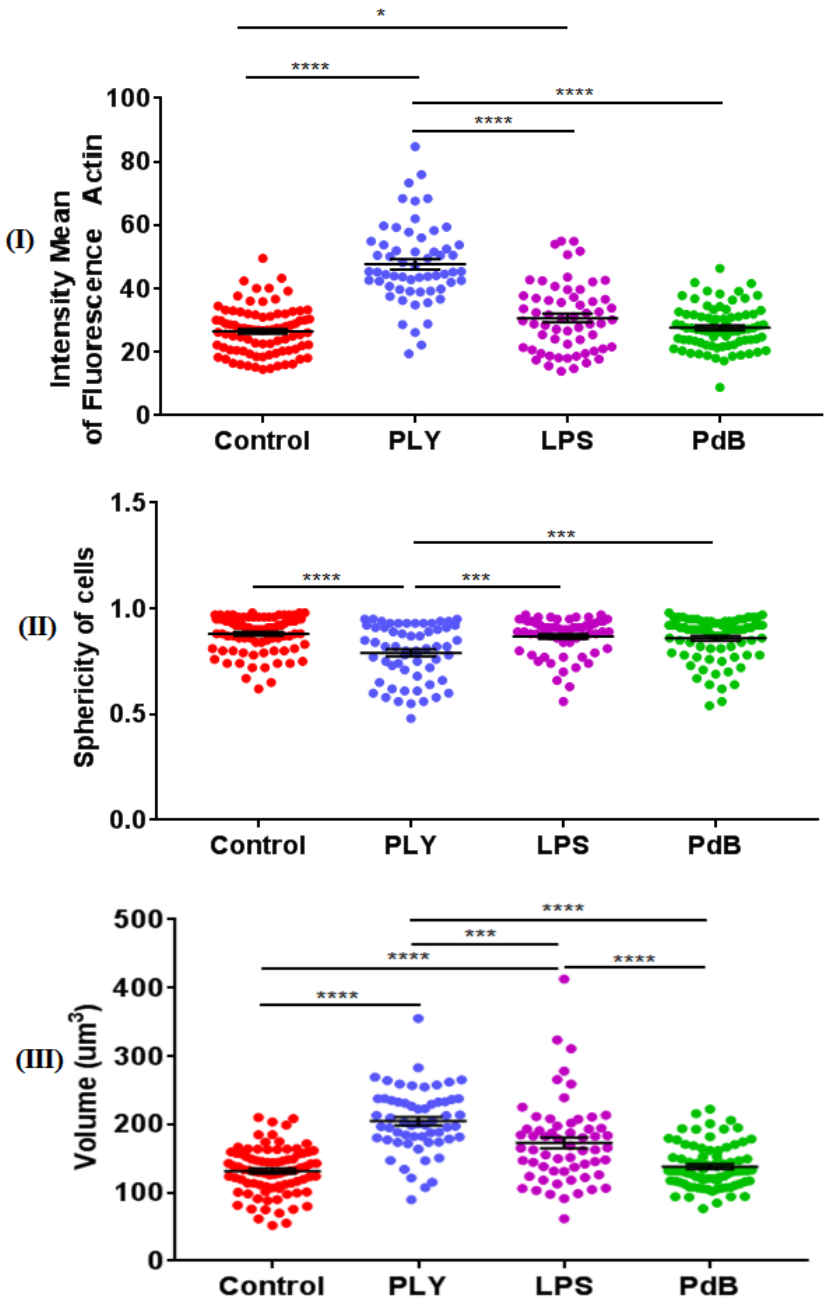

Figure 49: Neutrophils treated with PLY show increased f-actin polymerisation, increased volume, and decreased sphericity

Neutrophils were plated on glass coverslips and treated with PLY, LPS, or PdB for 45 minutes before fixation and staining with rhodamine-phalloidin and DAPI. Neutrophils were observed using 100x objective mounted on the Zeiss BIOAFM 880 confocal microscope. Graphs depict (I) fluorescence intensity of rhodamine-phalloidin, (II) cell sphericity, and (III) cell volume. Each point represents an individual cell. Mean $\pm$ SEM for a single experiment is shown. Statistical significance was determined using one-way ANOVA with Tukey's multiple comparisons test, with *($p<0.05$), **($p<0.01$), ***($p<0.001$) and ****($p<0.0001$).

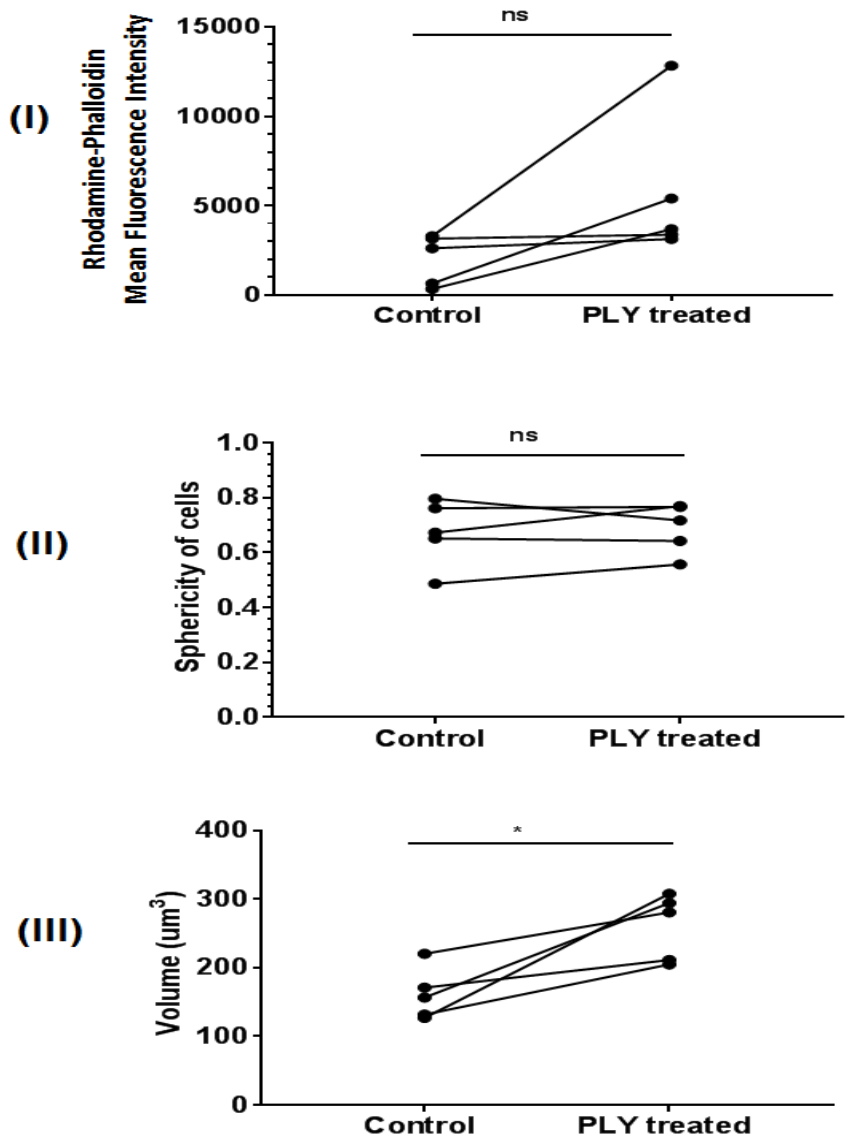

Figure 50: Neutrophils treated with PLY show increased volume, and a trend towards increased F-actin polymerisation

Neutrophils were plated on glass coverslips and treated with PLY, LPS, or PdB for 45 minutes before fixation and staining with rhodamine-phalloidin and DAPI. Neutrophils were observed using 100x objective mounted on the Zeiss BIOAFM 880 confocal microscope.

Graphs depict (I) fluorescence intensity of rhodamine-phalloidin, (II) cell sphericity, and (III) cell volume. Each point represents the mean for an individual experiment. 5 independent experiments are shown. Statistical significance was determined using paired t-test *$p<0.05$

4.2.2 Analysis of integrin expression on neutrophils following treatment with PLY

The data presented in this chapter show that PLY-treated neutrophils show increased adhesion to TC plastic and fibronectin, and a trend towards increased polymerisation of F-actin. Human neutrophils adhering to plastic surfaces are rapidly activated and spread quickly upon adhesion, inducing F-actin polymerization (Ginis et al. 1992). It has also been reported that binding of neutrophils to various biological substrates such as fibronectin and other non-biological surfaces such as plastic is dependent on the integrin subunit, CD18 (Werr et al. 1998). Neutrophils express a variety of adhesion receptors, including members of the well-studied integrin family. Integrins are connected to F-actin and mediate neutrophil adhesion to extracellular matrix proteins. Thus we thought increased expression or activity of integrins might explain these findings.

Here, we have assessed the effect of PLY on expression of : αMβ2 (CD11b/CD18), which plays a key role in transendothelial migration from blood to tissue during *S.pneumoniae* infection (Kadioglu et al. 2011); α2β1 (CD49b/CD29) which binds collagen and has been suggested to regulate neutrophil interstitial migration (Werr et al. 2000); and α4β1(CD49d/CD29) which binds fibronectin and may have an important role in neutrophil accumulation in *S. pneumoniae* infected lungs (Kadioglu et al. 2011).

4.2.2.1 Analysis of integrin expression on neutrophils stimulated with PLY *in vitro*

Neutrophils have previously been shown to upregulate CD11b following exposure to pneumococci (Cockeran et al. 2001). It also has been shown that CD11b expression is upregulated on neutrophils and endothelial cells in community acquired pneumonia (Glynn et al. 1999) and on neutrophils recruited to the lungs during bacterial pneumonia (Rijneveld et al. 2005). To confirm this finding we have performed experiments on neutrophils stimulated with PLY *in vitro*.

To assess changes in CD11b expression, neutrophils were stimulated with 1.5 HU/mL PLY for 30 minutes, 2 hours and 16 hours and further stained with a fluorescent live/dead dye before expression of CD11b was analysed by flow cytometry.

Our experiment concluded that treatment with PLY increased expression of CD11b on neutrophils at all time points (Figure 51). The highest median fluorescence intensity (MFI) was observed at 30 minutes of culture, and then decreased over time. There was also a transient increase in CD11b expression on untreated neutrophils after 30 minutes of culture, but this was substantially less than that observed for PLY-treated neutrophils (Figure 51).

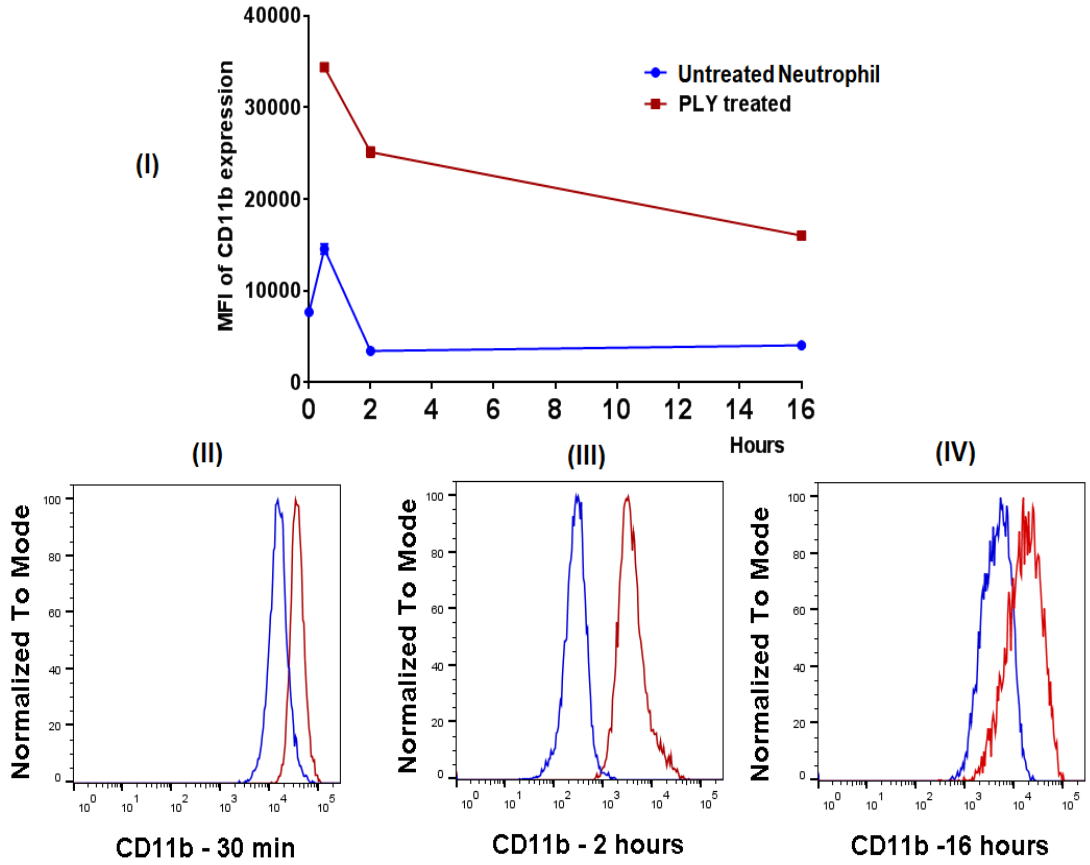

Figure 51: CD11b expression increased on neutrophils after exposure to PLY
Neutrophils were treated with 1.5 HU/mL PLY for the indicated times, stained with an antibody to CD11b, and analysed by flow cytometry (I) Graph depicts the MFI of CD11b expression on untreated neutrophils (blue) and treated neutrophils (red) at the indicated time point. (II-IV) Representative histograms depicting CD11b expression in control (blue) and PLY-treated (red) neutrophils at (II) 30 minutes, (III) 2 hours and (IV) 16 hours.

We next assessed changes in expression of the integrin subunits CD18, CD29, CD49b and CD49d. Since PLY treated neutrophils are larger, and more auto-fluorescent, fluorescence minus one (FMO) controls were used to determine gates and MFI normalised to FMO controls for the same experimental condition. Four independent experiments were performed, with a single replicate and time-point (45 minutes) in each. Again, a statistically significant increase in CD11b expression was observed (Figure 52(I) and 53(V)). CD29 and CD49d were both expressed on neutrophils, but there was no change in expression in response to PLY treatment (Figure 52(III), 53(I) and Figure 52(V), 53(V)). CD49b was not expressed by bone marrow derived neutrophils, and was not induced by treatment with PLY (Figure 52(IV) and 53(IV)). We also observed unexpectedly low levels of CD18 expression, either in the presence or absence of PLY (Figure 52(II) and 53(II)). This was surprising, as CD11b is expressed at very high levels, and pairs with CD18 at the cell surface. Similarly, a previous study showed that CD18 was absent or low on bone marrow neutrophils, and only increased upon exposure to *Leishmania* (Falcão et al. 2015). We hypothesis that this finding may be explained by the antibody clone we used only recognising active CD18, or less likely, that CD11b can be expressed at the cell surface in the absence of CD18. Even though heterodimers of CD11b/CD18 has been shown to play key roles in leukocyte adhesion and migration, transfection of cell lines with either CD11b or CD18 alone revealed distinct roles in attachment, spreading and migration (Solovjov et al. 2005).

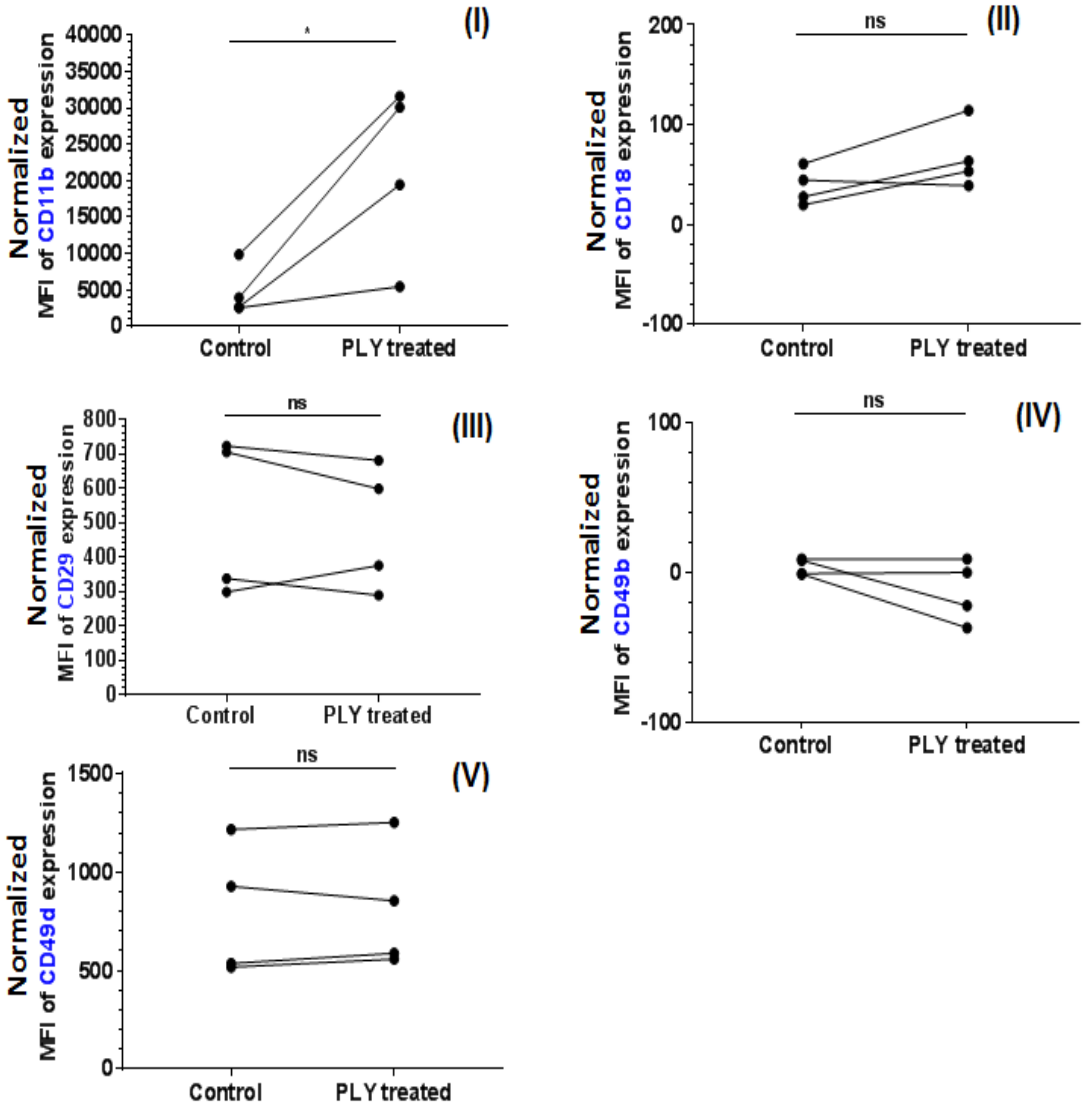

Figure 52: Summary of flow cytometric analysis of integrin expression on neutrophils treated with PLY

Neutrophils were treated with 1.5 HU/mL PLY for 45 minutes, stained with antibodies to CD11b (I), CD18 (II), CD 29 (III), CD49b (IV) and CD49d (V) and analysed by flow cytometry. Graphs show the normalized median fluorescence intensity (MFI) of the indicated integrin in control and PLY treated neutrophils. Each pair of data points represents one individual experiment, of four performed in total. Significance was determined using a paired t-test, *denotes $P<0.05$ and ns not significant.

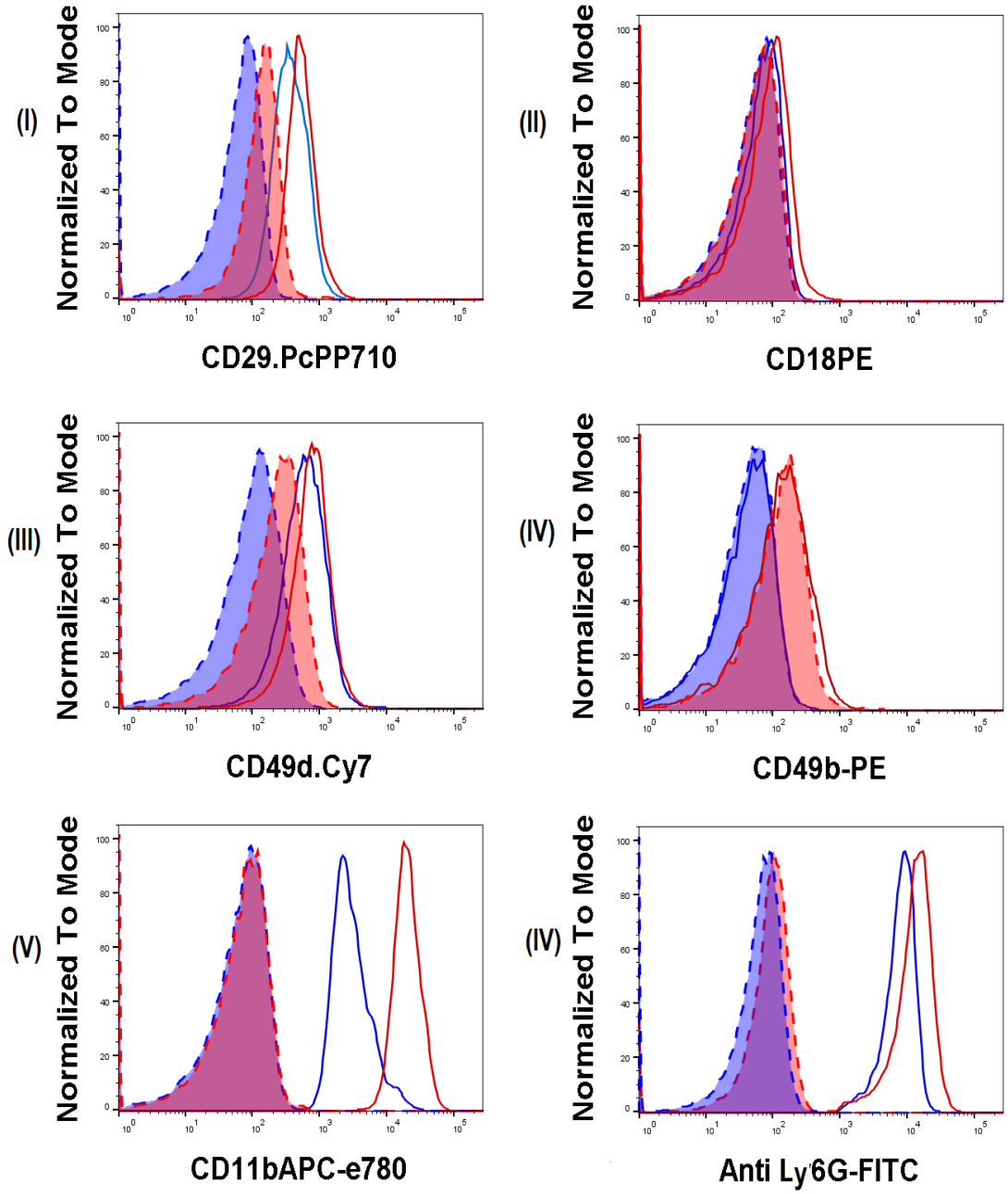

Figure 53: Representative histograms of integrin expression on neutrophils treated with PLY (Figure 52)

Neutrophils were treated with 1.5 HU/mL PLY for 45 minutes, stained with antibodies to (I) CD29, (II CD18, (III) CD49d, (IV) CD49b, (V) CD11b and (VI) Anti Ly6G and FMO before analysed by flow cytometry. The [blue] peak shows fluorescent intensity of control neutrophils. The [-------] peak shows intensity of FMO for control neutrophils. The [red] peak shows staining on neutrophils treated with PLY/mL and [------] peaks for FMO of PLY treated. Data are representative of four independent experiments.

4.2.2.2 Analysis of integrin expression on neutrophils in an *in vivo S. pneumoniae* infection model

Our *in vitro* analysis revealed no expression of CD49b on neutrophils isolated from bone marrow. This was not entirely surprising, since expression of this integrin has been shown to increase upon extravasation of neutrophils from blood to inflamed tissue. We therefore decided to assess integrin expression on neutrophils isolated from the blood and lungs of mice infected intranasally with *S. pneumoniae*. CD1 (female) mice were infected intranasally with 10^6 CFU of *S. pneumoniae* D39 strain. 24 hours post-infection, blood and lungs were collected from three infected and three control mice. Successful infection was confirmed by analysis of bacterial CFU in both blood and lung (Figure 54 I-II).

Single cell suspensions were prepared from lung tissue, and both blood and lung samples were analysed by flow cytometry. Neutrophils ($CD11b^+Ly6G^+$) increased in proportion in both blood and lung following infection (Figure 55 I-II). We next assessed integrin expression on neutrophils. We focused on CD49d as it has been suggested to play a role in recruitment of neutrophils to *S. pneumoniae* infected lungs (Kadioglu et al. 2011), and CD49b as it has been suggested to promote intersitital migration (Werr et al. 2000), and migration from the interstitum to inflamed alveoli (Ridger et al. 2001).

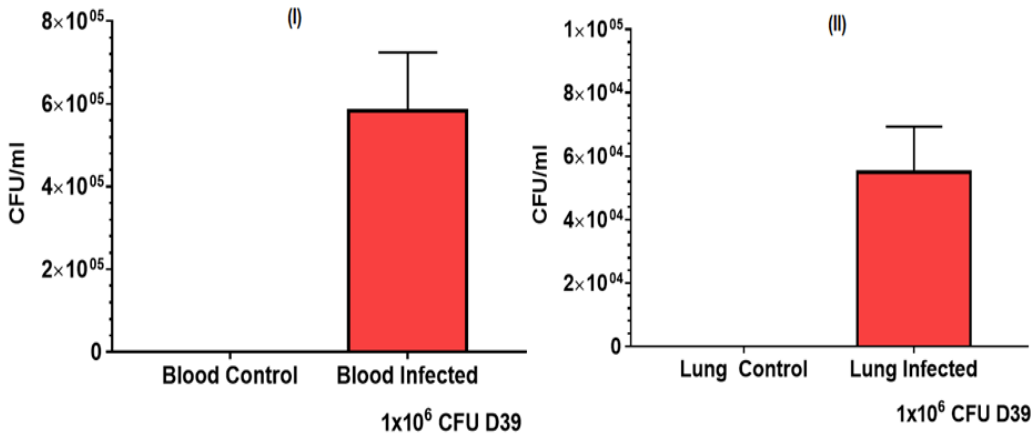

Figure 54: Bacterial load in blood and lungs following intranasal infection with *S.pneumoniae*

CD1 mice were infected intranasally with 10^6 CFU of *S. pneumoniae* D39 strain. Samples of blood (I) and lung tissue (II) were collected from control (n=3) and infected (n=3) mice 24 hours post-infection and plated on blood agar for Miles & Misra counts. Graphs depict CFU/mL for (1) Blood and (II) Lung. Mean ± SEM for 3 mice per condition is shown (n=3 mice).

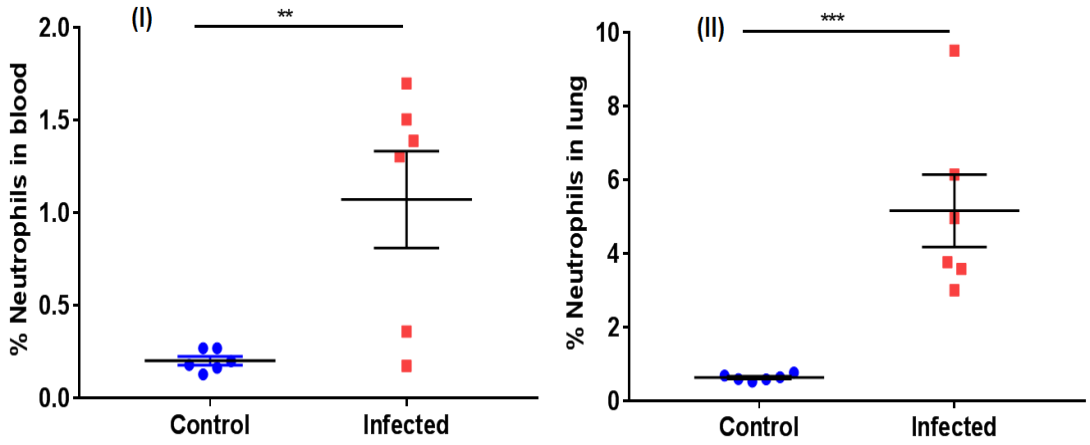

Figure 55: Neutrophils significantly increase in proportion in infected blood and lung

CD1 mice were infected intranasally with 10^6 CFU of *S.pneumoniae* D39 strain. Samples of blood (I) and lung tissue (II) were collected from control (n=6) and infected (n=6) mice 24 hours post-infection and processed for flow cytometry. Graphs depict proportion of neutrophils ($CD11b^+Ly6G^+$) after gating on $CD45^+$ cells in (I) blood and (II) lung. Mean ± SEM for 3 mice per condition is shown. Significance of $p<0.05$ was determined using an unpaired t-test (two-tailed) and denotes with **($p<0.01$) and ***($p<0.001$).

We found that, unlike bone marrow neutrophils, blood and lung neutrophils expressed CD49b on the cell surface (Figure 56, 57 and 58). However, blood and lung neutrophils expressed similar levels of CD49b, indicating that expression is not modulated by extravasation from blood to tissue. There was also no change in CD49b expression in response to infection in either tissue (Figure 57 III and 58 III).

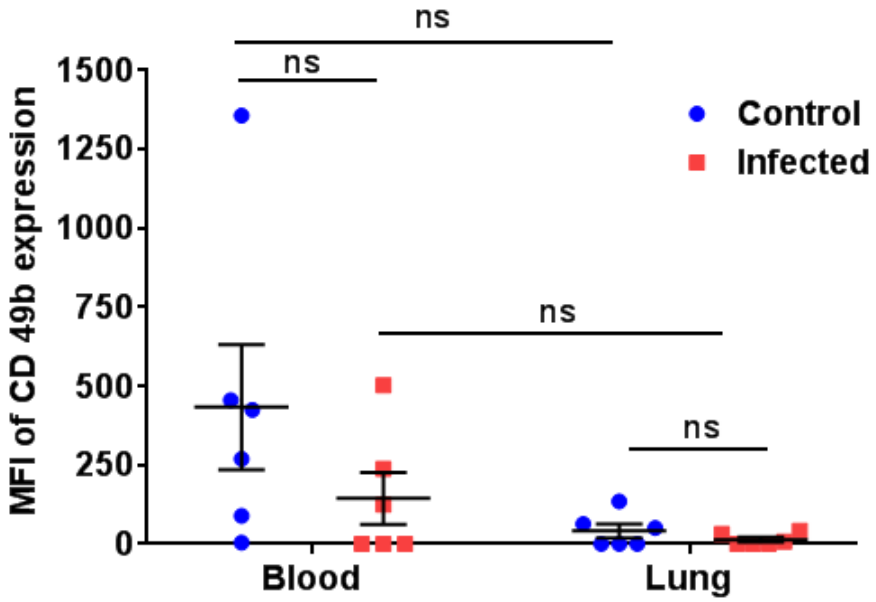

Figure 56: No increase in CD49b expression in response to infection in blood and lung neutrophils

CD1 mice were infected intranasally with 10^6 CFU of *S.pneumoniae* D39 strain. Samples of blood and lung were collected from control (n=6) and infected (n=6) mice 24 hours post infection and processed for flow cytometry. Graphs depict MFI expression of CD49b of neutrophils ($CD11b^+Ly6G^+$) after gating on $CD45^+$ cells in blood and lung. The data represent the means $\pm$ SEM of 6 mice and statistical significant using two-way ANOVA with post-hoc Tukey's multiple comparison ($p<0.05$), ns denote not significant.

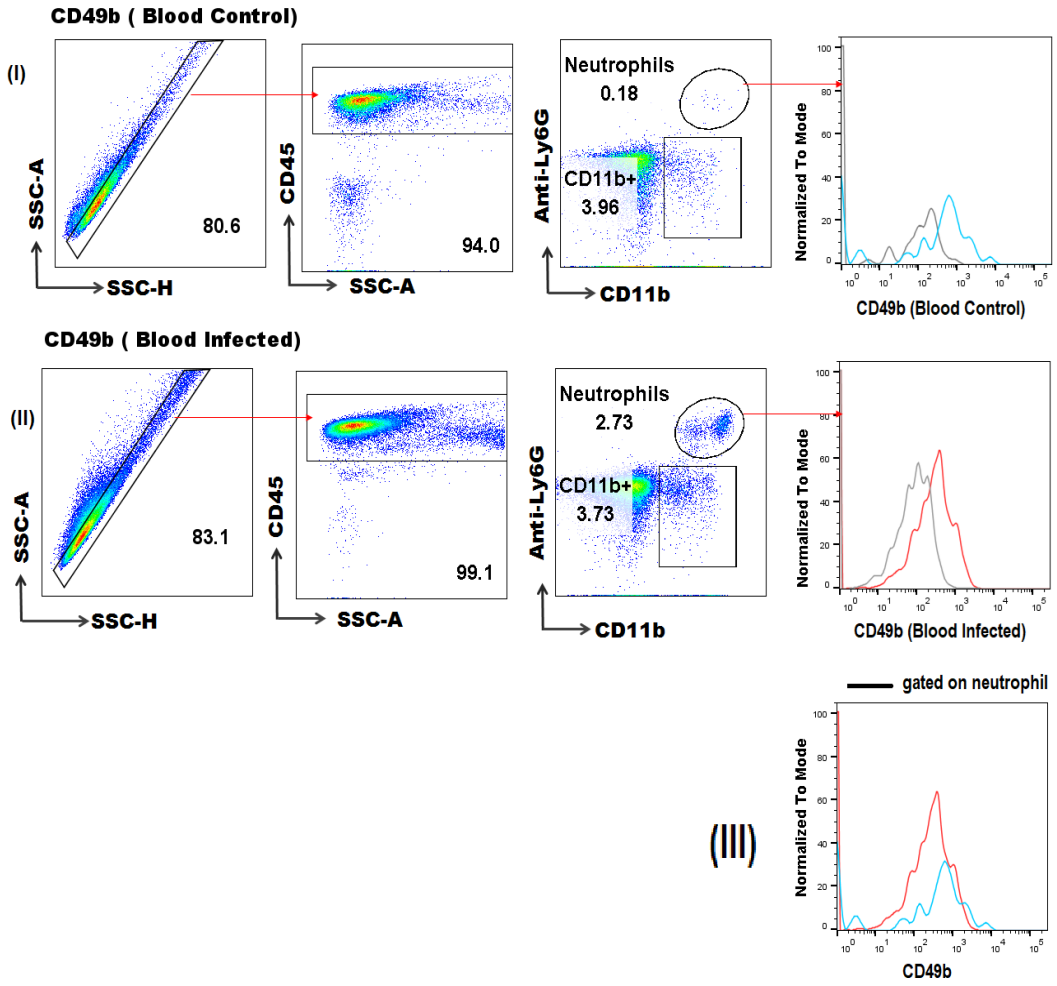

Figure 57: Representative flow cytometric analysis of CD49b in blood (for Figure 56)
CD1 mice were infected intranasally with 10^6 CFU of *S.pneumoniae* D39 strain. Samples of blood were collected from control (n=6) and infected (n=6) mice 24 hours post-infection and processed for flow cytometry. (I-II) Flow cytometric analysis of neutrophils from (I) control (n=6), and (II) infected (n=6) mice. Plots on the far left show discrimination of single cells from doublets (SSC-H vs SSC-A), followed by discrimination of leukocytes based on CD45 expression. Next neutrophils ($CD11b^+Ly6G^+$) were gated on, and analysed for expression of CD49b. [Grey] histograms indicate FMO controls. (III) The [blue] histogram indicates CD49b expression on neutrophils control in blood. The [red] indicates CD49b expression on neutrophils infected with D39 bacteria in blood. Data are representative of two independent experiments.

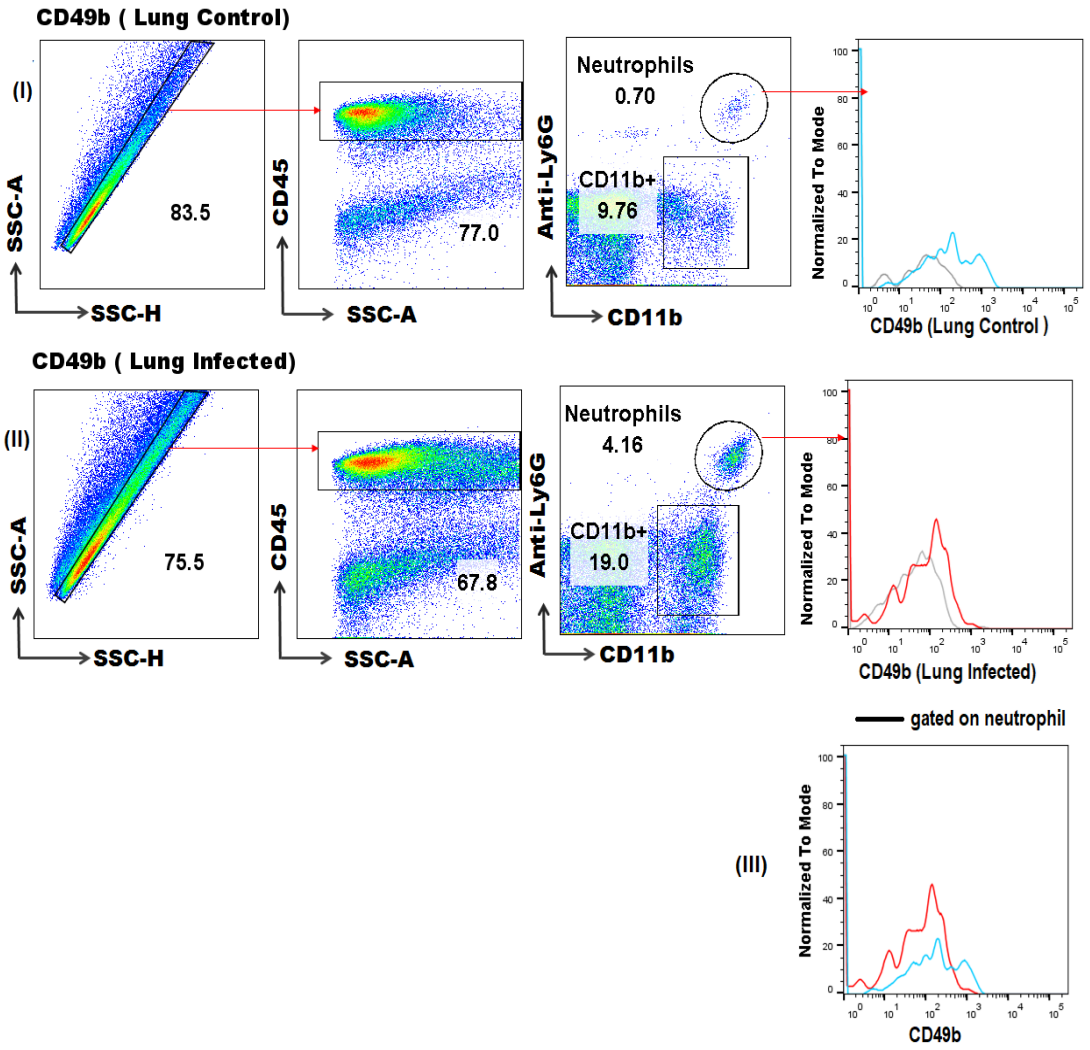

Figure 58: Representative flow cytometric analysis of CD49b in lung (for Figure 56) CD1 mice were infected intranasally with 10^6 CFU of *S.pneumoniae* D39 strain. Samples of blood were collected from control (n=6) and infected (n=6) mice 24 hours post-infection and processed for flow cytometry. (I-II) Flow cytometric analysis of neutrophils from (I) control (n=6), and (II) infected (n=6) mice. Plots on the far left show discrimination of single cells from doublets (SSC-H vs SSC-A), followed by discrimination of leukocytes based on side scatter and CD45 expression. Next neutrophils ($CD11b^+Ly6G^+$) and other $CD11b^+$ cells ($CD11b^+Ly6G^-$) cells were gated on, and analysed for expression of CD49b. [Grey] histograms indicate FMO controls. (III) The [blue] histogram indicates CD49b expression on neutrophils control in lung. The [red] indicates CD49b expression on neutrophils infected with D39 bacteria in lung. Data are representative of two independent experiments.

Our *in vitro* data showed that CD49d is expressed on isolated neutrophils, although no changes in expression were seen after PLY stimulation. Nevertheless, we analysed expression of CD49d on neutrophils from infected mice, as previous studies

have shown that neutrophil accumulation in *S. pneumoniae* infected lungs is related to CD49d expression (Kadioglu et al. 2011).

We found that, similar to bone marrow neutrophils, blood and lung neutrophils also expressed CD49d on the cell surface (Figure 59, 60 and 61). However, blood and lung neutrophils expressed similar levels of CD49d, indicating that expression is not modulated by extravasation from blood to tissue. There was also no change in CD49d expression in response to infection in either tissue (Figure 60 III and 61 III). This agreed with our *in vitro* findings, which also showed no change in CD49d expression in response to PLY treatment.

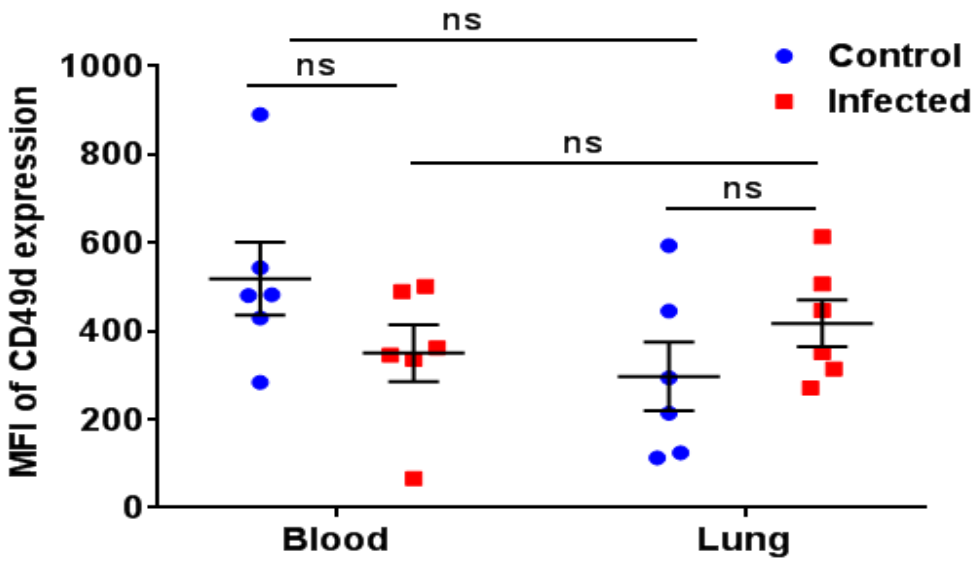

Figure 59: No changes in CD49d expression in response to infection in blood and lung neutrophils
CD1 mice were infected intranasally with 10^6 CFU of *S.pneumoniae* D39 strain. Samples of blood and lung were collected from control (n=6) and infected (n=6) mice 24 hours post-infection and processed for flow cytometry. Graphs depict MFI expression of CD49d of neutrophils ($CD11b^+Ly6G^+$) after gating on $CD45^+$ cells in blood and lung. The data represent the means ± SEM of 6 mice and statistical significance was determined using two-way ANOVA with post-hoc Tukey's multiple comparison ($p<0.05$), ns denote not significant.

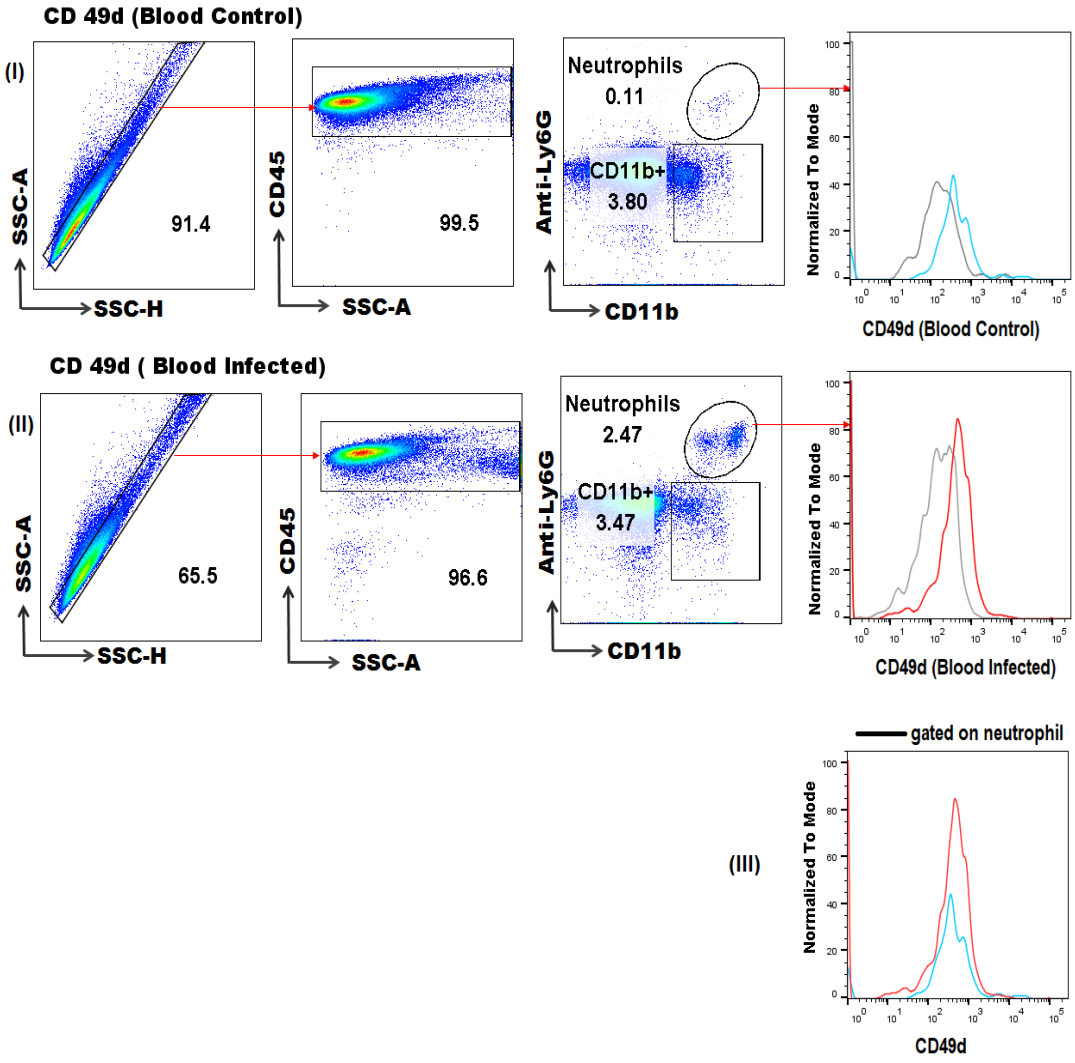

Figure 60: Representative flow cytometric analysis of CD49d in blood for (Figure 59) CD1 mice were infected intranasally with 10^6 CFU of *S.pneumoniae* D39 strain. Samples of blood were collected from control (n=6) and infected (n=6) mice 24 hours post-infection and processed for flow cytometry. (I-II) Flow cytometric analysis of neutrophils from (I) control (n=6), and (II) infected (n=6) mice. Plots on the far left show discrimination of single cells from doublets (SSC-H vs SSC-A), followed by discrimination of leukocytes based on side scatter and CD45 expression. Next neutrophils ($CD11b^+Ly6G^+$) and other $CD11b^+$ cells ($CD11b^+Ly6G^-$) cells were gated on, and analysed for expression of CD49d. [Grey] histograms indicate FMO controls. (III) The [blue] histogram indicates CD49d expression on neutrophils control in blood. The [red] indicates CD49d expression on neutrophils infected with D39 bacteria in blood. Data are representative of two independent experiments.

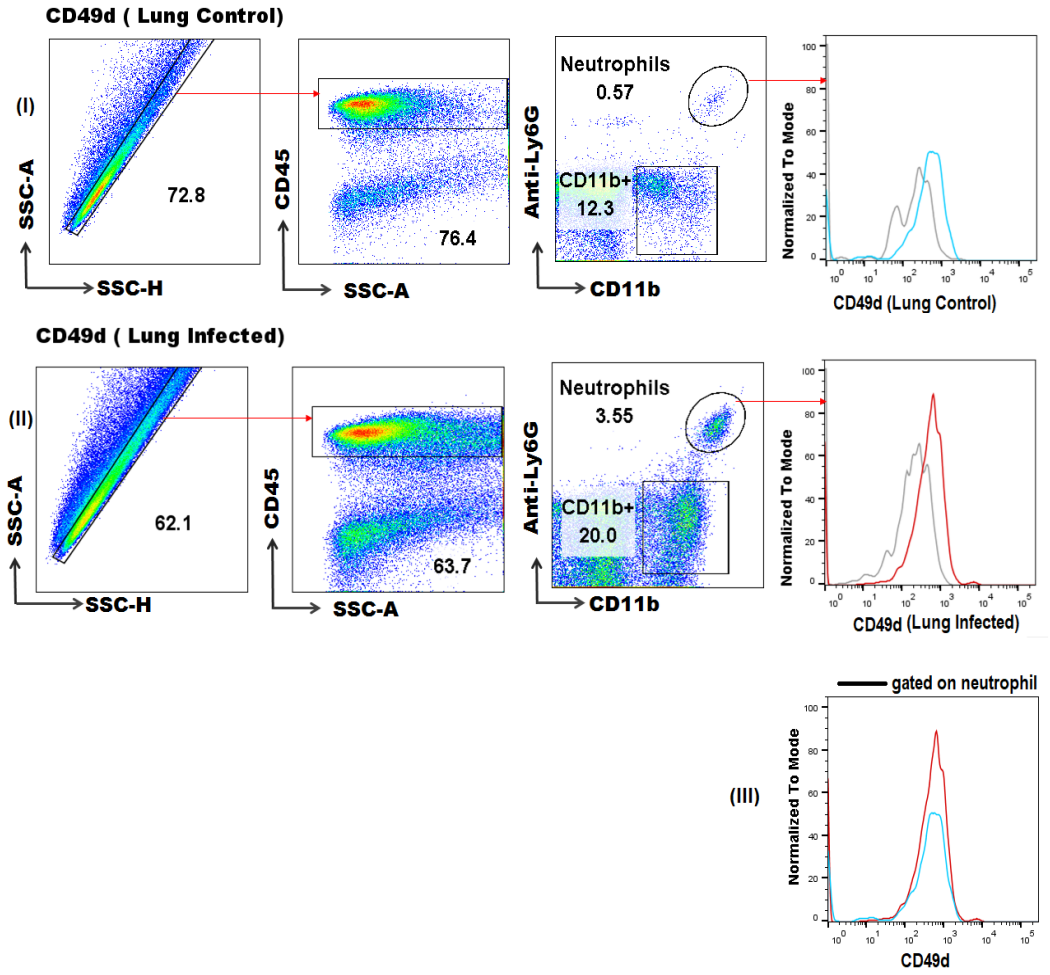

Figure 61: Representative flow cytometric analysis of CD49d in lung for (Figure 59)
CD1 mice were infected intranasally with 10^6 CFU of *S.pneumoniae* D39 strain. Samples of blood were collected from control (n=6) and infected (n=6) mice 24 hours post-infection and processed for flow cytometry. (I-II) Flow cytometric analysis of neutrophils from (I) control (n=6), and (II) infected (n=6) mice. Plots on the far left show discrimination of single cells from doublets (SSC-H vs SSC-A), followed by discrimination of leukocytes based on side scatter and CD45 expression. Next neutrophils ($CD11b^+Ly6G^+$) and other $CD11b^+$ cells ($CD11b^+Ly6G^-$) cells were gated on, and analysed for expression of CD49d. [Grey] histograms indicate FMO controls. (III) The [blue] histogram indicates CD49d expression on neutrophils control in lung. The [red] indicates CD49d expression on neutrophils infected with D39 bacteria in lung. Data are representative of two independent experiments.

Our *in vitro* data showed an increase in CD11b expression on neutrophils treated with purified PLY. Here, we assessed changes in CD11b expression on neutrophils in the blood and lungs of mice infected with D39 bacteria. We found that CD11b expression on neutrophils was increased in lung tissue compared to blood (Figure 62 I-III).

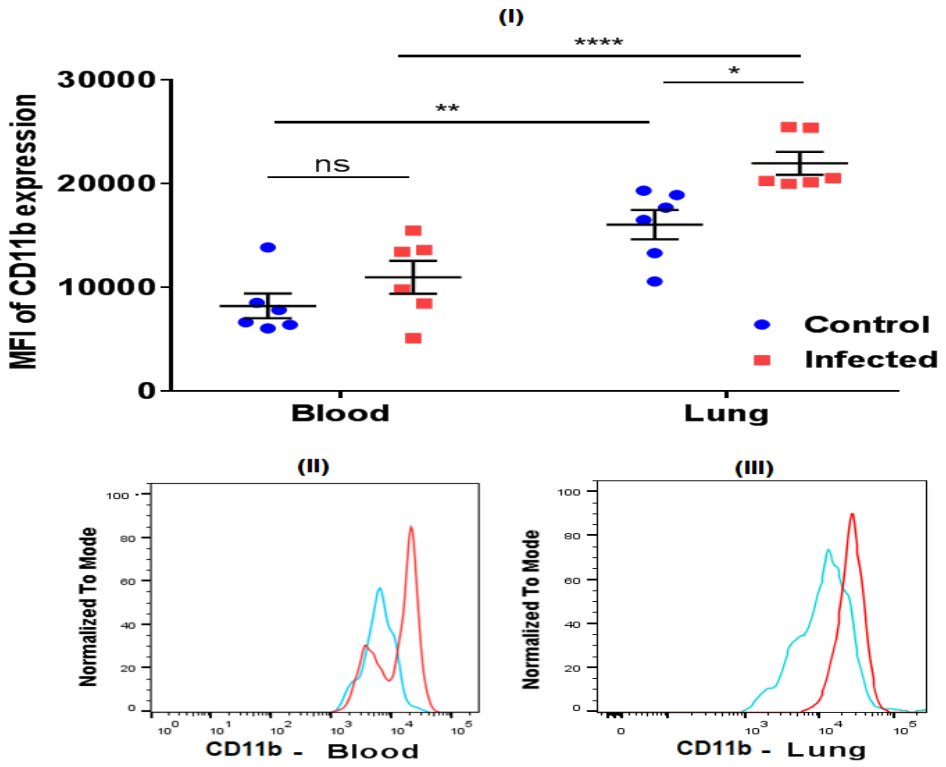

Figure 62: CD11b expression is significantly increased on neutrophil that have extravastated into lung in mice with *S. pneumonia*

CD1 mice were infected intranasally with 10^6 CFU of *S.pneumoniae* D39 strain. Samples of blood and lung were collected from control (n=6) and infected (n=6) mice 24 hours post-infection and processed for flow cytometry. (I) Graphs depict MFI expression of CD11b of neutrophils ($CD11b^+Ly6G^+$) after gating on $CD45^+$ cells in blood and lung. (II) The [blue] histogram indicates CD11b expression on neutrophils control. The [red] histogram indicates CD11b expression on neutrophils infected with D39 bacteria. Data are representative of two independent experiments. The data represent the means ± SEM of 6 mice and statistical significance was determined using two-way ANOVA with post-hoc Tukey's multiple comparison * ($p<0.05$), **($p<0.01$) and ****($p<0.0001$) and ns denote not significant.

4.3 Discussion

In this chapter we aimed to better understand the molecular mechanism by which PLY inhibits neutrophil migration. Treatment with PLY increased CD11b expression on neutrophils, together with actin polymerisation and adhesion. How these finding might explain the impaired migration in 2D and 3D assays observed in Chapter 3 will be discussed here.

4.3.1 PLY increased neutrophil adhesion and actin polymerization

We found that treatment with PLY increased neutrophil adhesion to both TC treated plastic and fibronectin-coated plates, although the latter was only transient. Adhesion to plastic is likely mediated by adhesion factors present in serum, such as vitronectin (Reutter 1985), and is accompanied by an increase in intracellular Ca^{2+}, an increase in F-actin, and activation of the respiratory burst (Ginis et al. 1992). Meanwhile, adhesion to fibronectin results in a smaller increase in intracellular Ca^{2+}, actin depolymerisation, and priming of the cells for subsequent activation of the respiratory burst by exogenous factors (Ginis et al. 1992). These differences might help explain why PLY treated neutrophils showed sustained increases in adhesion to plastic, but only transient increased adhesion to fibronectin in this study.

Chemoattractants induce regular transient increases in intracellular free Ca^{2+} in neutrophils. Experiments where intracellular Ca^{2+} is buffered have shown that these transient fluxes are required for motility by promoting uropod retraction through activation of myosin II, and detachment and endocytosis of integrins. Blocking integrins in calcium-buffered neutrophils restores motility (Mandeville & Maxfield 1997). By forming pores in the cell membrane, PLY can produce a strong cellular

Ca^{2+} influx (Stringaris et al. 2002), which may promote initial adhesion, but also mask the transient Ca^{2+} fluxes required for motility.

We also found that treatment with PLY produced increased actin polymerisation in some experiments. At sub-lytic concentrations, the pore forming function of PLY has been shown to be essential for rapid cytoskeletal reorganization leading to changes in astrocyte shape (Förtsch et al. 2011). In addition, PLY was shown to bind actin directly to increase actin polymerization in an *in vitro* assay (Hupp et al. 2013). This increase in actin polymerisation might explain increased adhesion to TC plastic, and decreased chemotaxis observed in Chapter 3, where PLY inhibited neutrophil chemotaxis in 2D and 3D assays.

Meanwhile, LPS has already been shown to stimulate neutrophil adhesion to plastic (Dahinden et al. 1983). Studies have shown that stiffness of neutrophils was increased after stimulation with LPS, which related to actin re-organisation, and led to cell retention in pores of transwell filters (Erzurum et al. 1992). Another study found neutrophil chemotaxis was inhibited in response to LPS-induced autocrine ATP signalling, and increases in intracellular calcium (Wang et al. 2017). These studies contrast with our 2D and 3D chemotaxis assays, where LPS-treated neutrophils migrated normally, compared to untreated neutrophils.

Signals induced by LPS or PLY may lead to activation of integrins (inside-out process) which changes the conformation and clustering of integrin on the cell membrane. This increases the affinity and avidity/valency of the integrin for its ligand, respectively. Ligand-occupied integrins connect to the actin cytoskeleton

regulating its reorganization, and driving outside-in signalling, which regulates activities such as cell spreading, adhesion and migration (Langereis 2013).

4.3.2 PLY increased CD11b expression on neutrophils

CD11b forms a heterodimer with CD18, known as Mac-1 or complement receptor 3 (CR3). CD11b is expressed on neutrophils and has important role in migration (Wang et al. 2002) *in vitro* and *in vivo* during extravasation. It also plays a direct role in the phagocytosis of iC3b-coated bacteria.

We showed that CD11b expression markedly increased on neutrophils after exposure to PLY *in vitro*, and in the lungs following intranasal infection with *S.pneumoniae*. Interestingly, calcium flux increases expression and activation of CD11b (Petersen et al. 1993). The strong cellular Ca^{2+} influx produced by PLY may therefore explain the increase in CD11b.

Previous studies have shown that during pneumococcal infection, modulation of CD11b expression on the neutrophil surface plays a functionally significant role in the recognition and clearance of these bacteria (Williams et al. 2003), PLY-mediated up-regulation of CD11b/CD18 expression on neutrophils (Cockeran et al. 2001) and upregulation of CD11b expression on neutrophils has been shown during pneumococcal infection (Glynn et al. 1999; Rijneveld et al. 2005). CD11b is an important regulator of neutrophil adhesion and migration, including recruitment to the lung during *S.pneumoniae* infection (Kadioglu et al. 2011). It has broad ligand specificity, including components of the ECM, cell surface receptors, and proteases. Therefore, the increase in CD11b expression upon treatment with PLY might help to explain the observed changes in neutrophil motility and adhesion.

4.3.3 Increased CD11b expression might explain increased adhesion to fibronectin

CD11b has been shown to be involved in neutrophil adhesion to fibronectin (van den Berg et al. 2001). In addition, S100A9 (small abundant proteins found in human neutrophil cytosol) can promote neutrophil adhesion to fibronectin through activation of CD18, though in this case, blocking CD11b had only a minor effect on adhesion (Anceriz et al. 2007). Consequently, increased adhesion to fibronectin might be explained by increased CD11b expression.

Surprisingly, we found that CD18 expression was almost absent on neutrophils, even after stimulation with PLY. Studies where CD11b and CD18 were expressed individually in cell lines showed each subunit has a distinct function, where CD11b to important for firm adhesion and CD18 is critical for cell migration. This would fit with our data, where increased CD11b expression is linked to increased adhesion. However , the physiological relevance of this finding, such as whether or not CD11b would ever be expressed on the cell surface in the absence of CD18, is unclear (Solovjov et al. 2005).

4.3.4 CD49b and CD49d

Since PLY can modulate surface expression of CD11b, we investigated the effects of PLY treatment on a panel of other integrin subunits, including CD49b and CD49d.

Studies have shown CD49b/CD29 (collagen-binding) and CD49d/CD29 (VCAM-1/fibronectin-binding) have an important role in regulating neutrophil interstitial migration and accumulation in the lungs, respectively (Werr et al. 2000; Kadioglu et al. 2011; Hynes 1992; Plow et al. 2000; Ridger et al. 2001).

4.3.4.1 CD49b

In the absence of infection, we found that neutrophils in the mouse bone marrow did not express CD49b, while those in the blood and lung did. Previous studies using rat models have shown that CD49b is absent on blood neutrophils, and is only expressed during neutrophil extravasation to sites of inflammation in response to chemotactic stimuli (Werr et al. 2000). However others have shown that CD49b is expressed on neutrophils in mouse peripheral blood (Ridger et al. 2001). It is possible that lack of expression in bone marrow is due to negative selection of $CD49b^+$ NK cells in our neutrophil isolation procedure, which could also remove $CD49b^+$ neutrophils. Alternatively, CD49b may be expressed upon export from the bone marrow to blood stream, rather than during extravasation from blood to tissue. It is unclear why rats and mice would differ in this respect. CD49b is highly expressed on platelets (Madamanchi et al. 2014), and platelets and neutrophils can adhere to each other to form platelet-neutrophil complexes, particularly in bacterial infection (Johansson et al. 2011). Therefore, CD49b expression on blood neutrophils may be an artefact of platelet-neutrophil complexes.

We observed no change in CD49b expression upon exposure to PLY, or following intranasal infection with *S.pneumoniae*. Furthermore, no change in CD49b expression was found following extravasation from blood to lung. This contrasts with the findings of Werr *et al*, who showed that CD49b expression was induced during PMN extravasation in response to chemotactic stimulation. Studies done by Werr *et al* have shown CD49b/CD29 is a key factor in neutrophil locomotion and recruitment to extravascular tissue. Expression of CD49b/CD29 also supported neutrophil motility in 3D collagen gels (Werr et al. 2000). However, our findings

here show that alteration in CD49b expression cannot explain the observed motility defect in 3D collagen gel assays in this study.

4.3.4.2 CD49d

CD49d expression was observed in bone marrow, blood and lung neutrophils. However, CD49d expression was not significantly altered following treatment with PLY, or intranasal infection with *S.pneumoniae*. It has been shown that CD49d is expressed at low levels on rodent neutrophils and its expression is elevated as neutrophils are mobilized from the bone marrow (Furze & Rankin 2008). Meanwhile, other studies show that CD49d/CD29 expression on migrated neutrophils decreased during pneumococcus infection (Tasaka et al. 2002). During pneumococcus infection, neutrophil adherence to the vasculature and accumulation into the lung tissue is dependent on CD49d/CD29 (Kadioglu et al. 2011). Our findings here do not support the idea that alteration in CD49d expression could explain the observed motility defect following treatment with PLY. We cannot rule out that changes in activation of the integrin at the cell surfaces might explain the observed defect in migration.

4.4 Conclusion

The data presented in this chapter gives rise to a hypothesis where impaired chemotaxis in PLY-treated neutrophils may be linked to increased CD11b expression, which drives firm adhesion to ECM-components, limiting migration. The role of Ca^{2+} flux in this process should also be investigated. We unexpectedly found low or absent levels of CD18 expression on neutrophils, whether or not CD11b would ever be expressed on the cell surface in the absence of CD18, remains unclear. It is possible that there was a technical issue with the antibody, and the use of a positive control cell known to express CD18 may help to elucidate this matter. Nevertheless, since CD18 staining was absent in both presence and absence of PLY, it cannot explain the observed differences in migration

Chapter 5: Global proteomic analysis of PLY-stimulated neutrophils

5.1 Brief Introduction

The *S. pneumoniae* toxin, pneumolysin (PLY) alters neutrophil migration and function, For example, PLY alters the respiratory burst and bactericidal activity in neutrophils, and our own experiments show a reduction in chemotaxis in 2D and 3D environments. However, the exact molecular mechanisms underpinning these functional changes remain unclear. Global analysis of changes in gene or protein expression following exposure of neutrophils to PLY might help to identify the molecular pathways involved in these functional changes.

In Chapter 3 it was determined that PLY inhibited neutrophil chemotaxis in 2D and 3D migration assays, and that inhibition depended on the haemolytic activity of the toxin. In Chapter 4, the aim was to understand the molecular mechanism by which PLY inhibits neutrophil migration. We found that PLY increased CD11b expression on neutrophils *in vitro* and infection with *S. pneumoniae* increased CD11b expression on blood and lung neutrophils *in vivo.* PLY also increased actin polymerization, and adhesion to tissue culture plastic and fibronectin. While these findings may help to explain impaired migration, they do not provide a detailed molecular mechanism for our findings.

The aim of this chapter was to obtain further clues as to how PLY inhibits neutrophil chemotaxis and defensive function, revealing novel influences of PLY on neutrophil function. To achieve this, we used label-free quantitative mass spectrometry to perform a global analysis of the effect of PLY on protein expression in neutrophils.

The knowledge gained from this global analysis will identify candidate proteins involved in regulating neutrophil migration and function, which may be targeted therapeutically to modulate neutrophil function.

5.2 Results

5.2.1 Preliminary proteomic analysis of isolated neutrophils

Mass spectrometry analysis was performed on isolated neutrophils to determine the minimum number of cells required to be able to detect proteins involved in neutrophil defensive function and motility.

Neutrophils were harvested from bone marrow before being plated and incubated for 4 hours. From a single mouse, $0.95x10^6$ neutrophils were obtained, with a purity of 89% ($Ly6G^+CD11b^+$) determined by flow cytometry. After incubation, neutrophils were washed twice in PBS to remove remaining serum, and cell pellets immediately frozen. Protein extraction, protein digestion, LC-MS/MS analysis, and identification of differentially expressed peptides were performed by Dr Stuart Armstrong from Department of Infection Biology, IGH.

Using an exclusion criterion of ≥ 2 peptides identified per protein, 1600 proteins were identified in the preliminary experiment. The gene list analysis tool Panther was used to characterise the identified proteins according to biological process. A number of proteins categorised as "immune system process", "biological adhesion" and "locomotion" were identified (Figure 63A). Data were compared with predicted proteins from the whole *Mus musculus* proteome, derived from Uniprot (Figure 63B). We found that the proportion of proteins categorised under each biological process was similar in our dataset, as in the whole mouse proteome, suggesting there

was no enrichment or bias in the collection of data. Our dataset contained 7.52% of all proteins classified as “immune system process”, 7.41% of all proteins classified as “biological adhesion”, and 5.86% of all proteins classified as “locomotion” (Table 11). Specific proteins identified in these categories are listed in Table 12, 13 and 14. Of these, integrin alpha-M, integrin alpha-L, L-selectin, integrin beta-2 are already known to play a role in neutrophil migration or adhesion. From a single mouse, we were able to detect a number of proteins involved in neutrophil defensive function and motility, validating the approach.

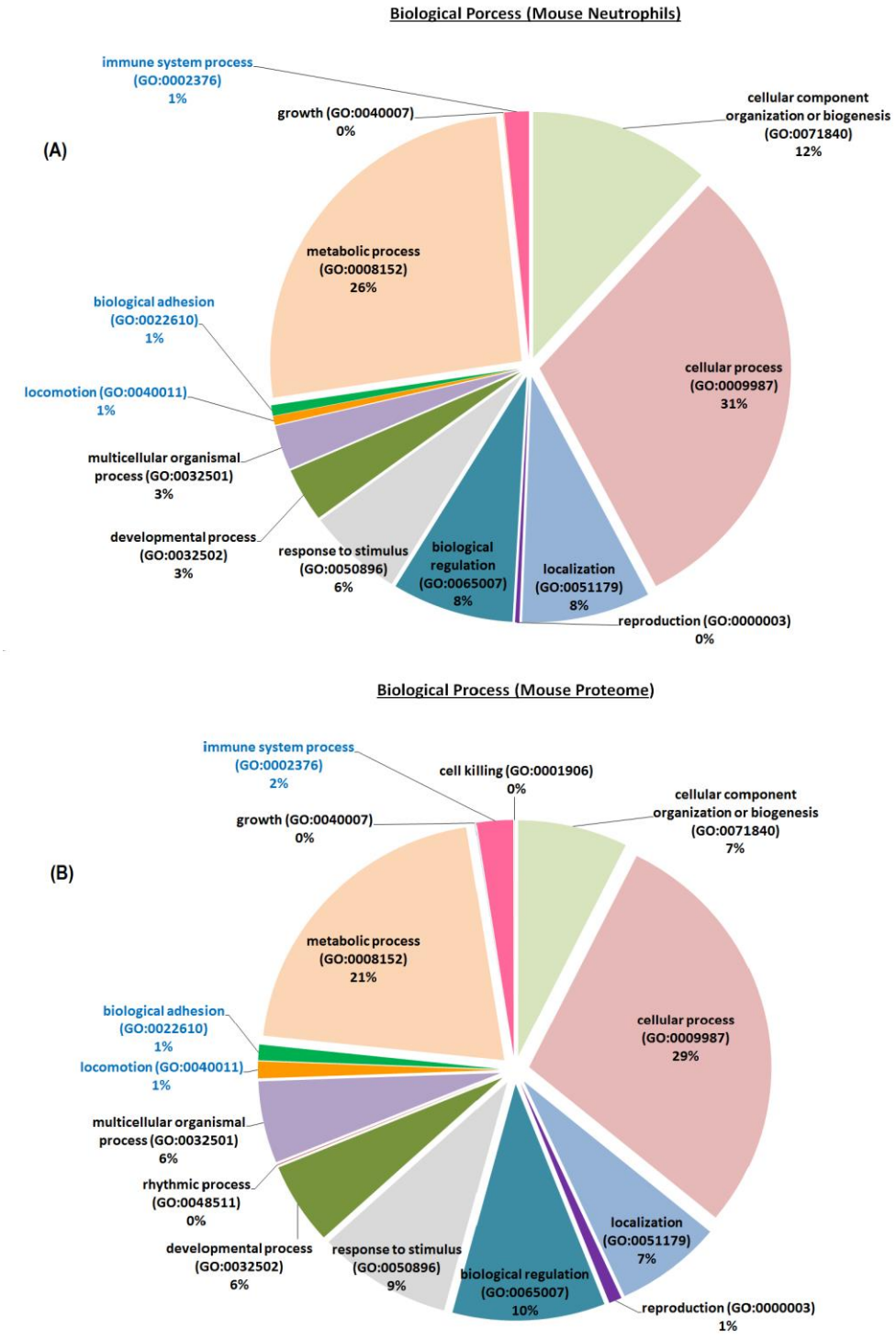

Figure 63: The percentage of proteins classified under each biological process is similar in isolated bone marrow neutrophils as in the whole mouse proteome.
Neutrophils were purified from bone marrow before being plated and incubated for 4 hours at 37°C. Proteins were extracted, digested, and subjected to mass spectrometry. 1600 identified proteins were classified using Panther (A) and compared with the whole mouse (B).

Table 11: Comparison of proteins identified in three biological process categories

Biological Process	Mouse (Proteome)	Mouse (Neutrophils)	% Identified
	IDs/Gene	IDs/Gene	
Immune System Process	612	46	7.52
Biological Adhesion	270	20	7.41
Locomotion	290	17	5.86

Table 12: Proteins identified in bone marrow neutrophils and classified in Panther as belonging to the biological process, "biological adhesion"

	Mapped IDs	Gene Name	Gene Symbol
1	Q61411	GTPase HRas	*Hras*
2	Q3UV74	Integrin beta-2-like protein	*Itgb2l*
3	P05555	Integrin alpha-M	*Itgam*
4	Q3U2S8	Voltage-gated hydrogen channel 1	*Hvcn1*
5	P61226	Ras-related protein Rap-2b	*Rap2b*
6	Q80ZJ1	Ras-related protein Rap-2a	*Rap2a*
7	Q9QVP9	Protein-tyrosine kinase 2-beta	*Ptk2b*
8	P62835	Ras-related protein Rap-1A	*Rap1a*
9	Q9ERD8	Gamma-parvin	*Parvg*
10	Q8BU31	Ras-related protein Rap-2c	*Rap2c*
11	P32883	GTPase KRas	*Kras*
12	Q60875	Rho guanine nucleotide exchange factor 2	*Arhgef2*
13	P24063	Integrin alpha-L	*Itgal*
14	P18337	L-selectin	*Sell*
15	P08556	GTPase NRas	*Nras*
16	Q4LDD4	Arf-GAP with Rho-GAP domain, ANK repeat and PH domain-containing protein 1	*Arap1*
17	Q9JIW9	Ras-related protein Ral-B	*Ralb*
18	P11835	Integrin beta-2	*Itgb2*
19	P16879	Tyrosine-protein kinase Fes/Fps	*Fes*
20	P97797	Tyrosine-protein phosphatase non-receptor type substrate 1	*Sirpa*

Table 13: Proteins identified in bone marrow neutrophils and classified in Panther as belonging to the biological process, "immune system process"

	Mapped IDs	Gene Name	Gene Symbol
1	Q04207	Transcription factor p65	*Rela*
2	P11352	Glutathione peroxidase 1	*Gpx1*
3	P42232	Signal transducer and activator of transcription 5B	*Stat5b*
4	Q9CXY6	Interleukin enhancer-binding factor 2	*Ilf2*
5	P06339	H-2 class I histocompatibility antigen, D-37 alpha chain	*H2-T23*
6	P48453	Serine/threonine-protein phosphatase 2B catalytic subunit beta isoform	*Ppp3cb*
7	Q8BK64	Activator of 90 kDa heat shock protein ATPase homolog 1	*Ahsa1*
8	Q3U2S8	Voltage-gated hydrogen channel 1	*Hvcn1*
9	P48025	Tyrosine-protein kinase SYK phosphatase 2B catalytic subunit alpha isoform	*Syk*
10	P48722	Heat shock 70 kDa protein 4L	*Hspa4l*
11	Q9QZS3	Protein numb homolog	*Numb*
12	P97315	Cysteine and glycine-rich protein 1	*Csrp1*
13	P63087	Serine/threonine-protein phosphatase PP1-gamma catalytic subunit	*Ppp1cc*
14	Q9QVP9	Protein-tyrosine kinase 2-beta	*Ptk2b*
15	P63330	Serine/threonine-protein phosphatase 2A catalytic subunit alpha isoform	*Ppp2ca*
16	P63328	Serine/threonine-protein	*Ppp3ca*
17	P41216	Long-chain-fatty-acid--CoA ligase 1	*Acsl1*
18	P30993	C5a anaphylatoxin chemotactic receptor 1	*C5ar1*
19	P14234	Tyrosine-protein kinase Fgr	*Fgr*
20	O08807	Peroxiredoxin-4	*Prdx4*
21	P18337	L-selectin	*Sell*
22	P42230	Signal transducer and activator of transcription 5A	*Stat5a*
23	Q64277	ADP-ribosyl cyclase/cyclic ADP-ribose hydrolase 2	*Bst1*
24	P48999	Arachidonate 5-lipoxygenase	*Alox5*
25	P27784	C-C motif chemokine 6	*Ccl6*
26	P62137	Serine/threonine-protein phosphatase PP1-alpha catalytic subunit	*Ppp1ca*
27	P08103	Tyrosine-protein kinase HCK	*Hck*
28	Q91VI7	Ribonuclease inhibitor	*Rnh1*
29	P25911	Tyrosine-protein kinase Lyn	*Lyn*

30	O88536	Formyl peptide receptor 2	*Fpr2*
31	Q8K4I3	Rho guanine nucleotide exchange factor 6	*Arhgef6*
32	P42225	Signal transducer and activator of transcription 1	*Stat1*
33	Q61805	Lipopolysaccharide-binding protein	*Lbp*
34	O54950	5'-AMP-activated protein kinase subunit gamma-1	*Prkag1*
35	Q3UND0	Src kinase-associated phosphoprotein 2	*Skap2*
36	Q91XR9	Phospholipid hydroperoxide glutathione peroxidase, nuclear	*Gpx4*
37	P28293	Cathepsin G	*Ctsg*
38	Q91VE0	Long-chain fatty acid transport protein 4	*Slc27a4*
39	P27870	Proto-oncogene vav	*Vav1*
40	P22437	Prostaglandin G/H synthase 1	*Ptgs1*
41	Q99J93	Interferon-induced transmembrane protein 2	*Ifitm2*
42	P41241	Tyrosine-protein kinase CSK	*Csk*
43	P42227	Signal transducer and activator of transcription 3	*Stat3*
44	P16879	Tyrosine-protein kinase Fes/Fps	*Fes*
45	Q61316	Heat shock 70 kDa protein 4	*Hspa4*
46	P97797	Tyrosine-protein phosphatase non-receptor type substrate 1	*Sirpa*

Table 14: Proteins identified in bone marrow neutrophils and classified in Panther as belonging to the biological process, "locomotion"

	Mapped IDs	**Gene Name**	**Gene Symbol**
1	Q3UV74	Integrin beta-2-like protein	*Itgb2l*
2	Q8R527	Rho-related GTP-binding protein RhoQ	*Rhoq*
3	Q62178	Semaphorin-4A	*Sema4a*
4	P60766	Cell division control protein 42 homolog	*Cdc42*
5	O35904	Phosphatidylinositol 4,5-bisphosphate 3-kinase catalytic subunit delta isoform	*Pik3cd*
6	P30993	C5a anaphylatoxin chemotactic receptor 1	*C5ar1*
7	Q7TMB8	Cytoplasmic FMR1-interacting protein 1	*Cyfip1*
8	Q9CPW4	Actin-related protein 2/3 complex subunit 5	*Arpc5*
9	P27784	C-C motif chemokine 6	*Ccl6*
10	Q9QUI0	Transforming protein RhoA	*Rhoa*

11	P60764	Ras-related C3 botulinum toxin substrate 3	*Rac3*
12	O88536	Formyl peptide receptor 2	*Fpr2*
13	P62746	Rho-related GTP-binding protein RhoB	*Rhob*
14	P11835	Integrin beta-2	*Itgb2*
15	Q99J93	Interferon-induced transmembrane protein 2	*Ifitm2*
16	Q62159	Rho-related GTP-binding protein RhoC	*Rhoc*
17	P16879	Tyrosine-protein kinase Fes/Fps	*Fes*

5.2.2 Proteomic analysis of the effect of PLY on neutrophils

We next proceeded with proteomic analysis of neutrophils stimulated with PLY. Unstimulated neutrophils were used as a negative control, and LPS treated neutrophils used to (1) reveal unique aspects of the neutrophil response to PLY vs general activation, and (2) control for any contaminating LPS in the PLY preparation. Neutrophils were isolated from bone marrow of four mice in each of three independent experiments. Neutrophils were left untreated, or treated with PLY or LPS, and plated for 4 hours at 37°C. Prior to proteomic analysis, quality control was performed by withdrawing small numbers of cells for flow cytometric analysis of purity, survival and CD11b expression. Since we observed increased adhesion of PLY-treated cells to TC plastic in Chapter 4, cells from each condition were also counted to check cell recovery was roughly equivalent. A summary of the quality control data is presented in Table 15. Purity exceeded 95% in all experiments; with more than 90% viable cells in all conditions with MFI ratio for CD11b expression on neutrophil at more than 3.0 for PLY and LPS treated neutrophils. Results for quality control were further supported by Figures in 64, 65, 66 and 67 with bar charts and representative flow cytometry histogram and plots.

Table 15: Summary of quality control results for proteomic samples
(A) Neutrophils were stained with anti-CD11b and anti-Ly6G and analysed by flow cytometry to check pre-culture purity (B) Neutrophils was plated alone, or with PLY or LPS, and incubated at 37°C for 4 hours. After incubation, cells were stained with Live /Dead dye and anti-CD11b, and analysed by flow cytometry.

Samples isolated (3 independent isolations, 4 mice pooled for each)	**Yield (n=3)**	**Purity (%)(n=3)**
(A) Neutrophils	$3.37 \times 10^7 \pm 2.5 \times 10^6$	96.7 ± 1.4
(B) Staining: Live/ Dead and CD11b	% of Live cells (n=3)	MFI Ratio (n=3)
Neutrophils	97 ± 0.2	1.0 ± 0.0
Neutrophils + PLY	95 ± 0.5	3.6 ± 0.5
Neutrophils +LPS	93 ± 1.0	12.9 ± 2.2

In Figure 64 (I), a summary of total cell counts recovered at the end of the culture period is presented. Even after thoroughly scraping off the neutrophils attached to the TC plastic plate, we still recovered slightly fewer PLY-treated neutrophils than untreated or LPS-treated neutrophil, which agrees with increased adhesion in our earlier experiments. In Figure 66, CD11b expression on neutrophils was increased after treatment with PLY and this agreed with our previous data in Chapter 3. This confirmed that the neutrophils had responded appropriately to PLY treatment. However, we also found that LPS treated neutrophils showed a more dramatic increase in CD11b expression when compared to PLY-treated neutrophils, and to our previous data in Chapter 3. This may due to the timing of the exposure to PLY: 45 minutes in Chapter 3, and 4 hours in this chapter. As a final assessment of sample quality, Figure 67 shows that PLY (II) and LPS (III) -treated neutrophils have a good viability, comparable with control, untreated neutrophils. Our quality control results concluded we have sufficient high quality neutrophils ($1.04 \times 10^7 \pm 3.1 \times 10^5$), PLY-treated neutrophils ($8.8 \times 10^6 \pm 1.6 \times 10^5$) and LPS-treated neutrophils ($9.4 \times 10^6 \pm 1.7 \times 10^5$) to proceed with the full proteomic analysis.

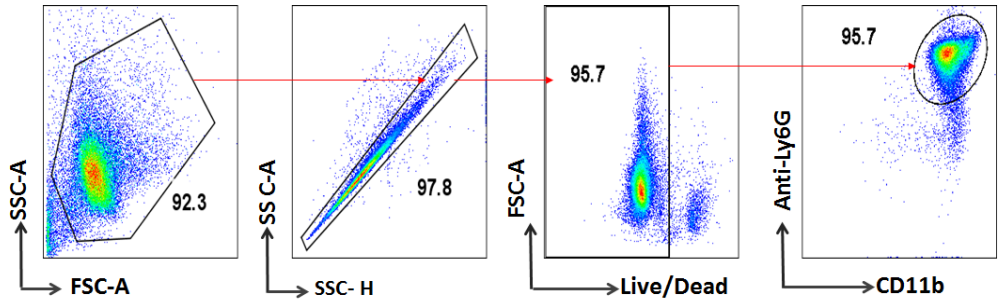

Figure 64: Flow cytometry analysis of neutrophil purity in samples used for proteomic analysis.

Neutrophils were purified from bone marrow and a small aliquot withdrawn and stained with anti-CD11b and anti Ly6G to check purity. From left to right, plots show discrimination of live cells based on forward and side scatter, discrimination of single cells from doublets, discrimination of live cells, and neutrophils identified by positive staining for CD11b and Ly6G. Data are representative of 3 independent experiments.

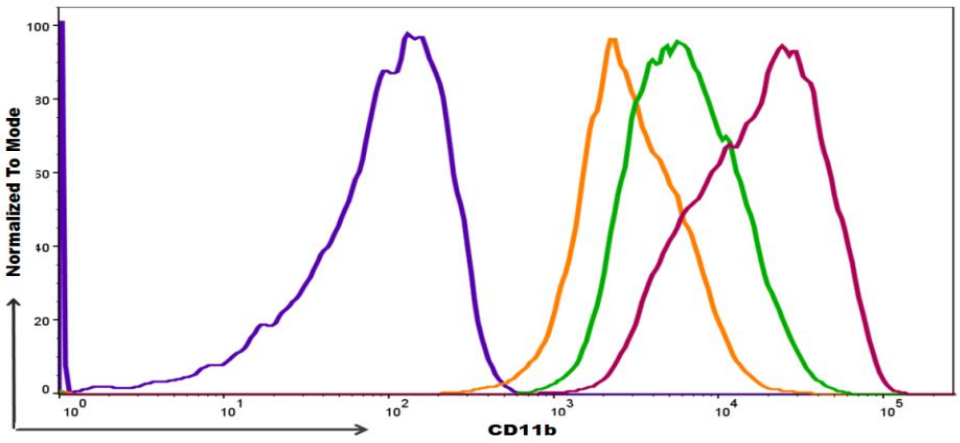

Figure 65: CD11b expression was increased on PLY-treated neutrophils used for proteomic analysis

Neutrophils were plated alone, or with PLY or LPS, and incubated at 37°C for 4 hours before small aliquots were withdrawn for analysis of CD11b expression. The [purple] peak shows fluorescent intensity of unstained control cells. The [orange] peak shows CD11b staining on untreated neutrophils. The [green] peak shows CD11b staining on neutrophils treated with PLY and [red] peak for LPS treated neutrophils. Data are representative of three independent experiments.

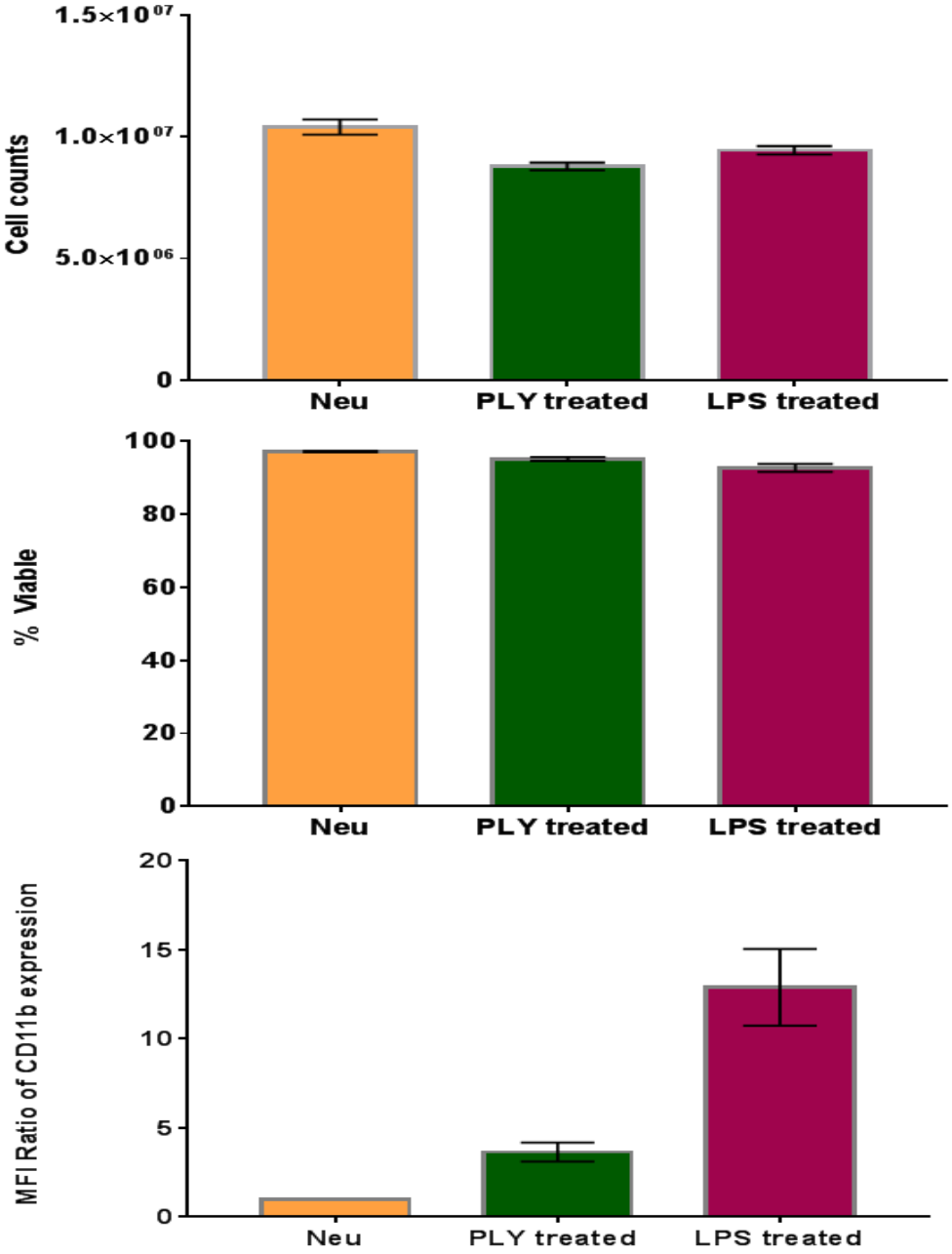

Figure 66: Summary of quality control analysis for proteomic studies
Neutrophils was plated alone, or with PLY or LPS, and incubated at 37°C for 4 hours. After incubation, cells were recovered and analysed by flow cytometry. Graphs depict (I) Total cell counts at the end of the culture period (II) Percentage viability of neutrophils assessed by LIVE/DEAD staining, (III) Ratio of CD11b MFI in treated compared to untreated neutrophils. Data are combined from 3 independent experiments. Mean ± SEM is shown.

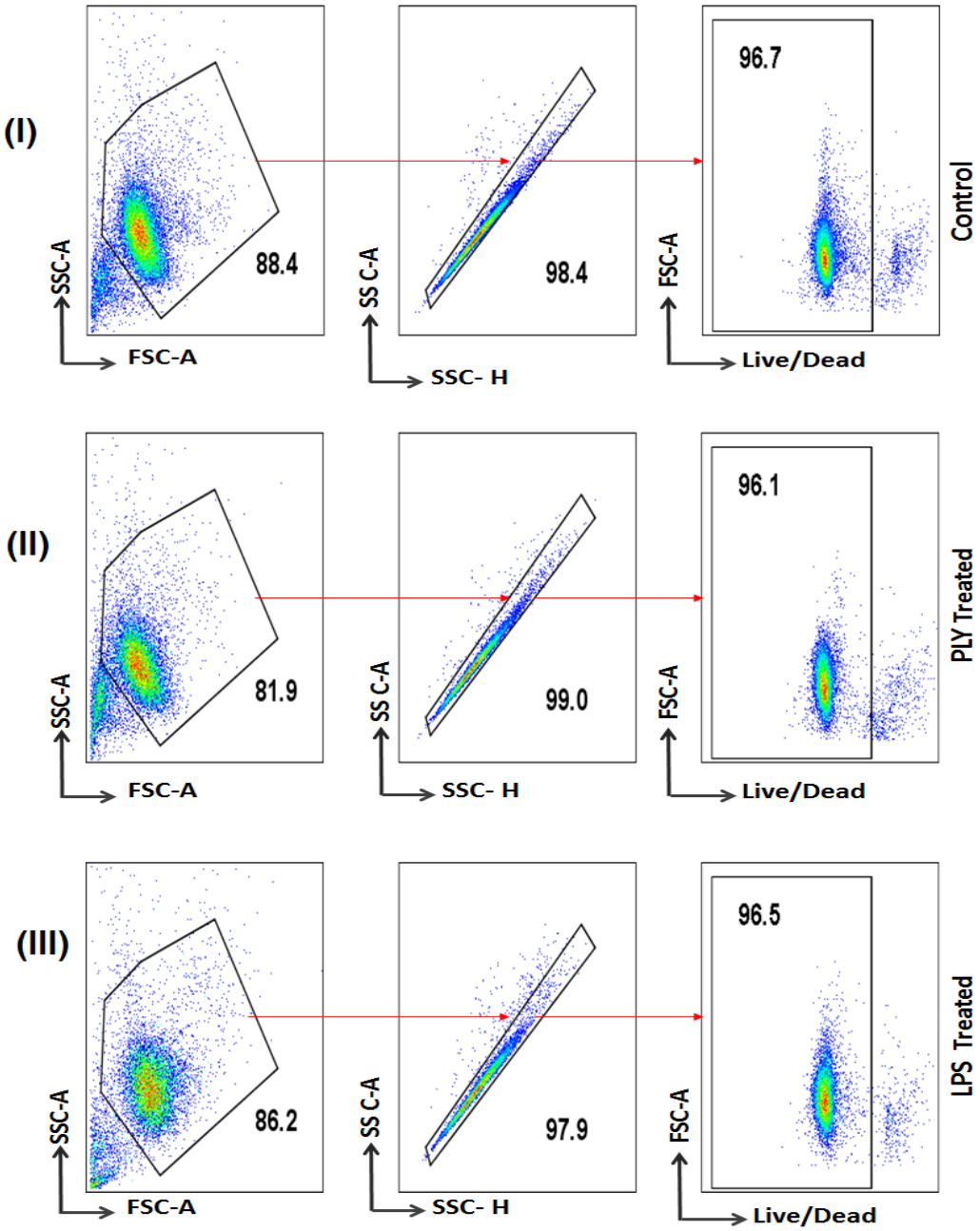

Figure 67: Flow cytometry analysis of cell viability in neutrophils used for proteomic analysis

Neutrophils were plated alone, or with PLY or LPS, and incubated at 37°C for 4 hours. After incubation small aliquots were withdrawn for Live/Dead Staining dye and analysed by flow cytometry. (I) Untreated neutrophils (II) Neutrophils treated with PLY (III) Neutrophils treated with LPS. Plots are representative of 3 independent experiments.

5.2.3 Global Analysis of the neutrophil response to PLY treatment

Having confirmed sample quality for nine samples from three replicates for each condition (control, PLY and PLY –treated neutrophils) we proceeded to label free quantitative proteomic analysis. Sample processing and data analysis was performed by Dr Stuart Armstrong. Group comparisons were performed using the Progenesis LC-MS proteomics software platform. Statistically significant differentially abundant proteins (ANOVA) from both pairwise comparisons and between all groups were used to investigate protein function and enrichment using the online tools DAVID and STRING, this was assisted by Dr Stuart Armstrong. Data obtained were run through UniProt Programme for additional protein identification and function. Candidate proteins from the analysis where then validated based on function related to migration using western blot, immunofluorescence staining and 2D chemotaxis assay. The summary of schematic workflow performed during this process is in Figure 68.

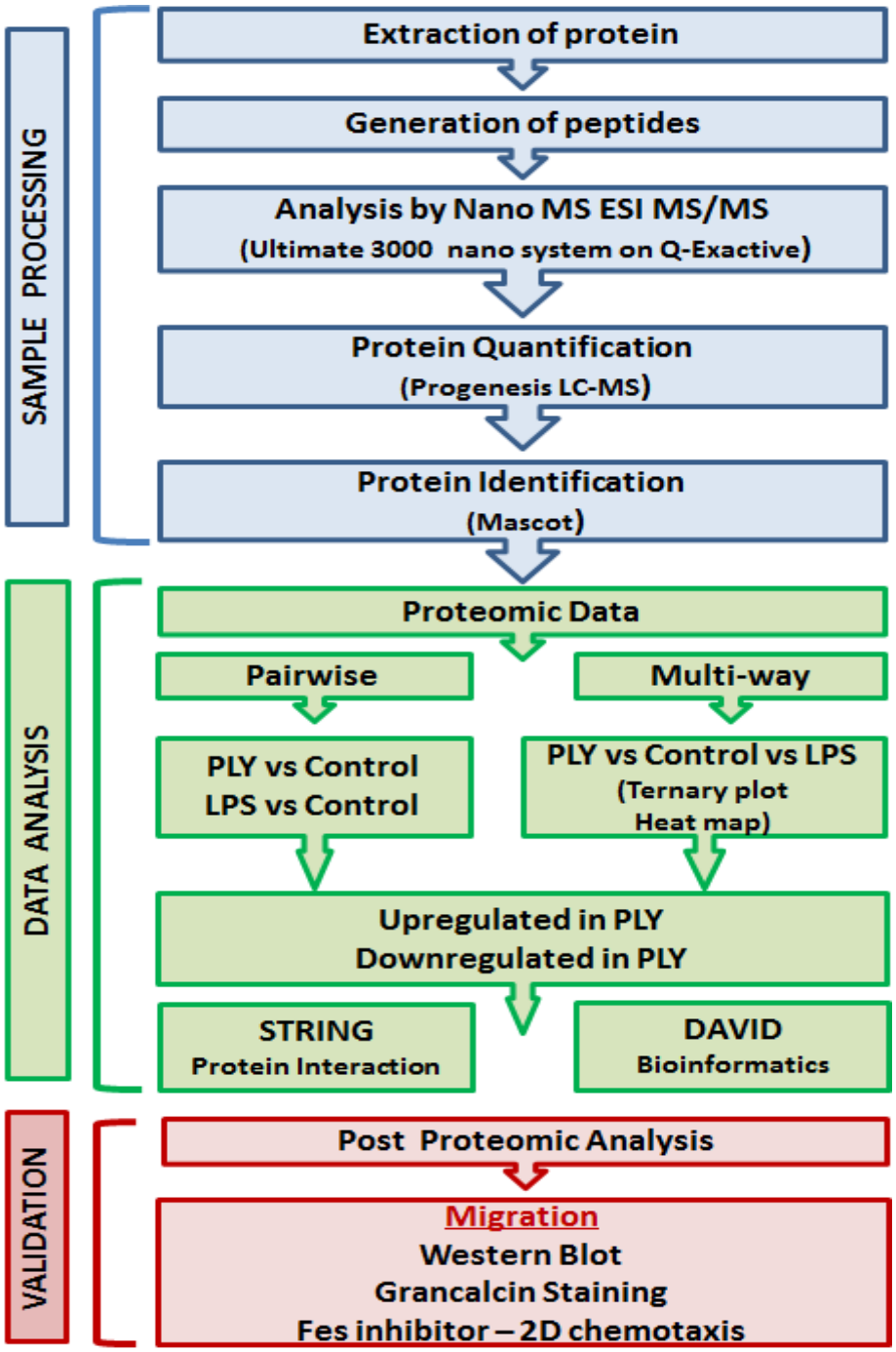

Figure 68: Schematic diagram of the workflow for proteomic analysis.
Neutrophils were purified from bone marrow, and plated alone or with PLY or LPS. After 4 hours, samples were collected for proteomic analysis. Following protein extraction and digestion, samples were analysed by label free quantitative mass spectrometry. Following quantification and identification of proteins, data were analysed in two ways to identify proteins altered in abundance by PLY, but not LPS; pairwise and multi-way comparisons. Post proteomic analysis to validate targets with a putative role in cell migration included western blotting, immunofluorescent staining, and function blocking experiments.

5.2.3.1 Pairwise comparison between PLY vs control and LPS vs Control, to identify proteins significantly changed only by PLY.

Initially, pairwise comparisons between PLY-treated and control neutrophils, and between LPS-treated and control neutrophils were performed by Progenesis LC-MS where the peptide intensities were normalised against the reference, highlighting the differences in protein expression between both samples. Spectral data were then exported for peptide identification using Mascot. Using an exclusion criteria of q <0.05, >2 unique peptides, >2 fold change, 82 proteins changed in abundance following treatment with PLY (41 upregulated and 41 downregulated), and 57 proteins changed in abundance following treatment with LPS (22 upregulated and 35 downregulated) (Appendix 1-2).

PLY-treatment of neutrophils results in impaired chemotaxis, whereas treatment with LPS does not. To identify proteins that change in abundance in response to PLY, but not LPS, we compared the lists of proteins significantly changed in abundance in PLY-treated samples vs controls, and in LPS-treated samples vs controls.

We found 22 proteins significantly increased in abundance in PLY-treated neutrophils compared to control, but *not* in LPS-treated samples compared to control (Figure 69, Table 16, Table 17 and Table 18)

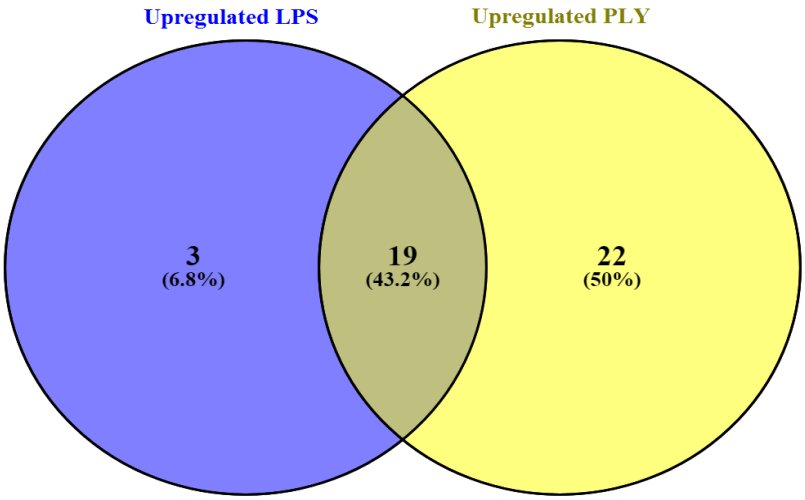

Figure 69: Venn diagram of the proteins upregulated in LPS-treated neutrophils (blue), and PLY treated neutrophils (yellow) vs control
Proteins were segregated using Venny 2.1 Bioinfo CNB-CSIC tool: http:// bioinfogp.cnbcsic.es/tools/venny

Table 16: List of protein upregulated in LPS- treated neutrophils vs control

No.	Accession	Gene	Protein
1.	Q9R0U0	*Srsf10*	Serine/arginine-rich splicing factor 10
2.	Q8VDM6	*Hnrnpul1*	Heterogeneous nuclear ribonucleoprotein U-like protein 1
3.	Q8CHK3	*Mboat7*	Lysophospholipid acyltransferase 7
4.	Q8BTI9	*Pik3cb*	Phosphatidylinositol 4,5-bisphosphate 3-kinase catalytic subunit beta isoform
5.	P36371	*Tap2*	Antigen peptide transporter 2
6.	Q99MK8	*Adrbk1*	Beta-adrenergic receptor kinase 1
7.	O88668	*Creg1*	Protein CREG1
8.	Q8K352	*Sash3*	SAM and SH3 domain-containing protein 3
9.	Q8QZY6	*Tspan14*	Tetraspanin-14
10.	P58021	*Tm9sf2*	Transmembrane 9 superfamily member 2
11.	O35841	*Api5*	Apoptosis inhibitor 5
12.	Q9Z1F9	*Uba2*	SUMO-activating enzyme subunit 2
13.	Q9JKB1	*Uchl3*	Ubiquitin carboxyl-terminal hydrolase isozyme L3
14.	Q9D6R2	*Idh3a*	Isocitrate dehydrogenase [NAD] subunit alpha, mitochondrial
15.	Q6P1F6	*Ppp2r2a*	Serine/threonine-protein phosphatase 2A 55 kDa regulatory subunit B alpha isoform
16.	P97484	*Lilrb3*	Leukocyte immunoglobulin-like receptor

			subfamily B member 3
17.	Q80UG5	*Sept9*	Septin-9 OS
18.	O08749	*Dld*	Dihydrolipoyl dehydrogenase, mitochondrial
19.	Q9DBC7	*Prkar1a*	cAMP-dependent protein kinase type I-alpha regulatory subunit
20.	Q9R062	*Gyg1*	Glycogenin-1
21.	Q03267	*Ikzf1*	DNA-binding protein Ikaros
22.	P63082	*Atp6v0c*	V-type proton ATPase 16 kDa proteolipid subunit

Table 17: List of protein upregulated in PLY-treated neutrophils vs control

No.	Accession	Gene	Protein
1.	Q9Z1F9	*Uba2*	SUMO-activating enzyme subunit 2
2.	Q9R0U0	*Srsf10*	Serine/arginine-rich splicing factor 10
3.	Q9CR68	*Uqcrfs1*	Cytochrome b-c1 complex subunit Rieske, mitochondrial
4.	O88668	*Creg1*	Protein CREG1
5.	Q60931	*Vdac3*	Voltage-dependent anion-selective channel protein 3
6.	Q9JHK5	*Plek*	Pleckstrin
7.	Q8CHK3	*Mboat7*	Lysophospholipid acyltransferase 7
8.	Q8BTI9	*Pik3cb*	Phosphatidylinositol 4,5-bisphosphate 3-kinase catalytic subunit beta isoform
9.	Q9D6R2	*Idh3a*	Isocitrate dehydrogenase [NAD] subunit alpha, mitochondrial
10.	P58021	*Tm9sf2*	Transmembrane 9 superfamily member 2
11.	Q8VDM6	*Hnrnpul1*	Heterogeneous nuclear ribonucleoprotein U-like protein 1
12.	P36371	*Tap2*	Antigen peptide transporter 2
13.	Q8QZY6	*Tspan14*	Tetraspanin-14
14.	Q9D0M3	*Cyc1*	Cytochrome c1, heme protein, mitochondrial
15.	Q8K352	*Sash3*	SAM and SH3 domain-containing protein 3
16.	P63028	*Tpt1*	Translationally-controlled tumor protein 7
17.	Q6P8X1	*Snx6*	Sorting nexin-6
18.	Q9JKB1	*Uchl3*	Ubiquitin carboxyl-terminal hydrolase isozyme L3
19.	P97484	*Lilrb3*	Leukocyte immunoglobulin-like receptor subfamily B member 3
20.	P63082	*Atp6v0c*	V-type proton ATPase 16 kDa proteolipid subunit
21.	Q9WTP6	*Ak2*	Adenylate kinase 2, mitochondrial
22.	Q61768	*Kif5b*	Kinesin-1 heavy chain
23.	Q6P1F6	*Ppp2r2a*	Serine/threonine-protein phosphatase 2A 55 kDa regulatory subunit B alpha isoform

24.	O09043	*Napsa*	Napsin-A
25.	Q99MK8	*Adrbk1*	Beta-adrenergic receptor kinase 1
26.	Q9R062	*Gyg1*	Glycogenin-1
27.	P54775	*Psmc4*	26S protease regulatory subunit 6B
28.	Q80W54	*Zmpste24*	CAAX prenyl protease 1 homolog
29.	Q80UG5	*Sept9*	Septin-9
30.	Q921F4	*Hnrnpll*	Heterogeneous nuclear ribonucleoprotein L-like
31.	P16879	*Fes*	Tyrosine-protein kinase Fes/Fps
32.	B2RQC6	*Cad*	CAD protein
33.	A3KGF7	*Plcb2*	1-phosphatidylinositol 4,5-bisphosphate phosphodiesterase beta-2
34.	Q8QZS1	*Hibch*	3-hydroxyisobutyryl-CoA hydrolase, mitochondrial
35.	P50637	*Tspo*	Translocator protein
36.	Q571E4	*Galns*	N-acetylgalactosamine-6-sulfatase
37.	O35593	*Psmd14*	26S proteasome non-ATPase regulatory subunit 14
38.	Q03267	*Ikzf1*	DNA-binding protein Ikaros
39.	Q3UMR5	*Mcu*	Calcium uniporter protein, mitochondrial
40.	Q8BGQ7	*Aars*	Alanine--tRNA ligase, cytoplasmic
41.	Q9WV54	*Asah1*	Acid ceramidase

Table 18: List of proteins significantly upregulated in PLY-treated neutrophils only

No.	UniP Accession	Gene	Protein
1.	Q8BGQ7	*Aars*	Alanine--tRNA ligase, cytoplasmic
2.	Q9WTP6	*Ak2*	Adenylate kinase 2, mitochondrial
3.	Q9WV54	*Asah1*	Acid ceramidase
4.	B2RQC6	*Cad*	CAD protein
5.	Q9D0M3	*Cyc1*	Cytochrome c1, heme protein, mitochondrial
6.	P16879	*Fes*	Tyrosine-protein kinase Fes/Fps
7.	Q571E4	*Galns*	N-acetylgalactosamine-6-sulfatase
8.	Q8QZS1	*Hibch*	3-hydroxyisobutyryl-CoA hydrolase, mitochondrial
9.	Q921F4	*Hnrnpll*	Heterogeneous nuclear ribonucleoprotein L-like
10.	Q61768	*Kif5b*	Kinesin-1 heavy chain
11.	Q3UMR5	*Mcu*	Calcium uniporter protein, mitochondrial
12.	O09043	*Napsa*	Napsin-A
13.	A3KGF7	*Plcb2*	1-phosphatidylinositol 4,5-bisphosphate phosphodiesterase beta-2
14.	Q9JHK5	*Plek*	Pleckstrin
15.	P54775	*Psmc4*	26S protease regulatory subunit 6B
16.	Q6P8X1	*Snx6*	Sorting nexin-6
17.	P63028	*Tpt1*	Translationally-controlled tumor protein

18.	Q9CR68	*Uqcrfs1*	Cytochrome b-c1 complex subunit Rieske, mitochondrial
19.	Q60931	*Vdac3*	Voltage-dependent anion-selective channel protein 3
20.	Q80W54	*Zmpste24*	CAAX prenyl protease 1 homolog
21.	O35593	*Psmd14*	26S proteasome non-ATPase regulatory subunit 14
22.	P50637	*Tspo*	Translocator protein

Meanwhile, 16 proteins significantly decreased in PLY-treated neutrophils compared to control, but not in LPS-treated neutrophils compared to control (Figure 70, Table 19, Table 20 and Table 21).

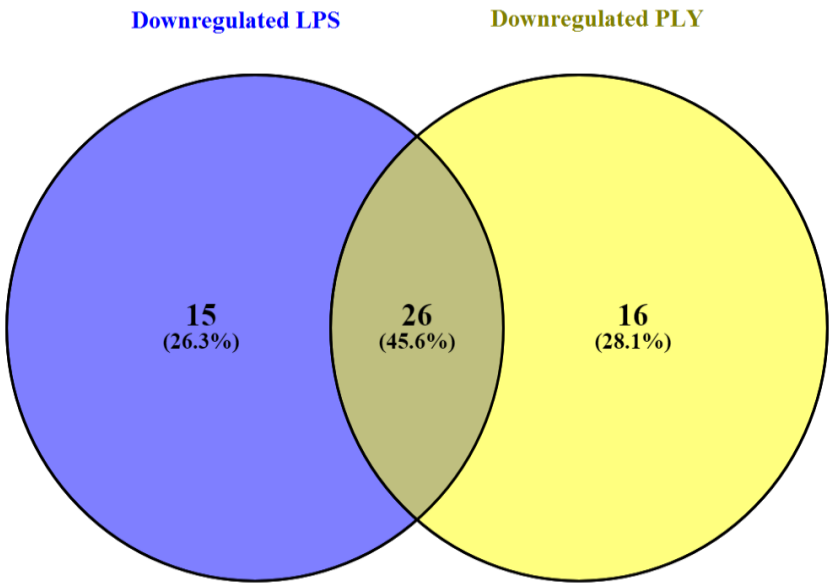

Figure 70:Venn diagram of the proteins of downregulated in LPS-treated neutrophils (blue), and PLY-treated neutrophils (yellow) vs control
Proteins were segregated using Venny 2.1 Bioinfo CNB-CSIC tool: http://bioinfogp.cnb.csic.es/tools/venny/

Table 19: List of proteins downregulated in LPS-treated neutrophils vs control

No.	Accession	Gene	Protein
1.	Q08093	*Cnn2*	Calponin-2
2.	P80316	*Cct5*	T-complex protein 1 subunit epsilon
3.	Q99LF4	*Rtcb*	tRNA-splicing ligase RtcB homolog
4.	P15702	*Spn*	Leukosialin
5.	Q9QZD9	*Eif3i*	Eukaryotic translation initiation factor 3 subunit I
6.	P97797	*Sirpa*	Tyrosine-protein phosphatase non-receptor type substrate 1
7.	Q99KE1	*Me2*	NAD-dependent malic enzyme, mitochondrial
8.	Q9R1T4	*Sept6*	Septin-6
9.	Q64324	*Stxbp2*	Syntaxin-binding protein 2
10.	P27601	*Gna13*	Guanine nucleotide-binding protein subunit alpha-13
11.	Q64277	*Bst1*	ADP-ribosyl cyclase/cyclic ADP-ribose hydrolase 2
12.	P97315	*Csrp1*	Cysteine and glycine-rich protein 1
13.	P99026	*Psmb4*	Proteasome subunit beta type-4
14.	Q60590	*Orm1*	Alpha-1-acid glycoprotein 1
15.	Q62426	*Cstb*	Cystatin-B
16.	P49446	*Ptpre*	Receptor-type tyrosine-protein phosphatase epsilon
17.	P82198	*Tgfbi*	Transforming growth factor-beta-induced protein ig-h3
18.	Q8BZQ2	*Crispld2*	Cysteine-rich secretory protein LCCL domain-containing 2
19.	Q504P2	*Clec12a*	C-type lectin domain family 12 member A
20.	Q9DCL9	*Paics*	Multifunctional protein ADE2
21.	Q6WVG3	*Kctd12*	BTB/POZ domain-containing protein
22.	P51675	*Ccr1*	C-C chemokine receptor type 1
23.	P07724	*Alb*	Serum albumin
24.	Q9EP69	*Sacm1l*	Phosphatidylinositide phosphatase SAC1
25.	Q8BK64	*Ahsa1*	Activator of 90 kDa heat shock protein ATPase homolog 1
26.	Q8VH51	*Rbm39*	RNA-binding protein 39
27.	Q9WTL7	*Lypla2*	Acyl-protein thioesterase 2
28.	O70138	*Mmp8*	Neutrophil collagenase
29.	Q8BGB5	*Limd2*	LIM domain-containing protein
30.	Q52KI8	*Srrm1*	Serine/arginine repetitive matrix protein
31.	Q8VEM8	*Slc25a3*	Phosphate carrier protein, mitochondrial
32.	Q8R016	*Blmh*	Bleomycin hydrolase
33.	P35174	*Stfa2*	Stefin-2

34.	O09044	*Snap23*	Synaptosomal-associated protein 23
35.	P40240	*Cd9*	CD9 antigen
36.	Q6P5F9	*Xpo1*	Exportin-1
37.	P11928	*Oas1a*	2'-5'-oligoadenylate synthase 1A
38.	Q9R0X4	*Acot9*	Acyl-coenzyme A thioesterase 9, mitochondrial
39.	Q9D154	*Serpinb1a*	Leukocyte elastase inhibitor A
40.	P50637	*Tspo*	Translocator protein
41.	O35593	*Psmd14*	26S proteasome non-ATPase regulatory subunit 14

Table 20: List of proteins downregulated in PLY-treated neutrophils vs control

No.	Accession	Gene	Protein
1.	P97797	*Sirpa*	Tyrosine-protein phosphatase non-receptor type substrate
2.	P80316	*Cct5*	T-complex protein 1 subunit epsilon
3.	Q08093	*Cnn2*	Calponin-2
4.	P97315	*Csrp1*	Cysteine and glycine-rich protein 1
5.	P07724	*Alb*	Serum albumin
6.	Q9R1T4	*Sept6*	Septin-6
7.	Q9QZD9	*Eif3i*	Eukaryotic translation initiation factor 3 subunit I
8.	Q504P2	*Clec12a*	C-type lectin domain family 12 member A
9.	P12815	*Pdcd6*	Programmed cell death protein 6
10.	P15702	*Spn*	Leukosialin
11.	Q9DB05	*Napa*	Alpha-soluble NSF attachment protein
12.	Q64324	*Stxbp2*	Syntaxin-binding protein 2
13.	Q8VC88	*Gca*	Grancalcin
14.	P99026	*Psmb4*	Proteasome subunit beta type-4
15.	Q8BFY6	*Pef1*	Peflin
16.	Q99LF4	*Rtcb*	tRNA-splicing ligase RtcB homolog
17.	Q9CPQ8	*Atp5l*	ATP synthase subunit g, mitochondrial
18.	P59108	*Cpne2*	Copine-2
19.	Q60590	*Orm1*	Alpha-1-acid glycoprotein 1
20.	Q9EP69	*Sacm1*	Phosphatidylinositide phosphatase SAC1
21.	P82198	*Tgfbi*	Transforming growth factor-beta-induced protein ig-h3
22.	Q9DCL9	*Paics*	Multifunctional protein ADE2
23.	Q6P5F9	*Xpo1*	Exportin-1
24.	P27601	*Gna13*	Guanine nucleotide-binding protein subunit alpha-13
25.	P41241	*Csk*	Tyrosine-protein kinase CSK

26.	P56376	*Acyp1*	Acylphosphatase-1
27.	Q52KI8	*Srrm1*	Serine/arginine repetitive matrix protein 1
28.	Q99L04	*Dhrs1*	Dehydrogenase/reductase SDR family member 1
29.	Q8BGB5	*Limd2*	LIM domain-containing protein 2
30.	Q8BFR5	*Tufm*	Elongation factor Tu, mitochondrial
31.	Q64277	*Bst1*	ADP-ribosyl cyclase/cyclic ADP-ribose hydrolase 2
32.	P35174	*Stfa2*	Stefin-2
33.	P47968	*Rpia*	Ribose-5-phosphate isomerase
34.	Q501J6	*Ddx17*	Probable ATP-dependent RNA helicase DDX17
35.	P40240	*Cd9*	CD9 antigen
36.	P51675	*Ccr1*	C-C chemokine receptor type 1
37.	Q8BK64	*Ahsa1*	Activator of 90 kDa heat shock protein ATPase homolog 1
38.	P11928	*Oas1a*	2'-5'-oligoadenylate synthase 1A
39.	O88842	*Fgd3*	FYVE, RhoGEF and PH domain-containing protein 3
40.	P97930	*Dtymk*	Thymidylate kinase
41.	Q8BUK6	*Hook3*	Protein Hook homolog 3
42.	P17433	*Spi1*	Transcription factor PU.1

Table 21: List of proteins significantly downregulated in PLY-treated neutrophils only

No.	UniP Accession	Gene	Protein
1.	P56376	*Acyp1*	Acylphosphatase-1
2.	Q9CPQ8	*Atp5l*	ATP synthase subunit g, mitochondrial
3.	P59108	*Cpne2*	Copine-2
4.	P41241	*Csk*	Tyrosine-protein kinase CSK
5.	Q501J6	*Ddx17*	Ddx17
6.	Q99L04	*Dhrs1*	Dehydrogenase/reductase SDR family member 1
7.	P97930	*Dtymk*	Thymidylate kinase
8.	O88842	*Fgd3*	FYVE, RhoGEF and PH domain-containing protein 3
9.	Q8VC88	*Gca*	Grancalcin
10.	Q8BUK6	*Hook3*	Protein Hook homolog 3
11.	Q9DB05	*Napa*	Alpha-soluble NSF attachment protein
12.	P12815	*Pdcd6*	Programmed cell death protein 6
13.	Q8BFY6	*Pef1*	Peflin
14.	P47968	*Rpia*	Ribose-5-phosphate isomerase
15.	Q8BFR5	*Tufm*	Elongation factor Tu, mitochondrial
16.	P17433	*Spi1*	Transcription factor PU.1

In order to assign functional information to all proteins identified, Uniprot Protein knowledgebase (http://www.uniprot.org/) was used. Using UniProt, we identified four proteins related to migration, or involved in adhesion and actin cytoskeleton (Table 22).

Table 22: List of proteins significantly changed in PLY treated neutrophils related to adhesion and actin cytoskeleton

Expression	UniP Accession	Gene	Protein	Function/Role (source UniProt)
Up regulated	P16879	*Fes*	Tyrosine-protein kinase Fes/Fps	• Regulation and rearrangement of the actin cytoskeleton, cell adherence, spreading and migration.
Down regulated	P41241	*Csk*	Tyrosine-protein kinase CSK	• Involved in the regulation of cell migration and immune responses.
Down regulated	O88842	*Fgd3*	FYVE, RhoGEF and PH domain-containing protein 3	• Filopodia organisation. • Regulation of CDC42 activation in cells for; movement, actin cytoskeleton and shape.
Down regulated	Q8VC88	*Gca*	Grancalcin	• Increased neutrophil adhesion on fibronectin. • Involved in the arrangement of focal adhesions.

5.2.3.2 Multi-way comparison of PLY-treated, LPS-treated, and control neutrophils

A multiway comparison of PLY-treated, LPS-treated, and control neutrophils was also performed. We detected 1410 proteins in our experiment, which were filtered and the results are presented as a ternary plot (Figure 71) and heat map (Figure 72).

For the ternary plot a filter of q ≤ 0.05 and ≥ 2 peptides per protein was applied resulting in 404 proteins being displayed in the plot (Figure 71). A list of proteins upregulated in PLY-treated neutrophils compared to both LPS-treated neutrophils and control, and a list of proteins downregulated PLY-treated neutrophils compared to both LPS-treated neutrophils and control is presented in Table 23.

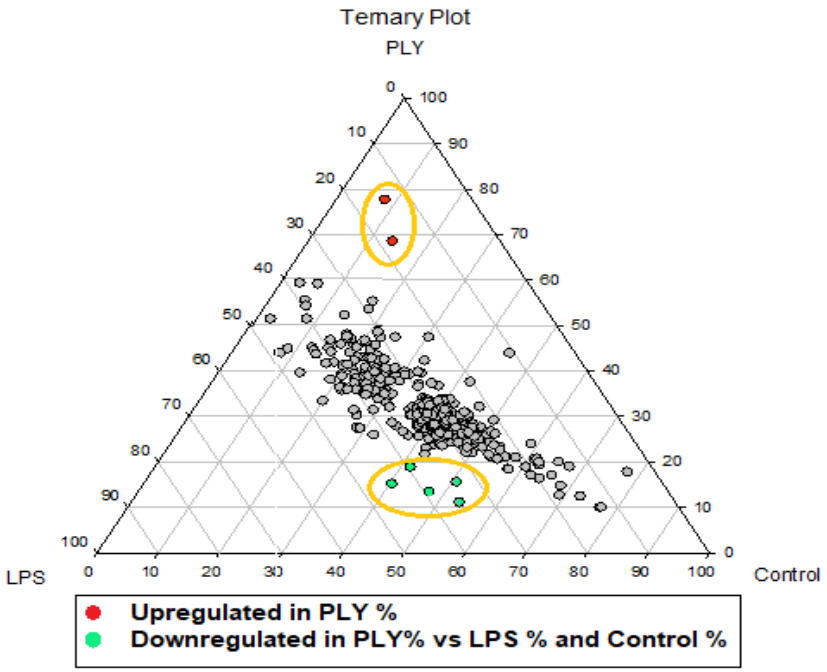

Figure 71: Ternary plot of normalized protein abundances in neutrophils treated with PLY or LPS compared to control

Relative protein abundance was measured using a label free proteomic approach. Proteins with a q-value ≤ 0.05 and ≥ 2 peptides identified were included in the plot. Numbers along the three sides of the triangle represent the proportion of the total signal that belongs to each of the three groups and each point the summed value should equal to 100. Highly up-regulated proteins for PLY-treated neutrophils only (proportion of signal >68%) are highlighted in red. Down-regulated proteins for PLY-treated neutrophil vs LPS and Control (proportion of signal < 20%) are highlighted in green.

Table 23: List of proteins (red) more abundant in PLY-treated neutrophils vs LPS-treated /control (more than 68% signal belongs to PLY) and (green) less abundant in PLY-treated neutrophils vs LPS-treated /control (less than 20 % signal belongs to PLY)

UniP Accession	Gene	Protein
Q9CR68	*Uqcrfs1*	Cytochrome b-c1 complex subunit Rieske, mitochondrial
Q6P8X1	*Snx6*	Sorting nexin-6
P59108	*Cpne2*	Copine-2
Q8VC88	*Gca*	Grancalcin
Q8BFY6	*Pef1*	Peflin
P97930	*Dtymk*	Thymidylate kinase
P12815	*Pdcd6*	Programmed cell death protein 6

The multi-way analysis is also presented as a heat-map (Figure 72). The colours represent the relative abundance of the indicated proteins: proteins with the highest intensity are highlighted in orange, while proteins with lowest intensity are white.

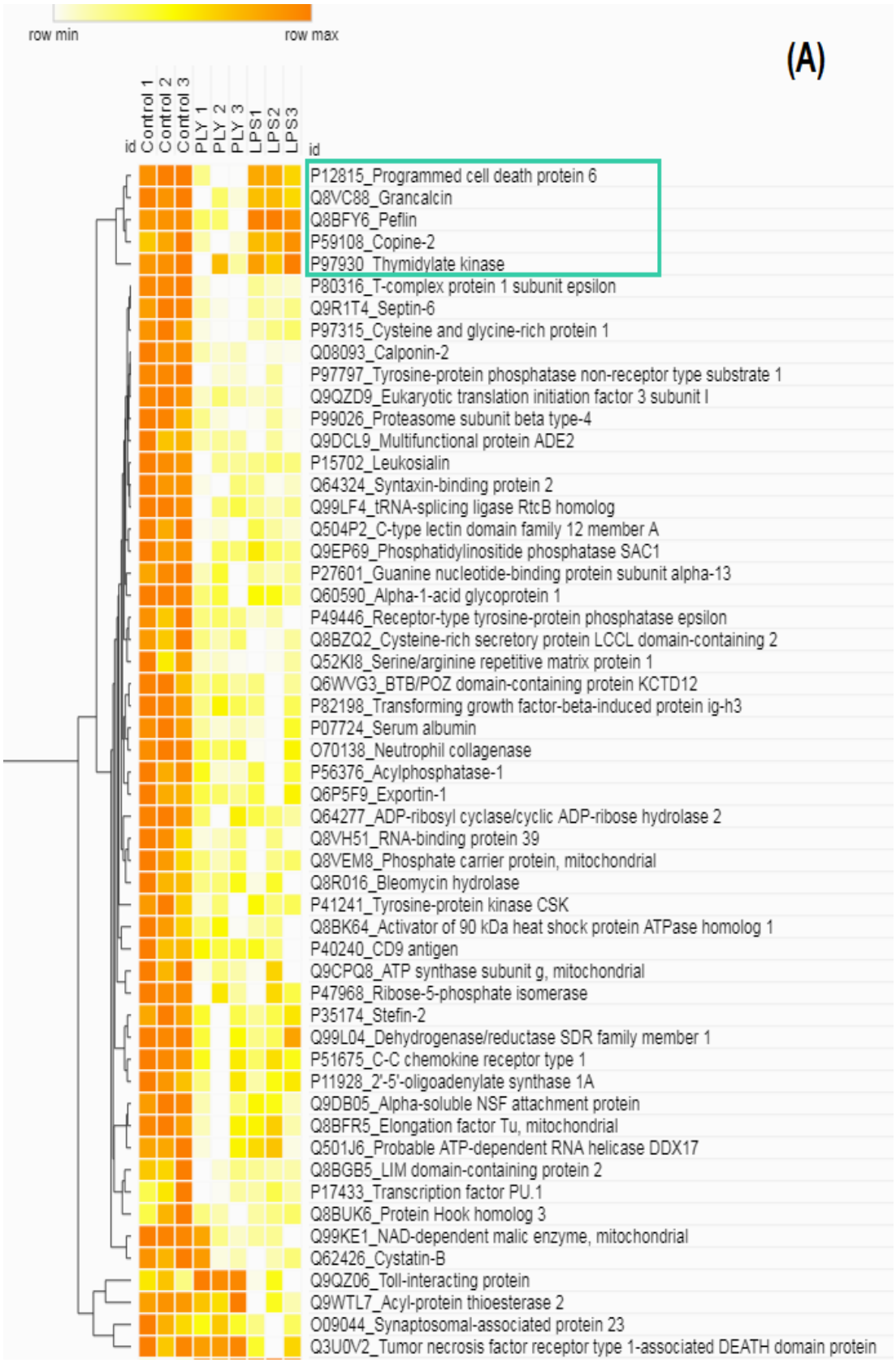
row min
row max
(A)
id
Control 1
Control 2
Control 3
PLY 1
PLY 2
PLY 3
LPS1
LPS2
LPS3
id
P12815_Programmed cell death protein 6
Q8VC88_Grancalcin
Q8BFY6_Peflin
P59108_Copine-2
P97930_Thymidylate kinase
P80316_T-complex protein 1 subunit epsilon
Q9R1T4_Septin-6
P97315_Cysteine and glycine-rich protein 1
Q08093_Calponin-2
P97797_Tyrosine-protein phosphatase non-receptor type substrate 1
Q9QZD9_Eukaryotic translation initiation factor 3 subunit I
P99026_Proteasome subunit beta type-4
Q9DCL9_Multifunctional protein ADE2
P15702_Leukosialin
Q64324_Syntaxin-binding protein 2
Q99LF4_tRNA-splicing ligase RtcB homolog
Q504P2_C-type lectin domain family 12 member A
Q9EP69_Phosphatidylinositide phosphatase SAC1
P27601_Guanine nucleotide-binding protein subunit alpha-13
Q60590_Alpha-1-acid glycoprotein 1
P49446_Receptor-type tyrosine-protein phosphatase epsilon
Q8BZQ2_Cysteine-rich secretory protein LCCL domain-containing 2
Q52KI8_Serine/arginine repetitive matrix protein 1
Q6WVG3_BTB/POZ domain-containing protein KCTD12
P82198_Transforming growth factor-beta-induced protein ig-h3
P07724_Serum albumin
O70138_Neutrophil collagenase
P56376_Acylphosphatase-1
Q6P5F9_Exportin-1
Q64277_ADP-ribosyl cyclase/cyclic ADP-ribose hydrolase 2
Q8VH51_RNA-binding protein 39
Q8VEM8_Phosphate carrier protein, mitochondrial
Q8R016_Bleomycin hydrolase
P41241_Tyrosine-protein kinase CSK
Q8BK64_Activator of 90 kDa heat shock protein ATPase homolog 1
P40240_CD9 antigen
Q9CPQ8_ATP synthase subunit g, mitochondrial
P47968_Ribose-5-phosphate isomerase
P35174_Stefin-2
Q99L04_Dehydrogenase/reductase SDR family member 1
P51675_C-C chemokine receptor type 1
P11928_2'-5'-oligoadenylate synthase 1A
Q9DB05_Alpha-soluble NSF attachment protein
Q8BFR5_Elongation factor Tu, mitochondrial
Q501J6_Probable ATP-dependent RNA helicase DDX17
Q8BGB5_LIM domain-containing protein 2
P17433_Transcription factor PU.1
Q8BUK6_Protein Hook homolog 3
Q99KE1_NAD-dependent malic enzyme, mitochondrial
Q62426_Cystatin-B
Q9QZ06_Toll-interacting protein
Q9WTL7_Acyl-protein thioesterase 2
O09044_Synaptosomal-associated protein 23
Q3U0V2_Tumor necrosis factor receptor type 1-associated DEATH domain protein

Figure 72: Heatmap highlighting proteins with differential abundance following treatment with PLY or LPS

Control, PLY-treated and LPS-treated neutrophils were stimulated for 4 hours before proceeding to proteomic analysis. Intensity values (log2) from proteins with a q-value ≤ 0.05, ≥ 2-fold change and ≥ 2 peptides identified per protein were used to create the heatmap. Hierarchical clustering (one minus Pearson correlation, average linkage method) of the rows was performed using the Morpheus online tool (https:// software.broadinstitute .org/morpheus/). The heatmap is split into two halves, A and B, to assist viewing. Proteins upregulated in PLY-treated neutrophils, but not LPS-treated neutrophils are highlighted in red, while proteins downregulated in PLY-treated neutrophils but not LPS-treated neutrophils are shown in green.

5.2.3.3 Comparison between pair-wise and multi-way analysis

We found some differences in the proteins identified using the pairwise and multi-way comparisons. Comparison of datasets from pairwise analysis likely overestimated the differences between PLY- and LPS-treated neutrophils by including proteins that were similarly regulated in both conditions, but only reached statistical significance in one. All proteins identified in the multi-way analysis were also present in the pairwise analysis. Integrin alpha-M (CD11b), expression of which increased on the neutrophil surface in response to PLY (Chapter 2), was present in the proteomic analysis but did not change in abundance following treatment with either PLY or LPS. This could be explained by the cell redistributing CD11b to the cell surface, rather than making more CD11b proteins.

5.2.3.4 Functional annotation of differentially expressed proteins

Using DAVID Bioinformatics Database, we performed a functional annotation of proteins identified by pairwise analysis as being significantly changed in PLY-treated, but not LPS-treated, neutrophils. We found no significant enrichment for any biological functions among the dataset (compared to whole *Mus musculus* genome). However, when the proteins identified ($q \leq 0.05$, ≥ 2 fold abundance change) in the multi-way analysis (PLY v LPS v Control) were analysed in the same way, a significant enrichment (p-value 7.7E-4, 70 fold enrichment) for calcium-dependent cysteine-type endopeptidase activity (3/7 proteins, GO term Molecular function). These three proteins were grancalcin (GCA), penta-EF hand domain containing1 (PEF1) and programmed cell death6 (PDCD6). The involvement of these three proteins will be reviewed in discussion.

5.2.4 Interactions between up-regulated and down-regulated proteins

We wanted to understand on how proteins upregulated in PLY-treated neutrophils could affect neutrophil functions such as migration and defense. Thus, using data from pairwise and multi-ways comparison, we looked for interactions between proteins upregulated and downregulated in PLY-treated neutrophils (Figure 73). Our protein network exhibited more interactions than expected, with a PPI enrichment p-value calculated as 0.00568 by STRING, meaning this group of proteins has more interaction among themselves than expected for a random set of proteins of similar size from the same genome, indicating that the proteins are at least partially biologically connected, as a group (Szklarczyk et al. 2017).

CAD is multifunctional protein that showed the most interactions. CAD proteins together with UMP synthase are localized around and outside the mitochondria in the cytosolic compartment. CAD has a possible association with the cytoskeleton, since mitochondria themselves are known to be anchored to the cytoskeletal network (Evans & Guy 2004).

Functional enrichment analysis of the network analysis highlighted that calcium-dependent cysteine-type endopeptidase activity (GO: 0004198, false discovery rate = 0.00394) is enriched, as observed previously.

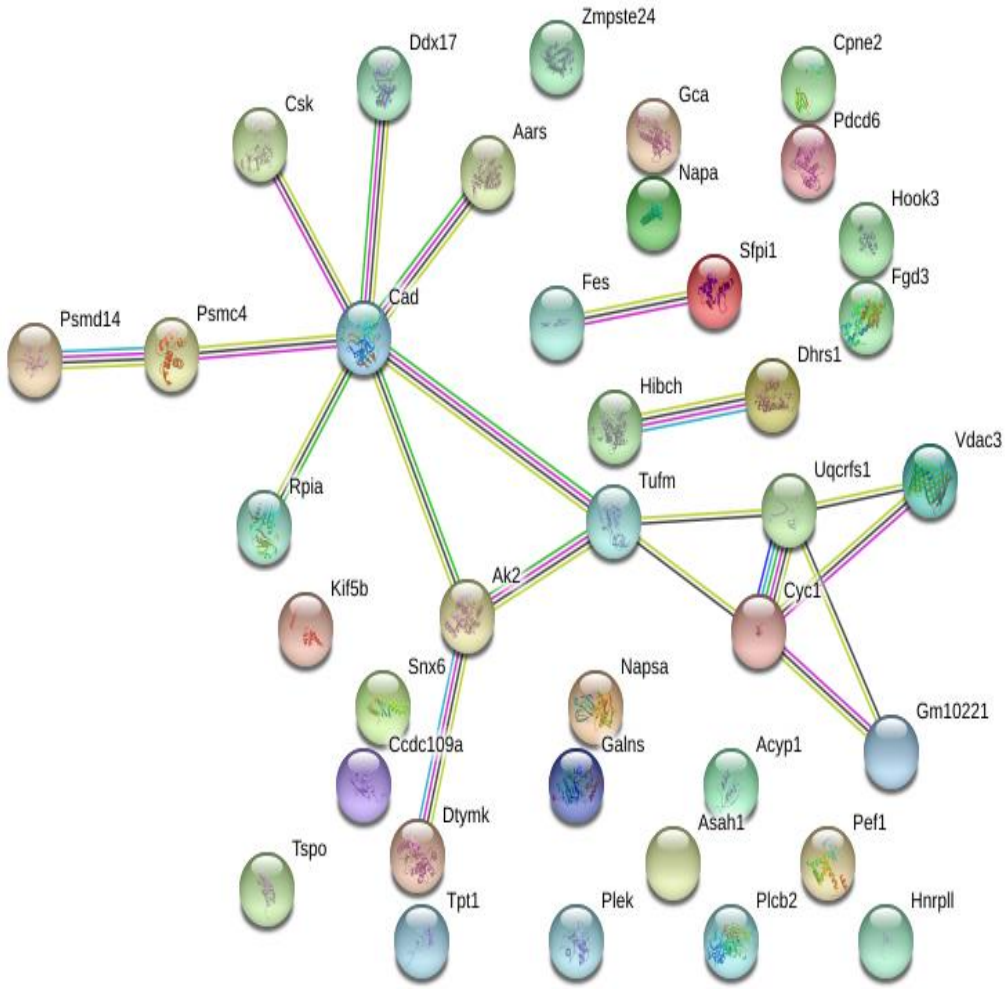

Figure 73: Maps showing putative protein-protein interactions between differentially abundant proteins in PLY treated neutrophils
Neutrophil proteins increasing or decreasing in abundance (q-value ≤ 0.05, ≥ 2-fold change and ≥ 2 peptides identified per protein) compared to control on treatment with PLY were entered into the online tool STRING version 10.5 (https://string-db.org/) (Szklarczyk et al. 2017) using default settings for proteins up and down -regulated in PLY.

While there is no direct link observed in STRING for grancalcin (GCA), Peflin (PEF1) and programmed cell death6 (PDCD6) they share a putative link through programmed cell death6- interacting protein (PDCD6IP), which is present in the proteomic dataset but does not change in abundance when treated with either PLY or LPS (Figure 74).

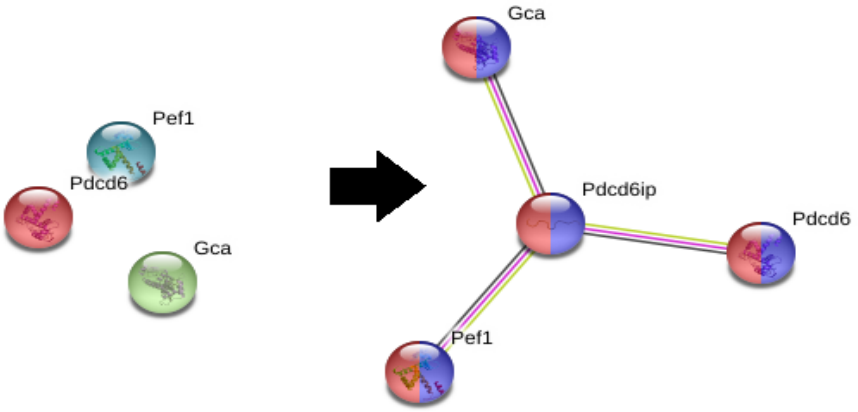

Figure 74: Maps showing interactions between 3 penta-EF-hand (PEF) proteins with programmed cell death6- interacting protein
Identified proteins GCA, PEF1 and PDCD6 accession number were entered into the online tool STRING version 10.5 (https://string-db.org/) and observed on additional network available. Functional network enrichment, pathway description colour coded for proteolysis (blue) and protein dimerization activity (red).

5.2.5 Post proteomic analysis

To validate our data, we have performed post proteomic analysis focusing on four proteins identified in the pair-wise analysis, which have evidence for a role in cell migration (Table 22). Firstly, we tried to confirm changes in the abundance of the selected proteins by western blot (Figure 75). However, of the four antibodies tested, only the grancalcin antibody showed bands of the expected size using a 1:100 dilution (Figure 75V). Using Image Lab version 5.2.1 Analysis Tool from Bio-Rad we measured the volume intensity of bands and found a reduction of 47.4 % in grancalcin band intensity in PLY-treated compared to control neutrophils. However, we also saw a 59.5% decrease in GAPDH band intensity, meaning that we can only conclude from this experiment that grancalcin is expressed in neutrophils, not that it is regulated by treatment with PLY.

5.2.5.1 Antibody analyses of grancalcin expression confirmed by western blot

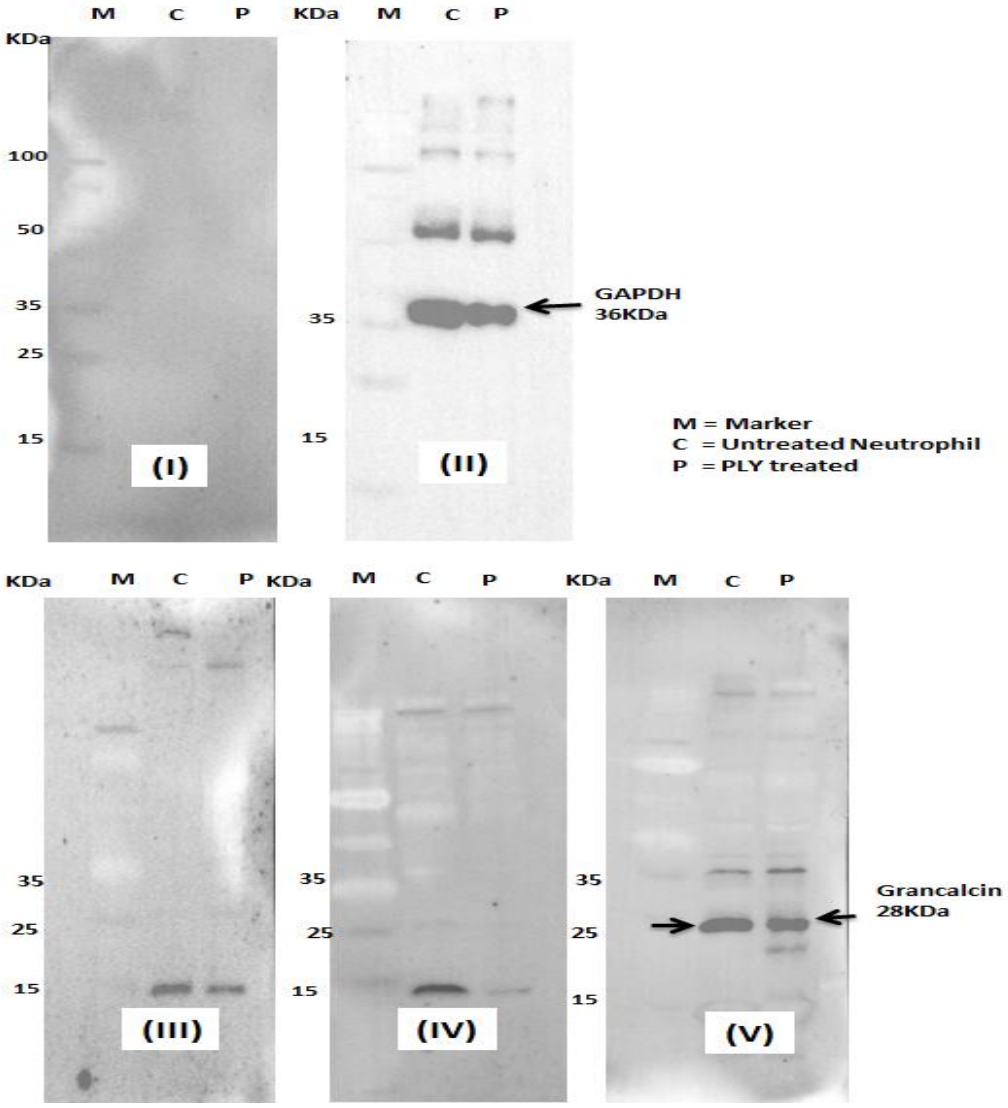

Figure 75: Western blot analysis of grancalcin expression in control and PLY-treated neutrophils

Neutrophils were treated with PLY or media alone for 45 minutes prior to analysis of protein expression by western blot. (I) Samples were stained only with a secondary goat anti-mouse IgG antibody at 1:10000 dilution. (II) Samples wre stained with anti-GADPH antibody at 1:2500 dilution. (III-V) Samples were stained with an anti-grancalcin antibody plus conjugated-secondary at (III) 1:1000 , (IV) 1: 500, and (V) 1: 100 dilutions. Arrows indicate molecular weight for specific band for GAPDH control at 36KDa (II) and grancalcin at 28KDa (V).

5.2.5.2 PLY treated neutrophils show decreased expression of grancalcin by confocal microscopy

Our results agree with previous studies showing that grancalcin is abundant in neutrophils. To verify that grancalcin expression is decreased upon exposure to PLY, neutrophils were plated onto glass coverslips and stained with a primary antibody to grancalcin, followed by a secondary antibody conjugated to a fluorescent dye, AF467. Despite several attempts at optimisation, staining was weak, and would need to be repeated with a different antibody in order to be convincing. Nevertheless, staining intensity was greater in untreated neutrophils than in PLY-treated neutrophils, or neutrophils stained with only the secondary antibody (Figure 76, and 77). This result supports the idea that expression of grancalcin in neutrophils is reduced after treated with PLY.

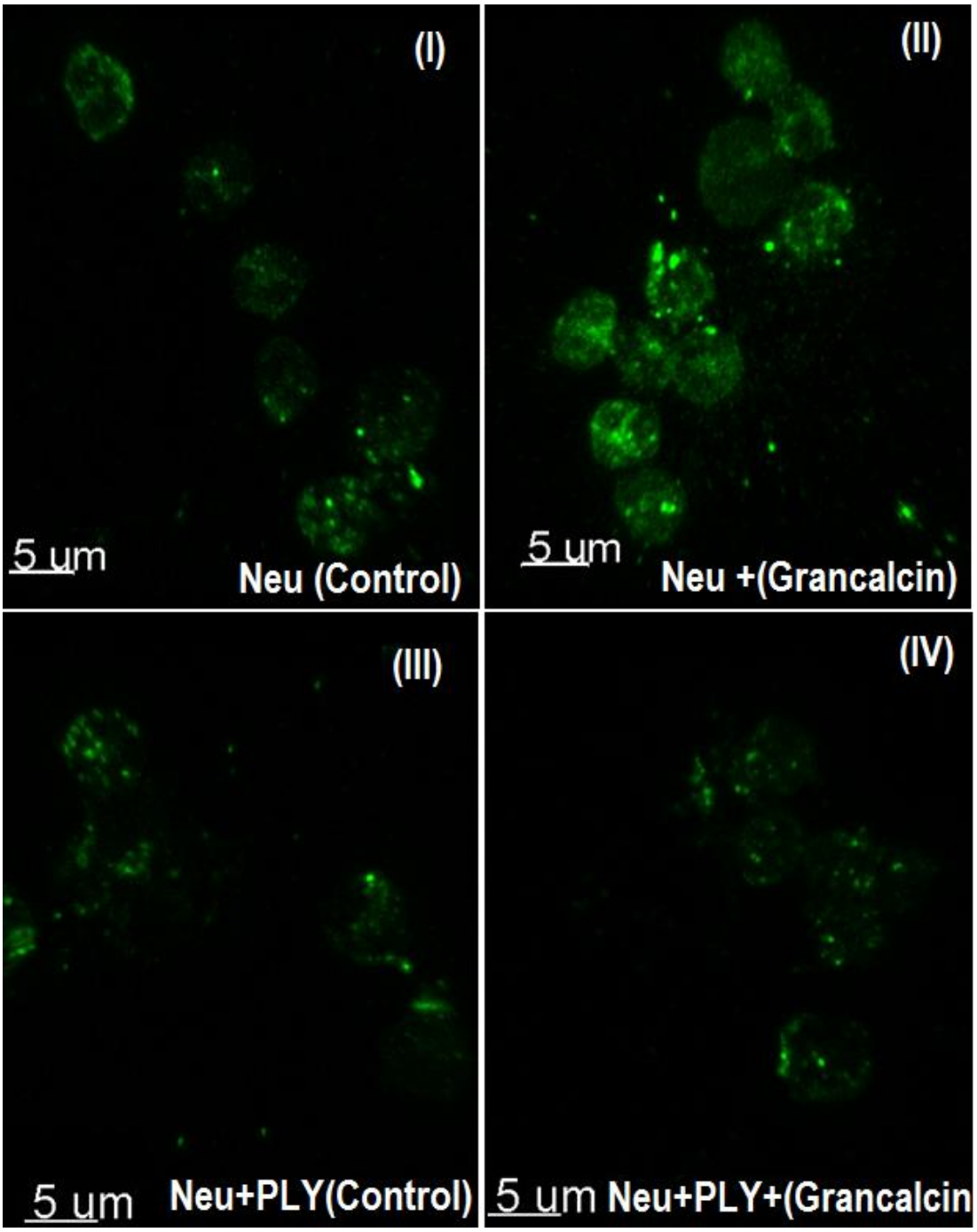

Figure 76: Neutrophils treated with PLY show weaker staining for grancalcin than untreated neutrophils

Neutrophils were plated on glass coverslips alone (I, II) or in the presence of PLY (III, IV). Subsequently, neutrophils were fixed and stained with a goat-anti-mouse-AF647 secondary only (I and III) or an anti-grancalcin primary antibody plus secondary (II and IV). Neutrophils were observed using 100x/1.45 oil objective mounted on the Zeiss LSM780 confocal microscope. Images are representative from 3 independent experiments.

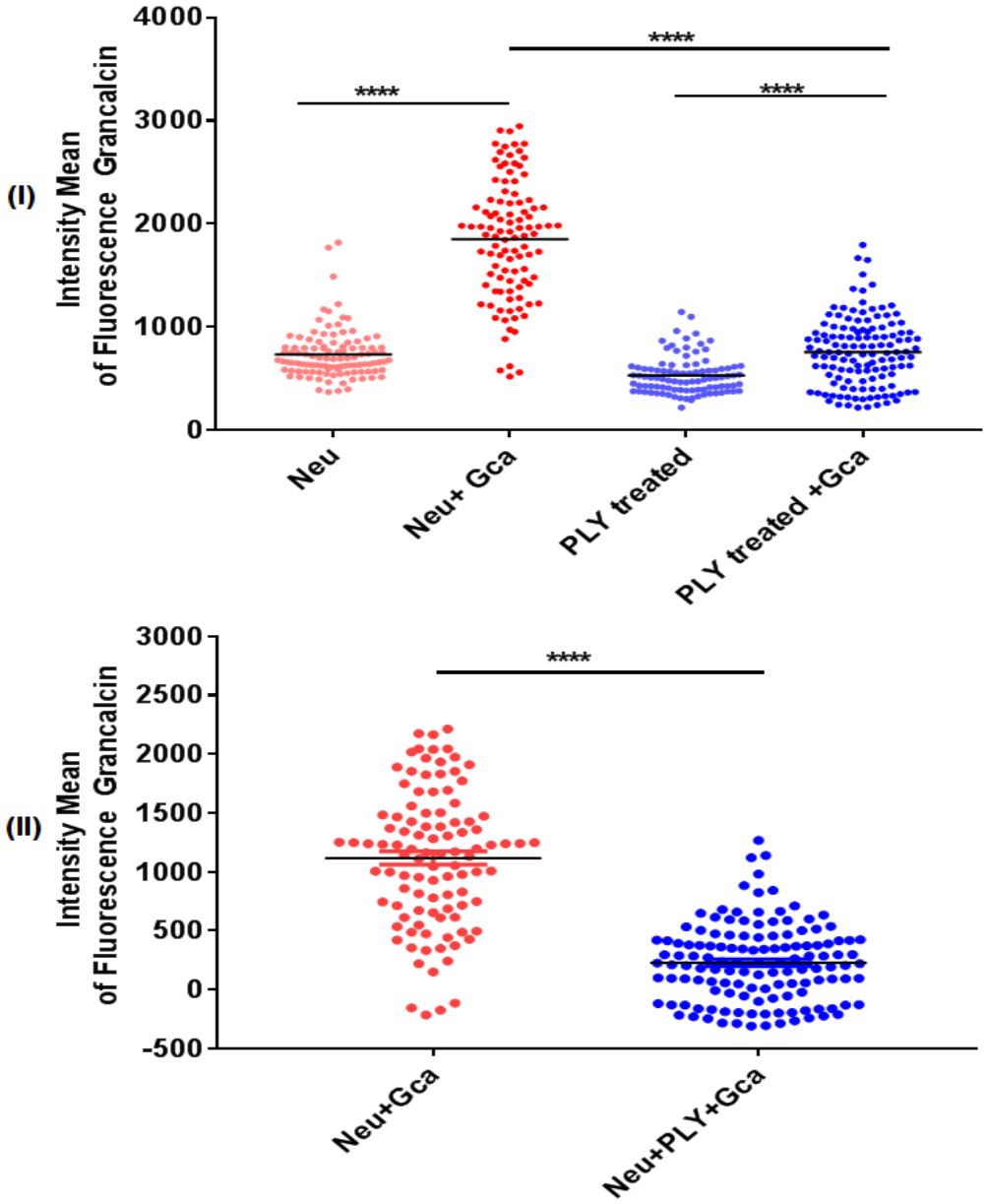

Figure 77: Neutrophils treated with PLY show weaker staining for grancalcin than untreated neutrophils

Neutrophils were plated on glass coverslips and treated with PLY for 45 minutes before fixation and staining with anti-grancalcin plus secondary antibody, or secondary antibody only. Graphs depict (I) fluorescence intensity of grancalcin staining for the indicated conditions (II) fluorescence intensity of grancalcin staining after subtracting background fluorescence from the secondary only controls. Statistical significance was determined using one-way ANOVA with Tukey's multiple comparisons test with ***($p<0.001$) and ****($p<0.0001$) for (I) and unpaired t-test with ****($p<0.0001$) for (II). Mean $\pm$ SEM for a single experiment is shown and each point represents an individual cell.

5.2.5.3 Treatment of neutrophils with a FES inhibitor, Herbimysin A, partially restores chemotaxis following exposure to PLY

The tyrosine-protein kinase, FES, was found to increase in abundance following treatment with PLY. To assess if this increase in FES accounted for the observed migration defect, neutrophils were treated with herbimycin A, which acts as a FES inhibitor by irreversibly and selectively inhibiting tyrosine kinases.

Following treatment with herbimycin A and/or PLY, chemotaxis towards KC was assessed using the 2D chemotaxis assay described in chapter 3 (Figure 78).

We found that neutrophils treated with herbimysin A alone did not show any significant differences in chemotaxis compared to untreated controls (Figure 78A). However, herbimysin A was found to partially restore chemotaxis of PLY-treated neutrophil toward KC at 10uM (Figure 78B).

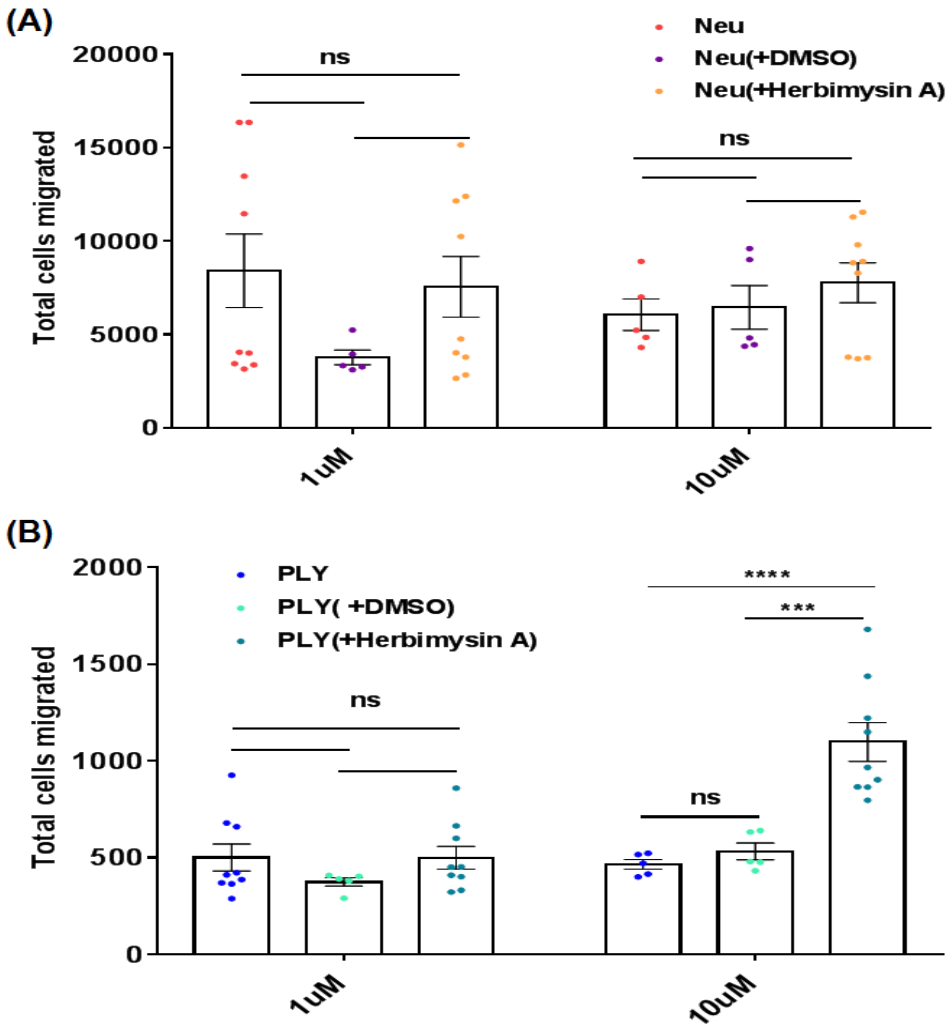

Figure 78: Herbimysin A partially restores chemotaxis of PLY-treated neutrophil toward KC

Untreated neutrophils (A) and PLY-treated neutrophil (B) were treated with DMSO vehicle or herbimysin A at the indicated concentrations, and placed in the upper well of a 96-Transwell® plate. Chemotaxis towards KC placed in the bottom well was assessed by counting the total number of migrated cells on a MACS Quant Flow Cytometer. Graph depicts the total number of neutrophils migrating to the bottom well under the indicated conditions. Each dot represents a single well of an assay performed in duplicate or greater. Data are combination of 2 independent experiments (with the exception of DMSO controls, which are from a single experiment). Statistical significance was determined using one-way ANOVA with post-hoc analysis by Tukey's multiple comparisons with ***($p<0.001$), **** ($p<0.0001$) and , ns denotes not significant.

5.3 Discussion

In this chapter we aimed to obtain further clues on how PLY inhibits neutrophil chemotaxis and defensive function, revealing novel pathways targeted by PLY to influences the neutrophil response. We used label-free quantitative mass spectrometry to perform a global analysis of the effect of PLY on protein expression in neutrophils. Our results revealed two interesting clues: Firstly, using pair-wise analysis we found four candidate proteins with confirmed roles in cell migration; FES (Tyrosine-protein kinase Fes/Fps), CSK (Tyrosine-protein kinase CSK), FGD3(FYVE, RhoGEF and PH domain-containing protein 3) and GCA (Grancalcin). Preliminary experiments revealed that treating neutrophils with an inhibitor of FES partially restored the PLY-mediated chemotaxis defect. Secondly, the group of proteins found to be significantly downregulated in the multi-way analysis was enriched for calcium-dependent cysteine-type endopeptidase activity and EF-hand domains (containing a calcium binding site). This is of interest, since PLY-treatment of neutrophils results in elevated intracellular calcium levels. The knowledge gained from this global analysis may give clues both to how PLY manipulates neutrophil function, and also to the basic molecular mechanisms regulating neutrophil migration, which may be targeted therapeutically to modulate neutrophil function in disease.

5.3.1 Grancalcin

We found that after exposure to PLY, grancalcin expression was downregulated in neutrophils. It has been shown grancalcin is highly expressed in neutrophils and monocytes/macrophage, and is also highly expressed in leukocytes that have extravasated to sites of infection, suggesting that it plays an important role in host defense activities (Liu et al. 2004). However, studies in grancalcin knock-out mice

showed that the protein was largely dispensable for neutrophil recruitent and function. Knock-out mice were however more resistant to endotoxic shock, which may implicate grancalcin is restraining host-damaging functions of neutrophils (Roes et al. 2003). Upon neutrophil activation, grancalcin has been shown to translocate to the granule membrane (Roes et al. 2003). It is possible that this occurs upon exposure to PLY, and the change in protein localisation (and/or extrusion of membrane bound secretory granules) may explain the reduction in grancalcin we observed in the mass spectrometry data. On the other hand, PLY has been shown to inhibit neutrophil degranulation (Paton & Ferrante 1983; Nandoskar et al. 1986) thus the decrease in expression of grancalcin may have another explanation. Studies using grancalcin-deficient neutrophils conducted by Xu *et al* shown neutrophil adherence to fibronection decreases by 60% in the absence of grancalcin (Xu et al. 2006). This contrasts to our results where PLY-treated neutrophils showed reduced grancalcin expression, but increased adhesion. However, we were not able to perform any functional assays to confirm a role for grancalcin in PLY-mediated inhibition of chemotaxis. Future experiments could include using grancalcin-knockout mouse compared with wild type mouse to assess chemotactic responses of isolated neutrophils.

5.3.2 FES

FES expression in PLY-treated neutrophils was found to be upregulated in our proteomic study. FES is a protein-tyrosine kinase (PTK) that participates in many processes such as cell survival and migration, and is highly expressed in hematopoietic cells and their progenitors. It activity can enhanced by ligand binding to the SH2 domain, resulting in regulation of the actin cytoskeleton and membrane

trafficking (Craig 2012). FES may also participate in cytoskeletal reorganization and motility by regulating cross-talk between Kit receptor PTK and β1 integrins in mast cells (Smith et al. 2010). Although, no studies of FES in neutrophils have been performed, the related protein, FER, has been shown inhibit neutrophil chemotaxis, suggesting that increased levels of FES could explain the chemotactic defect we observe in PLY-treated neutrophils (Khajah et al. 2013). To assess this we used herbimysin A, an inhibitor of FES, in the 2D chemotaxis assay, and showed partially restored chemotaxis in PLY–treated neutrophils exposed to herbimysin A. Herbimysin A is an antibiotic that can react with thiol groups and permanently inhibits tyrosine kinase activation (Fukazawa et al. 1991). Beside FES, it can also inhibit other tyrosine kinases such as SRC, YES, ROS, ABl, and ERBB (Uehara & Fukazawa 1991) and heat shock protein 90 (HSP90) (Santa Cruz Biotechnology-CAS 70563-58-5). Therefore, we cannot yet conclude that upregulation of FES explains the chemotaxis defect in PLY-treated neutrophils. For example, another target of herbimysin A, HSP90, plays a role in cell migration (Snigireva et al. 2014; Kim et al. 2014). Another example is ABl, which has a role in regulation of the actin cytoskeleton for normal cells (Panjarian et al. 2013). Thus, a more specific inhibitor, or disruption of the *Fes* gene, will be required to confirm its role.

5.3.3 Calcium

Using DAVID Bioinformatics Database, the differentially regulated proteins identified in the multiway comparison were analysed, and we found a significant enrichment for calcium-dependent cysteine-type endopeptidase activity (3/7 proteins, Goterm MF direct), and EF-hand 1 calcium-binding site (3/7 proteins, Interpro). These proteins were: Peflin (PEF1), programmed cell death 6 (PDCD6) and

grancalcin (GCA). In addition, Copine-2 (CPNE2) is a calcium-dependent membrane binding protein (Cowland et al. 2003).

Grancalcin, a 28 kDa protein (Maki et al. 2002), displays a Ca^{2+}-dependent translocation to the granules and plasma membrane upon the activation of neutrophils (Boyhans et al. 1992). Grancalcin also increases adhesion of neutrophils to fibronectin (Xu et al. 2006), and binds to the actin-bundling protein, L-plastin, in a Ca^{2+} dependent manner (Lollike et al. 2001). Peflin (also known as penta-EF hand domain containing1 protein) form cytosolic heterodimers with PDCD6, which dissociate in response to calcium. PDCD6 was also found to be down-regulated in PLY-treated neutrophils in our analysis. Recently, under basal conditions peflin was found to negatively regulate PDCD6/sec31A interactions and ER to Golgi transport (Rayl et al. 2016). PDCD6 has been shown by Vito *et al* to be involved in apoptosis in response to T cell receptor-, Fas-, and glucocorticoid receptor signalling. This protein has a function in Alzheimer's where it mediates Ca^{2+} regulated signals resulting in cell death and disease. Copine-2 (CPNE2) is from the C2-domain protein family which is another Ca^{2+}-binding protein family (in addition to EF-hand and annexins). Copine-2 has been found to be expressed in immature neutrophil precursors, though the function remains unclear (Cowland et al. 2003).

In our study we were treating neutrophils with sub-lytic concentrations of PLY. PLY is a thiol-activated cytolysin membrane-damaging toxin synthesized by *S. pneumoniae* (Paton et al. 1993). PLY can mediate Ca^{2+} influx by forming pores in the host cell membrane. PLY-driven Ca^{2+} influx may potentiate neutrophil pro-inflammatory activities such as CD11b-mediated adhesion, degranulation, and induction of NO synthase, for which increases in intracellular free calcium have previously been shown to be pre-requisite (Cockeran, Steel, et al. 2001; Lew et al.

1986; Pettit & Hallett 1996). Transient increases in cytosolic Ca^{2+} are important in cell migration, however sustained Ca^{2+} signalling in PLY-treated neutrophils may result in dysregulation of migration machinery, and impaired neutrophil chemotaxis (Cockeran, Steel, et al. 2001; Paton & Ferrante 1983).

5.4 Conclusion

The aim of this chapter was to obtain further clues was succeeded. We found four candidate proteins which may be involved in migration; FES (Tyrosine-protein kinase Fes/Fps), CSK (Tyrosine-protein kinase CSK), FGD3 (FYVE, RhoGEF and PH domain-containing protein 3) and GCA (Grancalcin). We also found decreases in three calcium binding proteins GCA (Grancalcin)), PEF1 (Peflin) and PDCD6 (programmed cell death6).

Chapter 6: Conclusion

The aim of this thesis was to understand how neutrophil migration is modulated by the *Streptococcus pneumoniae* toxin, PLY.

In Chapter 3, we determined that PLY could inhibit neutrophil chemotaxis in 2D and 3D assays. This inhibitory activity was direct, and depended on the pore-forming function of the toxin, since PdB was unable to inhibit chemotaxis. However, in experiments with live bacteria, inhibition of chemotaxis did not completely correlate with haemolytic activity. Thus, we suggesting other virulence factors might also contribute to inhibition of neutrophil chemotaxis, which remain unidentified. What might be the outcome of PLY-mediated inhibition of neutrophil migration? We hypothesise that impaired neutrophil migration to the infection site will give an advantage to the bacteria, allowing them to multiply. To control the situation, more neutrophils will be recruited, leading to tissue damage. Alternatively, PLY may simply provide a "stop" signal once neutrophils reach the site of infection, allowing them to perform host defensive functions. Future studies should address the molecular details of how neutrophil behaviour is altered in tissue after PLY stimulation, or infection with *S. pneumoniae.* This will help us to understand the mechanism closely, and might allow neutrophil migration to be manipulated in other settings.

In Chapter 4, we found PLY-treated neutrophil increased CD11b expression, increased actin polymerisation and increased adhesion to plastics. It has been shown that neutrophils adhesion to plastic is accompanied by an increase in intracellular Ca^{2+}, an increase in F-actin, and activation of the respiratory burst (Ginis et al. 1992).

PLY can produce a strong cellular Ca^{2+} influx (Stringaris et al. 2002) by forming pores in the cells membrane, potentially resulting in actin rearrangement, increased adhesion, and reduced motility. This is supported by our finding that PdB (a PLY toxoid without pore-forming function) does not inhibit neutrophil migration, nor increase F-actin intensity, sphericity or volume when compared to untreated neutrophils.

CD11b alone has been shown to establish firm adhesion of neutrophils (Solovjov et al. 2005). Thus we raise the hypothesis that impaired chemotaxis in PLY-treated neutrophils may be linked to increased CD11b expression, which drives firm adhesion to the plate, thus limiting migration. This may also related to pore-forming activity and Ca^{2+} influx: PLY-driven Ca^{2+} influx potentiate neutrophil pro-inflammatory activities such as CD11b-mediated adhesion, as has been shown in previous studies (Cockeran, Steel, et al. 2001; Lew et al. 1986; Pettit & Hallett 1996).

In Chapter 5, through global proteomic analysis, we found two sets of proteins regulated by PLY which might explain the observed changes in cell migration: those with confirmed roles in cell migration (FES, CSK, FGD3 and GCA), and members of penta-EF-hand family of Ca^{2+}-binding proteins (GCA, PEF1 and PDCD6). FES, a protein tyrosine kinase, was upregulated during treatment with PLY, and has previously been shown to be involved in regulation of the actin cytoskeleton reorganization and motility in other cells (e.g. mast cells). In our study, treating neutrophils with an inhibitor of FES partially restored the PLY-mediated chemotaxis defect, however further validation will be needed. Grancalcin (GCA) has been shown to be involved in neutrophil defense mechanisms (Liu et al. 2004), and increased

adhesion on fibronectin (Xu et al. 2006). In addition to this, not only GCA but PEF1 and PDCD6 are from the same family of penta-EF-hand Ca^{2+} binding proteins, which form cytosolic heterodimers which dissociate in response to calcium. PDCD6 itself has an important role in apoptotic cell death. How reduced abundance of these proteins regulates neutrophil motility, and how it may be related to sustained Ca^{2+} levels following treatment with PLY, remains unclear.

Data presented in our study may help our understanding of the pathogenesis of *S. pneumoniae*, it is useful to understand how neutrophils migrate through inflamed tissues in order to develop therapies which can prevent neutrophil-mediated damage to host tissues in sterile injury.

Appendix 1: List of Control vs PLY (Reference Table)

No	Uni P Accession	Anova (p)	q Value	Unique peptides	Confidence score	Max fold change	Highest mean condition	Lowest mean condition
1.	O88842	0.0365878	0.041979438	2	115.76	285.0000728	Control	PLY
2.	Q501J6	0.0149568	0.0255264	5	983.83	13.40821995	Control	PLY
3.	P51675	0.0187957	0.029425617	2	119.64	7.649242456	Control	PLY
4.	Q9R1T4	0.0001439	0.002905883	2	374.59	7.645676727	Control	PLY
5.	P80316	6.383E-06	0.000483377	13	1277.32	5.813265792	Control	PLY
6.	Q60590	0.0021747	0.010057787	2	183.6	5.419246827	Control	PLY
7.	P12815	0.000273	0.003846594	4	282.38	4.795014896	Control	PLY
8.	Q6P5F9	0.0032626	0.011979957	4	177.57	4.612835257	Control	PLY
9.	P15702	0.0003689	0.004297827	2	291.51	3.900050721	Control	PLY
10.	Q52KI8	0.0072771	0.01763585	2	155.12	3.814544545	Control	PLY
11.	Q8BUK6	0.0459055	0.048568039	2	245.45	3.618174545	Control	PLY
12.	Q8BK64	0.0285445	0.036603165	3	298.47	3.547858251	Control	PLY
13.	P97930	0.0415324	0.045738784	2	153.87	3.503542666	Control	PLY
14.	P82198	0.0026802	0.010898281	2	123.5	3.251812501	Control	PLY
15.	Q8VC88	0.0007583	0.006380612	4	324.39	3.237152563	Control	PLY
16.	Q64277	0.0104532	0.021252593	3	127.82	3.209977538	Control	PLY
17.	P07724	0.0001316	0.002794996	25	3100.84	3.195460599	Control	PLY
18.	P97315	0.0001166	0.002716354	4	376.23	3.14772092	Control	PLY
19.	Q9EP69	0.0023733	0.01031226	2	86.91	3.122163117	Control	PLY
20.	Q08093	1.84E-05	0.001013547	11	924.56	3.103282651	Control	PLY
21.	Q9QZD9	0.0001819	0.003302468	4	278.82	2.948884264	Control	PLY
22.	Q9DCL9	0.0028303	0.011198748	5	329.74	2.945982943	Control	PLY
23.	Q64324	0.000671	0.005807896	8	1041.52	2.748842828	Control	PLY
24.	P11928	0.0298225	0.037667079	3	228.56	2.662365212	Control	PLY
25.	Q8BFY6	0.0018397	0.009685055	3	297.94	2.652681799	Control	PLY
26.	Q8BGB5	0.009083	0.020200613	2	171.49	2.644583931	Control	PLY
27.	Q504P2	0.0002414	0.00382513	6	313.2	2.530457392	Control	PLY
28.	P35174	0.0110263	0.021895767	2	140.21	2.452092699	Control	PLY
29.	P40240	0.0186613	0.029290935	3	299.39	2.437635852	Control	PLY
30.	P97797	4.998E-06	0.000432571	3	145.4	2.401825412	Control	PLY
31.	Q99LF4	0.0019023	0.009685055	2	92.01	2.308335451	Control	PLY
32.	Q9DB05	0.0005576	0.005672782	4	318.52	2.275569489	Control	PLY
33.	P27601	0.0044214	0.014036592	2	184.62	2.216869654	Control	PLY
34.	P41241	0.005179	0.015457173	4	126.24	2.215873034	Control	PLY
35.	P47968	0.0117639	0.022210637	6	713.06	2.196685098	Control	PLY
36.	P59108	0.0020329	0.009853429	6	616.09	2.191263599	Control	PLY
37.	Q8BFR5	0.0095958	0.020689729	2	204.6	2.180606727	Control	PLY
38.	P99026	0.0015139	0.009238946	6	688.99	2.125548737	Control	PLY
39.	Q99L04	0.0085311	0.019578559	4	132.06	2.060601484	Control	PLY
40.	Q9CPQ8	0.0020297	0.009853429	3	215.36	2.042066723	Control	PLY
41.	P56376	0.0060161	0.016136021	3	230.18	2.018735289	Control	PLY

42.	Q8QZY6	0.0012275	0.008547971	2	90.94	22.84828451	PLY	Control
43.	O88668	0.0002462	0.00382513	2	183.51	19.27277039	PLY	Control
44.	Q9CR68	0.0001853	0.003302468	2	58.61	9.770416919	PLY	Control
45.	P50637	0.0206002	0.030553931	2	138.17	9.683984955	PLY	Control
46.	Q8BTI9	0.0003481	0.004218207	2	32.35	9.503131362	PLY	Control
47.	P36371	0.0010132	0.007486491	2	87.64	8.154471751	PLY	Control
48.	Q9JKB1	0.0028086	0.011194924	2	73.97	6.276746414	PLY	Control
49.	Q9R0U0	6.319E-05	0.002046041	2	80.7	5.674920404	PLY	Control
50.	Q9Z1F9	3.842E-05	0.001454965	3	166.06	5.391237635	PLY	Control
51.	Q6P8X1	0.0023668	0.01031226	2	64.81	4.978218746	PLY	Control
52.	P63082	0.0029177	0.011402307	2	225.3	3.742700111	PLY	Control
53.	Q9D6R2	0.0003881	0.004437029	2	71.93	3.687065805	PLY	Control
54.	Q8CHK3	0.0003026	0.00389502	3	214.06	3.444056854	PLY	Control
55.	P97484	0.0028465	0.011198748	3	180.55	3.241184918	PLY	Control
56.	Q3UMR5	0.0316744	0.038668455	3	134.96	3.233488891	PLY	Control
57.	P58021	0.0004702	0.005070038	3	130.81	3.204308426	PLY	Control
58.	Q9JHK5	0.000293	0.00389502	4	330.55	3.082501484	PLY	Control
59.	Q80UG5	0.0110794	0.021895767	3	88.86	3.028984504	PLY	Control
60.	Q9WV54	0.0416229	0.045738784	3	132.27	2.995008879	PLY	Control
61.	Q8K352	0.0016252	0.00928918	4	283.62	2.914438493	PLY	Control
62.	Q03267	0.0313252	0.038668455	3	163.72	2.830604805	PLY	Control
63.	O35593	0.0276605	0.035892248	2	189.41	2.793714592	PLY	Control
64.	Q8BGQ7	0.0319081	0.038819419	2	103.36	2.768705818	PLY	Control
65.	A3KGF7	0.0177778	0.02834467	3	182.64	2.767238083	PLY	Control
66.	Q8QZS1	0.018113	0.028677584	2	119.47	2.633048383	PLY	Control
67.	Q8VDM6	0.000477	0.005070038	5	461.13	2.556843668	PLY	Control
68.	Q9WTP6	0.0032535	0.011979957	9	735.16	2.508224533	PLY	Control
69.	Q99MK8	0.0059217	0.016088535	5	222.33	2.390539564	PLY	Control
70.	P63028	0.0018892	0.009685055	5	555.09	2.332319438	PLY	Control
71.	Q60931	0.0002705	0.003846594	8	752.68	2.326708026	PLY	Control
72.	O09043	0.0058401	0.015938521	4	345.24	2.30900194	PLY	Control
73.	B2RQC6	0.0146186	0.025161674	4	126.6	2.281366423	PLY	Control
74.	Q9D0M3	0.0013245	0.008679737	3	158.59	2.261408343	PLY	Control
75.	Q9R062	0.0068486	0.017005549	6	423.97	2.141446938	PLY	Control
76.	Q80W54	0.0105412	0.021359731	7	469.47	2.117800839	PLY	Control
77.	Q61768	0.0037047	0.012974388	6	312.38	2.081376144	PLY	Control
78.	P16879	0.0137322	0.024373772	4	323.6	2.080058639	PLY	Control
79.	P54775	0.0087423	0.019763825	5	204.93	2.049196828	PLY	Control
80.	Q571E4	0.0207772	0.030553931	3	304.51	2.038553168	PLY	Control
81.	Q921F4	0.0111485	0.021895767	5	280.51	2.032927852	PLY	Control
82.	Q6P1F6	0.0056851	0.015775858	3	208.33	2.031302144	PLY	Control

Appendix 2: List of Control vs LPS (Reference Table)

No	UniP accession	Anova (p)	q Value	Unique peptides	Confidence score	Max fold change	Highest mean condition	Lowest mean condition
1.	Q99KE1	0.0001429	0.0048657	2	100.21	17.146468	Control	LPS
2.	P51675	0.0042407	0.022489	2	119.64	6.0797201	Control	LPS
3.	Q9R1T4	0.0001674	0.0051483	2	374.59	5.9323713	Control	LPS
4.	Q8BK64	0.0050269	0.0231882	3	298.47	5.0343103	Control	LPS
5.	P80316	2.763E-05	0.0022299	13	1277.32	4.862362	Control	LPS
6.	P82198	0.0022063	0.0164914	2	123.5	4.4221119	Control	LPS
7.	Q52KI8	0.0084222	0.0301831	2	155.12	3.808754	Control	LPS
8.	Q60590	0.0016795	0.0160762	2	183.6	3.7903199	Control	LPS
9.	Q08093	9.815E-06	0.0016044	11	924.56	3.4727571	Control	LPS
10.	Q9DCL9	0.0026708	0.018017	5	329.74	3.4404281	Control	LPS
11.	Q64277	0.0004921	0.0091417	3	127.82	3.4263484	Control	LPS
12.	P40240	0.0207516	0.0472458	3	299.39	3.4059111	Control	LPS
13.	Q9QZD9	7.925E-05	0.0035008	4	278.82	3.3478351	Control	LPS
14.	P15702	5.419E-05	0.0031014	2	291.51	3.2530028	Control	LPS
15.	P07724	0.0045736	0.0231882	25	3100.84	2.9340495	Control	LPS
16.	Q64324	0.0002288	0.0057853	8	1041.52	2.7251972	Control	LPS
17.	Q8BGB5	0.0082371	0.0297902	2	171.49	2.4482476	Control	LPS
18.	P97315	0.0006639	0.0115014	4	376.23	2.441635	Control	LPS
19.	Q9EP69	0.0049147	0.0231882	2	86.91	2.4307097	Control	LPS
20.	Q62426	0.0018402	0.0163292	2	154.49	2.4160873	Control	LPS
21.	Q99LF4	3.231E-05	0.0022299	2	92.01	2.3863395	Control	LPS
22.	P97797	0.0001085	0.0042248	3	145.4	2.3659165	Control	LPS
23.	O70138	0.0079248	0.02947	15	1319.53	2.3556364	Control	LPS
24.	P49446	0.0021822	0.0164914	4	245.93	2.2712067	Control	LPS
25.	P27601	0.000298	0.0071647	2	184.62	2.2543541	Control	LPS
26.	Q8BZQ2	0.0023213	0.0169399	6	275.03	2.1850341	Control	LPS
27.	P99026	0.0011722	0.0142369	6	688.99	2.1664273	Control	LPS
28.	Q6WVG3	0.0032309	0.019656	8	728.24	2.1524471	Control	LPS
29.	O09044	0.0150089	0.0414139	2	225.94	2.1463496	Control	LPS
30.	Q504P2	0.0024535	0.017225	6	313.2	2.1160534	Control	LPS
31.	P35174	0.0141065	0.0400344	2	140.21	2.0949734	Control	LPS
32.	Q9WTL7	0.0057014	0.0251892	5	209.25	2.0608326	Control	LPS
33.	Q8R016	0.0140952	0.0400344	2	104.16	2.0532288	Control	LPS
34.	Q8VEM8	0.0105922	0.0337021	8	325.84	2.0512815	Control	LPS
35.	Q8VH51	0.005589	0.0250999	3	155.89	2.03636	Control	LPS
36.	O08749	0.0112942	0.0345332	4	339.53	2.0004381	LPS	Control
37.	O35841	0.0014071	0.0145585	2	275.41	2.0212475	LPS	Control
38.	Q9R062	0.0183236	0.0450278	6	423.97	2.0507925	LPS	Control
39.	Q03267	0.0211852	0.0474952	3	163.72	2.1144002	LPS	Control
40.	Q8K352	0.0009682	0.0136434	4	283.62	2.1401487	LPS	Control
41.	Q6P1F6	0.0040053	0.0221197	3	208.33	2.2864333	LPS	Control

42.	Q99MK8	0.0007025	0.0115014	5	222.33	2.3092782	LPS	Control
43.	Q9DBC7	0.0124534	0.0366407	3	249.55	2.3413522	LPS	Control
44.	P63082	0.0233685	0.0495674	2	225.3	2.4536399	LPS	Control
45.	Q8VDM6	0.0003216	0.0074808	5	461.13	2.5709448	LPS	Control
46.	P97484	0.004046	0.022184	3	180.55	2.6713044	LPS	Control
47.	P58021	0.0013836	0.0145585	3	130.81	3.1141283	LPS	Control
48.	Q8CHK3	0.0004196	0.008165	3	214.06	3.2794242	LPS	Control
49.	Q9D6R2	0.0032386	0.019656	2	71.93	3.4569697	LPS	Control
50.	Q80UG5	0.010099	0.0335815	3	88.86	3.6088672	LPS	Control
51.	Q9JKB1	0.0027226	0.0180919	2	73.97	4.9835972	LPS	Control
52.	Q9Z1F9	0.001517	0.0151211	3	166.06	5.6112069	LPS	Control
53.	P36371	0.0005291	0.0096108	2	87.64	5.9417368	LPS	Control
54.	Q9R0U0	0.0001519	0.0049673	2	80.7	6.2109502	LPS	Control
55.	Q8BTI9	0.0004452	0.0084632	2	32.35	6.6660153	LPS	Control
56.	O88668	0.0008152	0.0123389	2	183.51	12.352202	LPS	Control
57.	Q8QZY6	0.00133	0.0145585	2	90.94	20.819341	LPS	Control

References

Alexander, J.E. et al., 1998. Amino acid changes affecting the activity of pneumolysin alter the behaviour of pneumococci in pneumonia. *Microbial Pathogenesis*, 24(3), pp.167–174.

Alonso, D.E. et al., 1995. Streptococcus pneumoniae: virulence factors, pathogenesis, and vaccines. *Microbiological reviews*, 59(4), pp.591–603. Available at: http://www.pubmedcentral.nih.gov/articlerender.fcgi?artid=239389&tool=pmcentrez&rendertype=abstract.

Amulic, B. et al., 2012. Neutrophil Function: From Mechanisms to Disease. *Annual Review of Immunology*, 30(1), pp.459–489. Available at: http://www.annualreviews.org/doi/10.1146/annurev-immunol-020711-074942.

Anceriz, N. et al., 2007. Through Activation of B2 Integrins. *Biochemical and Biophysical Research Communications*, 354(1), pp.84–89.

Anderluh, G. & Gilbert, R., 2014. MACPF/CDC Proteins - Agents of Defence, Attack and Invasion. In pp. 145–160. Available at: http://link.springer.com/10.1007/978-94-017-8881-6.

Artemenko, Y., Swaney, K.F. & Devreotes, P.N., 2011. Cell Migration. In *Methods in Molecular Biology*. pp. 287–309.

Asano, Y. & Horn, E., 2011. Chemotaxis and Migration Tool 2.0. *ibidi GmbH*, pp.1–21.

Ba, M. et al., 2011. International Union of Basic and Clinical Pharmacology . LXXXIV : Leukotriene Receptor Nomenclature , Distribution , and Pathophysiological Functions. , 63(3), pp.539–584.

Bardoel, B.W. et al., 2014. The balancing act of neutrophils. *Cell Host and Microbe*, 15(5), pp.526–536. Available at: http://dx.doi.org/10.1016/j.chom.2014.04.011.

van den Berg, J.M. et al., 2001. Beta1 integrin activation on human neutrophils promotes beta2 integrin-mediated adhesion to fibronectin. *European journal of*

immunology, 31(1), pp.276–84. Available at: http://www.ncbi.nlm.nih.gov/pubmed/11265644.

Bogaert, D., de Groot, R. & Hermans, P.W.M., 2004. Dynamics of nasopharyngeal colonisation. *Lancet Infectious Diseases*, 4(March), pp.144–154. Available at: http://infection.thelancet.com.

Borregaard, N., 2010. Neutrophils, from Marrow to Microbes. *Immunity*, 33(5), pp.657–670. Available at: http://dx.doi.org/10.1016/j.immuni.2010.11.011.

Borregaard, N., Sørensen, O.E. & Theilgaard-Mönch, K., 2007. Neutrophil granules: a library of innate immunity proteins. *Trends in Immunology*, 28(8), pp.340–345.

Boyhans, A. et al., 1992. Angela BoyhanS, Colin M. Casimir, John K. French, Carmel G. Teahan, and Anthony. , 267(5), pp.2928–2933.

Cera, M.R. et al., 2009. JAM-A promotes neutrophil chemotaxis by controlling integrin internalization and recycling. *Journal of Cell Science*, 122(2), pp.268–277. Available at: http://jcs.biologists.org/cgi/doi/10.1242/jcs.037127.

Chalovich, J.M. & Eisenberg, E., 2013. NIH Public Access. *Magn Reson Imaging*, 31(3), pp.477–479.

Cockeran, R., Durandt, C., et al., 2002. Pneumolysin activates the synthesis and release of interleukin-8 by human neutrophils in vitro. *The Journal of infectious diseases*, 186(4), pp.562–565.

Cockeran, R. et al., 2009. Pneumolysin induces release of matrix metalloproteinase-8 and -9 from human neutrophils. *European Respiratory Journal*, 34(5), pp.1167–1170.

Cockeran, R., Steel, H.C., et al., 2001. Pneumolysin Potentiates Production of Prostaglandin E 2 and Leukotriene B 4 by Human Neutrophils. *Infection and Immunity*, 69(5), pp.3494–3496.

Cockeran, R., Theron, A.J., et al., 2001. Proinflammatory interactions of pneumolysin with human neutrophils. *The Journal of infectious diseases*, 183(4), pp.604–611.

Cockeran, R., Anderson, R. & Feldman, C., 2002. The role of pneumolysin in the pathogenesis of Streptococcus pneumoniae infection. *Current Opinion in Infectious Diseases*, 15(3), pp.235–239.

Condliffe, A.M. et al., 2011. Sequential activation of class IB and class IA PI3K is important for the primed respiratory burst of human but not murine neutrophils Sequential activation of class IB and class IA PI3K is important for the primed respiratory burst of human but not murine. , 106(4), pp.1432–1440.

Condliffe, A.M., Kitchen, E. & Chilvers, E.R., 1998. Neutrophil priming: pathophysiological consequences and underlying mechanisms. *Clin Sci (Lond)*, 94(5), pp.461–471.

Cowland, J.B. et al., 2003. Tissue expression of copines and isolation of copines I and III from the cytosol of human neutrophils. *Journal of Leukocyte Biology*, 74(3), pp.379–388. Available at: http://doi.wiley.com/10.1189/jlb.0203083.

Craig, A. et al., 2009. Neutrophil recruitment to the lungs during bacterial pneumonia. *Infection and Immunity*, 77(2), pp.568–575.

Craig, A.W.B., 2012. Department of Biochemistry, Queen's University, Division of Cancer Biology and Genetics, Queen's Cancer Research Institute, Kingston, Ontario K7L 3N6 Canada. , (19), pp.861–875.

Dahinden, C. et al., 1983. Granulocyte activation by endotoxin . I . Correlation between adherence and other granulocyte functions , and role of endotoxin structure on biologic activity . *J Immunol*, 130(2), pp.857–862.

Day, R.B. & Link, D.C., 2012. Regulation of neutrophil trafficking from the bone marrow. *Cellular and Molecular Life Sciences*, 69(9), pp.1415–1423.

Diamond, M.S. et al., 1990. ICAM-1 (CD54): A counter-receptor for Mac-1 (CD11b/CD18). *Journal of Cell Biology*, 111(6 II), pp.3129–3139.

Doeing, D.C., Borowicz, J.L. & Crockett, E.T., 2003. Gender dimorphism in differential peripheral blood leukocyte counts in mice using cardiac, tail, foot, and saphenous vein puncture methods. *BMC Clinical Pathology*, 3, pp.1–6.

Dong, X. et al., 2017. Draft genome of the honey bee ectoparasitic mite, Tropilaelaps

mercedesae, is shaped by the parasitic life history. *GigaScience*, 6(3), pp.1–17.

Dzhagalov, I.L. et al., 2012. Two-photon imaging of the immune system. *Current protocols in cytometry / editorial board, J. Paul Robinson, managing editor ... [et al.]*, Chapter 12, p.Unit12.26.

Ekman, A. & Olaf, L., 2009. The expression and function of Nod-like receptors in neutrophils. , 1, pp.55–63.

Erzurum, S.C. et al., 1992. Mechanisms of lipopolysaccharide-induced neutrophil retention. Relative contributions of adhesive and cellular mechanical properties. *Journal of immunology (Baltimore, Md. : 1950)*, 149(1), pp.154–62. Available at: http://www.ncbi.nlm.nih.gov/pubmed/1376747.

Evans, D.R. & Guy, H.I., 2004. JBC Papers in Press. Published on April 19, 2004 as Manuscript R400007200. , (313).

Falcão, S.A.C. et al., 2015. Exposure to Leishmania braziliensis Triggers Neutrophil Activation and Apoptosis. *PLoS Neglected Tropical Diseases*, 9(3), pp.1–19.

Feldman, C. & Anderson, R., 2016. Epidemiology, virulence factors and management of the pneumococcus. *F1000Research*, 5(0), p.2320. Available at: http://f1000research.com/articles/5-2320/v1.

Förtsch, C. et al., 2011. Changes in astrocyte shape induced by sublytic concentrations of the cholesterol-dependent cytolysin pneumolysin still require pore-forming capacity. *Toxins*, 3(1), pp.43–92.

Förtsch, C., 2012. Pneumolysin : the state of pore-formation in context to cell trafficking and inflammatory responses of astrocytes Pneumolysin : Einfluss der Porenbildung auf zelluläre Transportprozesse und inflammatorische Antworten in Astrozyten. , (January).

Fukazawa, H. et al., 1991. Specific inhibition of cytoplasmic protein tyrosine kinases by herbimycin A in vitro. *Biochemical Pharmacology*, 42(9), pp.1661–1671.

Furze, R.C. & Rankin, S.M., 2008. Neutrophil mobilization and clearance in the bone marrow. *Immunology*, 125(3), pp.281–288.

Futosi, K., Fodor, S. & Mócsai, A., 2013. Neutrophil cell surface receptors and their intracellular signal transduction pathways. *International Immunopharmacology*, 17(3), pp.638–650. Available at: http://dx.doi.org/10.1016/j.intimp.2013.06.034.

Galli, S., Borregaard, N. & Wynn, T., 2011. Phenotypic and functional plasticity of cells of innate immunity: macrophages, mast cells and neutrophils. *Nature immunology*, 12(11), pp.1035–1044. Available at: http://www.nature.com/ni/journal/v12/n11/abs/ni.2109.html.

Ginis, I. et al., 1992. Comparison of actin changes and calcium metabolism in plastic- and fibronectin-adherent human neutrophilsle. *J Immunol*, 149(4)(15), pp.1388–9.

Glynn, P. et al., 1999. Neutrophil CD11b and soluble ICAM-1 and E-selectin in community acquired pneumonia. *European Respiratory Journal*, 13(6), pp.1380–1385.

Grant, C.C. et al., 2003. Invasive pneumococcal disease in Oxford, 1985-2001: a retrospective case series. *Archives of Disease in Childhood*, 88(8), pp.712–714. Available at: http://adc.bmj.com/cgi/doi/10.1136/adc.88.8.712.

Hausdorff, W.P. et al., 2000. Which Pneumococcal Serogroups Cause the Most Invasive Disease: Implications for Conjugate Vaccine Formulation and Use, Part I. *Clinical Infectious Diseases*, 30(1), pp.100–121. Available at: https://academic.oup.com/cid/article-lookup/doi/10.1086/313608.

Hayashi, F., Means, T.K. & Luster, A.D., 2003. Toll-like receptors stimulate human neutrophil function. *Blood*, 102(7), pp.2660–2669.

Heit, B. et al., 2002. An intracellular signaling hierarchy determines direction of migration in opposing chemotactic gradients. *Journal of Cell Biology*, 159(1), pp.91–102.

Heit, B., 2005. Fundamentally different roles for LFA-1, Mac-1 and 4-integrin in neutrophil chemotaxis. *Journal of Cell Science*, 118(22), pp.5205–5220. Available at: http://jcs.biologists.org/cgi/doi/10.1242/jcs.02632.

Henrichsen, J., 1995. Six newly recognized types of Streptococcus pneumoniae.

Journal of Clinical Microbiology, 33(10), pp.2759–2762.

Henry, S.J., Crocker, J.C. & Hammer, D.A., 2013. Fibronectin Induces Beta2-Integrin-Mediated Neutrophil Haptokinesis Independent of Chemoattractant. *Biophysical Journal*, 104(2), p.320a. Available at: http://linkinghub.elsevier.com/retrieve/pii/S0006349512030226.

Hirst, R. a. et al., 2004. The role of pneumolysin in pneumococcal pneumonia and meningitis. *Clinical and Experimental Immunology*, 138(2), pp.195–201.

Hogg, J., 1995. Leukocyte Traffic in the Lung. *Annual Review of Physiology*, 57(1), pp.97–114. Available at: http://physiol.annualreviews.org/cgi/doi/10.1146/annurev.physiol.57.1.97.

Houldsworth, S., Andrew, P.W. & Mitchell, T.J., 1994. Pneumolysin Stimulates Production of Tumor Necrosis Factor Alpha and Interleukin-13 by Human Mononuclear Phagocytes. , 62(4), pp.1501–1503.

Huang, D.W., Sherman, B.T. & Lempicki, R.A., 2009a. Bioinformatics enrichment tools: Paths toward the comprehensive functional analysis of large gene lists. *Nucleic Acids Research*, 37(1), pp.1–13.

Huang, D.W., Sherman, B.T. & Lempicki, R.A., 2009b. Systematic and integrative analysis of large gene lists using DAVID bioinformatics resources. *Nature Protocols*, 4(1), pp.44–57.

Hupp, S. et al., 2013. Direct transmembrane interaction between actin and the pore-competent, cholesterol-dependent cytolysin pneumolysin. *Journal of Molecular Biology*, 425(3), pp.636–646. Available at: http://dx.doi.org/10.1016/j.jmb.2012.11.034.

Hynes, R.O., 1992. Integrins: Versatility, modulation, and signaling in cell adhesion. *Cell*, 69(1), pp.11–25.

ibdi GmbH, 2016. Application Note 17 2D and 3D Chemotaxis Assays Using µ -Slide Chemotaxis Important Notes ¾ Read the related document first : " Important Handling Information for the µ -Slide Chemotaxis – READ THIS BEFORE USE ". ¾ Follow all of the steps in this Applicat. , pp.1–18.

Iliev, A.I. et al., 2007. Cholesterol-dependent actin remodeling via RhoA and Rac1 activation by the Streptococcus pneumoniae toxin pneumolysin. *Proceedings of the National Academy of Sciences of the United States of America*, 104(8), pp.2897–902. Available at: http://www.pnas.org/content/104/8/2897.abstract.

Johansson, D., Shannon, O. & Rasmussen, M., 2011. Platelet and neutrophil responses to Gram positive pathogens in patients with bacteremic infection. *PLoS ONE*, 6(11).

Johnson, M.K., Boese-Marrazzo, D. & Pierce, W. a., 1981. Effects of pneumolysin on human polymorphonuclear leukocytes and platelets. *Infection and Immunity*, 34(1), pp.171–176.

Jounblat, R. et al., 2003. Pneumococcal behavior and host responses during bronchopneumonia are affected differently by the cytolytic and complement-activating activities of pneumolysin. *Infection and Immunity*, 71(4), pp.1813–1819.

Justus, C.R. et al., 2014. In vitro cell migration and invasion assays. *Journal of visualized experiments : JoVE*, 752, p.e51046. Available at: http://www.jove.com/video/51046/in-vitro-cell-migration-and-invasion-assays.

Kadioglu, A. et al., 2000. Host cellular immune response to pneumococcal lung infection in mice. *Infection and immunity*, 68(2), pp.492–501.

Kadioglu, A. et al., 2011. The integrins Mac-1 and alpha4beta1 perform crucial roles in neutrophil and T cell recruitment to lungs during Streptococcus pneumoniae infection. *Journal of immunology (Baltimore, Md. : 1950)*, 186(10), pp.5907–5915.

Kadioglu, A. et al., 2008. The role of Streptococcus pneumoniae virulence factors in host respiratory colonization and disease. *Nature reviews. Microbiology*, 6(4), pp.288–301.

Kanneganti, T.D., Lamkanfi, M. & Núñez, G., 2007. Intracellular NOD-like Receptors in Host Defense and Disease. *Immunity*, 27(4), pp.549–559.

Karmakar, M. et al., 2015. Neutrophil IL-1β Processing Induced by Pneumolysin Is

Mediated by the NLRP3/ASC Inflammasome and Caspase-1 Activation and Is Dependent on K^+ Efflux. *The Journal of Immunology*, 194(4), pp.1763–1775. Available at: http://www.jimmunol.org/lookup/doi/10.4049/jimmunol.1401624.

Katanaev, V.L., 2001. Signal transduction in neutrophil chemotaxis. *Biochemistry. Biokhimiia*, 66(4), pp.351–68. Available at: http://www.ncbi.nlm.nih.gov/pubmed/11403641.

Khajah, M. et al., 2013. Fer Kinase Limits Neutrophil Chemotaxis toward End Target Chemoattractants. *The Journal of Immunology*, 190(5), pp.2208–2216. Available at: http://www.jimmunol.org/cgi/doi/10.4049/jimmunol.1200322.

Kim, J. et al., 2014. The role of heat shock protein 90 in migration and proliferation of vascular smooth muscle cells in the development of atherosclerosis. *Journal of Molecular and Cellular Cardiology*, 72, pp.157–167. Available at: http://dx.doi.org/10.1016/j.yjmcc.2014.03.008.

Kirkham, L.A.S. et al., 2006. Identification of invasive serotype 1 pneumococcal isolates that express nonhemolytic pneumolysin. *Journal of Clinical Microbiology*, 44(1), pp.151–159.

Koedel, U., Scheld, W.M. & Pfister, H.W., 2002. Pathogenesis and pathophysiology of pneumococcal meningitis. *Lancet Infectious Diseases*, 2(12), pp.721–736.

Kolaczkowska, E. & Kubes, P., 2013. Neutrophil recruitment and function in health and inflammation. *Nature reviews. Immunology*, 13(3), pp.159–75. Available at: http://www.ncbi.nlm.nih.gov/pubmed/23435331.

Koppe, U., Suttorp, N. & Opitz, B., 2012. Recognition of Streptococcus pneumoniae by the innate immune system. *Cellular Microbiology*, 14(4), pp.460–466.

Kruger, P. et al., 2015. Neutrophils: Between Host Defence, Immune Modulation, and Tissue Injury. *PLoS Pathogens*, 11(3), pp.1–22.

Kumar, V. & Sharma, A., 2010. Neutrophils: Cinderella of innate immune system. *International Immunopharmacology*, 10(11), pp.1325–1334. Available at: http://dx.doi.org/10.1016/j.intimp.2010.08.012.

Küng, E. et al., 2014. The pneumococcal polysaccharide capsule and pneumolysin

differentially affect CXCl8 and IL-6 release from cells of the upper and lower respiratory tract. *PLoS ONE*, 9(3), pp.4–9.

Lämmermann, T. et al., 2013. Neutrophil swarms require LTB4 and integrins at sites of cell death in vivo. *Nature*, 498(7454), pp.371–375.

Lämmermann, T. et al., 2008. Rapid leukocyte migration by integrin-independent flowing and squeezing. *Nature*, 453(7191), pp.51–55.

Lämmermann, T. & Germain, R.N., 2014. The multiple faces of leukocyte interstitial migration. *Seminars in Immunopathology*, 36(2), pp.227–251.

Lämmermann, T. & Sixt, M., 2009. Mechanical modes of "amoeboid" cell migration. *Current Opinion in Cell Biology*, 21(5), pp.636–644.

Langereis, J.D., 2013. Neutrophil integrin affinity regulation in adhesion, migration, and bacterial clearance. *Cell Adhesion and Migration*, 7(6).

Lew, P.D. et al., 1986. Quantitative analysis of the cytosolic free calcium dependency of exocytosis form three subcellular compartments in intact human neutrophils. *J. Cell Biol.*, 102(June), pp.2197–2205.

Ley, K. et al., 2007. Getting to the site of inflammation: The leukocyte adhesion cascade updated. *Nature Reviews Immunology*, 7(9), pp.678–689.

Libman, E., 1905. A pneumococcus producing a peculiar form of hemolysis. *Proc. N.Y. Pathol. Soc.*, 5, p.168.

Littmann, M. et al., 2009. Streptococcus pneumoniae evades human dendritic cell surveillance by pneumolysin expression. *EMBO Molecular Medicine*, 1(4), pp.211–222.

Liu, F. et al., 2004. Characterization of murine grancalcin specifically expressed in leukocytes and its possible role in host defense against bacterial infection. *Bioscience, biotechnology, and biochemistry*, 68(4), pp.894–902. Available at: http://www.ncbi.nlm.nih.gov/pubmed/15118320.

Liu, G.Y. et al., 2005. *Staphylococcus aureus* golden pigment impairs neutrophil killing and promotes virulence through its antioxidant activity. *The Journal of*

Experimental Medicine, 202(2), pp.209–215. Available at: http://www.jem.org/lookup/doi/10.1084/jem.20050846.

Lollike, K. et al., 2001. Biochemical Characterization of the Penta-EF-hand Protein Grancalcin and Identification of L-plastin as a Binding Partner. *Journal of Biological Chemistry*, 276(21), pp.17762–17769.

Lyck, R. & Enzmann, G., 2015. The physiological roles of ICAM-1 and ICAM-2 in neutrophil migration into tissues. *Current Opinion in Hematology*, 22(1), pp.53–59. Available at: http://content.wkhealth.com/linkback/openurl?sid=WKPTLP:landingpage&an=00062752-201501000-00010.

Madamanchi, A., Santoro, S.A. & Zutter, M.M., 2014. I Domain Integrins. , 819. Available at: http://link.springer.com/10.1007/978-94-017-9153-3.

Maki, M. et al., 2002. Structures, functions and molecular evolution of the penta-EF-hand Ca2+-binding proteins. *Biochimica et biophysica acta*, 1600(1–2), pp.51–60.

Mandeville, J.T.H. & Maxfield, F.R., 1997. Effects of buffering intracellular free calcium on neutrophil migration through three-dimensional matrices. *Journal of Cellular Physiology*, 171(2), pp.168–178.

Manuscript, A., 2013. NIH Public Access. , 32(4), pp.856–864.

Marino, J. et al., 1985. Fibronectin mediates chemotactic factor-stimulated neutrophil substrate adhesion. *The Journal of Laboratory and Clinical Medcine*, 105(6), pp.725–730.

Marriott, H.M., Mitchell, T.J. & Dockrell, D.H., 2008. Pneumolysin : A Double-Edged Sword During the Host-Pathogen Interaction. , 44(0), pp.497–509.

Martin, K.J.S. et al., 2015. The Role of Phosphoinositide 3-Kinases in Neutrophil Migration in 3D Collagen Gels. *Plos One*, 10(2), p.e0116250. Available at: http://dx.plos.org/10.1371/journal.pone.0116250.

Martner, A. et al., 2008. Pneumolysin released during Streptococcus pneumoniae autolysis is a potent activator of intracellular oxygen radical production in

neutrophils. *Infection and Immunity*, 76(9), pp.4079–4087.

Maus, U.A. et al., 2007. Importance of phosphoinositide 3-kinase γ in the host defense against pneumococcal infection. *American Journal of Respiratory and Critical Care Medicine*, 175(9), pp.958–966.

Maus, U.A. et al., 2004. Pneumolysin-Induced Lung Injury Is Independent of Leukocyte Trafficking into the Alveolar Space. *The Journal of Immunology*, 173(2), pp.1307–1312. Available at: http://www.jimmunol.org/cgi/doi/10.4049/jimmunol.173.2.1307.

Mayadas, T.N., Cullere, X. & Lowell, C.A., 2014. The Multifaceted Functions of Neutrophils. *Annual Review of Pathology: Mechanisms of Disease*, 9(1), pp.181–218. Available at: http://www.annualreviews.org/doi/10.1146/annurev-pathol-020712-164023.

McNeela, E.A. et al., 2010. Pneumolysin activates the NLRP3 inflammasome and promotes proinflammatory cytokines independently of TLR4. *PLoS Pathogens*, 6(11).

Mestas, J. & Hughes, C.C.W., 2004. Of Mice and Not Men: Differences between Mouse and Human Immunology. *The Journal of Immunology*, 172(5), pp.2731–2738. Available at: http://www.jimmunol.org/cgi/doi/10.4049/jimmunol.172.5.2731.

Mi, H., Muruganujan, A. & Thomas, P.D., 2013. PANTHER in 2013: Modeling the evolution of gene function, and other gene attributes, in the context of phylogenetic trees. *Nucleic Acids Research*, 41(D1), pp.377–386.

Mitchell, a. M. & Mitchell, T.J., 2010. *Streptococcus pneumoniae*: virulence factors and variation. Available at: http://eprints.gla.ac.uk/29958/.

Mitchell, T.J. et al., 1991. Complement activation and antibody binding by pneumolysin via a region of the toxin homologous to a human acute-phase protein. *Molecular Microbiology*, 5(8), pp.1883–1888.

Mitchell, T.J. et al., 1989. Expression of the pneumolysin gene in Escherichia coli: rapid purification and biological properties. *BBA - Gene Structure and*

Expression, 1007(1), pp.67–72.

Moore, K. et al., 1995. P-selectin glycoprotein ligand-1 mediates rolling of human neutrophils on P selectin. *Journal of Cell Biology*, 128(4), pp.661–671.

Moreland, J.G. & Bailey, G., 2006. Neutrophil transendothelial migration in vitro to Streptococcus pneumoniae is pneumolysin dependent. *American journal of physiology. Lung cellular and molecular physiology*, 290(5), pp.L833–L840.

Nandoskar, M. et al., 1986. Inhibition of human monocyte respiratory burst, degranulation, phospholipid methylation and bactericidal activity by pneumolysin. *Immunology*, 59(4), pp.515–20. Available at: http://www.pubmedcentral.nih.gov/articlerender.fcgi?artid=1453333&tool=pmcentrez&rendertype=abstract.

Neill, D.R., Mitchell, T.J. & Kadioglu, A., 2015. *Pneumolysin*, Elsevier Inc. Available at: http://linkinghub.elsevier.com/retrieve/pii/B9780124105300000144.

Nel, J.G. et al., 2016. Pneumolysin activates neutrophil extracellular trap formation. *Clinical and Experimental Immunology*, 184(3), pp.358–367.

Nuzzi, P. a., Lokuta, M. a. & Huttenlocher, A., 2007. Analysis of Neutrophil Chemotaxis. In pp. 23–35. Available at: http://www.springerlink.com/content/un2535qk7l236695/abstract/%5Cnhttp://www.springerlink.com/content/un2535qk7l236695/abstract/#section=96093&page=1.

Obaro, S. & Adegbola, R., 2002. The pneumococcus: Carriage, disease and conjugate vaccines. *Journal of Medical Microbiology*, 51(2), pp.98–104.

Panjarian, S. et al., 2013. Structure and dynamic regulation of abl kinases. *Journal of Biological Chemistry*, 288(8), pp.5443–5450.

Parker, L.C. et al., 2005. The expression and roles of Toll-like receptors in the biology of the human neutrophil.

Paterson, G.K. & Orihuela, C.J., 2011. Pneumococci: immunology of the innate host response - PATERSON - 2010. , 15(7), pp.1057–1063.

Paton, J.C. et al., 1993. Molecular Analysis of The Pathogenicity of Streptococcus Pneumoniae: The Role of Pneumococcal Proteins. *Annual Review of Microbiology*, 47(1), pp.89–115. Available at: http://www.annualreviews.org/doi/10.1146/annurev.mi.47.100193.000513.

Paton, J.C. et al., 1991. Purification and immunogenicity of genetically obtained pneumolysin toxoids and their conjugation to Streptococcus pneumoniae type 19F polysaccharide. *Infection and Immunity*, 59(7), pp.2297–2304.

Paton, J.C. & Ferrante, A., 1983. Inhibition of human polymorphonuclear leukocyte respiratory burst, bactericidal activity, and migration by pneumolysin. *Infection and immunity*, 41(3), pp.1212–6. Available at: http://www.pubmedcentral.nih.gov/articlerender.fcgi?artid=264628&tool=pmcentrez&rendertype=abstract.

Paton, J.C., Rowan Kelly, B. & Ferrante, A., 1984. Activation of human complement by the pneumococcal toxin pneumolysin. *Infection and Immunity*, 43(3), pp.1085–1087.

Perez-Castillejos, R., 2010. Replication of the 3D architecture of tissues. *Materials Today*, 13(1–2), pp.32–41. Available at: http://dx.doi.org/10.1016/S1369-7021(10)70015-8.

Perobelli, S.M. et al., 2015. Plasticity of neutrophils reveals modulatory capacity. *Brazilian Journal of Medical and Biological Research*, 48(8), pp.665–675.

Petersen, M., Williams, J.D. & Hallett, M.B., 1993. of CDl lb. , pp.157–159.

Pettit, E.J. & Hallett, M.B., 1996. Localised and global cytosolic Ca2+ changes in neutrophils during engagement of Cd11b/CD18 integrin visualised using confocal laser scanning reconstruction. *Journal of cell science*, 109 (Pt 7(7), pp.1689–94. Available at: http://www.ncbi.nlm.nih.gov/pubmed/8832391.

Phillipson, M. et al., 2006. Intraluminal crawling of neutrophils to emigration sites: a molecularly distinct process from adhesion in the recruitment cascade. *The Journal of Experimental Medicine*, 203(12), pp.2569–2575. Available at: http://www.jem.org/lookup/doi/10.1084/jem.20060925.

Pillay, J. et al., 2010. Brief report In vivo labeling with 2 H 2 O reveals a human neutrophil lifespan of 5 . 4 days. *Blood*, 116(4), pp.625–627.

Plow, E.F. et al., 2000. Ligand binding to integrins. *Journal of Biological Chemistry*, 275(29), pp.21785–21788.

Quinn, M.T., Editors, F.R.D. & Walker, J.M., 2014. *Neutrophil Methods and Protocols IN Series Editor*,

Rabiet, M.J., Huet, E. & Boulay, F., 2007. The N-formyl peptide receptors and the anaphylatoxin C5a receptors: An overview. *Biochimie*, 89(9), pp.1089–1106.

Randle, E., Ninis, N. & Inwald, D., 2011. Invasive pneumococcal disease. *Archives of Disease in Childhood: Education and Practice Edition*, 96(5), pp.183–190.

Rankin, S.M., 2010. The bone marrow: a site of neutrophil clearance. *Journal of Leukocyte Biology*, 88(2), pp.241–251. Available at: http://www.jleukbio.org/cgi/doi/10.1189/jlb.0210112.

Ratner, A.J. et al., 2006. Pore-Forming Toxins. , 281(18), pp.12994–12998.

Rayl, M. et al., 2016. Penta-EF-hand protein peflin is a negative regulator of ER-to-Golgi transport. *PLoS ONE*, 11(6), pp.1–18. Available at: http://dx.doi.org/10.1371/journal.pone.0157227.

Renkawitz, J. et al., 2009. Adaptive force transmission in amoeboid cell migration. *Nature Cell Biology*, 11(12), pp.1438–1443. Available at: http://dx.doi.org/10.1038/ncb1992.

Reutter, W., 1985. Hepatocyte Adhesion on Plastic 288 Neumeier and Reutter Isolation of Hepatocytes and Adhesion Inhibiting Assay Antisera and IgG Isolation. , 160.

Ridger, V.C. et al., 2001. Differential effects of CD18, CD29, and CD49 integrin subunit inhibition on neutrophil migration in pulmonary inflammation. *Journal of immunology*, 166(5), pp.3484–3890. Available at: http://www.ncbi.nlm.nih.gov/pubmed/11207307.

Rijneveld, A.W. et al., 2005. CD11b limits bacterial outgrowth and dissemination

during murine pneumococcal pneumonia. *The Journal of infectious diseases*, 191, pp.1755–1760.

Rijneveld, A.W. et al., 2002. Roles of Interleukin-6 and Macrophage Inflammatory Protein–2 in Pneumolysin-Induced Lung Inflammation in Mice. *The Journal of Infectious Diseases*, 185(1), pp.123–126. Available at: https://academic.oup.com/jid/article-lookup/doi/10.1086/338008.

Roes, J. et al., 2003. Granulocyte function in grancalcin-deficient mice. *Mol.Cell Biol.*, 23(0270–7306 (Print)), pp.826–830.

Rossjohn, J. et al., 1998. The molecular mechanism of pneumolysin, a virulence factor from Streptococcus pneumoniae. *Journal of Molecular Biology*, 284(2), pp.449–461.

Rubins, J.B. et al., 1995. Dual function of pneumolysin in the early pathogenesis of murine pneumococcal pneumonia. *Journal of Clinical Investigation*, 95(1), pp.142–150.

Rubins, J.B. & Janoff, E.N., 1998. Pneumolysin: a multifunctional pneumococcal virulence factor. *The Journal of laboratory and clinical medicine*, 131(1), pp.21–27.

Rudan, I. et al., 2008. Epidemiology and etiology of childhood pneumonia. *Bulletin of the World Health Organization*, 86(5), pp.408–416.

Sadik, C.D., Kim, N.D. & Luster, A.D., 2011. Neutrophils cascading their way to inflammation. *Trends in Immunology*, 32(10), pp.452–460. Available at: http://dx.doi.org/10.1016/j.it.2011.06.008.

Sahai, E. & Pinner, S., 2009. Integrin-independent movement of immune cells. *F1000 Biology Reports*, 1(September), pp.2–6. Available at: http://www.f1000.com/reports/b/1/67/.

Sawtell, A.K., 2015. *Investigating neutrophil phenotype and migration mechanisms in the tissue draining lymph node during acute pulmonary infection with Streptococcus pneumoniae University of York Biology January*.

Smith, J.A., Samayawardhena, L.A. & Craig, A.W.B., 2010. Fps/Fes protein-tyrosine

kinase regulates mast cell adhesion and migration downstream of Kit and β1 integrin receptors. *Cellular Signalling*, 22(3), pp.427–436. Available at: http://dx.doi.org/10.1016/j.cellsig.2009.10.014.

Smith, J.D. et al., 1998. Induction of beta2 integrin-dependent neutrophil adhesion to human alveolar epithelial cells by type 1 Streptococcus pneumoniae and derived soluble factors. *The Journal of infectious diseases*, 177(4), pp.977–985.

Snigireva, A. V et al., 2014. Effect of Heat Shock Protein 90 (Hsp90) on Migration and Invasion of Human Cancer Cells in Vitro. *Biophysics and Biochemistry*, 157(4), pp.476–478.

Solovjov, D.A., Pluskota, E. & Plow, E.F., 2005. Distinct roles for the ?? and ?? subunits in the functions of integrin ??M??2. *Journal of Biological Chemistry*, 280(2), pp.1336–1345.

Song, J.Y., Eun, B.W. & Nahm, M.H., 2013. Diagnosis of pneumococcal pneumonia: Current pitfalls and the way forward. *Infection and Chemotherapy*, 45(4), pp.351–366.

Spaan, A.N. et al., 2013. Neutrophils Versus *Staphylococcus aureus* : A Biological Tug of War. *Annual Review of Microbiology*, 67(1), pp.629–650. Available at: http://www.annualreviews.org/doi/10.1146/annurev-micro-092412-155746.

Stark, M.A. et al., 2005. Phagocytosis of apoptotic neutrophils regulates granulopoiesis via IL-23 and IL-17. *Immunity*, 22(3), pp.285–294.

Stringaris, A.K. et al., 2002. Neurotoxicity of pneumolysin, a major pneumococcal virulence factor, involves calcium influx and depends on activation of p38 mitogen-activated protein kinase. *Neurobiology of Disease*, 11(3), pp.355–368.

Summers, C. et al., 2010. Neutrophil kinetics in health and disease. *Trends in Immunology*, 31(8), pp.318–324. Available at: http://dx.doi.org/10.1016/j.it.2010.05.006.

Szklarczyk, D. et al., 2017. The STRING database in 2017: Quality-controlled protein-protein association networks, made broadly accessible. *Nucleic Acids Research*, 45(D1), pp.D362–D368.

Takeuchi, O. & Akira, S., 2010. Pattern Recognition Receptors and Inflammation. *Cell*, 140(6), pp.805–820. Available at: http://dx.doi.org/10.1016/j.cell.2010.01.022.

Tarabykina, S. et al., 2000. Two forms of the apoptosis-linked protein ALG-2 with different Ca2+ affinities and target recognition. *Journal of Biological Chemistry*, 275(14), pp.10514–10518.

Tasaka, S. et al., 2002. Very late antigen-4 in CD18-independent neutrophil emigration during acute bacterial pneumonia in mice. *American Journal of Respiratory and Critical Care Medicine*, 166(1), pp.53–60.

Thomas, C.J. & Schroder, K., 2013. Pattern recognition receptor function in neutrophils. *Trends in Immunology*, 34(7), pp.317–328. Available at: http://dx.doi.org/10.1016/j.it.2013.02.008.

Thomas, P.D. et al., 2003. PANTHER: A library of protein families and subfamilies indexed by function. *Genome Research*, 13(9), pp.2129–2141.

Thornton, J. et al., 2005. THP-1 Monocytes Up-Regulate Intercellular Adhesion Molecule 1 in Response to Pneumolysin from Streptococcus pneumoniae THP-1 Monocytes Up-Regulate Intercellular Adhesion Molecule 1 in Response to Pneumolysin from Streptococcus pneumoniae. , 73(10), pp.6493–6498.

Tilley, S.J. et al., 2005. Structural basis of pore formation by the bacterial toxin pneumolysin. *Cell*, 121(2), pp.247–256.

Torres, A. & Cilloniz, C., 2014. Pneumococcal disease: Epidemiology and new vaccines. *Community Acquired Infection*, 1(2), p.35. Available at: http://www.caijournal.com/text.asp?2014/1/2/35/147647.

Trinchieri, G. & Sher, A., 2007. Cooperation of Toll-like receptor signals in innate immune defence. , 7(March), pp.179–190.

Uehara, Y. & Fukazawa, H., 1991. Protein Kinase Inhibitors. *Method in Enzymology*, 201(Academic Press, Inc), pp.370–378.

Vestweber, D., 2007. Adhesion and signaling molecules controlling the transmigration of leukocytes through endothelium. *Immunological Reviews*,

218(1), pp.178–196.

Wang, C. et al., 2002. Modulation of Mac-1 (CD11b/CD18)-Mediated Adhesion by the Leukocyte-Specific Protein 1 Is Key to Its Role in Neutrophil Polarization and Chemotaxis. *The Journal of Immunology*, 169(1), pp.415–423. Available at: http://www.jimmunol.org/cgi/doi/10.4049/jimmunol.169.1.415.

Wang, X. et al., 2017. Endotoxin-induced autocrine ATP signaling inhibits neutrophil chemotaxis through enhancing myosin light chain phosphorylation. *Proceedings of the National Academy of Sciences*, 114(17), pp.4483–4488. Available at: http://www.pnas.org/lookup/doi/10.1073/pnas.1616752114.

Watanabe, J. et al., 2003. Endotoxins stimulate neutrophil adhesion followed by synthesis and release of platelet-activating factor in microparticles. *Journal of Biological Chemistry*, 278(35), pp.33161–33168.

Weiser, J.N., Ferreira, D.M. & Paton, J.C., 2018. Streptococcus pneumoniae: Transmission, colonization and invasion. *Nature Reviews Microbiology*, 16(6), pp.355–367. Available at: http://dx.doi.org/10.1038/s41579-018-0001-8.

Weninger, W., Biro, M. & Jain, R., 2014. Leukocyte migration in the interstitial space of non-lymphoid organs. *Nature reviews. Immunology*, 14(4), pp.232–46. Available at: http://www.ncbi.nlm.nih.gov/pubmed/24603165.

Wennerberg, K., 2004. Rho-family GTPases: it's not only Rac and Rho (and I like it). *Journal of Cell Science*, 117(8), pp.1301–1312. Available at: http://jcs.biologists.org/cgi/doi/10.1242/jcs.01118.

Werr, J. et al., 1998. beta1 integrins are critically involved in neutrophil locomotion in extravascular tissue In vivo. *The Journal of experimental medicine*, 187(12), pp.2091–2096.

Werr, J. et al., 2000. Integrin alpha(2)beta(1) (VLA-2) is a principal receptor used by neutrophils for locomotion in extravascular tissue. *Blood*, 95(5), pp.1804–9. Available at: http://www.ncbi.nlm.nih.gov/pubmed/10688841.

Wiesner, S., Legate, K.R. & Fässler, R., 2005. Integrin-actin interactions. *Cellular and Molecular Life Sciences*, 62(10), pp.1081–1099.

Williams, J.H. et al., 2003. Modulation of neutrophil complement receptor 3 expression by pneumococci. *Clinical science (London, England : 1979)*, 104(6), pp.615–625.

Xu, P. et al., 2006. The role of grancalcin in adhesion of neutrophils. *Cellular Immunology*, 240(2), pp.116–121.

Yamahashi, Y. et al., 2015. Integrin associated proteins differentially regulate neutrophil polarity and directed migration in 2D and 3D. *Biomedical Microdevices*, 17(5).